DOCTORAL THESIS

Research and Development of Explicit Demand Flexibility Management Methods for Ventilation Systems

Vahur Maask

TALLINNA TEHNIKAÜLIKOOL
TALLINN UNIVERSITY OF TECHNOLOGY
TALLINN 2023

TALLINN UNIVERSITY OF TECHNOLOGY
DOCTORAL THESIS
70/2023

Research and Development of Explicit Demand Flexibility Management Methods for Ventilation Systems

VAHUR MAASK

TAL TECH PRESS

TALLINN UNIVERSITY OF TECHNOLOGY
School of Engineering
Department of Electrical Power Engineering and Mechatronics
This dissertation was accepted for the defence of the degree 07/11/2023

Supervisor: Argo Rosin, Dr.Sc.Eng., Tenured Associate Professor
School of Engineering
Tallinn University of Technology
Tallinn, Estonia

Co-supervisor: Tarmo Korõtko, Ph.D., Senior Researcher
School of Engineering
Tallinn University of Technology
Tallinn, Estonia

Opponents: Rui Miguel Amaral Lopes, Ph.D., Assistant Professor
NOVA School of Science and Technology
Department of Electrical and Computer Engineering
NOVA University Lisbon
Lisbon, Portugal

Ansis Avotiņš, Ph.D., Leading Researcher and Docent
Faculty of Electrical and Environmental Engineering
Institute of Industrial Electronics and Electrical Engineering
Riga Technical University
Riga, Latvia

Defence of the thesis: 18/12/2023, Tallinn

Declaration:
Hereby I declare that this doctoral thesis, my original investigation and achievement, submitted for the doctoral degree at Tallinn University of Technology has not been submitted for doctoral or equivalent academic degree.

Vahur Maask

---
signature

European Union
European Regional
Development Fund

Investing
in your future

Copyright: Vahur Maask, 2023
ISSN 2585-6898 (publication)
ISBN 978-9916-80-085-0 (publication)
ISSN 2585-6901 (PDF)
ISBN 978-9916-80-086-7 (PDF)
Printed by Koopia Niini & Rauam

TALLINNA TEHNIKAÜLIKOOL
DOKTORITÖÖ
70/2023

Ventilatsioonisüsteemidele otsese energiapaindlikkuse juhtimismeetodite uurimine ja arendamine

VAHUR MAASK

TAL TECH
KIRJASTUS

Content

List of publications 7
Author's contribution to the publications 8
Abbreviations 9
Symbols 10
1 Introduction 14
1.1 Background 14
1.2 Motivation 17
1.3 Aims, hypotheses, and research tasks 17
1.4 Contribution and dissemination 18
1.5 Application 18
1.6 Thesis outline 19
2 State of the art 20
2.1 Energy flexibility 20
2.1.1 Demand-side flexibility 21
2.1.2 Aggregation and explicit demand flexibility 24
2.1.3 Virtual energy storage 26
2.1.4 Balancing services in Europe 27
2.2 Management algorithms 29
2.2.1 Types of management algorithms 29
2.2.2 Algorithms used for flexible loads 30
2.3 Ventilation systems 31
2.3.1 Ventilation system control 31
2.3.2 Methods used for ventilation systems 32
2.3.3 Ventilation in nearly zero-energy buildings 32
2.4 Conclusions 34
3 Development of flexibility management methods of a ventilation system 36
3.1 Flexible power of a ventilation system 36
3.1.1 Constant air volume type of a system 37
3.1.2 Variable air volume type system 38
3.1.3 Power consumption relations and forecasting 39
3.2 Duration of forced ventilation rate 40
3.2.1 Open-loop type of system flexibility estimation 40
3.2.2 CO_2 concentration based flexibility estimation 44
3.2.3 Temperature-based flexibility estimation 44
3.2.4 Humidity-based flexibility estimation 46
3.3 Boundary condition corrections 47
3.3.1 Evaluation of uneven occupancy 47
3.3.2 Correction of IAQ parameter limit 49
3.4 Implementation of the developed flexibility management method 49
3.4.1 Adjustment method for duration estimations 49
3.4.2 Calculation method for the regulation price 50
3.4.3 Addressing the rebound effect 52
3.4.4 Selection of flexibility management algorithm 53
3.4.5 Applying flexibility management methods 54
3.5 Ventilation system as a virtual energy storage 55

3.5.1 Power capacity of virtual energy storage 55
3.5.2 Energy capacity of virtual energy storage 56
3.5.3 Virtual energy storage state of charge 58
3.5.4 Self-discharge rate of virtual energy storage 59
3.6 Conclusions 60

4 Validation of the developed flexibility management method 61
4.1 Technical and economic constraints 62
4.1.1 Determination of ventilation system parameters 62
4.1.2 Determination of building usage and internal gains 64
4.1.3 Determination of economic constraints for the flexibility service 64
4.2 Description of object models 65
4.2.1 Object 1: Small room in a building 65
4.2.2 Object 2: Single-family house 67
4.2.3 Air handling unit 69
4.2.4 Description of simulation scenarios 70
4.3 Analysis of simulation results 71
4.3.1 Object 1: Small room in a building 71
4.3.2 Object 2: Single-family house 79
4.4 Conclusions 85

5 Case studies with the developed flexibility management methods 87
5.1 Description of the building ventilation systems and experimental setups 87
5.1.1 Case study 1: Ventilation system 306SV and auditorium room 89
5.1.2 Case study 2: Ventilation system 303SV and lecture rooms 90
5.2 Analysis of case study results 92
5.2.1 Case study 1: Ventilation system 306SV and auditorium room 92
5.2.2 Case study 2: Ventilation system 303SV and lecture rooms 96
5.3 Conclusions 99

6 Conclusions and future work 100
6.1 Future work 102

List of figures 103

List of tables 105

References 106

Acknowledgements 116

Abstract 117

Lühikokkuvõte 118

Appendix 119

Curriculum vitae 176

Elulookirjeldus 177

List of Publications

The list of author's publications, on the basis of which the thesis has been prepared:

I **Maask, V.**, Rosin, A., Korõtko, T., Thalfeldt, M., Syri, S., Ahmadiahangar, R. (2023), "Aggregation ready flexibility management methods for mechanical ventilation systems in buildings," Energy and Buildings, vol. 296, Oct. 2023 doi: https://doi.org/10.1016/j.enbuild.2023.113369.

II **Maask, V.**, Rosin, A., Korõtko, T. (2023), "Virtual Energy Storage Model of Ventilation System for Flexibility Service," 17th IEEE International Conference on Compatibility, Power Electronics and Power Engineering, CPE-POWERENG 2023 (1–6). IEEE.

III **Maask, V.**, Mikola, A., Korõtko, T., Rosin, A., Thalfeldt, M. (2021), "Contributions to ventilation system demand response: a case study of an educational building," Cold Climate HVAC & Energy 2021 (1–6). E3S Web of Conferences.

IV Ferrantelli, a., Aljas, H. K., **Maask, V.**, Thalfeldt, M. (2021), "Tenant-based measured electricity use in 4 large office buildings in Tallinn, Estonia," Cold Climate HVAC & Energy 2021 (1–10). E3S Web of Conferences.

V **Maask, V.**, Häring, T., Ahmadiahangar, R., Rosin, A., Korõtko, T. (2020), "Analysis of Ventilation Load Flexibility Depending on Indoor Climate Conditions," 21st International Conference on Industrial Technology, ICIT2020 (1–6). IEEE.

VI **Maask, V.**, Rosin, A., Roasto, I. (2018), "Development of Experimental Load Management System for Nearly Zero-Energy Building," 59th International Scientific Conference on Power and Electrical Engineering of Riga Technical University, RTUCON 2018 (1–5). IEEE.

Author's Contribution to the Publications

Contribution to the papers in this thesis are:

I Vahur Maask, as the paper's main author, developed the concept for the publication. Researched and developed novel methods to quantify energy flexibility in ventilation systems, conducted simulations, and analyzed the results.

II Vahur Maask, as the paper's main author, developed the concept for the publication. Researched and developed novel methods to describe ventilation systems as virtual energy storage, conducted simulations, and analyzed the results.

III Vahur Maask, as the paper's primary author, was responsible for the method development, conducting the experiment, and analysis of the results.

IV Vahur Maask, as the third author of the paper, was responsible for the data collection and pre-processing.

V Vahur Maask, as the main author of the paper, developed the concept for the publication, selected research methods, constructed models, and carried out the analysis.

VI Vahur Maask, as the paper's main author, was responsible for developing the concept for the publication, creating models, and analyzing the results.

Abbreviations

AHU	Air handling unit
AIC	Akaike information criterion
ARMA	Autoregressive moving average
BES	Battery energy storage
BMS	Building management system
CAV	Constant air volume
CO_2	Carbon dioxide
DR	Demand response
EMS	Energy management system
EU	European Union
FMS	Flexibility management system
FVR	Forced ventilation rate
HVAC	Heating, cooling, and air conditioning
IAQ	Indoor air quality
IPS	Integrated power system
MAPE	Mean absolute percentage error
nZEB	Nearly zero-energy building
OECD	Organization for Economic Co-operation and Development
PV	Photovoltaic
QoS	Quality of service
RMSE	Root means square error
SoC	State of charge
SPG	Specific pollutant generation
TSO	Transmission system operator
UPS	Unified power system of Russia
V2G	Vehicle to grid
V2L	Vehicle to load
VAV	Variable air volume
VES	Virtual energy storage
VPP	Virtual power plant

Symbols

A_D	The DuBois surface area (m^2)
A_R	Zone floor area (m^2)
C	CO_2 concentration in a zone (ppm)
C_{amb}	Ambient CO_2 concentration (ppm)
c_{amort}	The regulation cost on amortization (€)
c_{comf}	The regulation cost on comfort (€/kWh)
C_{design}	The design CO_2 concentration for a zone (ppm)
$C_{h,i}$	The guideline value of the substance (µg/m^3)
c_{mgn}	Margin for regulations (€/kWh)
C_{limit}	CO_2 concentration limit value (ppm)
$C_{h,o}$	The concentration of the substance in the supply air (µg/m^3)
C_t	CO_2 concentration at timestep *t* (ppm)
C_{t-1}	CO_2 concentration at previous timestep *t* - 1 (ppm)
$c_{t,el}$	Electricity price including electricity market price and electricity supplier profit margin at timestep *t* (€/kWh)
$c_{t,fees}$	The sum of all the fees includes transmission costs and taxes added to the consumed energy price at timestep *t* (€/kWh).
$C_{t,min}$	Minimum CO_2 concentration for maximum airflow rate at timestep *t* (ppm)
C_t^{st}	Stable condition CO_2 concentration at timestep *t* (ppm)
$E_{t,\,dec}$	The energy capacity for up-regulation at timestep *t* (kWh)
$E_{t,\,inc}$	The energy capacity for down-regulation at timestep *t* (kWh)
G	CO_2 generation rate (m^3/s)
g	Local acceleration of gravity (m/s^2)
G_h	The generation rate of the substance (µg/s)
G_{pers}^{co2}	CO_2 generated by a person (m^3/s)
G_{pers}^{w}	Humidity generated by a person (m^3/s)
G_{max}^{co2}	Maximum estimated CO_2 generation rate (m^3/s)
G_t^{co2}	CO_2 generation rate during the timestep *t* (m^3/s)
G_t^{heat}	Heat generation rate during the timestep *t* (W)
G_t^{w}	Humidity generation rate during the timestep *t* (g/s)
K_{design}	Design value for the number of persons in a zone (pers)
K_t	Number of people inside a zone at timestep *t* (pers)
K_{t-1}	Number of people inside a zone at timestep *t* - 1 (pers)
k_t^{self}	The self-discharge or self-charge rate at timestep t (Ws/s)
MET	The level of physical activity
m_{final}	The final mass of a zone (kg)
m_{in}	The mass of the entering medium (kg)
$m_{initial}$	The initial mass of a zone (kg)

m_{out}	The mass of leaving medium (kg)
n	Total number of rooms
N_1	Fan rotational speed for the state 1 (rpm)
N_2	Fan rotational speed for the state 2 (rpm)
p	The order of the autoregressive polynomial or pressure (Pa)
P_1	Power consumption for the state 1 (kW)
P_2	Power consumption for the state 2 (kW)
P_{bias}	Power consumption bias (kW)
$p_{s,1}$	Pressure for the state 1 (Pa)
$p_{s,2}$	Pressure for the state 2 (Pa)
P_{max}	Maximum power consumption (kW)
P_{min}	Minimum power consumption (kW)
$price_t$	The calculated regulation price at time *t* (€/kWh)
$p_{s,1}$	Pressure for the state 1 (Pa)
$p_{s,2}$	Pressure for the state 2 (Pa)
P_t	Power consumption for timestep *t* (kW)
$P_{t,dec}$	Flexible power for up-regulation at timestep *t* (kW)
$P_{t,inc}$	Flexible power for down-regulation at timestep *t* (kW)
Q	Ventilation rate for the zone (m^3/s)
q	The order of the moving average polynomial or heat generated inside a zone (J)
Q_1	Airflow rate for the state 1 (m^3/s)
Q_2	Airflow rate for the state 2 (m^3/s)
Q_B	Ventilation rate for emissions from the zone ($l/[s \cdot m^2]$)
Q_{fvr}	Forced ventilation rate (m^3/s)
Q_h	The ventilation rate required for dilution (m^3/s)
Q_i	Airflow rate from a room *i* (m^3/s)
Q_{max}	Maximum ventilation rate (m^3/s)
Q_{min}	Minimum ventilation rate (m^3/s)
Q_p	Ventilation rate for the number of persons in the zone (l/s)
Q_{resp}	Person respiration rate (m^3/s)
Q_{return}	Airflow rate in the return air duct (m^3/s)
Q_t	Ventilation rate at timestep *t* (m^3/s)
q_t	The heat generated inside a zone during timestep *t* (J)
Q_{t-1}	Ventilation rate at previous timestep *t* - 1 (m^3/s)
Q_t^{return}	Airflow rate in the return air duct at the timestep *t* (m^3/s)
Q_t^{room}	Airflow rate from the room (m^3/s)
Q_{tot}	Total ventilation rate for the zone (l/s)
$Q_{tot,min}$	Total minimum ventilation rate for the zone with zero occupancy (l/s)
RH	Relative humidity (%)

RQ	A respiratory quotient
SPG_t^{room}	Specific pollutant generation for the room at the timestep *t* [(m³/s)/m², W/m² or (g/s)/m²]
SPG_t^{zone}	Specific pollutant generation for the zone at the timestep *t* [(m³/s)/m², W/m² or (g/s)/m²]
T	The temperature of the air (K)
T_i	Indoor air temperature (°C)
T_{supply}	Supply air temperature (°C)
T_t	Temperature at timestep *t* (°C)
T_{t-1}	Temperature at the previous timestep *t* – 1 (°C)
u	Internal energy per unit mass (J/kg)
V	Air volume in a zone or specific volume (m³)
v	The velocity of molecules (m/s)
W	Absolute humidity (g/m³)
W_i	Water vapor concentration in indoor air (g/m³)
W_{limit}	Humidity concentration limit value (g/m³)
W_{supply}	Supply air humidity concentration (g/m³)
W_t	Humidity concentration at timestep *t* (g/m³)
W_{t-1}	Humidity concentration at previous timestep *t* – 1 (g/m³)
w	Energy converted into work (J)
X_i	IAQ parameter value in room *i* (ppm, °C or g/m³)
X_{limit}	IAQ parameter limit according to the standard or set value (ppm, °C, or g/m³)
X_t^{limit}	IAQ parameter calculated limit for the timestep *t* (ppm, °C, or g/m³)
X_{return}	IAQ parameter value in return air (ppm, °C or g/m³)
Y_t^{fcst}	ARMA(p, q) model forecast for timestep *t*
Y_{t-i}	The autoregressive model lag
z	Elevation above the horizontal reference plane (m)
α	ARMA model constant
β_i	The autoregressive model's coefficient for the lag *i*
ΔP_t	Available flexible power at timestep *t* (kW)
Δt	Timestep length (s)
ε_t	Error terms
ε_{t-i}	The moving average model's error lag
ε_v	Effectiveness of ventilation
τ_t	FVR duration estimate at timestep *t* (s) or duration of regulation at timestep *t* (h)
τ_{t-i}	FVR duration estimate lag (s)
τ_t^{FVR}	Forced ventilation rate duration at time *t* (s)
$\tau_{t,i}^{FVR}$	An estimate of FVR duration at timestep *t* during correction iteration *i* (s)

$\tau_{t,i-1}^{FVR}$	An estimate of FVR duration at timestep *t* during previous correction iteration *i* – 1 (s)
$\tau_t^{FVR,co2}$	CO_2 concentration based FVR duration at timestep *t* (s)
$\tau_t^{FVR,T}$	Temperature based FVR duration at timestep *t* (s)
$\tau_t^{FVR,W}$	Humidity-based FVR duration at timestep *t* (s)
$\tau_t^{rb,CO2}$	CO_2 concentration based rebound duration at timestep *t* (s)
ϕ_i	The moving average model's coefficient for the lag *i*

1 Introduction

1.1 Background

Increasing environmental awareness and climate change have pushed the EU towards climate neutrality. Renewable Energy Directive [1] will force member states to fulfill at least 32% of overall energy needs with renewable energy by 2030. Furthermore, the provisional agreement is to increase the share of renewable energy goal from 32 to 42.5%. The European Green Deal [2] states that the long-term strategy will become the first climate-neutral continent by 2050. According to the Eurostat [2], the share of renewable energy consumption in gross final energy consumption during the period from 2010 to 2021 has increased from 12.5 to 21.8% in the EU, while in Estonia, renewable energy share during the same period has increased from 24.6 to 38%. Increasing the share of distributed volatile renewable energy generation makes maintaining the equilibrium between supply and demand increasingly challenging. It raises the importance of demand response and energy flexibility managed by aggregators, as described in [3]. Furthermore, the Baltic desynchronization of the IPS/UPS synchronous area will be conducted by 2026 [4]. It will further increase the importance of grid services, which Baltic electricity consumers could provide to system operators by taking advantage of their flexible loads.

According to the European Commission [5], buildings consume around 40% of the total energy produced in the EU, being the largest energy consumers in Europe. It is applying pressure on building more energy-efficient buildings and raising interest in flexible loads inside a building. In Estonia, all new buildings must be nZEB from 2020 onwards, which means that the building must not exceed the set energy performance indicator value, which for multi-apartment and office buildings is 100 kWh/(m^2·y) [6]. Another aspect is the demand-side flexibility inside a building. According to Eurelectric [7], flexibility is the modification of energy generation or consumption in reaction to an external signal to provide a service to the grid. Flexibility can be characterized by the following parameters: the amount of power modulation, the duration, the rate of change, the response time, the location, etc.

Typical flexible loads in buildings are heating, ventilation, air conditioning, lighting, appliances (e.g., laundry, dishwasher, tumble dryer), and electric vehicle chargers [8]–[10]. The study in [11] showed that HVAC systems account for up to 62% of overall electrical energy consumption in a building. In contrast, ventilation system fans can have up to 20% of the share. Therefore, ventilation systems are the biggest electricity consumers in a building after heating, cooling, and lighting. While heating, cooling, and lighting electricity consumption relies on ambient conditions and has high seasonal dependence, a ventilation system operation correlates with building usage, thus making it a valuable flexibility source throughout the year.

Ventilation systems can be characterized by their system type or control topology (Figure 1.1). There are two types of ventilation systems: natural and mechanical. Natural ventilation systems rely on airflows driven by gravity forces without electricity consumption [12]. Therefore, natural ventilation systems have no value from an energy flexibility standpoint. Mechanical ventilation systems depend on airflows generated by fans and can be divided into four: exhaust, supply, balanced, and energy recovery [13]. Exhaust and supply ventilation systems commonly use only one extract or supply air fan. Balanced ventilation systems use at least two fans, one installed in the exhaust and the

other in the supply air duct. It gives better indoor climate control and is universally applicable to all climates. The energy recovery ventilation type also has at least two fans but includes additional equipment to provide energy recovery that is essential for constructing nZEB. Energy recovery can be in the form of heat recovery or enthalpy recovery. Both have a heat exchanger, but the enthalpy recovery system retracts some water vapor from the exhaust air and transfers it back to the supply air.

From the control perspective, a ventilation system can be divided into a constant air volume (CAV) and variable air volume (VAV) type of a system. CAV system has the simplest control topology and commonly operates in an open loop configuration without feedback. This system type does not change its ventilation rate and has power consumption with low fluctuation. CAV is controlled by switching the system on, off, or between operation modes. Only adjustments are made in temperature control where the temperature can be regulated in a single point (single-zone) or multiple points (multi-zone). VAV system has a more complex system control topology and can handle the ventilation rate according to indoor air quality (IAQ). A single-zone VAV ventilation system adjusts its ventilation rate mainly by changing the fans' rotational speed directly through IAQ parameters (e.g., pollutant concentration, temperature, humidity). A multi-zone VAV type system has multiple dampers that adjust their position according to the zone's IAQ parameter, and the fans' rotational speed is changed through pressure shifts in air ducts.

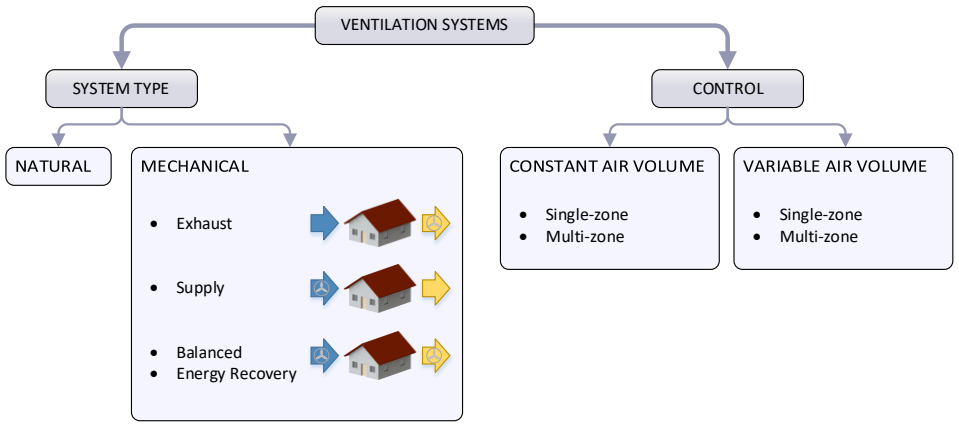

Figure 1.1. Characterization of ventilation systems by system type and control.

The installation and electrical loads of a building can be considered one nanogrid [14]. As proposed in studies [15]–[17], a central controller is used to manage nanogrid's energy flows and flexibility, which in this thesis is denoted as a flexibility management system (FMS). Changes in the ventilation system structure must be introduced to provide flexibility service to the grid. The concept of flexible control is explained in Figure 1.2, where the structure is divided into four hierarchical layers: ventilation system, measurement, management, and aggregation. No changes are needed on the ventilation system level if connecting the control with FMS is possible.

Based on the system type, an appropriate flexibility management algorithm is chosen. On the measurement level, power metering must be achieved. It is required to install an electricity meter to measure the power consumption of a ventilation system, or an existing meter will be used if available. Air duct sensors are needed to boost the performance of

the flexibility estimation algorithm, and room IAQ sensors are recommended for improvements. The flexibility can also be estimated in a sensorless mode, increasing the uncertainty in flexibility estimations. On a management level, an FMS must be installed. It can also be a remote server communicating with the building management system (BMS). If the building has no BMS, the FMS must directly control the ventilation system and acquire sensor data. Depending on the system configuration, a ventilation system can be controlled through switches or frequency converters. The aggregation level consists of the aggregator communicating with different FMSs and providing services to the transmission system operator (TSO).

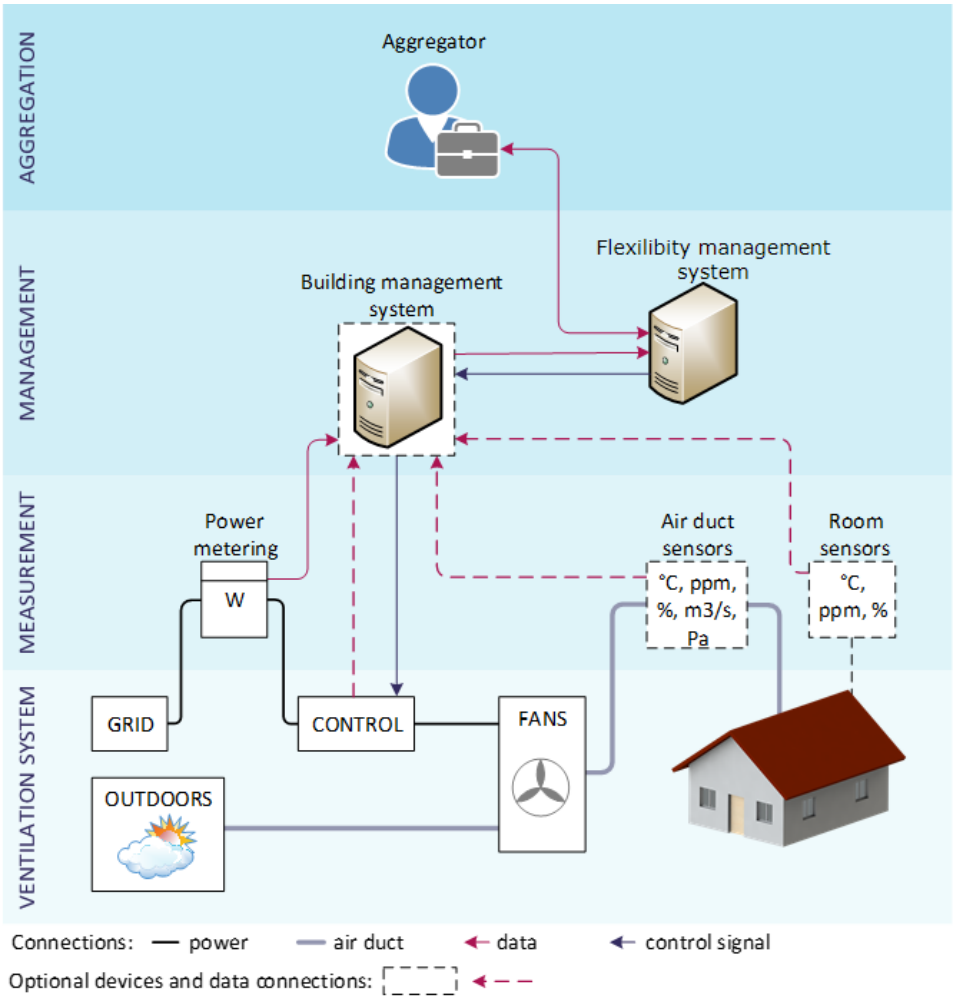

Figure 1.2. The concept of flexible control of a ventilation system.

1.2 Motivation

The author of this thesis carried out a comprehensive study on ventilation systems and addressed restrictions that can jeopardize the use of these systems in the flexibility service. The motivation to conduct this research came from the lack of appropriate methods that could be used to assess and include ventilation systems in the flexibility service. This research will bridge the gap in research by proposing appropriate methods for ventilation system flexibility management. The developed methods are modeled and tested in simulations, and experiments have been conducted on an actual building to verify the applicability of the developed method. Based on the results presented here, it is possible to assess the flexibility potential of the selected system and select an appropriate control algorithm to include the ventilation system in the flexibility service. The thesis can also be a source for future developments and research topics in the field of energy flexibility and load aggregation. This research was supported by the Estonian Research Council grant (PUT1680), Estonian Centre of Excellence in Zero Energy and Resource Efficient Smart Buildings and Districts ZEBE (grant 2014-2020.4.01.15-0016) funded by the European Regional Development Fund. Additional support was received from the European Commission through the H2020 project Finest Twins (grant no 856602). This doctoral thesis was supported by the project "Increasing the knowledge intensity of Ida-Viru entrepreneurship" co-funded by the European Union (2021-2027.6.01.23-0034).

1.3 Aims, hypotheses, and research tasks

The main aim of this Ph.D. research is to study and develop methods for harvesting mechanical ventilation system flexibility on the building level to ensure electricity cost reduction, create conditions for wider use of renewable energy in buildings, and provide services to a balancing authority.

Hypotheses:

1. Combining mass and energy balance analysis with sensor data will enable estimating forced ventilation rate duration.
2. The forced ventilation rate duration methods will forecast the maximum delivery period, wherein, in at least 95% of cases, the requirements for indoor air quality are guaranteed.
3. With the implementation of ventilation system flexibility management methods, it is possible to provide up-regulations for at least 30 min without exceeding set requirements for indoor air quality in at least 50% of the cases where the reserve is activated.
4. Using flexibility management methods to provide the flexibility service with a ventilation system will reduce the total energy cost of ventilation by at least 5%.

Research tasks:

- Analysis and classification of approaches for managing ventilation system flexibility to develop novel mathematical methods to quantify the flexibility.
- Development of novel ventilation system flexibility management methods to consider different system configurations and available sensor data.
- Improvement and validation of developed flexibility management methods on a simulated building model to analyze the performance characteristics and behavior of these methods.

- Improvement and validation of the developed flexibility management methods on a test building to test these methods under the conditions that would occur in actual use.

1.4 Contribution and dissemination

This thesis addresses comprehensive research on demand flexibility in ventilation systems, focusing on quantifying this flexibility and integrating the selected system into the flexibility service. The author proposes flexibility management methods that consider system type, available sensor data, and layout, covering most of the ventilation systems used in buildings. Knowledge and results included in this research have increased the awareness of ventilation system usability in flexibility service programs and facilitated the integration of these systems.

The findings of this research have been introduced in six research publications. Five of the papers have been published at Scopus-indexed conferences. One of the articles was published in a peer-reviewed journal. Intermediate results of the research have been presented in four sequential doctoral schools.

Scientific novelties:

- A novel method for calculating forced ventilation rate duration that considers sensor data, building size, and ventilation system parameters without the need for complex system models, large training datasets, and tuning of the hyperparameters. The method is applied to different pollutants to calculate changes in their concentration.
- A novel approach to cope with limited or nonexistent sensor data in applications where it is impossible or infeasible to install additional measurement devices.
- Definitions of ventilation system flexibility characteristics, instructions to aid the recognition process of these characteristics, and specification of ventilation system parameters that affect the flexibility.

Practical novelties:

- A set of methods developed from an aggregator's viewpoint enables integrating most ventilation systems into flexibility service.
- Comprehensive guidelines on integrating a ventilation system in a flexibility service include the needed parameters, sensor data, sources of the input, and algorithm selection procedure.
- Calculations made on the 2022 energy prices and reserve activations provide a clear picture of how the ventilation system exploitation in the flexibility service can reduce energy consumption and most importantly, the total energy costs.

1.5 Application

Within the last decade in Estonia, 212 new office buildings, 583 new commercial buildings, and 46,723 new dwellings were built, which corresponds to a floor area of 794,800 m^2 for office buildings, 1,038,300 m^2 for commercial buildings, and 4,571,600 m^2 for dwellings [18]. According to the Estonian regulation [19] the airflow rate for office and commercial buildings is 2 $l/(s \cdot m^2)$. The same regulation states the airflow rate for dwellings, which is 0.5 $l/(s \cdot m^2)$. The total calculated airflow rate is 5,952 m^3/s for all the office, commercial buildings, and dwellings built within the last decade. The average specific fan power is

between 2.0 and 2.7 kW/(m^3/s) [20]. Therefore, the total installed power for selected buildings built during the last ten years is 11.9 MW and 16.1 MW. The share of total power consumption of the ventilation system of each building type is roughly equal (Figure 1.3). Considering building size, office and commercial buildings have larger ventilation systems, which makes them preferable in the flexibility service. It does not mean that dwelling ventilation systems should be set aside. If many dwelling ventilation systems are concentrated under an aggregator, considerable power for the flexibility service can be harvested. According to the study [22], up to 15% of the rated fan power can be used for flexibility services without substantially affecting the IAQ of the building. The total available power for the flexibility service in the selected buildings is around 2.1 MW.

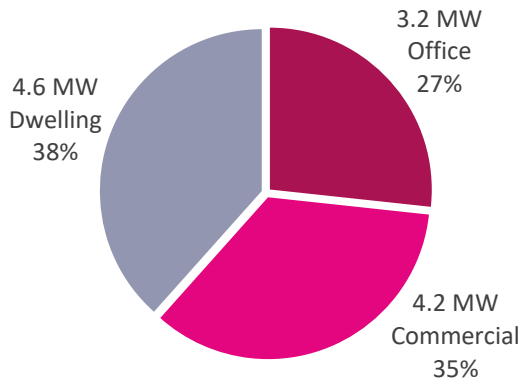

Figure 1.3. Share of the installed power of the ventilation system for each building type during the last decade.

According to Estonia's 2022-year manual frequency restoration reserve (mFRR) activations, the average energy utilized during up-regulation was around 8.7 MWh [22]. During the same time frame, regulations consumed a maximum of 98.9 MWh of energy. According to Elering AS [23], an Estonian transmission system operator (TSO), the average hourly energy usage in 2022 was 934 MWh. Since ventilation systems are known to use at least 2% of the energy generated in the EU, their greatest potential is to provide about 19 MWh of energy for the flexibility service. Therefore, ventilation systems use more energy than is needed during most regulations. As a result, the potential for the flexibility offered by ventilation systems is rather significant.

1.6 Thesis outline

The thesis is divided into four main topics and sections. Chapter 2 covers the previous research on demand-side flexibility and gives an overview of ventilation types and relevant parameters. Chapter 3 discusses the development of ventilation system flexibility management methods where different system types and available data are used to propose an appropriate flexibility management algorithm. Chapter 4 presents modeling and assessment of the flexibility management methods developed in Chapter 3 based on the results acquired from simulations. Chapter 5 addresses case studies with flexibility management methods on a test building to evaluate the performance of the method under real conditions. Finally, Chapter 6 concludes all the results gathered during this research and recommends future research topics.

2 State of the art

This chapter presents a background study of flexibility, characterization of demand-side flexibility, flexibility management algorithms, and ventilation system control from a flexibility standpoint. The state of the art study is based on various research papers to give insight and an overview of current trends and relevant research results. Firstly, energy flexibility definitions and relevant research are addressed, with the focus mainly on buildings and demand-side flexibility. Secondly, the characterization of the flexibility algorithm is given, and the main approaches are discussed. Lastly, ventilation systems and their control discussed in research papers are studied.

2.1 Energy flexibility

Energy flexibility in the context of electric system flexibility is the system's ability to adjust generation or consumption to maintain a secure system operation considering grid stability constraints and volatile renewable energy sources [24]. By Eurelectric [7] definitions, the modification of generation or consumption is done through an external signal, which can be price or activation. Electric system flexibility can be divided into demand-side and generation flexibility (Figure 2.1). Demand-side flexibility can be differentiated into explicit and implicit demand flexibility. Implicit demand flexibility uses different electricity tariffs to stimulate prosumers to consume or generate at certain hours [24]. With advancements in smart grid technology and distributed energy generation, a passive energy consumer can become an active energy prosumer [25]. Explicit demand flexibility considers committed prosumers who increase or decrease consumption or generation in response to the system's needs [24].

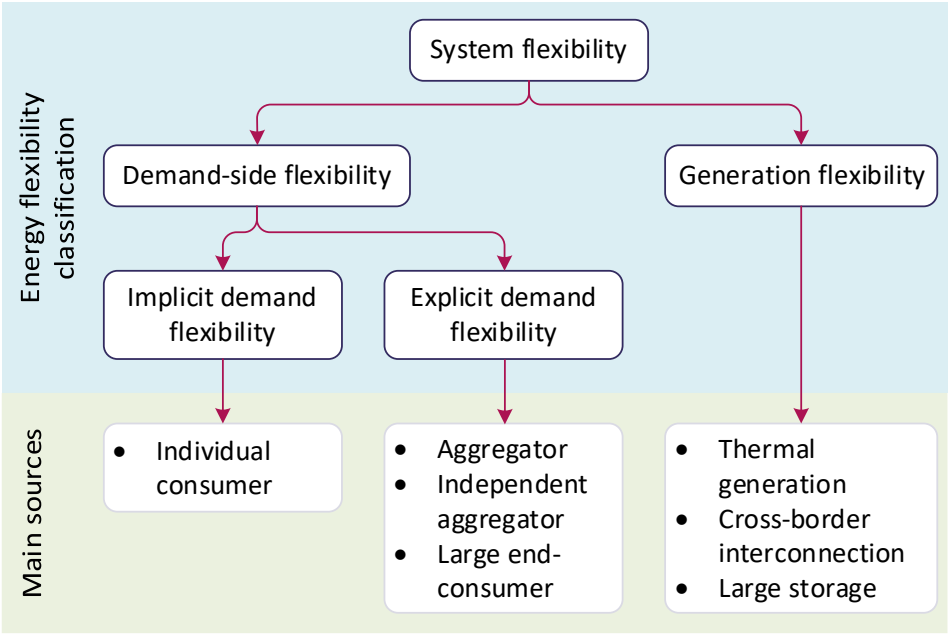

Figure 2.1. Classification of energy flexibility and main sources of flexibility [24].

Generation flexibility has been the main source of system flexibility long before the cost-effectiveness of changing demand patterns was evaluated [26]. The primary sources of generation-side flexibility have been:

- **Thermal generation** uses fossil fuel-based power plants to provide flexibility to the system. If there is a need for more energy, then more fuel is burned and vice versa [24].
- **Cross-border interconnection** enables large-scale sharing of energy, ancillary services, and backup resources [27].
- **Large energy storage** can adapt its energy production and consumption according to the system's needs. Hydroelectric plants have been the main energy storage for a long time but are limited by the location where they can be installed [28]–[30]. With the advancements in battery technology and increased efficiency in production, energy storage can have a significant role in providing stability to the energy system if safety and environmental aspects are addressed [31], [32].

2.1.1 Demand-side flexibility

In 2019, the total electricity consumption in the world reached 22.8 PWh, with a 1.7% increase compared to the previous year. In the same year, the total electricity consumed in OECD countries was 9.7 PWh, around 42% of the total electrical energy consumption in the world. Compared to the previous year, electricity consumption in OCED countries decreased by 1.1%. The main sectors where electricity is consumed are residential, industrial, commercial, and public services (Figure 2.2). Under others, electricity consumption in agriculture, forestry, fishing, and other non-specified sectors is presented [33].

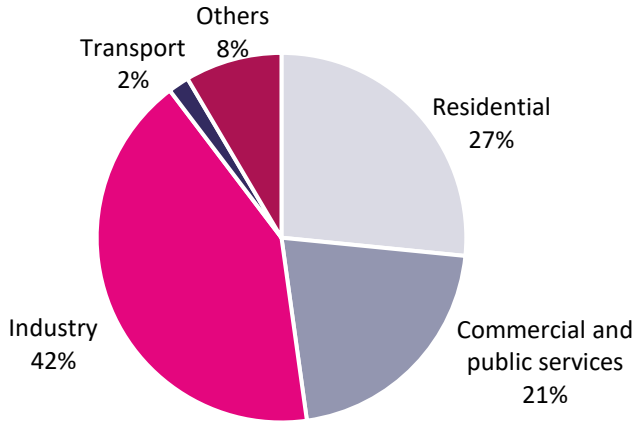

Figure 2.2. World electricity consumption by sector in 2019 [33].

According to the Global Alliance for Buildings and Construction, nearly 55% of global energy consumption is represented by buildings. A share of energy consumed by residential buildings is around 73%, and non-residential buildings are around 27%. In Estonia, 76% of the floor area in the building stock comprises residential buildings. Annual energy consumption per floor area in Estonian residential buildings is around

270 kWh/m^2, while the same parameter for non-residential buildings is around 400 kWh/m^2. Non-residential buildings in Estonia by floor area are about 20% wholesale and retail trade, 18% hotels and restaurants, 18% health care, 19% education, and the rest of 25% are used by other non-residential sectors. Residential buildings can be classified into multi- and single-family dwellings, where the share of the residential building stock is 75% and 25%, respectively. In summary, buildings can be considered valuable assets in demand-side flexibility programs [34], [35].

Flexible loads in buildings play a crucial role in the demand-side flexibility. Flexible loads are differentiated from all the other devices and systems by the ability to vary power consumption over their baseline demand without jeopardizing their Quality of Service (QoS). The amount of deviation from the baseline demand requested by an aggregator or balancing authority (usually TSO) is the reference signal [36]. Buildings, devices and systems that correspond to flexible loads have electrical storage, discrete (on/off) and dimming control of the lighting system, discrete and variable frequency control of the components in an HVAC system, and shiftable appliances [37]. According to the study [11] where electricity consumption in two office buildings was measured, it can be stated that most of the energy in office buildings is consumed by HVAC systems (Figure 2.3). The mentioned study was conducted in Estonian office buildings where the need for building cooling is around 3% of total electricity consumption, which is insignificant compared to the heating load. Ventilation systems with air heaters account for about 31% of total energy consumption in the monitored buildings. In the residential sector, space heating has the highest share of total electricity consumption in Estonian dwellings, while cooling load is non-existent in residential buildings (Figure 2.4) [35].

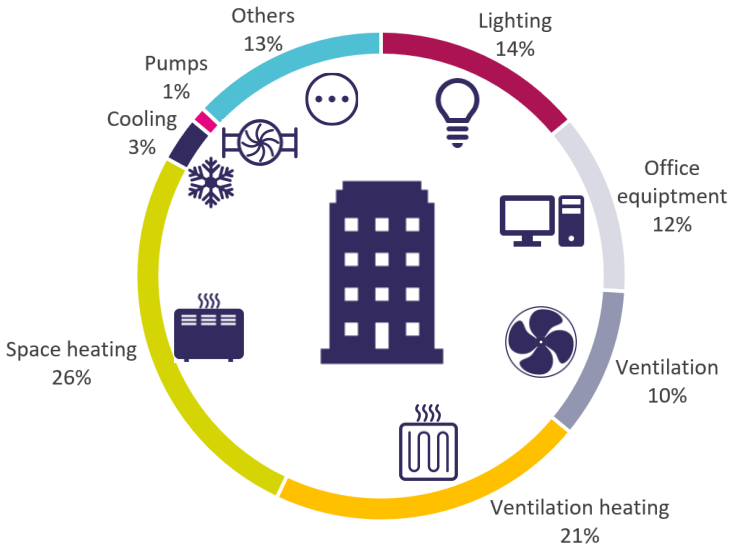

Figure 2.3. Weighted distribution of electricity consumption in two office buildings [11].

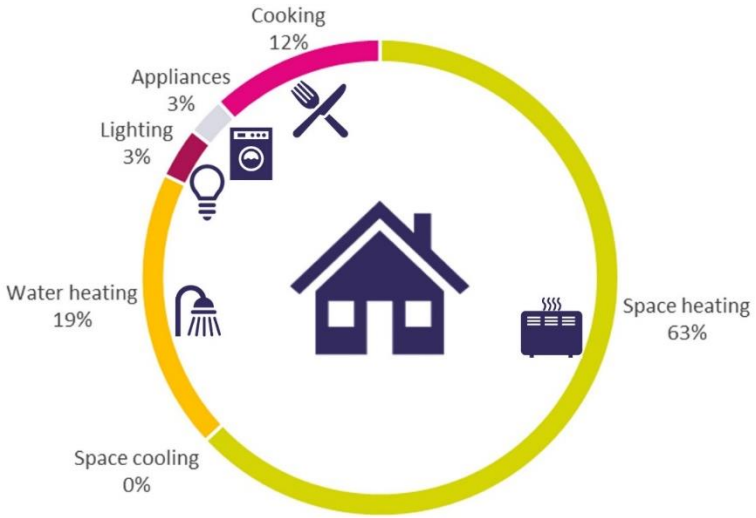

Figure 2.4. Distribution of electricity consumption in Estonian residential buildings [35].

Flexible loads and their usage in the flexibility service are as follows:

- **Electrical storage** has increased its necessity in energy flexibility in buildings aided by the wider use of stationary battery systems in buildings and electric vehicles with bidirectional charging possibilities, e.g., vehicle to load (V2L), vehicle to grid (V2G) [38]. One of the research topics is to use electrical storage to increase the share of locally produced electrical energy from on-site renewable energy generation, also called self-consumption. Luthander et al. [39] have reported that a battery storage system of 0.5 to 1 kWh per kWp of PV panels can increase the relative self-consumption rate by 13 to 24%. Kempener and Borden [40] showed that 4 kWh electric storage with 5 kWp PV panels could improve self-consumption from 30 to 60%. Another field of research is to optimize electrical storage's discharging/charging process to smoothen load fluctuations and shape load profiles for economic benefits [41], [42]. Phan et al. [43] proposed a method to optimize battery usage over a 24-hour period, which can achieve cost reduction on consumed energy by 28 to 31%. Battery energy storage is also used to provide services to the electrical system. The study [44] showed that when using batteries in both the energy and regulation market, 12% of total revenue is gathered from regulations.
- **A lighting system** in buildings has changed in the last two decades from being manually controlled by the occupants to automatically adjusting to visual comfort, efficiency, and economics [45]. Compared to other flexible loads in buildings, a lighting system's power consumption can be altered within seconds [46]. In the study [46], it is reported that for large California buildings (i.e., more than 4645 m^2), a 25% reduction in lighting system power consumption could provide a 2.5 GW regulation reserve. The same report found that when the lighting system operates around 80% light level, then ±8% power consumption can be altered without notice.
- **HVAC systems** are the largest energy consumers in a building, and through demand-side management, substantial environmental and economic benefits can be gained [47], [48]. Nyholm et al. [49] showed that pre-heating and operation

duration of 5.5 GW of peak-load shifting can be achieved by optimizing an electric heating system in Sweden based on the Swedish electricity prices during the study. The study [51] analyzed load shifting for a heat pump and a thermal storage tank by considering different temperature setpoints and tank sizes. The results showed that the proposed method can save 10% of annual costs. During up-regulations, when air-conditioners are switched off, the delay after giving the activation signal (to switch off) is around 12 to 60 s until the final load curtailment [50]. Bode et al. [51] made a similar study about shutting down and cycling air-conditioning compressors, which responded within 60 s after the activation signal was given and reached total capacity within 6 min. Cai and Braun [52] proposed a control method for a rooftop unit with a variable speed supply fan, compressor, and condenser fan to provide frequency regulation service, reducing the energy cost for buildings by 12 to 26%. Authors of the study [53] reported that 15% of the ventilation system-rated power could be used for the flexibility service without jeopardizing occupants' thermal comfort.

- **Shiftable appliances** have a significant potential to provide flexibility in the residential sector where washing machines, dishwashers, tumble dryers, and other similar home equipment time of use can be altered [37]. According to the study [54], an average maximum down-regulation of 430 W at midnight on the weekend and an average maximum up-regulation of 65 W during the weekend can be achieved per household. The study in [55] used a mixed-integer nonlinear optimization model to control shiftable appliances and reduce the cost of electricity by 25%.

Nearly half of the global energy consumption is represented by buildings, making them valuable sources for the demand-side flexibility. In Estonia, around 60% of energy consumption is represented by the HVAC systems, and when comparing different flexible loads, they can provide cost-effective capacity to the flexibility service.

2.1.2 Aggregation and explicit demand flexibility

The explicit demand flexibility approach involves re-scheduling consumption or onsite generation with a specific objective. For example, to stabilize the electric system, lessen the effect of peak electricity prices, or deal with congestion problems [24], [56]. Therefore, offering competition to power plants in the form of Virtual Power Plants (VPP), which aggregates distributed energy generation and flexible loads to participate in the wholesale market, balancing markets, reserves markets, and providing grid services [24], [57], [58]. For large prosumers, individual participation in the mentioned markets can be considered. In all other cases, aggregation is needed to concentrate multiple prosumers' ability to change their consumption or generation to fulfill all the requirements stated by the market operator [59], [60]. Aggregators concentrate and manage the flexibility offered by buildings or other sources and make a combined offer to the balancing authority or transmission system operator (Figure 2.5) [61].

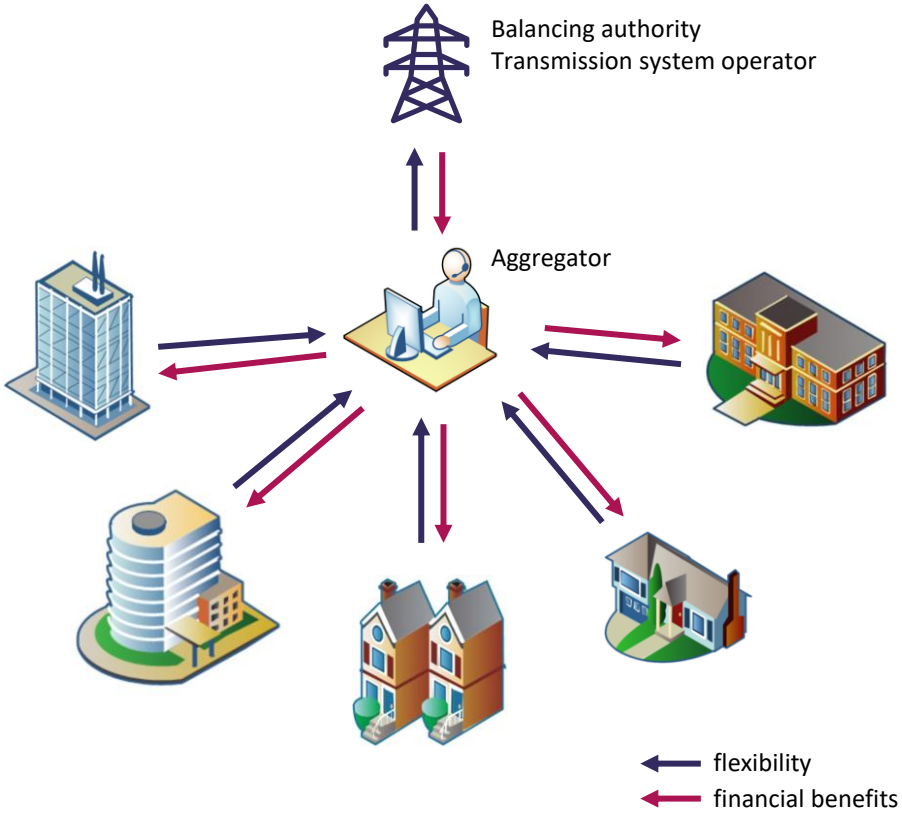

Figure 2.5. Concept of aggregating flexible loads in buildings.

An independent aggregator manages prosumers' flexible loads without being the utility that supplies energy to prosumers [60]. Therefore, an independent aggregator must be able to harvest the flexibility without signing a contract with an energy supplier servicing the same prosumer [62]. The following difficulties are encountered that impede an aggregator's actions:

- **The bulk energy issue** is a problem caused by the difference between actual consumption and the forecast made on the previous day. The retailer will not invoice the total electricity procured cost [63].
- **The imbalance issue** is a problem where retailers are reacting to the activation of the reserve. Volume correction or energy transfer is essential for imbalance settlement. The aftermath of the activation can cause a "rebound effect" where the consumption is less or more than usual, which causes a second imbalance problem [63].

Aggregation is essential to the flexibility service to take advantage of explicit demand flexibility inside buildings. If the aggregator is independent of the energy-supplying utility, problems that require tight cooperation with different parties can arise.

2.1.3 Virtual energy storage

Renewable distributed power generation causes high and rapid fluctuation in the net demand, which is a concern from the grid stability perspective since the frequency nominal value of 50 Hz is more challenging to sustain with conventional generators [64]. There are three possible ways to mitigate the volatility in the electric system:

- **Standby generation** in the form of hydro or fossil fuel-based power stations. Hydroelectric power stations are limited by geographical location and environmental restrictions. Using fossil fuel-based power stations as a backup will harm the goal of changing energy production to fully renewable [64]. Also, keeping these power plants on standby will cause a situation where the plant does not sell enough energy to cover basic costs, and it must be closed, as is happening all around Europe [65].
- **Energy storage** by using pumped hydro, batteries, compressed air, and flywheels. The major downside of using and implementing energy storage is the cost of building this system [64]. With the increasing use of Li-ion technology-based mobile and stationary energy storage, concerns about safety and environmental aspects are still topical and need to be addressed before large-scale storage can be built [66]–[70].
- **Virtual energy storage (VES)** is a concept where flexible loads can manipulate demand around a nominal baseline so that power consumption increases or decreases, like charging or discharging a battery. The use of flexible loads to provide grid services has an accelerating interest in research and among parties of an electric system. The significant advantage of VES is its lower cost of implementation compared to a real BES since there is little change in hardware and most of the work revolves around software and communication [64].

The QoS constrains the full exploitation of VES. QoS is a parameter or a group defined through the flexible load's primary purpose. For the HVAC system, the QoS can be measured through IAQ parameters (e.g., temperature, humidity, CO_2 concentration) [64]. For the pool pump, QoS can be defined through the water circulation pump running time, which is a surrogate for water cleanliness [71], [72]. Also, under QoS, running costs of flexible loads and equipment lifetime are considered independent of the sector (e.g., residential, commercial, industrial) [64].

The grid authority can activate the VES reserve through a reference signal, expecting loads to track it with sufficient accuracy. Loads that fail to do so are considered unreliable, e.g., loads that violate their QoS unilaterally abort the regulation. Therefore, the reference signal must be crafted according to the capacity of flexible loads. The capacity of a flexible load represents limitations in aggregate behavior caused by the required QoS for this load [73]. The most widely used approach to determine flexible loads' capacity is to develop a group of necessary conditions that ensure that the flexible load can track reference signals and provide the required QoS [74], [75]. Kundu et al. [76] proposed a geometric approach to characterize the flexibility of distributed energy resources. Lin and Adetola [77] proposed a load-centric approach for characterizing flexible loads. Barooah [64] proposed a power spectral density (PSD) approach that does not rely on the knowledge of a specific reference signal but only on its statistics. According to this approach, the grid-level demand of PSD can be allocated to resources (Figure 2.6).

VES is an approach that can exploit flexible loads similar to battery energy storage. There are different approaches to characterize the flexibility of VES, but QoS is the most essential group of parameters used.

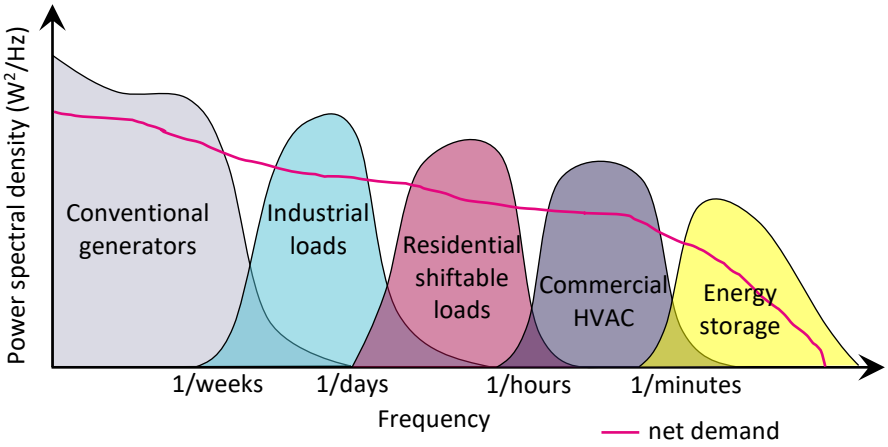

Figure 2.6. Example of power spectral density of net demand and allocation of resources to cover the electric system needs [64].

2.1.4 Balancing services in Europe

Balancing services restore the frequency to the nominal value of 50 Hz and maintain equilibrium between active power demand and supply within the electric system. The Transmission System Operator (TSO) procures and manages balancing services [78]. There are four balancing services (Figure 2.7) that differ from each other by the response time and activation method:

- **Frequency containment reserve (FCR),** a primary reserve, is usually activated automatically within milliseconds in response to the frequency deviation. For a long time, thermal power plants have been the only party in the electric system supplying FCR. However, with the increase of connected, flexible loads (e.g., electric heaters, electric vehicles, energy storage, etc.), their importance in FCR is decreasing. Fast ramp rates and frequency-based activation are causing aggregators difficulty in participating in this service [79].
- **Automatic frequency restoration reserve (aFRR),** or a secondary reserve, will be activated if the frequency has not returned to its threshold. The activation is done automatically between 30 s and 15 min after the frequency deviation [80]. The primary purpose of aFRR is to replace FCR and release the capacity for the following situations.
- **Manual frequency restoration reserve (mFRR)** has similar reasons as aFRR by restoring frequency to its nominal value, but the activation is done manually (e.g., using electronic messages or calling). Since it has a longer reaction time and slower ramp rate, aggregators have a high potential to exploit all the available flexible loads in this service.
- **Replacement reserve (RR),** or the quaternary reserve, is a long-lasting reserve that releases previous reserves' capacity after activation. It will provide the possibility to react to the subsequent failure or disturbance in the electric system again with faster reserves. Activation is done automatically or semi-automatically, and the reserve must be active for 15 min up to 2 h [80].

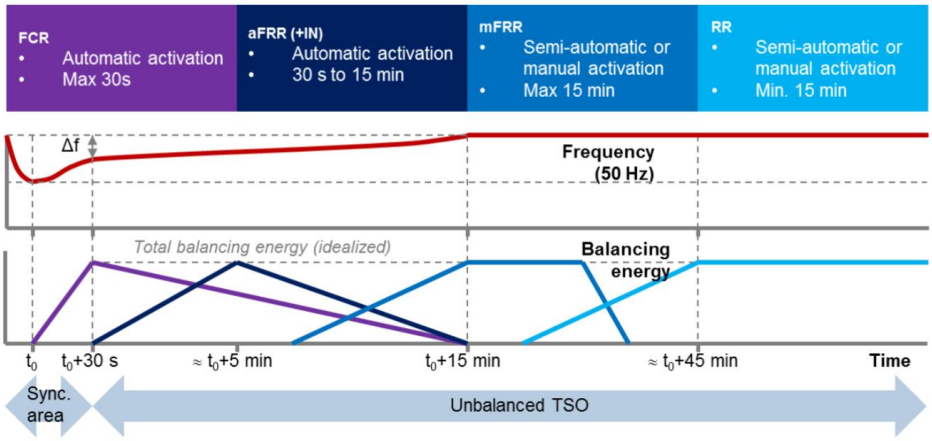

Figure 2.7. Activation process of balancing market reserves [81].

In Europe, harmonizing different balancing services is essential, meaning that regulatory measures are unified and markets are extended internationally between countries. For this balancing, service platforms are introduced:

- **PICASSO** is the Platform for the International Coordination of Automated Frequency Restoration and Stable System Operation. It is a platform to exchange balancing energy from aFRR with an activation time of 30 s to 15 min. Estonia is an observer state of this platform [82].
- **MARI** is the Manually Activated Reserves Initiative for the mFRR service. Activation time in this platform is less than 15 min. Estonia is a member state of this platform [83].
- **TERRE** is the Trans European Replacement Reserves Exchange for the RR service. Activation time in this platform for the RR service is up to 30 min. Currently, Estonia has no interaction with this platform [84].

Currently, the main balancing service available in the Baltic electric system is the Manual Frequency Restoration Reserve (mFRR). It states the limitation for the flexible load, meaning that the reaction time with the transition from one power level to another cannot be longer than 12.5 min (Table 2.1). Other parameters constrain the prospective systems to be used in the flexibility service. The minimum quantity is most important, meaning that 1 MW of ventilation systems must be combined to achieve the set minimum power level [85].

Table 2.1. Baltic mFRR standard product characteristics [85].

Parameter	mFRR standard product requirement
Mode of activation	Manual
Activation type	Direct or scheduled
Direction	Upward or downward
Full activation time	12.5 min
Minimum quantity	1 MW
Minimum duration of the delivery period	5 min
Price resolution	0.01 €/MWh
Preparation period	Not higher than 7 min
Ramping period	Not higher than 12 min
Deactivation period	Not higher than 10 min
Maximum duration of the delivery period	Not higher than 20 min for scheduled activation and 35 min for direct activation

2.2 Management algorithms

Flexible load management requires algorithms and methods which consider the following:

- **Quantification** is needed to measure the flexibility and provide metrics for the aggregator. The flexibility can be quantified through properties such as flexible power, delay, duration, etc [86].
- **The forecast** is an important part of the flexibility service. Short-term forecast (e.g., from hours to one day or a week) estimates flexibility ahead and makes tenders to the market operator.
- **Delivery** is part of aggregation where flexible loads are selected, and the activation signal is sent to the selected loads. The delivery must schedule and revise activation when needed to provide the required capacity to the grid.
- **The control** must consider specifics of each system, usually inside a primary controller. The control can include scheduling time-of-use, adaption to external signals (e.g., day-ahead price, multiple tariff system), and feedback controller such as PID.

2.2.1 Types of management algorithms

Algorithms must react to the real system behavior, and to do so, models are used for forecasting, scheduling, and control, which can be divided into three:

- **White-box** models are deterministic and defined through constants, constraints, and static and dynamic equations. Modeling a complex system with this kind of approach can be challenging. The most noticeable drawback is the need for a detailed model and complete physical knowledge of the system [87]. Also, using a white-box model with many relations between different system parts can be computationally heavy, which is unsuitable for modeling complex real-time systems [88]. Physics-based models are well suited for simple and well-established systems such as thermal electric and battery energy storage [89], [90].
- **Black-box** models ignore the physics and rely on empirical data [87]. This approach needs vast data to determine the connections and behavior of a

system, for example, HVAC power usage, interior and outdoor temperatures, and setpoints. Large (encompassing all seasons) and rich (covering all conceivable operational envelopes) training datasets are required [91], [92], which is frequently the most challenging part of creating data-driven models for flexibility management. If there are any detailed simulation models for the building, they can be used to generate this training data. However, they frequently fall short of capturing the stochastic character of actual data. Feature evaluation and selection become essential for creating an accurate but effective model when dealing with big datasets with several features (variables or sensors) [93]. It explains the significance of feature choice in data-driven models for using the flexibility of building energy. Data-driven regression-based models [94], [95], decision trees [96], and entirely black-box models like neural networks and support vector machines [97] are all employed to assess demand response (DR) potential.

- **Gray-box** models combine physics with empirical methods. One type of the model where experimental data determine the parameters is the resistance-capacitance (RC) (or lumped-capacitance) model. Continuous time (stochastic) differential equations are developed here, and parameter estimation is done using system identification approaches [98]. It focuses primarily on gray-box models when describing a method for creating and choosing a model appropriate for predictive control [99]. Furthermore, gray-box models are advised for sub-space techniques and are perfect for moderately complicated buildings. A state-space (SS) model is a class of first-order differential equations describing input, output, and state variables. The advantages of gray-box models are frequently described in the literature, allowing physical interpretation of the model parameters and comprehension of some of the underlying physical processes underpinning the behavior of buildings [100], [101].

2.2.2 Algorithms used for flexible loads

Algorithms are needed to forecast, schedule, and control flexible loads. Models that employ these algorithms are divided into three groups: white-box, gray-box, and black-box. White-box control or forecasting models implement physical and mathematical relationships and transfer functions to estimate or forecast one parameter out of others. White-box modeling has the advantage of traceability and robustness, but with complex systems, perfect behavior, and good accuracy are hard to achieve. Black-box models typically apply machine learning to describe input and output relationships. It can adapt to any system if set up correctly but lacks traceability and robustness. Gray-box models are hybrids that implement white-box mathematical relationships with added historical data-based methods to improve accuracy [102].

In the study [103] multi-criteria analysis (MCA) was conducted on eight algorithms used in energy management systems. This study analyzed six parameters: implementation feasibility, usability, computational time, accuracy, randomization, and adaptability. Implementation feasibility considers the ease of implementing the technique in a restricted amount of time and resources. Usability emphasizes the capacity to provide a condition for its users to perform the tasks safely, effectively, efficiently, and satisfactorily. Computational time values the time it takes for the technique to converge to an outcome. Accuracy is the size of the dispute between the outcome of the technique and the real

statistics. Randomization is the ability of the method to draw a pattern from a random dataset. Adaptability assumes that the same technique can be combined with other optimization techniques or used in a different environment. Artificial Neural Network has the highest score based on the MCA.

Table 2.2. List of algorithms used in energy management systems [103].

Algorithm	MCA score
ANFIS (Adaptive Neural Fuzzy Interference System)	187
ANN (Artificial Neural Network)	189
MLR (Multiple Linear Regression)	170
XGBoost (eXtreme Gradient Boosting)	185
WNN (Wavelet Neural Network)	181
SVM (Support Vector Machine)	169
ARIMA (Auto Regressive Integrated Moving Average)	140
Gaussian Process Regression	144

2.3 Ventilation systems

A ventilation system is used to provide fresh air to the building and to extract polluted air. Ventilation system operation depends on the usage of a building while providing required indoor air quality [104].

2.3.1 Ventilation system control

The traditional ventilation system is set up to provide a fixed minimum ventilation rate per person based on the maximum occupancy of a building or a space [105]. According to the standard EN-16798 [106] ventilation rate for normal conditions is 7 l/s per person and 0.7 l/s per m^2. The standard ventilation rates differ based on the building type and pollutant generation. Since the building is not occupied by the maximum number of people daily, this ventilation rate is higher than needed. Demand Controlled Ventilation (DCV) uses one or multiple Indoor Air Quality (IAQ) parameters to control the ventilation system according to the setpoint or limit values where actual demand for fresh air is estimated. It has been found that with DCV, about 62% of ventilation reduction can be achieved compared to a system without DCV [105].

DCV can be based on temperature [107], [108] or based on CO_2 concentration, which is discussed in [109], [110]. DCV with closed-loop control needs sensors to monitor IAQ. These sensors can be placed in rooms or air ducts. As suggested in [111], placing sensors in both the supply and return air ducts allows one to actively see contamination or temperature differences. The drawback of this setup is that during ventilation shutdown, the state of IAQ is unknown, and contamination or temperature can exceed the limits. Placing sensors in each room or space of the building requires higher investment costs and a complex sensor network.

Closed loop control needs a regulator to control the airflow accurately. A conventional system uses PID control to hold the IAQ within its setpoint value. The drawback of PID control is high overshoot and oscillation. In [100], direct feedback linearization is applied to overcome this issue to obtain a linear input-output model characterized by no overshoot and minimal oscillation.

Multiple studies consider temperature-based ventilation control with the thermal comfort of occupants. Ventilation demand response is considered in [110] where a study was made for commercial buildings to minimize the sum of HVAC energy and thermal discomfort costs related to occupants.

2.3.2 Methods used for ventilation systems

Studies in [10], [11] focus on temperature-based ventilation control while also considering the thermal comfort of occupants. Ventilation DR is considered in [10], where the study was made for a commercial building to minimize the sum of HVAC energy- and thermal discomfort costs related to occupants. In [11], testing was not based on any detailed model but on the actual measurement from the on-site experiments. Those studies did not consider all IAQ parameters but focused merely on the temperature. Controlling a ventilation system only by measured indoor temperature does not guarantee that other IAQ parameters are within the required limits.

An HVAC system for frequency regulation service is studied in [12]. Up to 15% of the rated fan power can be implemented in the frequency regulation without substantially affecting indoor temperature. The DR potential of ventilation systems in residential buildings is discussed in [13], where it is stated that a single 13 kW ventilation system in a 12-story apartment building can provide 4.5 kW of power increase and 1.0 kW of power reduction when needed without compromising IAQ. The outcome of the study was that an automated DR for ventilation systems could provide prolonged load sheds and ancillary services without jeopardizing IAQ. Research in [4] shows that buildings can provide short-term energy flexibility without requiring substantial changes and extra investments in the HVAC system. The mentioned studies do not consider ventilation shutdown as an option to provide load flexibility. Furthermore, existing research mainly focuses on one IAQ parameter while discarding the influence of other parameters on system flexibility.

The study in [14] monitored indoor air pollutant concentration and climate factors based on occupants' number and activities. The measured parameters included particulate matter and the CO_2 concentration. It was found that the pollutant concentration increases along with the rise in the number of occupants and the level of their physical activities. The occupants' behavior was studied in [15], where it was concluded that the CO_2 concentration and the absolute humidity level correlate since both the CO_2 and the water vapor are generated during respiration. The findings imply that the absolute humidity level can be estimated based on CO_2 concentration measurements. In [16], classroom measurements were carried out to investigate the dependence of CO_2 concentration on the ventilation rate and the number of students. The study showed that in a poorly ventilated space with a volume of 210 m^3 and an occupancy of 20 persons, the CO_2 concentration rose from 472 ppm to 1732 ppm within 4 hours.

2.3.3 Ventilation in nearly zero-energy buildings

Estonian Government has issued a regulation [6] that states: *"A nearly zero-energy building is a building that is characterized by sound engineering solutions, that is built according to the best possible construction practice, that employs solutions based on energy efficiency and renewable energy technologies and whose energy performance indicator is greater than 0 kWh/($m^2 \cdot y$) but does not exceed the limit values (Table 2.3)."*

A mechanical ventilation system with a heat recovery is needed to fulfill these requirements. It means that instead of natural ventilation, there will be more electric drives that can provide flexibility to the electric power system. This tendency is covered by Estonian legislation [112] that requires new or significantly reconstructed buildings, with some exceptions, to have a ventilation system with heat recovery, supply, and extract air fans.

Table 2.3. Limit values for energy performance indicator in nZEB.

Building type	**kWh/(m^2·y)**
Small residential buildings	50
Multi-apartment buildings	100
Libraries, offices, and research buildings	100
Business buildings	130
Public buildings	120
Commerce buildings and terminals	130
Educational buildings	90
Pre-school institutions for children	100
Healthcare buildings	270

One nZEB can be seen as a nanogrid as it is a single-unit power distribution system connected to the other power units (e.g., microgrid) through a gateway. Nanogrid is characterized by local power production (e.g., PV plant) and local loads (e.g., domestic appliances) and can optionally include energy storage [113], [114], [115], [116], [117]. The gateway can be a bidirectional power electronic converter (e.g., energy router) with its control system, DC/DC converter for battery, and AC/DC converters for external and internal AC bus connections, as shown in Figure 2.8. By using this power electronic converter, the whole nanogrid can act as a controllable load for the main grid [118], [119], [120], [121], [122].

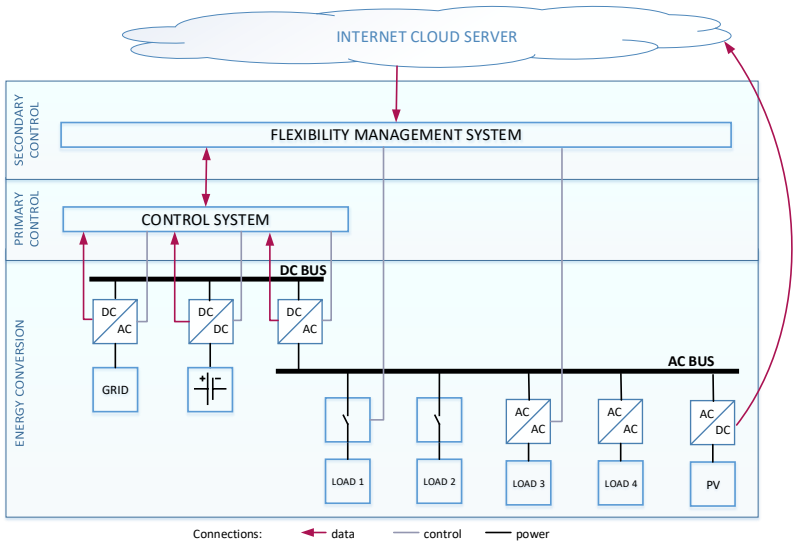

Figure 2.8. Proposed structure of nZEB nanogrid [Paper VI].

Nanogrid has different loads that can be switched or have variable power usage. Switched loads are divided into remotely controlled (load 1) and stand-alone (load 2). Simple ventilation systems are switched on and off using relays or contactors. However, typically, they work as a stand-alone system, which means that electrical installation must be changed to create the possibility of switching the ventilation system from the flexibility management system. Ventilation systems with variable drive frequency (loads 3 and 4) can change the power consumption within a specific range.

2.4 Conclusions

Characterization and quantification of flexibility are needed to aggregate flexible loads in the scope of explicit demand flexibility. Forecasts and system control are essential in placing tenders and activating reserves. Therefore, flexible load management is divided into the following parts:

- **Quantification** is needed to measure the flexibility and provide metrics for an aggregator. The flexibility cannot be quantified through a single metric, so multiple properties, such as capacity, delay, and duration, are considered [86]. Y. Chen et al. [123] have discussed some of the equations to quantify flexibility, but these mainly apply to heating and cooling systems. After all, the composition of the properties is dictated by the aggregator and the selected aggregation method.
- **Forecasting** is an important part of the flexibility service to schedule flexible loads and ensure regulation readiness. Short-term forecasts (i.e., from hours to one day or a week) are used to submit tenders to the market operator [124].
- **The interface** is a composition of methods, rules, and hardware to communicate with an aggregator and control flexible loads. It also includes building-level aggregation, where tenders from the flexible loads of the whole building are combined and submitted. If the flexibility management system receives an activation signal from an aggregator, the interface must deliver the required capacity within the given time constraints.

The literature reviewed did not give a complete package of methods to manage the energy flexibility of a ventilation system. The available methods were too time-consuming and costly to implement. Also, the research papers fail to guide the building owners or aggregators on implementing the provided methods on their systems. Estimations of how long a ventilation system can sustain a set power level were neglected in the studied literature. This thesis addresses these problems and proposes methods to manage ventilation system flexibility, enabling the use of ventilation in the flexibility service. Based on the literature analysis conducted in this chapter, it was found that flexibility management methods developed from an aggregator perspective and forced ventilation rate duration must be addressed in the following chapters. An in-depth study will be conducted in Chapter 3 to discover the connections between indoor air quality and FVR duration.

3 Development of flexibility management methods of a ventilation system

Parameters are needed to quantify a ventilation system's flexibility before it can be used in the flexibility service. These parameters must be recognized, measured, and forecasted. Parameters that quantify flexibility are flexible power, duration, rate of change, response time, location, etc. The flexible power quantifies how much of the power consumption of a ventilation system can be increased P_{inc} or decreased P_{dec} at a given time (Figure 3.1). The duration τ_{dur} shows how long the ventilation system power consumption can be changed. The rate of change indicates the speed at which the power consumption can be changed, and it can be calculated through the altered power consumption and the transition process durations for falling edge τ_{fal} and rising edge τ_{ris}. The response time is the delay from sending the command until the ventilation system takes action. The location is the geographic position of the ventilation system, which is also viewed from an electricity system perspective.

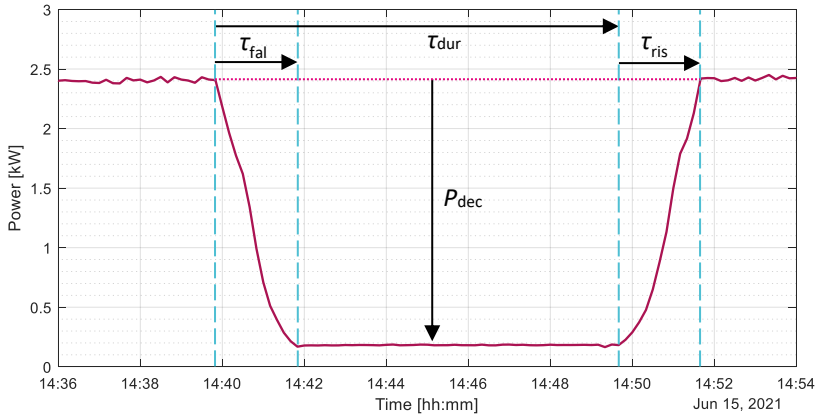

Figure 3.1. Flexible power and duration.

This chapter focuses on developing methods to measure and forecast flexible power and duration because these parameters depend on the building usage and the time of day. The rate of change, the response time, and the location characterize system properties, which can be considered constants because they are not dependent on building usage or the time of day. Changes in these values are insignificant and can mainly be caused by external factors.

3.1 Flexible power of a ventilation system

The flexible power at a specific timestep can be calculated from the system's maximum and minimum power consumption. These values can be taken from the system's documentation or measured onsite. Available power increase for a timestep t can be calculated through the forecasted power consumption for this timestep considering the maximum power consumption, as shown in (3.1). Available power decrease can be calculated similarly, regarding the minimum power consumption shown in (3.2). The minimum power consumption can be taken as 0 when the flexibility is harvested by shutting down the system.

$$P_{\mathrm{t,\,inc}} = P_{\mathrm{max}} - P_{\mathrm{t}} \tag{3.1}$$

$$P_{\mathrm{t,\,dec}} = P_{\mathrm{t}} - P_{\mathrm{min}} \tag{3.2}$$

where $P_{\mathrm{t,\,inc}}$ – maximum available power consumption increase (down-regulation) for timestep *t* (kW),
$P_{\mathrm{t,\,dec}}$ – maximum available power consumption decrease (up-regulation) for timestep *t* (kW),
P_{t} – forecasted power consumption for timestep *t* (kW),
P_{max} – maximum measured or given by documentation of power consumption (kW),
P_{min} – minimum measured or given by documentation of power consumption (kW).

The only difficulty is forecasting power consumption for the needed forecast horizon, which will be discussed in the following subsections. Depending on the system type, the power consumption is forecasted accordingly. Three ventilation system configurations have different power consumption behaviors: constant air volume, variable air volume single zone, and variable air volume multi-zone.

3.1.1 Constant air volume type of a system

A typical CAV type of a ventilation system operates according to a set schedule. This schedule is composed according to the building used to provide ventilation only when the building is occupied. Also, pre-ventilation before people enter the building or room is used to ensure fresh air is present before it is needed. The ventilation system operates only during workdays for office buildings that are used five days a week and 8 h a day. The schedule may differ within a day, but it can be assumed that the ventilation system is switched on early in the morning and off in the evening (Figure 3.2). Since the load for this system does not change during its operation, the power consumption is relatively constant compared to VAV-type systems.

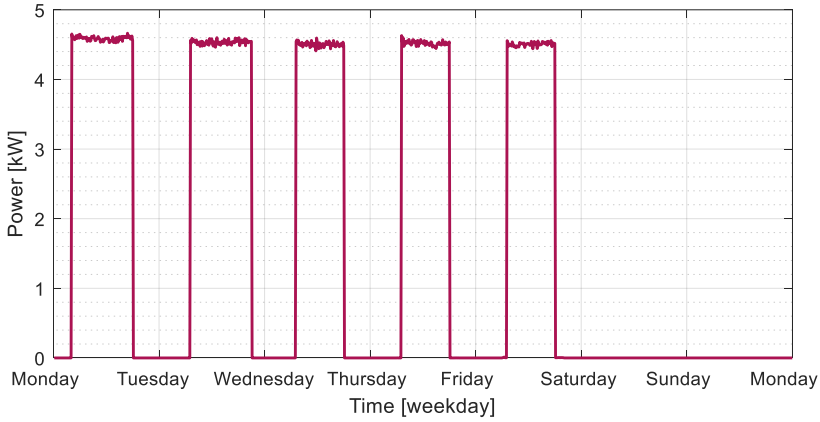

Figure 3.2. Example of weekly power consumption of a CAV type system.

3.1.2 Variable air volume type system

A VAV type ventilation system can also operate according to a schedule, but the airflow rate during the operational hours of a ventilation system is dependent on the building usage. It causes a situation where the power consumption of a ventilation system is not constant but is fluctuating. The schedule may differ for office buildings within a day, but it can be assumed that the ventilation system is operational during working hours and shut down for the rest of the time. Figure 3.3 shows an example of power consumption in a single-zone VAV type system during a week in an educational building. In a single-zone ventilation system, fluctuations are caused by a single sensor in the return air duct or the room. According to this sensor, the ventilation system changes the rotational speed of fans through a variable frequency drive and therefore, causes changes in the airflow rate.

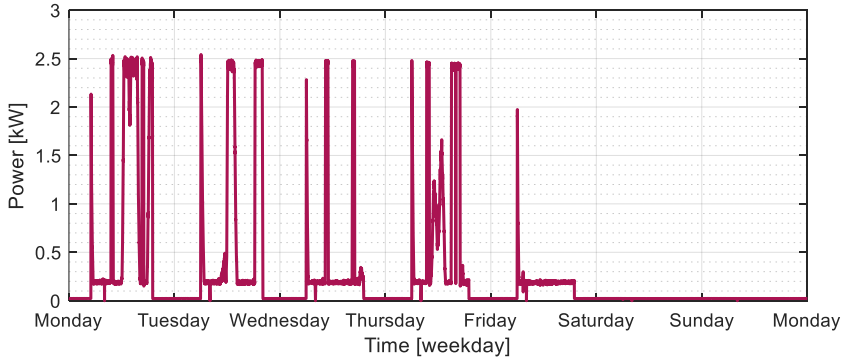

Figure 3.3. Example of weekly power consumption of a single-zone VAV type system.

Similar to a single-zone VAV type ventilation system, a multi-zone ventilation system can also operate according to a schedule. The difference is that the power consumption of the ventilation system is influenced by multiple valves that open and close according to the zone usage. The schedule may differ for office buildings within a day, but it can be assumed that the ventilation system is operational during working hours and shut down for the rest of the time. Figure 3.4 shows an example of a multi-zone VAV type system in an educational building where static pressure in the air duct is maintained. Power consumption fluctuations in this type of configuration are lower than for the single-zone VAV type system, which affects the forecasting accuracy positively.

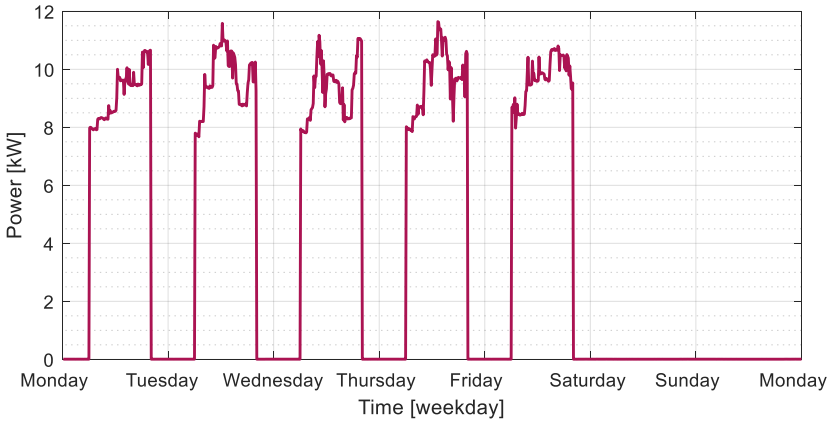

Figure 3.4. Example of weekly power consumption of a multi-zone VAV type system.

3.1.3 Power consumption relations and forecasting

Affinity laws, also known as fan laws, can be used to calculate power consumption from the change in the airflow rate [125] and vice versa. These laws are shown in (3.3) and are defined from the relationship between two operational points. Usually, measured, forecasted, or nominal values derive one value from the others.

$$\frac{P_1}{P_2} = \left(\frac{N_1}{N_2}\right)^3 = \left(\frac{Q_1}{Q_2}\right)^3 = \left(\frac{p_{s,1}}{p_{s,2}}\right)^{3/2} \tag{3.3}$$

where P_1 – power consumption for state 1 (kW),
P_2 – power consumption for state 2 (kW),
N_1 – fan rotational speed for state 1 (rpm),
N_2 – fan rotational speed for state 2 (rpm),
Q_1 – airflow rate for state 1 (m^3/s),
Q_2 – airflow rate for state 2 (m^3/s),
$p_{s,1}$ – pressure for state 1 (Pa),
$p_{s,2}$ – pressure for state 2 (Pa).

The real applied ventilation system does not strictly follow affinity laws, and typically, there is higher power consumption at a minimum ventilation rate. Self-consumption of the fan drive and losses cause higher power consumption at a minimum rate. Therefore, power consumption bias P_{bias} is calculated through maximum and minimum ventilation power consumption and airflow rate, as shown in (3.4). The power consumption for the timestep *t* is calculated using affinity law, which states the dependence between airflow rates and power consumption, as shown in (3.5).

$$P_{bias} = \frac{P_{min} - P_{max}\left(\frac{Q_{min}}{Q_{max}}\right)^3}{1 - \left(\frac{Q_{min}}{Q_{max}}\right)^3}, \tag{3.4}$$

where Q_{min} – minimum ventilation rate (m^3/s),
Q_{max} – maximum ventilation rate (m^3/s).

$$P_t = (P_{max} - P_{bias}) \cdot \left(\frac{Q_t}{Q_{max}}\right)^3 + P_{bias} \tag{3.5}$$

where Q_t – minimum ventilation rate at timestep *t* (m^3/s).

Forecasting the power consumption can be done by implementing appropriate forecasting models. Autoregressive moving average ARMA(p, q) model can be used to forecast CAV and VAV type of ventilation system power consumption, as shown in (3.6) [126]. A typical ventilation system operates according to a set schedule, and there are insignificant changes in a building's weekly or daily usage pattern, which means there is no need to use more complex and data-heavy algorithms.

$$Y_t^{fcst} = \alpha + \sum_{i=1}^{p} \beta_i Y_{t-i} + \varepsilon_t + \sum_{i=1}^{q} \phi_i \varepsilon_{t-i} \quad (3.6)$$

where Y_t^{fcst} – forecast for timestep *t* based on previous data,
Y_{t-i} – the autoregressive model lag,
ε_t – error terms,
α – ARMA model's model constant,
β_i – the autoregressive model's coefficient for the lag *i*,
ϕ_i – the moving average model's coefficient for the lag *i*,
ε_t – the moving average model's error lag,
p – the order of the autoregressive polynomial,
q – the order of the moving average polynomial.

The forecasting model must access the historical power consumption data of a ventilation system. ARMA model terms *p* and *q* are calculated using the Akaike information criterion (AIC) method. The forecast for timestep *t* is based on current and previous days or weeks' data, depending on the ventilation system schedule. If the previous week's data is used for the next week's forecast, then this time window is one week. Thus, each forecast considers the previous week's power consumption on the same weekday and time. The current day and day or week data is input into this forecasting model depending on the ventilation system schedule.

3.2 Duration of forced ventilation rate

A ventilation system must operate below or above its regular rate during reserve activation. It is forcing the ventilation system to reduce or increase its power consumption. This state can only be sustained for a certain duration because it affects IAQ in the building. In this section, methods to estimate and forecast the duration of the forced ventilation rate (FVR) are discussed. The proposed methods assume a mixing type of a ventilation system.

3.2.1 Open-loop type of system flexibility estimation

The open-loop type of a ventilation system has no feedback from a building. It causes the situation where the control system of the ventilation system has no information about the IAQ state in the building. Estimation and forecast of the FVR duration are made indirectly using information presented in the building design documentation, ventilation system datasheet, building usage profile, regulations, and standards. In estimations, only CO_2 concentration is used as it is the most volatile parameter compared to temperature and humidity.

CO_2 concentration in a zone must be estimated to calculate the FVR duration. It is done using an average CO_2 concentration for the building or calculated using mass balance analysis, as shown in (3.7). The study in [118] found that the average CO_2 concentration in an apartment building is 837 ppm. It is a good reference when the estimation is made but it does not consider fluctuations in the CO_2 concentration caused by changing building usage throughout the day. Therefore, occupant schedules given in the standard EN 16798-1:2019 are a better alternative (Figures 3.6 and 3.7). Furthermore, the standard occupant schedule can be tailored to a specific building according to the building's real usage, which would enhance flexibility estimation performance.

$$V\frac{dC}{dt} = G + QC_{amb} - QC \tag{3.7}$$

where V – air volume in a zone (m^3),
C – CO_2 concentration in a zone (ppm),
G – CO_2 generation rate (m^3/s),
Q – airflow rate for the zone (m^3/s),
C_{amb} – ambient CO_2 concentration (ppm).

To estimate CO_2 generation in a zone serviced by a selected ventilation system, the maximum number of people in this zone must be acquired. It is done according to the number of workplaces and seats in the zone, or the other alternative is to use values given in the standard EN 16798-1:2019 (Table 3.1). Maximum occupancy can be calculated accordingly if the zone floor area is known. CO_2 generated by a person during respiration is, according to the EN 16798-1:2019, around 20 l/h, or a more accurate estimation can be done by calculating one person's CO_2 generation through DuBois surface area, MET, and RQ (i.e., the rate of CO_2 produced to oxygen consumed) value, as shown in (3.8). An average size adult has a DuBois surface area of around 1.8 m^2 and an *RQ* of 0.83 [13]. The standard EN 16798-1:2019 states that humans in residential, educational, and office buildings are mainly occupied with sedentary activities; therefore, the MET value is 1.2.

$$G_{pers}^{co2} = \frac{0.00276 \cdot A_D \cdot \mathrm{MET}}{(0.23RQ + 0.77) \cdot 10^3} \tag{3.8}$$

where A_D – the DuBois surface area (m^2),
MET – the level of physical activity,
RQ – a respiratory quotient [125].

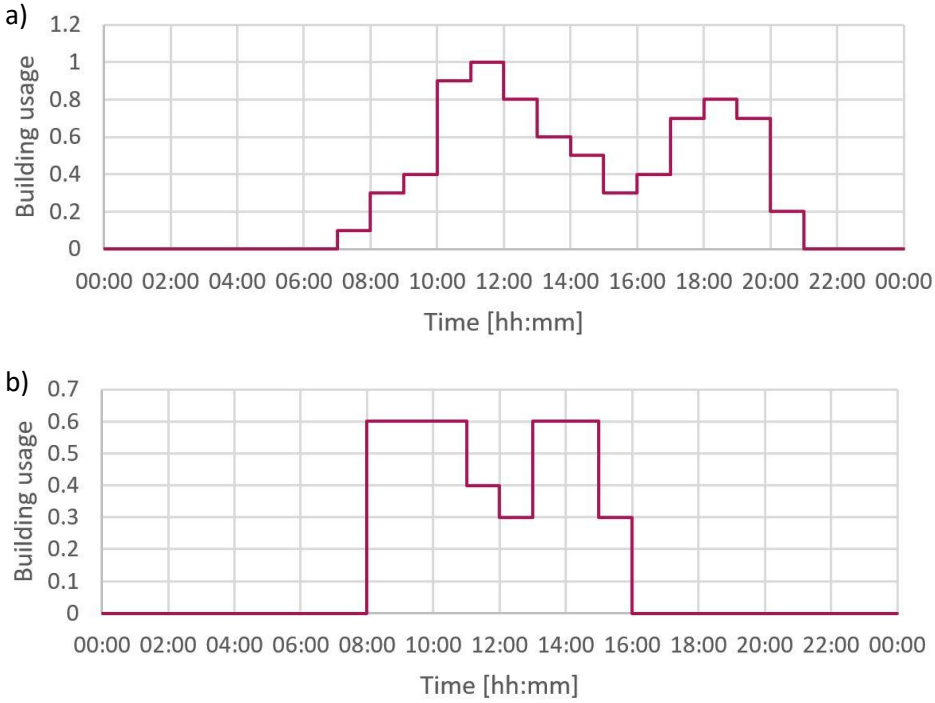

Figure 3.5. Occupant schedules for a) educational and b) commercial buildings [127].

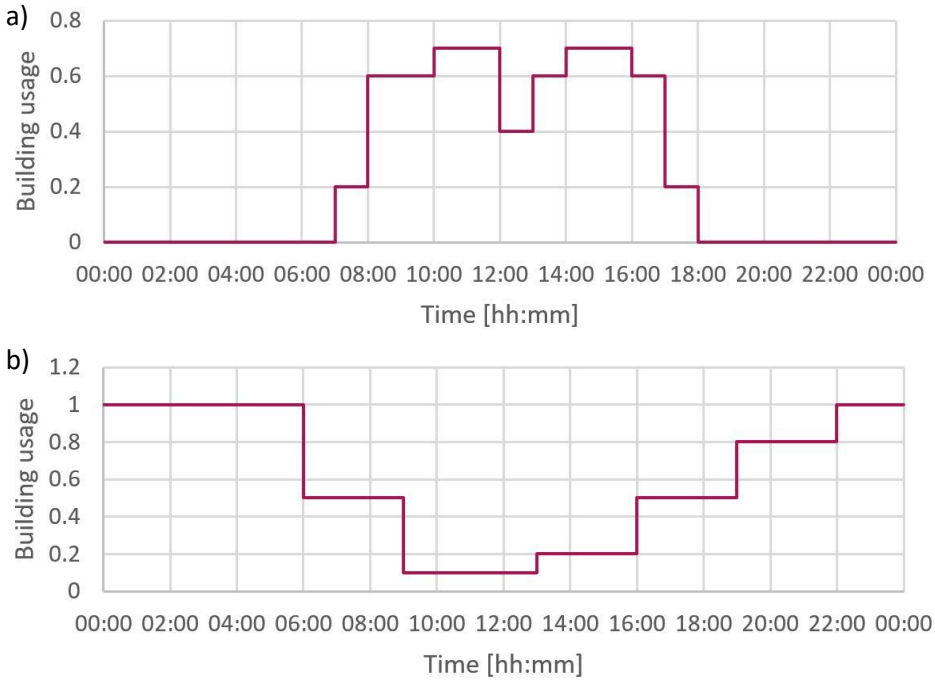

Figure 3.6. Occupant schedules for a) office buildings and b) dwellings [127].

Table 3.1. Building occupancy and ventilation rate ratios to a floor area [127].

Building type	Occupants, m^2/pers	Ventilation rate, l/(s·m^2)
Office	17	2
Educational	5,4	3
Commercial	17	2
Dwelling	28.3	0.5

CO_2 concentration in a zone must be estimated before an FVR duration can be calculated. It is done using mass balance analysis in a form where the current timestep CO_2 concentration will be calculated through CO_2 concentration of a previous timestep and change of CO_2 concentration, as shown in (3.9). CO_2 concentration change depends on CO_2 generation, the airflow of fresh ambient air, extraction of polluted air, timestep size, and the zone volume. CO_2 generation is calculated through the previously mentioned CO_2 generation rate for one person and the number of people acquired by multiplying building usage with maximum occupancy. If the airflow rate for supplying fresh air and extracting polluted air is unknown, then it can be calculated through floor area and minimum ventilation rate given by the standard EN 16798-1:2019 (Table 3.1).

$$C_t = C_{t-1} + \frac{\left(K_{t-1} \cdot G_{pers}^{co2} + Q_{t-1} \cdot C_{amb} - Q_{t-1} \cdot C_{t-1}\right) \cdot \Delta t}{V} \tag{3.9}$$

where C_t – CO_2 concentration at timestep *t* (ppm),
C_{t-1} – CO_2 concentration at previous timestep *t* – 1 (ppm),
K_{t-1} – number of people inside a zone at timestep *t* – 1 (pers),
Q_{t-1} – ventilation rate at previous timestep *t* – 1 (m^3/s),
C_{amb} – ambient CO_2 concentration (typically selected as 400 ppm),
Δt – timestep length (s),
V – zone volume (m^3).

When there is a need during regulations to force the ventilation system to operate at a minimum ventilation rate or shut it down (Q_{min} = 0), it is necessary to know how long this state can be held. During the FVR period of the ventilation system, the CO_2 concentration rises until it reaches its limit value. According to the standard EN 16798-1:2019, the limit is 800 ppm above ambient for the normal condition. Based on the calculated CO_2 concentration and the known CO_2 concentration limit value, the FVR duration can be calculated as follows:

$$\tau_t^{FVR} = \frac{V \cdot (C_{limit} - C_t)}{K_t \cdot G_{pers}^{co2} - Q_{min} \cdot \frac{C_t + C_{limit} - 2C_{amb}}{2}} \tag{3.10}$$

where τ_t^{fvr} – FVR duration at timestep *t* (s),
C_{limit} – CO_2 concentration limit value (ppm),
Q_{min} – minimum ventilation rate (m^3/s).

3.2.2 CO_2 concentration based flexibility estimation

If a zone has a CO_2 sensor in rooms or a return air duct, it is possible to calculate FVR duration based on measurements, thus improving estimations. The CO_2 generation rate during the last timestep can be calculated as shown in (3.11). This equation is derived from (3.7) and put into a discrete form more suitable for a control system.

$$G_t^{co2} = \frac{V \cdot (C_t - C_{t-1})}{\Delta t} + Q_t \cdot (C_t - C_{amb}) \tag{3.11}$$

The CO_2 generation rate at a given timestep enables the estimation of ventilation system FVR duration based on CO_2 concentration, as shown in (3.12). This equation is similar to (3.10), with the only difference that measurements are used instead of standard values. The main restriction for the FVR duration when the ventilation system operates at lowered power consumption is the upper limit of CO_2 concentration according to the standard EN 16798-1:2019, 800 ppm above ambient for normal conditions. This value depends on the building type and comfort level, meaning that it can be suited for specific needs. There is no lower limit for CO_2 concentration, which means that there is no limitation to increasing the power consumption of a ventilation system from the CO_2 concentration perspective.

$$\tau_t = \frac{V \cdot (C_{limit} - C_t)}{G_t^{co2} - Q_{min} \cdot \frac{C_t + C_{limit} - 2C_{amb}}{2}} \tag{3.12}$$

The FVR duration calculated with (3.12) is an instantaneous value considering conditions measured during the last timestep. It is not applicable when forecasts for future FVR durations are needed. Therefore, the ARMA(p, q) model is set up to forecast the future based on previous values. ARMA(p, q) model is also used for forecasting the CO_2 generation rate, which is needed to calculate the price for regulations. The ARMA(p, q) model forecasting is expressed in (3.6).

3.2.3 Temperature-based flexibility estimation

In some applications, a ventilation system provides thermal comfort to occupants or holds set temperatures for other purposes. It means that when the ventilation system is used for the flexibility service, the temperature effect should be included in the estimations. The standard EN 16798-1:2019 specifies temperature ranges according to building type and season. Seasons are defined by running mean external temperature. The heating season is considered when the seven-day running mean external temperature is above 17 °C, and the cooling season is considered when the running mean temperature is below 12 °C. All the temperature ranges for normal conditions according to space type and season are given in Table 3.2.

The first law of thermodynamics can be used to estimate energy flows into or out of a zone, as is expressed in (3.13). The difference between the initial and final states of the zone can be expressed through multiple mass flows with uniform properties, including the heat *q* generation by people, appliances, and room heating. Mechanical work *w* can be excluded from the equation because the zone is not doing any mechanical work, and all the energy used by appliances is converted into heat [128].

Table 3.2. Temperature ranges for normal conditions according to space type and season [127].

Building or space type	**Temperature range for the heating season**	**Temperature range for the cooling season**
Residential (bedroom, living room, etc.)	20 … 25 °C	23 … 26 °C
Residential (kitchen, storage, etc.)	17 … 25 °C	
Offices and similar (single office, open plan office, conference room, auditorium, cafeteria, restaurant, classroom, etc.)	20 … 24 °C	23 … 26 °C

$$\sum m_{in}\left(u+pV+\frac{v^2}{2}+gz\right)_{in}-\sum m_{out}\left(u+pV+\frac{v^2}{2}+gz\right)_{out}+q-$$
$$-w=\left[m_{final}\left(u+\frac{v^2}{2}+gz\right)_{final}-m_{initial}\left(u+\frac{v^2}{2}+gz\right)_{initial}\right]_{zone} \quad (3.13)$$

where m_{in} – the mass of the entering medium,
m_{in} – the mass of leaving medium,
m_{final} – the final mass of a zone,
$m_{initial}$ – the initial mass of a zone,
u – internal energy per unit mass,
p – pressure,
V – specific volume,
v – velocity of molecules,
g – local acceleration of gravity,
z – elevation above the horizontal reference plane,
q – heat generated inside a zone,
w – energy converted into work.

A ventilation system can be considered the only way entering and leaving airflow streams can move. All the other mass flows through openings and walls can be regarded as one variable: heat. From (3.13), only mass internal energy *u* is needed to estimate the heat generation between entering and leaving air, while pressure, volume, velocity, and potential energy have no significant difference. To evaluate ventilation system flexibility based on temperature, a heat generation rate must be calculated, which can be done as follows:

$$\frac{q_t}{\Delta t}=\frac{V\cdot(T_t-T_{t-1})}{\Delta t}+Q_t\cdot\left(T_t-T_{supply}\right) \quad (3.14)$$

where T_t – temperature at timestep *t* (°C),
T_{t-1} – temperature at the previous timestep *t* – 1 (°C),
T_{supply} – supply air temperature (°C),
Q_t – ventilation rate at timestep *t* (m^3/s),
Δt – timestep length (s),
V – zone volume (m^3).

The heat generation rate at a given timestep enables estimation of ventilation system FVR duration based on the temperature, as shown in (3.15). This equation is similar to CO_2 concentration based estimation, but it must consider seasonal effects. During summer, when the ventilation system is used for cooling, the temperature limit should be selected as the maximum temperature value given by the standard EN 16798-1:2019:2019, which is 26 °C. In winter, when the ventilation system acts as a heat source, the temperature limit should be the minimum allowable value, commonly 20 °C.

$$\tau_t = \frac{V \cdot (T_{limit} - T_t)}{\frac{q_t}{\Delta t} - Q_{fvr} \cdot \frac{T_t + T_{limit} - 2T_{supply}}{2}} \tag{3.15}$$

The FVR duration calculated with (3.15) is an instantaneous value considering conditions measured during the last timestep. It is not applicable when forecasts for future FVR durations are needed. Therefore, the ARMA(p, q) model is set up to forecast the future based on previous values. The ARMA(p, q) model for forecasting is expressed in (3.6).

3.2.4 Humidity-based flexibility estimation

Humidity is affected by persons inside the building where, during exhaling, some moisture is added to inhaled air; washing and drying also add moisture to the inside air. Typically, a ventilation system extracts excess moisture from the building. When the ventilation system is used for the flexibility service, the humidity effect should be included in estimations. The standard EN 16798-1:2019:2019 recommends limiting the absolute humidity to 12 g/kg or 14.45 g/m^3.

Commercially available humidity sensors typically measure relative humidity, thus outputting a value that is a percentage of the measured humidity level against maximum humidity at a given temperature. Relative humidity inside air depends on the air temperature, which means that relative humidity for entering and leaving air is not comparable. This issue is resolved by converting the relative humidity level into absolute (g/m^3), which can be calculated as follows [129]:

$$W = \frac{B \cdot C \cdot RH \cdot 10^{\left(\frac{m \cdot T}{T + T_n}\right)}}{100 \cdot T} \tag{3.16}$$

where T – temperature of the air (K),
RH – relative humidity,
C, B, T_n, m – constants given in Table 3.3.

Table 3.3. Values for the constants [129].

Constant	Value
B	6.116441
C	2.16679 gK/J
m	7.591386
T_n	240.7263

Like the CO_2 concentration estimation, the humidity level inside the building can be estimated by the mass balance analysis, as shown in (3.7). The humidity generation rate can be calculated as follows:

$$G_t^w = \frac{V \cdot (W_t - W_{t-1})}{\Delta t} + Q_t \cdot (W_t - W_{supply}) \quad (3.17)$$

where W_t – humidity concentration at timestep *t* (g/m^3),
W_{supply} – supply air humidity concentration (g/m^3).

The ventilation system provides dry air to the building. Therefore, the humidity will rise if the ventilation rate decreases until the maximum allowable level is reached. The same approach as was used for CO_2 concentration based flexibility estimation can be used also for humidity:

$$\tau_t = \frac{V(W_{limit} - W_t)}{G_t^w + Q_{min} \cdot \frac{W_t + W_{limit} - 2W_{supply}}{2}} \quad (3.18)$$

where W_{limit} is humidity concentration limit value (g/m3).

The FVR duration calculated with (3.18) is an instantaneous value with the same shortcomings as for the CO_2 concentration and temperature-based estimations. A separate model is needed to forecast FVR durations. Therefore, the same approach as for the temperature estimations is used. ARMA(p, q) model is set up to make forecasts for the future based on previous values. The ARMA(p, q) model for forecasting is expressed in (3.6).

3.3 Boundary condition corrections

One building can consist of multiple zones, each with multiple rooms. If there is an IAQ sensor in the return air duct, it does not represent the real situation in each room. The pollutant concentration is the average value for the whole zone. If there are rooms with uneven usage, then it can cause a situation where boundary conditions will be exceeded. It is especially troublesome if the ventilation system is forced to operate at its minimum rate. The regulation effect on IAQ is lessened by restricting the ventilation system flexibility and correcting the boundary condition. It is done by narrowing the range where the IAQ parameter can be.

3.3.1 Evaluation of uneven occupancy

IAQ parameters (e.g., CO2 concentration, temperature, humidity) are typically measured in a return air duct connected to multiple rooms. It causes the situation where, for ideal conditions, the measured value is a weighted average value for all the rooms, as shown in (3.19). If there is an uneven usage of rooms, then there is a possibility that the IAQ parameter limit value will be exceeded in high occupancy rooms during regulations.

$$X_{return} = \frac{\sum_{i=1}^{n} X_i Q_i}{Q_{return}} \quad (3.19)$$

where X_{return} – IAQ parameter value in return air,
X_i – IAQ parameter value in room *i*,
Q_{return} – airflow rate in the return air duct (m^3/s),
Q_i – airflow rate from a room *i* (m^3/s),
n – total number of rooms.

IAQ condition in a building must be measured or estimated to consider uneven occupancy in the flexibility estimation. For this, there are two approaches:

- Install temporary IAQ sensors in rooms of interest to log measurements for at least one week during normal building usage (i.e., avoid holidays). It is recommended to take repeated measurements at least once a year or after a change in room usage in a building (i.e., change of tenant).
- Evaluate rooms' usage according to the design documentation of a building or according to the real building usage, which requires manual logging of rooms' use for at least one week.

Suppose that one of the previously mentioned approaches is conducted. In that case, it is possible to estimate pollutant generation or heat generation according to the floor area of selected rooms, which in this thesis is named specific pollutant generation (SPG). Therefore, the SPG for CO_2 is defined as $(m^3/s)/m^2$, the SPG for temperature is defined as $W/m^{2,}$ and the SPG for humidity is defined as $(g/s)/m^2$. The SPG for CO_2 is calculated through CO_2 concentration change, as shown in (3.11) or using one person CO_2 generation rate, as shown in (3.8), multiplied by the number of people and divided by the floor area of the selected room. The SPG for temperature is calculated through the temperature change, as shown in (3.14), or by adding all the heat sources in a room and dividing by the floor area of the selected room. Heat sources are persons inside the room and appliances. According to the ASHRAE Handbook [44], one person's heat generation depends on the degree of activity, which must be multiplied by the number of people inside a room. The SPG for humidity is calculated through water vapor concentration change, as shown in (3.17) or using one-person humidity generation by multiplying it by the number of people. If the average person's respiration rate of 0.12 l/s is used, then the humidity generation rate for this person can be calculated as follows [130]:

$$G_{pers}^{w} = (A + BT_i - 0.798W_i) \cdot Q_{resp} \tag{3.20}$$

where A = 0.02645 – constant with the temperature in °C,
B = 0.000065 – constant with the temperature in °C,
T_i – indoor air temperature (°C),
W_i – water vapor concentration in indoor air (g/m^3),
Q_{resp} – person's respiration rate (m^3/s).

It is advised to consider water vapor release from showers and cooking for dwellings. Water vapor release from showers is 2.6 kg/h and 0.7 kg/h for baths. Additionally, 0.24 kg of water vapor per meal can be considered when cooking [130].

Table 3.4. Heat generation by human beings in different states of activity [128].

Degree of Activity	**Building type**	**Total heat generation by an adult male, W**	**Total adjusted heat generation by male, female, child, W**
Seated, very light work	Offices, hotels, apartments	130	115
Moderately active office work	Offices, hotels, apartments	140	130
Standing, light work, walking	Department store, retail store	160	130

3.3.2 Correction of IAQ parameter limit

IAQ parameter limit value can be corrected based on acquired SPGs. The room with the highest SPG for the selected IAQ parameter defines the corrected limit value. Spaces are not used equally throughout one day, and a room's maximum SPG can change. Therefore, it is reasonable to calculate the corrected limit value for each timestep. The corrected limit value is calculated based on the value given by the standard EN 16798-1:2019, from which the measured parameter value in the supply air is deducted. The difference is then multiplied by the room airflow rate and SPG for the selected IAQ parameter. The acquired value is divided by the return airflow rate and the zone's average SPG for all of the rooms in this zone and added to the supply air parameter value, as shown in (3.21).

$$X_t^{limit} = X_{supply} + \frac{\left(X_{limit} - X_{supply}\right) \cdot Q_t^{room} \cdot SPG_t^{room}}{Q_t^{return} \cdot SPG_t^{zone}} \tag{3.21}$$

where X_t^{limit} – IAQ parameter calculated limit in ppm, °C, or g/m^3,
X_{limit} – IAQ parameter limit according to the standard or set value in ppm, °C, or g/m^3,
Q_t^{room} – airflow rate from the room (m^3/s),
SPG_t^{room} – specific pollutant generation for the room in (m^3/s)/m^2, W/m^2 or (g/s)/m^2,
Q_t^{return} – airflow rate in the return air duct (m^3/s),
SPG_t^{zone} – specific pollutant generation for the zone in (m^3/s)/m^2, W/m^2 or (g/s)/m^2.

3.4 Implementation of the developed flexibility management method

Flexibility management methods are dependent on the ventilation system type and available data. The ventilation system type defines algorithms that can be implemented on the given system, and available data establishes the accuracy of the estimations. The flexible control concept of a ventilation system is discussed in section 1.1 (Figure 1.2), where all the needed flexibility service hardware and interconnections are described. This section presents guidance for implementing the developed methods with recommendations to improve data quality and optimize ventilation system operation during regulations.

3.4.1 Adjustment method for duration estimations

The FVR durations calculated using the methods described under section 3.2 do not consider variable building usage. Inconsistent building usage is considered by adjusting FVR duration according to the following timesteps. If the following timestep FVR duration estimation is shorter, caused by increased room usage, the estimation must be shortened, as described in (3.22). This adjustment is repeated, and after each iteration, the sum of all FVR duration estimations is calculated and compared with the previous iteration sum, as shown in (3.23). If they are equal, then the adjustment is completed. Adjustment is only done in one direction (e.g., shortened) to avoid overestimating FVR duration and therefore, jeopardizing IAQ in the building.

$$\tau_{t,i}^{FVR} = \begin{cases} \tau_{t+1,i-1}^{FVR} + \Delta t, & \tau_{t+1,i-1}^{FVR} < \tau_{t,i-1}^{FVR} - \Delta t \\ \tau_{t,i-1}^{FVR}, & \tau_{t+1,i-1}^{FVR} \geq \tau_{t,i-1}^{FVR} - \Delta t \end{cases} \quad (3.22)$$

where $\tau_{t,i}^{FVR}$ – an estimate of FVR duration at time *t* during correction iteration *i*,
$\tau_{t,i-1}^{FVR}$ – an estimate of FVR duration at time *t* during previous correction iteration *i* - 1,
Δt – timestep length (s).

$$\sum_{t=1}^{n} \tau_{t,i}^{FVR} = \sum_{t=1}^{n} \tau_{t,i-1}^{FVR} \quad (3.23)$$

3.4.2 Calculation method for the regulation price

Knowing the energy price for regulations is a crucial component for enabling the integration of a ventilation system in a flexibility service. It is the needed input for the aggregator, according to which the amount of regulated energy will be compensated to a building owner. A personalized pricing mechanism is used to achieve this, as shown in (3.24). The direction of regulation dictates the ingredients of the final regulation price. It is necessary to compensate for lower IAQ in the zone if up-regulation is activated and the ventilation system's power consumption is reduced. It can be done by considering variable building usage described through the CO_2 generation rate. Regulation-induced amortization of the system must also be addressed to compensate for additional wear (e.g., switching counts for contactors and movement of valves). If down-regulation is activated and the ventilation system's power consumption is increased, then this causes additional energy consumption, which must be compensated.

$$price_t = \begin{cases} \frac{G_t^{co2}}{G_{max}^{co2}} \cdot c_{comf} + \frac{c_{amort}}{\Delta P \cdot \tau_t} + c_{mgn}, & \Delta P < 0 \\ \frac{C_t - C_{t,min}}{C_{limit} - C_{t,min}} \cdot c_{t,el} - c_{t,fees} - \frac{c_{amort}}{\Delta P \cdot \tau_t} - c_{mgn}, & \Delta P > 0 \end{cases} \quad (3.24)$$

where $price_t$ – the calculated regulation price at time *t* (€/kWh),
G_t^{co2} – CO_2 generation rate at time *t* (m^3/s),
G_{max}^{co2} – maximum estimated CO_2 generation rate (m^3/s),
c_{comf} – the regulation cost on comfort (€/kWh),
τ_t – duration of regulation at time *t* (h),
c_{amort} – the regulation cost on amortization (€),
c_{mgn} – margin for regulations (€/kWh),
ΔP – change of power consumption during regulation (kW),
C_t – CO_2 concentration in the return air at time *t* (ppm),
$C_{t,min}$ – minimum CO_2 concentration for maximum airflow rate at time *t* (ppm),
C_{limit} – CO_2 concentration limit value (ppm),
$c_{t,el}$- electricity price including electricity market price and electricity supplier profit margin at time *t* (€/kWh),
$c_{t,fees}$– the sum of all the fees, which include transmission costs and taxes added to consumed energy price at time *t* (€/kWh).

The tendered price for up-regulation depends on the CO_2 generation rate, and the maximum price is achieved at maximum building usage (Figure 3.7 a). Cost on comfort can be selected according to historical balancing energy prices on the market, and in this thesis, the price data for the last two weeks is used. The same approach determines the maximum CO_2 generation rate where the previous two weeks' maximum value is used. Usually, regulations introduce an insignificant amount of additional wear to the system; therefore, amortization costs are neglected in the validation process of developed methods. The margin for regulation is a parameter that is dictated by the building owners, which increases the profitability of the flexibility service. In future studies, this margin can be optimized to maximize regulation activations and income since increasing the regulation price lowers the number of events where the market price is reached. In validating the developed method, the margin is not used, and the difference between the tendered and the market price is split between the building owner and the aggregator. The tendered down-regulation price depends on the CO_2 concentration in the return air (Figure 3.7 b). If the ventilation system's return air CO_2 concentration is higher than the minimum possible CO_2 concentration, the goal is to decrease the CO_2 concentration level by purchasing electricity at a lower price. When the CO_2 concentration is low due to the low occupancy, down-regulation is provided if the additional costs from grid fees and taxes are compensated.

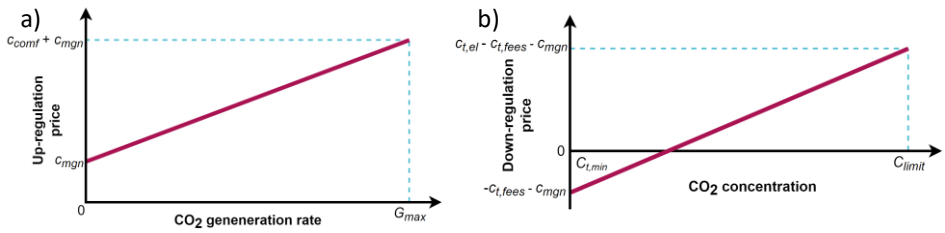

Figure 3.7. Dependence of the regulation price on a) CO_2 generation rate for up-regulation and b) CO_2 concentration for down-regulation.

The estimation of the forced ventilation rate duration dictates the maximum duration for each regulation. The regulation price is calculated for each period separately. Therefore, the duration of each regulation can be derived as follows:

$$\tau_t = \begin{cases} \tau_t^{FVR}, & \tau_t^{FVR} \leq \Delta t \\ \Delta t, & \tau_t^{FVR} > \Delta t \end{cases} \tag{3.25}$$

where τ_t^{FVR} – duration of the forced ventilation rate at time *t* (h),
Δt – duration between two sequent calculation steps (h).

For down-regulations, the minimum possible CO_2 concentration and CO_2 concentration at a specific time must be estimated ahead. It can be derived from the mass balance analysis, as shown in (3.26) and (3.27). Minimum CO_2 concentration depends on the maximum airflow and CO_2 generation rates at selected times. The FVR duration forecasts estimate CO_2 concentration ahead, as discussed in section 3.2.

$$C_{t,min} = \begin{cases} \frac{G_t^{co2}}{Q_{max}} + C_{amb}, & \frac{G_t^{co2}}{Q_{max}} \geq 0 \\ C_{amb}, & \frac{G_t^{co2}}{Q_{max}} < 0 \end{cases} \quad (3.26)$$

where G_t^{co2} – CO_2 generation rate at time t (m^3/s),
Q_{max} – maximum ventilation rate (m^3/s),
C_{amb} – ambient CO_2 concentration (ppm).

$$C_t = \frac{2V \cdot C_{limit} + 2\tau_t^{fvr,co2} \cdot G_t^{co2} - \tau_t^{fvr} \cdot Q_{fvr} \cdot (C_{limit} - 2C_{amb})}{2V - \tau_t^{fvr} \cdot Q_{fvr}} \quad (3.27)$$

where V – zone volume (m^3),
C_{limit} – CO_2 concentration limit value (ppm),
$\tau_t^{fvr,co2}$ – CO_2 concentration based forced ventilation rate duration at time t (s),
G_t^{co2} – CO_2 generation rate at time t (m^3/s),
Q_{fvr} – forced ventilation rate (m^3/s).

3.4.3 Addressing the rebound effect

Regulations can affect the energy consumption of the ventilation system even after activations. After activation of the reserve, the temporary power consumption increase is known as a rebound effect [131]. Power consumption of a CAV type ventilation system will be affected only during regulations, and no rebound effect exists. The reason is that the CAV type system only operates at a set ventilation rate and is not influenced by indoor air conditions. The system's cumulative energy consumption is also reduced if the power consumption is decreased during regulations. The VAV type ventilation system will be affected by regulations. The system controller and system layout influence the magnitude and duration of the rebound effect. If the power consumption of a VAV type ventilation system is decreased and CO_2 concentration-based control is implemented, then after the regulation, there is a temporary increase in power consumption (Figure 3.8). Effects of the regulation on cumulative energy consumption are investigated in simulations.

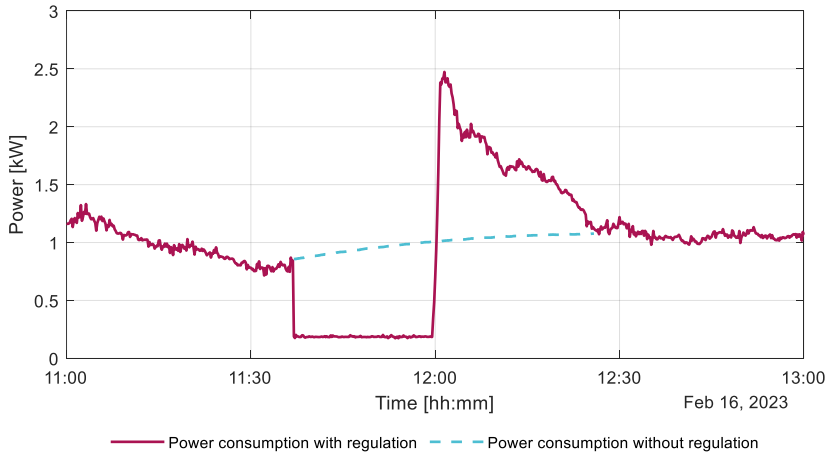

Figure 3.8. Rebound effect of a VAV type ventilation system.

After the deactivation of the reserve, the IAQ in the building is disturbed. It creates a need to know the subsequently allowed regulation since consecutive activations can too highly impact the IAQ. In this thesis, the rebound duration is the length of time that it takes for the ventilation system to change a sufficient amount of indoor air with fresh ambient air to reach normal IAQ conditions. The rebound duration can be estimated with the following two equations:

$$C_t^{st} = \frac{G_t^{co2}}{Q_t} + C_{amb} \tag{3.28}$$

$$\tau_t^{rb,CO2} = \frac{V \cdot (C_t^{st} - C_t)}{G_t^{co2} - Q_t \cdot \frac{C_t + C_t^{st} - 2C_{amb}}{2}} \tag{3.29}$$

where C_t^{st} – stable condition CO_2 concentration at timestep *t* (ppm),
$\tau_t^{rb,CO2}$ – CO_2 concentration-based rebound duration at timestep *t* (s).

$$\tau_t^{rb,CO2} = \frac{2V}{Q_t} \tag{3.30}$$

3.4.4 Selection of flexibility management algorithm

Different ventilation system configurations cause the flexibility management algorithm to be combined from the appropriate components described in this thesis. The procedure described in Figure 3.8 can be followed to ease the algorithm selection. First of all, a power consumption forecasting method must be selected. ARMA(p, q) model is suitable for this with the AIC method to tune it. For FVR duration estimations, available IAQ sensors and their locations must be made clear. If there is a CO_2 sensor that gives an adequate overview of CO_2 concentration in a zone, then FVR duration can be calculated accordingly. If sensors are absent, an open-loop approach can be implemented, or another option is to install a CO_2 concentration sensor. These can also be applied to FVR duration estimations if temperature and humidity sensors are available. If one zone includes multiple rooms, then it is necessary to have measurements or estimations from each room separately. A different approach is needed if there are no IAQ sensors in each room. The IAQ parameter limit value must be corrected to avoid exceeding the limit when only one sensor is installed in the return air duct. FVR durations must be adjusted to consider the variable usage of the building. The regulation price must be calculated to enable transactions with an aggregator. After each reserve activation, rebound duration must be calculated to avoid concurrent activations jeopardizing IAQ.

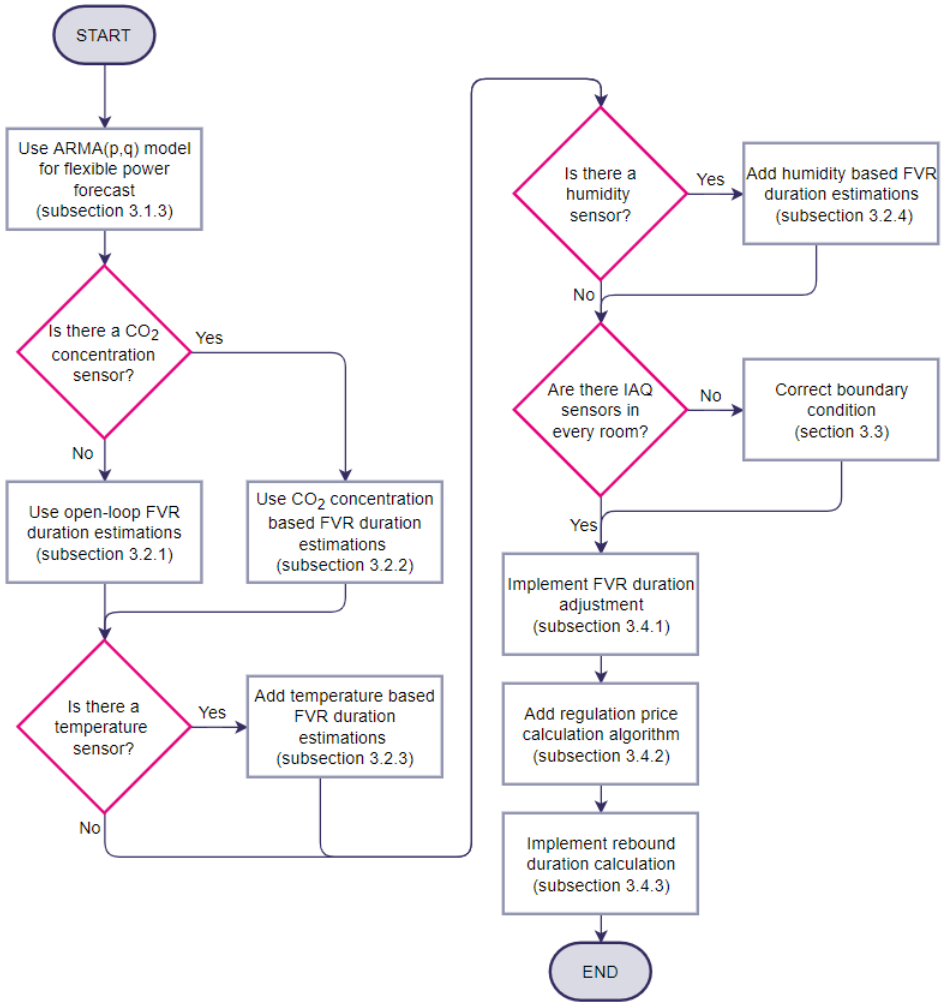

Figure 3.9. Algorithm selection procedure for flexibility management.

3.4.5 Applying flexibility management methods

Flexibility management methods can be applied using a flexibility management system that embeds all needed algorithms (Figure 3.10). The flexibility management system consists of modules, each having its purpose. The regulation activation module aims to listen for activation reserve activation signals, check if the ventilation system is available for regulation, and send commands to the ventilation system to force a defined ventilation rate. The flexible power forecasting module is responsible for acquiring power consumption measurement data and forecasting available power for up- and down-regulations. The pollutant generation calculation module aims to estimate building usage needed for FVR duration calculation. The FVR duration calculation algorithm acquires building usage data and calculates FVR durations based on the data gathered from sensors and building design documentation. The regulation price calculation module is responsible for putting together tendered prices for regulations based on the costs and building IAQ conditions. After calculating everything, the tender is sent to an aggregator of available flexible power, FVR duration, and price for each timestep.

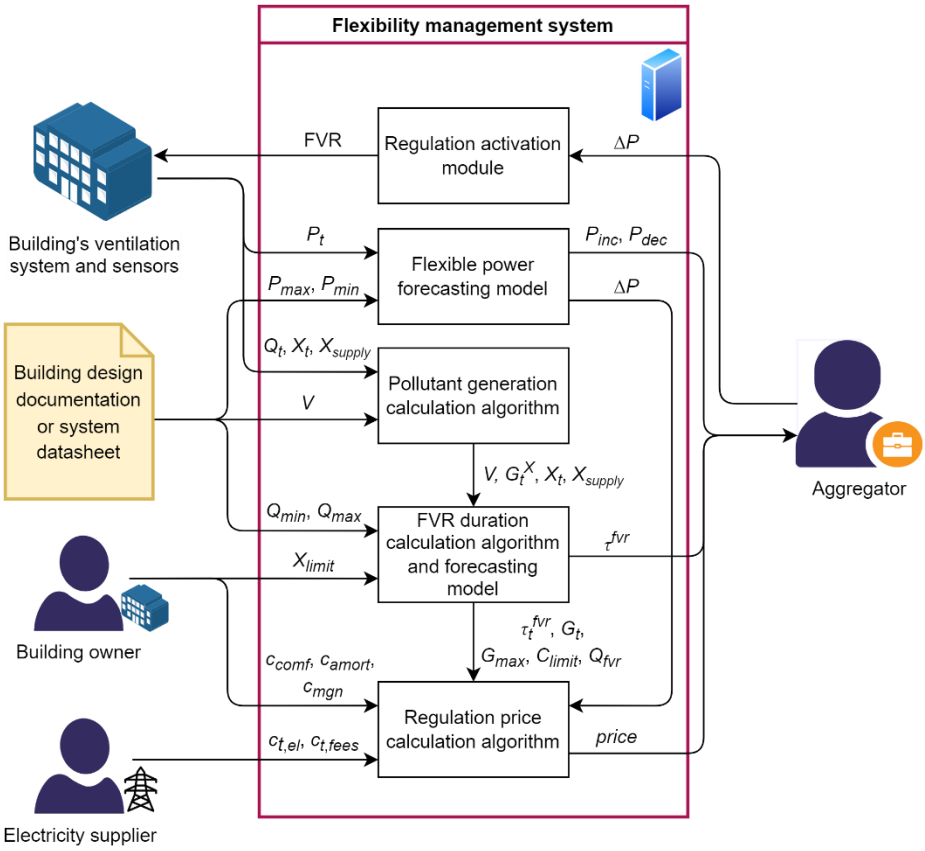

Figure 3.10. Implementation of the flexibility management methods [Paper I].

3.5 Ventilation system as a virtual energy storage

Ventilation systems can be considered a virtual energy storage (VES), which can behave similar to a battery energy storage (BES). Its characteristics and calculation methods must be understood to use a ventilation system as a VES. In this section, the following aspects are discussed:

- Power capacity,
- Energy capacity,
- State of Charge (SoC),
- Self-discharge rate.

3.5.1 Power capacity of virtual energy storage

The power capacity of a ventilation system is defined through its maximum and minimum power consumption, as discussed in section 3.1. The available power capacity depends on the power consumption of a ventilation system at a selected instance (Figure 3.11). The available power capacity for flexible power can be calculated and forecasted using the methods described in section 3.1.

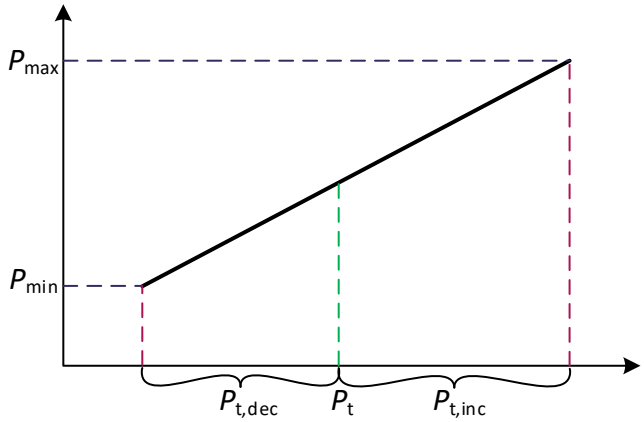

Figure 3.11. Available flexible power of a ventilation system at time t.

3.5.2 Energy capacity of virtual energy storage

A ventilation system differs from a BES by its energy capacity. A ventilation system can exceed its boundary conditions without causing irreversible damage to the system. During charging, the ventilation system consumes more power to increase the percentage of fresh air in the building, lowering the CO_2 concentration. From the IAQ viewpoint, the ventilation system can consume an infinite amount of energy during the charging cycle, but CO_2 concentration cannot decrease beyond the minimum concentration level, as shown in (3.26). The energy to reach the minimum CO_2 concentration level can be calculated with (3.31). During discharging, the power consumption of a ventilation system is reduced, and the air exchange rate is lowered, which causes CO_2 concentration to rise. During the discharging cycle, the ventilation system can operate at a lower power consumption level for a limited time, which is dictated by IAQ conditions in a building. Therefore, the energy capacity for up-regulation is limited, as shown in (3.32). IAQ parameter value at a specific timestep can be calculated according to the forced ventilation rate duration forecast, as shown in (3.27).

$$E_{t,\,inc} = P_{t,inc} \cdot \frac{V \cdot (C_{limit} - C_t)}{G_t^{co2} - Q_{max} \cdot \sqrt[3]{\frac{P_t + P_{t,inc} - P_{bias}}{P_{max} - P_{bias}}} \cdot \frac{C_t + C_{t,min} - 2C_{amb}}{2}} \tag{3.31}$$

$$E_{t,\,dec} = P_{t,dec} \cdot \frac{V \cdot (C_{limit} - C_t)}{G_t^{co2} - Q_{max} \cdot \sqrt[3]{\frac{P_t - P_{t,dec} - P_{bias}}{P_{max} - P_{bias}}} \cdot \frac{C_t + C_{limit} - 2C_{amb}}{2}} \tag{3.32}$$

where V – zone volume (m^3),
C_{limit} – CO_2 concentration limit value (ppm),
C_t – CO_2 concentration value at time *t* (ppm),
C_{supply} – CO_2 concentration value in supply air (ppm),
G_t^{co2} – CO_2 generation rate at time *t* (m^3/s),
Q_{max} – maximum ventilation rate (m^3/s),
P_{bias} – ventilation system power consumption bias (W).

Energy capacity during discharging is non-linearly dependent on the CO_2 concentration (Figure 3.12). Maximum energy capacity is achieved when the CO_2 concentration in the building is at the ambient level. When charging before discharging the VES is planned, it is reasonable not to attempt to lower the CO2 concentration close to the ambient level. The region close to the ambient level does not increase the capacity significantly but increases the self-discharge, as discussed in the following subsections.

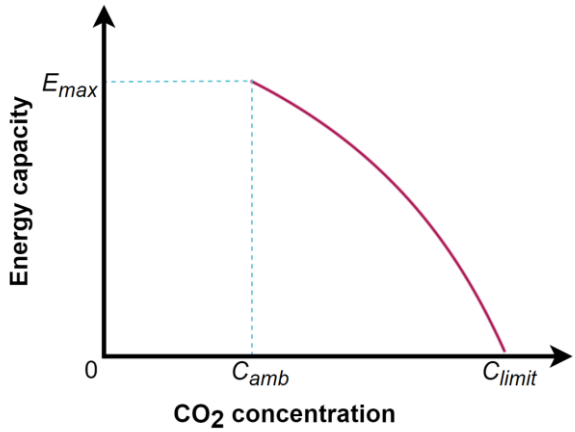

Figure 3.12. Energy capacity dependence on CO_2 concentration in a building.

During regulation, the flexible power can be in the range of current power consumption up or down to the limit. The more the power consumption changes, the more IAQ in a building is affected. Since the energy capacity has a nonlinear dependence on power consumption, there is a possibility to optimize the amount of power to maximize the total energy capacity for one regulation. A regulation duration can be a fixed length, which means that changing the power consumption less than possible will cause the effect where the CO_2 concentration limit is not reached before the regulation is ended. The consequence of this is the unused potential of the ventilation system. Decreasing power consumption to more than the optimal amount causes the situation where the CO_2 concentration limit is reached before the regulation is ended, which also causes lower energy capacity of the VES (Figure 3.13).

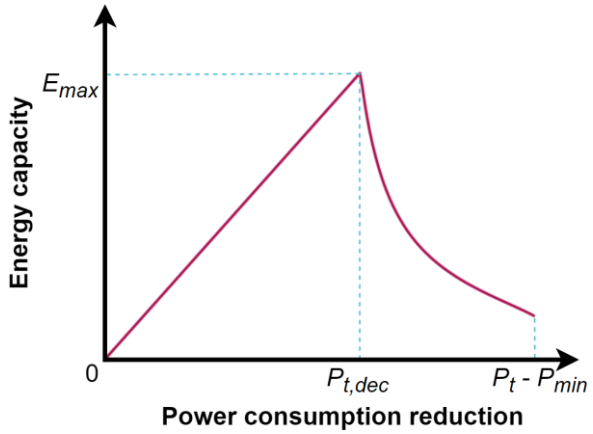

Figure 3.13. Energy capacity dependence on the reduction of power consumption.

If the length of regulation duration is known or estimated ahead, then the power consumption increase or decrease can be calculated as shown in (3.33) and (3.34), respectively. Before the power level can be computed, the CO_2 generation rate must be known. The method to estimate this is given in section 3.2. Power consumption at a specific time is also an important parameter that can be estimated using the method described in section 3.1.

$$P_{t,\,inc} = \left[\frac{\tau_t \cdot G_t^{co2} - V \cdot (C_{limit} - C_t)}{\tau_t \cdot Q_{max} \cdot \frac{C_t + C_{limit} - 2C_{supply}}{2}}\right]^3 \cdot (P_{max} - P_{bias}) - P_t + P_{bias} \qquad (3.33)$$

$$P_{t,\,dec} = \left[\frac{\tau_t \cdot G_t^{co2} - V \cdot (C_{limit} - C_t)}{\tau_t \cdot Q_{max} \cdot \frac{C_t + C_{limit} - 2C_{supply}}{2}}\right]^3 \cdot (P_{bias} - P_{max}) + P_t - P_{bias} \qquad (3.34)$$

where τ_t – regulation duration (s).

3.5.3 Virtual energy storage state of charge

A VES SoC can be described through CO_2 concentration in a building because this parameter is directly connected to building usage and is affected by the people inside. The VES's SoC can fluctuate throughout the day depending on the system type and building usage. When SoC is at 100%, the CO_2 concentration is at a minimum level, which can be calculated through the maximum ventilation rate and the CO_2 generation at the selected timestep, as shown in (3.26). Since the building usage changes throughout the day, the minimum CO_2 concentration also changes accordingly (Figure 3.14). The actual SoC is the CO_2 concentration in a building at each timestep, which can be calculated as shown in (3.27). When SoC is at 0%, the CO_2 concentration has reached its limit. The maximum CO_2 concentration limit does not change, except for a multi-zone ventilation system where the correction of the boundary condition is needed, which is discussed under section 3.3.

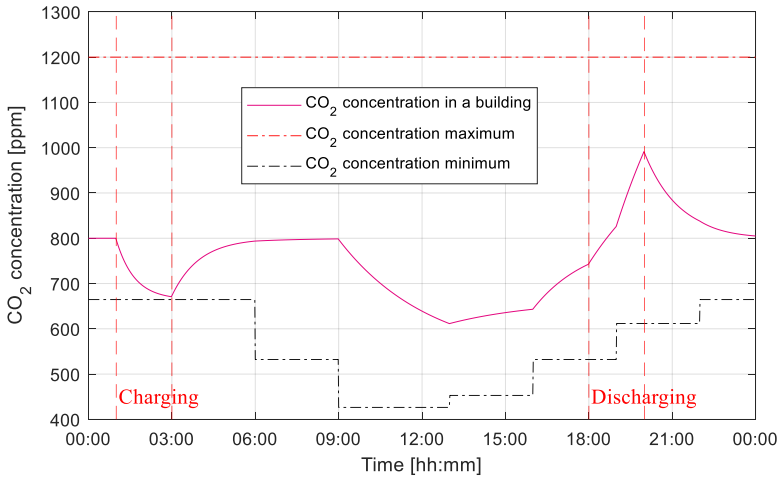

Figure 3.14. CO_2 concentration-based SoC estimation for a ventilation system.

3.5.4 Self-discharge rate of virtual energy storage

CO_2 concentration has always some stable level, which depends on the CO_2 generation and ventilation rates. If the VAV type system is used, the stable condition is around the setpoint C_{set}. This steady-state level causes the effect of self-discharge or self-charge of the VES. Self-discharge occurs when the CO_2 concentration level is lower than the stable level, and self-charge happens when the CO_2 concentration level is higher than the stable level. The self-discharge or self-charge rate can be calculated as follows:

$$k_t^{self} = \left[(P_{t-1} - P_{min}) \cdot \frac{V \cdot (C_{limit} - C_{t-1})}{G_{t-1}^{co2} - Q_{min} \cdot \frac{C_{t-1} + C_{limit} - 2C_{amb}}{2}} - (P_t - P_{min}) \cdot \frac{V \cdot (C_{limit} - C_t)}{G_t^{co2} - Q_{min} \cdot \frac{C_t + C_{limit} - 2C_{amb}}{2}} \right] \cdot \frac{1}{\Delta t} \quad (3.35)$$

where k_t^{self} – the self-discharge or self-charge rate at time t (Ws/s),
P_{min} – ventilation system minimum power consumption (W),
P_{t-1} – ventilation system power consumption at time $t-1$ (W),
C_{t-1} – CO_2 concentration at time $t-1$ (ppm),
Q_{min} – minimum ventilation rate (m^3/s),
Δt – duration between two sequent timesteps (s),
G_{t-1}^{co2} – CO_2 generation rate at time t (m^3/s).

When constant ventilation rate and building usage are considered, the maximum self-discharge rate is near ambient concentration (Figure 3.15). The self-discharge rate is zero when the stable CO_2 concentration level is reached, which can be the CO_2 concentration setpoint for the VAV type of system. The minimum self-discharge rate is present near the limit or maximum CO_2 concentration where the self-discharge is negative, meaning that the VES is charging and CO_2 concentration decreases. The self-discharge rate in the same CO_2 concentration range is lower than the self-charge rate. Therefore, the VES is prone to self-charge better than self-discharge.

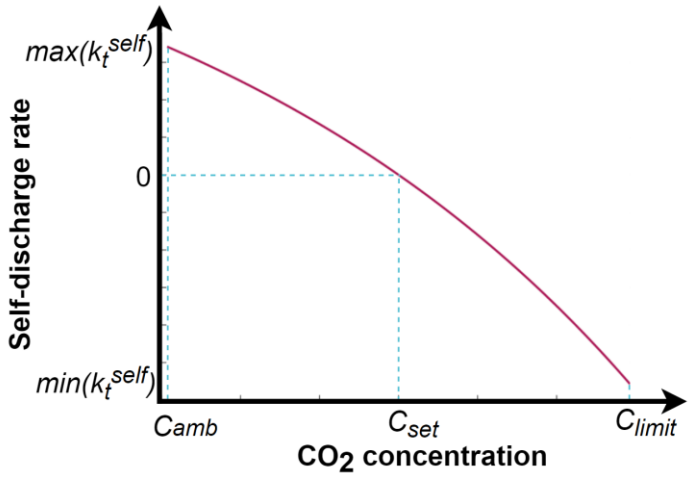

Figure 3.15. Dependence of the self-discharge rate on the CO_2 concentration.

3.6 Conclusions

This chapter described the development of the methods of ventilation system flexibility management. The methods were developed by the definitions of flexibility and the needed input data for an aggregator discussed in Chapter 2. Based on the provided data and estimation, the aggregator can manage each ventilation system or building separately to achieve optimum results.

The ventilation system management methods include flexible power, FVR duration estimation algorithms, and a pricing model. Since there are different types of ventilation systems with specific features, there is no single approach for every system. The following methods are used for the flexibility estimation of a ventilation system:

- Estimations of ventilation system flexible power are based on the measured data, and forecasts for specified horizons are done using the ARMA model.
- CO_2 concentration based FVR duration estimations are based on building usage data. If the CO_2 sensor is present, then through mass balance analysis, CO_2 generation is calculated.
- Temperature-based FVR duration estimations are based on temperature sensor readings, and by using the first law of thermodynamics, a heat generation rate is calculated.
- Humidity-based FVR duration estimations use a similar approach to the CO_2 concentration-based estimation, and estimations rely entirely on sensor data.
- FVR duration adjustment is done by shortening estimations based on the following time steps forecasted durations. It enables the capability to consider the variable usage of a building.
- The price for each regulation is calculated through a personalized pricing mechanism, which the building owner can adjust. The pricing model takes into account the building usage and IAQ conditions.
- A boundary condition correction algorithm is used when there are not enough sensors installed in crucial rooms where regulations affect IAQ the most. The range where the measured parameter can be is narrowed to lessen the regulation effect on the IAQ in high-usage rooms.
- After each reserve activation, the rebound is calculated to stabilize IAQ in a building.

A selection algorithm is described, and guidelines are given to implement the developed flexibility management methods. The flexibility management system to use all the described methods is also brought out to make the implementations as state-forward as possible. Finally, characteristics through which a ventilation system can be described as virtual energy storage are discussed, giving aggregators tools to use ventilation systems as battery energy storage. The assessment and verification of the developed methods will be provided in Chapter 4 and tested in case studies in Chapter 5. The development of the ventilation system flexibility management method showed that the first hypothesis is correct, as mass and energy balance analysis combined with sensor data enables the estimation of forced ventilation rate duration.

4 Validation of the developed flexibility management method

In this chapter, the developed flexibility methods are validated through MATLAB and IDA ICE simulations. First, technical and economic constraints are given as inputs to object models. Technical limitations parameterize inputs for building models in IDA ICE. Economic constraints define the parameters essential for the validation. Object models are described, which are composed in the IDA ICE building simulation tool. Simulations and calculations regarding the flexibility forecast and control are carried out in MATLAB, a programming and numeric computing platform. This chapter also describes control scenarios of a ventilation system to assess the performance of the developed flexibility management method. It includes the results of all the simulations and the evaluation of the effectiveness of the method.

The simulation process can be divided into steps, each conducted in one of the simulation tools (Figure 4.1). Each step can be described as follows:

I. The building model is configured, and the occupancy schedule is generated in MATLAB. All the data between MATLAB and IDA ICE is transferred using PRN files.
II. IDA ICE uses the building model and all the necessary information to run a year-long simulation. Each room and the AHU's measured data are logged into output files.
III. Flexibility management methods are used after importing the IDA ICE output files into MATLAB. It includes measuring and forecasting the energy flexibility of the ventilation system. The day-ahead price, mFRR activations, and the balancing energy price for 2022 are used to schedule activations.
IV. With activations of the reserve, a simulation lasting a year is repeated.
V. Data is collected from IDA ICE, and estimates of previously calculated flexibility are compared with the data acquired in step IV. The dataset is examined in MATLAB, and the conclusions are drawn.

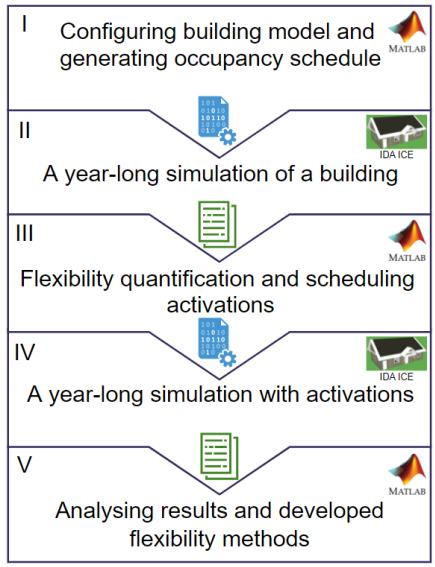

Figure 4.1. MATLAB and IDA ICE co-simulation process [Paper I].

4.1 Technical and economic constraints

This section discusses all the technical and economic constraints that are important to consider when assessing the developed flexibility method. Also, these constraints are essential to set up the object models in IDA ICE.

4.1.1 Determination of ventilation system parameters

For method validation, two main parameters for simulations are needed. These are ventilation rate and power consumption. The ventilation rate can be calculated according to the standard EN 16798-1:2019, which states that design parameters for IAQ shall be derived using one or more of the following methods:

1. Based on perceived air quality
2. By using limit values for substance concentration
3. Based on predefined ventilation air flow rates

The first method calculates the ventilation rate based on perceived air quality. The total ventilation rate is found by combining the ventilation rate for people and a building, as shown in (4.1). These specific ventilation rates are selected according to the building pollution level and IAQ category. For normal conditions, low-polluting buildings and IAQ category II are selected (Table 4.1). The first method is used to prepare models for the validation of the flexibility management method.

$$Q_{tot} = K_{design} \cdot Q_p + A_R \cdot Q_B \tag{4.1}$$

where Q_{tot} – total ventilation rate for the zone (l/s),
K_{design} – design value for the number of persons in a zone,
Q_p – ventilation rate for the number of persons in the zone (l/s),
A_R – zone floor area (m^2),
Q_B – ventilation rate for emissions from the zone (l/[s·m^2]).

Table 4.1. IAQ categories and values for calculating the ventilation rate [127].

Category		I	II	III	IV
Level of expectation		High	Medium	Moderate	Low
Low-polluting building, l/(s·m²)		1.0	0.7	0.4	0.3
Airflow per non-adapted person, l/(s·pers)		10	7	4	2.5
CO_2 concentration above outdoors for non-adapted persons, ppm		550	800	1350	1350
Total design ventilation rate for the zone or room	**l/(s·pers)**	20	14	8	5.5
	l/(s·m²)	2	1.4	0.8	0.55

The second method is using criteria for individual substances. The ventilation rate required to dilute a specific substance can be calculated as shown in (4.2). Typically, CO_2 is used for calculations, the limit values of which can be found in Table 4.1. Default values for ε_v can be found in the standard EN 16798-3. For complete mixing, the ventilation effectiveness equals 1.

$$Q_h = \frac{G_h}{C_{h,i} - C_{h,o}} \cdot \frac{1}{\varepsilon_v} \tag{4.2}$$

where Q_h – the ventilation rate required for dilution (m³/s),
G_h – the generation rate of the substance (µg/s),
$C_{h,i}$ – the guideline value of the substance (µg/m³),
$C_{h,o}$ – the concentration of the substance in the supply air (µg/m³),
ε_v – effectiveness of ventilation.

The third method uses a predefined total designed ventilation rate for the zone or room given in Table 4.1. If the ventilation rate is calculated using per-person and per-floor area approaches, then the highest ventilation rate should be used.

The CO_2 concentration in the return air is used to manage VAV system. Proportional control described in the Trane Engineers newsletter [132] is applied in simulations to control the VAV-type ventilation system. The following procedure is applied to calculate parameters for proportional control:

1. The required ventilation rate for the design zone population is calculated, as shown in (4.1).
2. The minimum ventilation rate is found using (4.1), where the number of persons in a zone is 0, and the rate is calculated only based on the zone floor area.
3. The target CO_2 concentration is found according to the design parameters, as shown in (4.3). This method uses minimum occupancy for the zone to calculate the CO_2 concentration setpoint. Minimum occupancy must be a reasonable non-zero value, which can be acquired from the occupancy schedule discussed in section 4.2. The minimum occupancy value calculates the minimum ventilation rate for the VAV system using equation (4.1). The acquired minimum ventilation rate is used to calculate the design CO_2 concentration for a zone, which can be expressed as follows:

$$C_{design} = C_{amb} + \frac{G_{pers}^{co2} \cdot K_{design}}{Q_{tot}} \tag{4.3}$$

where C_{amb} – ambient CO_2 concentration (ppm),
G_{pers}^{co2} – one person's CO_2 generation rate (m³/(s·pers)),
K_{design} – design value for the number of persons in a zone,
Q_{tot} – total ventilation rate for the zone (l/s).

4. The ventilation rate for the timestep *t* is calculated proportionally based on the CO_2 concentration, and the calculated ventilation rates, which can be expressed as follows:

$$Q_t = \frac{C_t - C_{amb}}{C_{design} - C_{amb}} \cdot \left(Q_{tot} - Q_{tot,min}\right) + Q_{tot,min} \tag{4.4}$$

where C_t – CO_2 concentration at timestep *t* (ppm),
$Q_{tot,min}$ – total minimum ventilation rate for the zone with zero occupancy (l/s).

The standard EN 16798-1:2019:2019 gives guidelines for controlling the ventilation system during unoccupied periods. If the ventilation system is shut off, the minimum air must be delivered to a zone before occupation. This minimum amount is 1 volume of the

zone that must be ventilated within 2 hours. If the ventilation rate is lowered during the unoccupied period, the total airflow for diluting emissions from the building must be at least 0.15 l/(s·m^2) in all rooms. The ventilation rate of 0.15 l/(s·m^2) is also used during regulations when the power consumption of the ventilation system is lowered.

The power consumption of a ventilation system can be calculated through SFP. On average, SFP ranges from 2.0 to 2.7 kW/(m^3/s) [20]. According to Estonian legislation [7], the SFP can be at a maximum of 2.0 kW/(m^3/s) for renovated and new dwellings. In nZEB, the SFP is 1.5 kW/(m^3/s) and even lower [133].

4.1.2 Determination of building usage and internal gains

Building usage and internal gains depend on the building type. Building usage is defined by the number of occupants, which can be calculated using values given by the standard EN 16798-1:2019 (Table 4.2). Building internal gains are heat sources that emit additional heat into a room. These internal gains are caused by occupants who dissipate body heat, lighting, and appliances. All the power consumed by the lighting and appliances is assumed to be converted into heat.

IAQ parameter setpoint can differ for every building or room. Minimum and maximum temperature setpoint values for heating and cooling are used in simulations. These values are given in the standard EN 16798-1:2019. The CO_2 setpoint is selected according to the maximum allowable CO_2 concentration setpoint value. IAQ parameters' limit values are discussed in section 3.2.

Table 4.2. Building parameters for simulations [127].

Building type	Office	Dwelling
Occupants, pers/m^2	0.0588	0.0353
Activity level, MET	1.2	1.2
Lights, W/m^2	10	8
Appliances, W/m^2	12	3
Minimum heating setpoint, °C	21	21
Maximum cooling setpoint, °C	25	27

4.1.3 Determination of economic constraints for the flexibility service

Four main parameters dictate activations in the flexibility service:

- **Available flexible power** – ventilation system is used in regulations only when it provides enough power to be altered. Suppose that there is a need to lower the power consumption and the ventilation system is already operating close to its minimum rate. In that case, this ventilation system will be ignored in regulations. A regulation is rejected in simulations if the available flexible power is less than half the maximum power consumption.
- **Regulation duration** – a ventilation system can operate at FVR for a given time until the IAQ parameter boundary condition is reached. If the allowed duration is already short, selecting a given ventilation system for regulations is not reasonable. It will be ignored until a longer duration is allowed. According to Baltic TSOs [81] the minimum duration of the delivery period is 5 min, which is used in simulations.
- **Regulation price** – each ventilation system operator or owner dictates its regulation price, which can be calculated as discussed in section 3.4.2. If the requested price for regulation is higher than the aggregator is willing to pay, then the given

ventilation system is ignored in regulations. The year 2022 balancing energy price is used to calculate the revenue generated for activations. The tendered price is paid to the ventilation system owner, and the difference between the balancing energy price and the tendered price is split between the system owner and the aggregator. Nord Pool Spot day-ahead prices for Estonia are used to calculate the cost of consumed energy during normal conditions, for which a 20% value-added tax (VAT) is added. Additional charges, such as a fixed tariff grid fee of 86.5 €/MWh, a renewable energy fee of 13.56 €/MWh, and an electricity excise duty of 1.2 €/MWh were added to the day-ahead prices. The energy that was not used was multiplied by the entire cost of power during up-regulation and deducted from the total energy cost used during the simulated period.

- **Activation** – marks the event when the reserve is activated (i.e., ventilation system power consumption is altered). The year 2022 mFRR standard product activations are used in simulations where the available flexible power, regulation duration, and price are checked.

4.2 Description of object models

Two object models are used in simulations to verify the performance of the developed method. The first object is a room in a building, which can be an apartment or an office. The second object is a single-family house. In this section, these two objects are described with building usage profiles used in simulations. Also, the air handling unit (AHU) for these two objects is described. These models are constructed in IDA Indoor Climate and Energy (IDA ICE), a specialized application to imitate building behavior. IDA ICE has been validated according to EN 15255:2007, EN 15265:2007, EN 13791, and ASHRAE 140-2004. EQUA AB website [134] provides reports about the test results of these validations.

4.2.1 Object 1: Small room in a building

The first object is a room that is part of a single-story building (Figure 4.2). This room has an independent ventilation system that was used in simulations. The room's floor area is 13.84 m^2, and the height is 2.7 m. The building with the room is located in Tallinn, Estonia, so weather data for Estonia is used. This room has three internal walls with a thickness of 0.1 m and one external with a thickness of 0.405 m. The floor is lifted 1 m above the ground, with a thickness of 0.293 m. The thickness of the ceiling, which is also a roof, is 0.713 m. The building has light-frame construction with thermal insulation in between wall panels. During winter, the temperature in the room is held with a wall-mounted radiator.

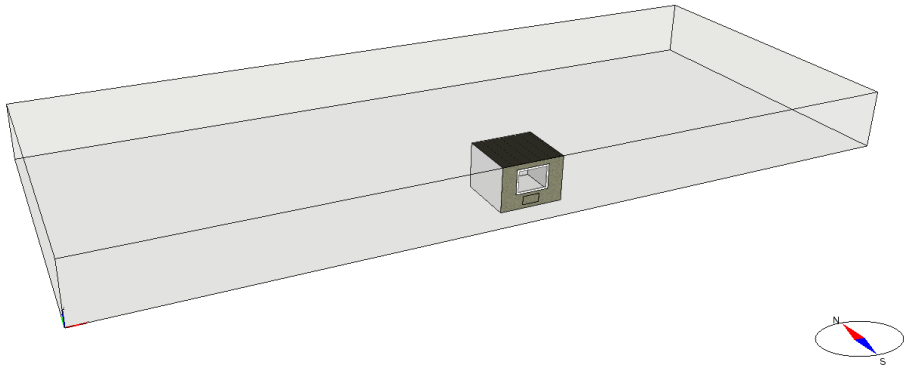

Figure 4.2. The room of a building used in simulations [Paper II].

This room can be an office or an apartment. The room type is changed through changes in occupancy, ventilation system operation schedule, and building-specific parameters discussed in the previous section. The occupancy schedule depends on the weekday and time. According to the standard EN 16798-1:2019, offices are not used during weekends and nighttime, which means that building usage at that time equals 0 (Table 4.3). Apartments have the highest usage during the night and the lowest during the daytime. All the presented data will be used in simulations, and schedules will be selected according to the building type.

Table 4.3. Occupancy schedule according to a room type.

Start time	End time	Office	Apartment
00:00	06:00	0	1
06:00	07:00	0	0.5
07:00	08:00	0.2	0.5
08:00	09:00	0.6	0.5
09:00	10:00	0.6	0.1
10:00	11:00	0.7	0.1
12:00	13:00	0.4	0.1
13:00	14:00	0.6	0.2
14:00	15:00	0.7	0.2
16:00	17:00	0.6	0.5
17:00	18:00	0.2	0.5
18:00	19:00	0	0.5
19:00	22:00	0	0.8
22:00	00:00	0	1

The room AHU power consumption is dependent on the room type. Office's AHU maximum power consumption is around 18% more than for an apartment due to higher occupancy (Table 4.4). Both room types have the same minimum ventilation rate since during up-regulation, a ventilation rate of 0.15 l/(s·m^2) is held.

Table 4.4. Parameters of the room ventilation system for simulations.

Parameter	Office	Apartment
AHU maximum power consumption	25.4 W	21.6 W
AHU minimum power consumption	0.9 W	0.9 W
Maximum ventilation rate	15.3 l/s	13.0 l/s
Minimum ventilation rate	2.0 l/s	2.0 l/s

4.2.2 Object 2: Single-family house

The second object is a single-family, single-story house (Figure 4.3). The house is divided into eleven rooms: utility room, bathroom, technical room, kitchen, main bedroom, living room, hall, vestibule, toilet, office, and bedroom (Figure 4.4). The total floor area of the building is 100.2 m^2, and the room height is 2.7 m. The building is located in Tallinn, Estonia, so weather data for Estonia is used. The internal walls of the building have a thickness of 0.126 m, and external walls - 0.366 m. The floor is placed at ground level with a thickness of 0.347 m. The ceiling thickness is 0.413 m, with an attic above. The building has light-frame construction with thermal insulation in between wall panels. During winter, room temperature is held with central heating using wall-mounted radiators with a total heating power of 9.65 kW. The building has a central AHU responsible for exchanging air from the room and outdoors but also provides cooling when needed. AHU has integrated a 2 kW electrical air heater to warm the supply air with a heating setpoint of 18 °C. This air heater is only used when the heat recovery is insufficient.

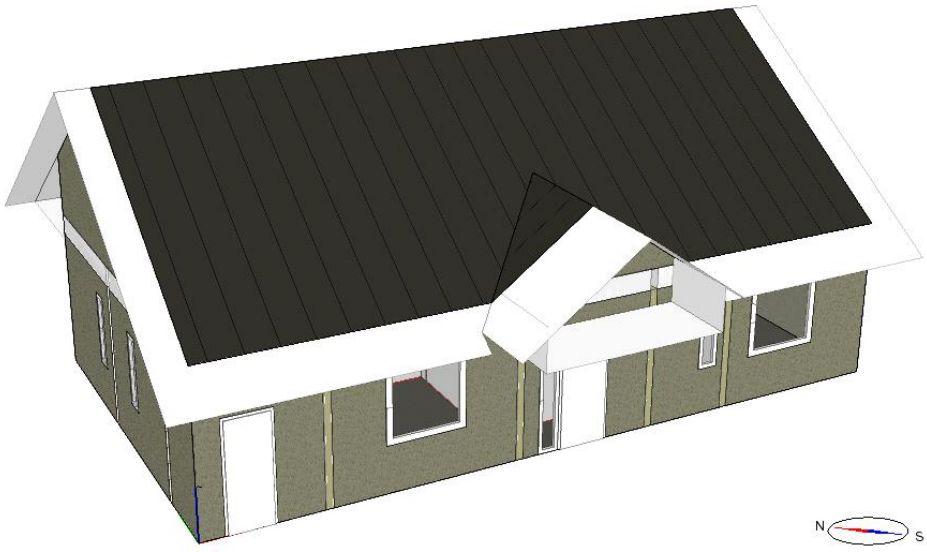

Figure 4.3. The single-family house used in simulations.

Figure 4.4. Floor plan of the single-family house [Paper I].

The building model is based on a small single-family home that serves as a model for redefining the cost-optimality threshold for new nearly zero-energy dwellings in Estonia [135]. The relevant documentation is provided, and the model has been validated in a related project [136]–[140]. According to statistics [141], a single-floor level building with a total floor size of 100 m^2 can be considered a typical single-family dwelling in Estonia. The study in [142] discusses the application of a neural network to construct a thermal model of the same building and includes a more comprehensive description of this model.

The building is used by a three-person family with two adults and one child. An occupancy simulation tool [143] generated a building occupancy schedule for each room (Figure 4.5). As a result, bedrooms have the highest usage at night and the lowest during the day when there are few or no residents at home. The rest of the rooms have a volatile usage profile dependent on the residents' daytime activities. The technical room, utility room, and vestibule are expected to have very low usage if used only for short durations. It is the reason why they are not included in the occupancy schedule. The occupancy simulation tool was used twice to generate profiles for the toilet and office using second-run bathroom and living room profiles. As a result, the building can accommodate a maximum of five people, which can be reasonable when guests are considered. The metabolic equivalent of task (MET) of 1.2 was chosen for the building object.

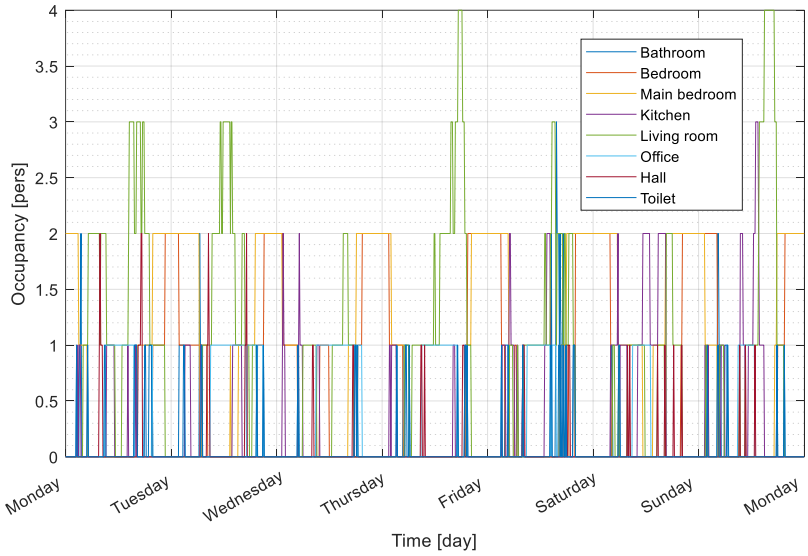

Figure 4.5. Room-specific occupancy schedule.

4.2.3 Air handling unit

An energy recovery type of a ventilation system was used for simulations. Estonian legislation [136] requires that this ventilation system must be used in low-energy buildings and nZEB. This requirement is not mandatory if one of the following statements is true:

1) The heat source is the extract air heat pump.
2) There is no constructional possibility to install an energy recovery ventilation system.
3) The extracted air contains pollutants that must not be introduced into the heat recovery.
4) The planned operating time of the AHU is less than four hours a day.
5) During significant reconstruction, installing ventilation ducts in the building is not technically possible.
6) A different ventilation system ensures the required energy efficiency of the building, IAQ, and thermal comfort.

None of these statements are true for objects used in the simulations. This means that the AHU has heat recovery and air ducts for supplying fresh air and extracting polluted air from the building (Figure 4.6). In total, two fans are used for air exchange. The supply air is also heated or cooled depending on the ambient conditions. The supply air temperature setpoint is defined to be 18 °C. In total, six sensors are placed into air ducts. The flexibility method developed in the previous chapter requires CO_2 concentration, humidity, and temperature data in the extracted air to estimate the FVR duration. Temperature and humidity are measured in the supply air, which is also needed for FVR duration estimations. An airflow rate sensor is required to measure the ventilation rate; this can be done indirectly using fan laws, but direct measurements are taken in simulations.

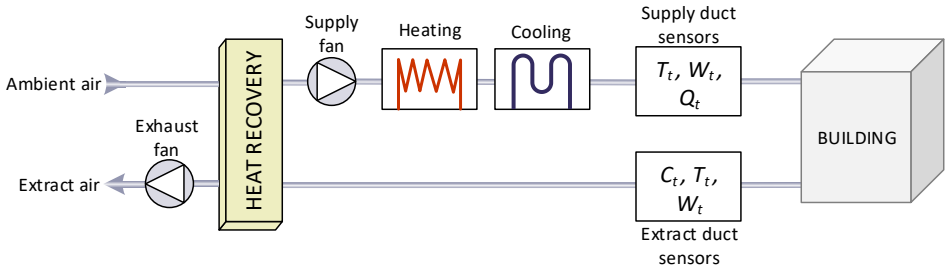

Figure 4.6. System layout of the air handling unit [Paper I].

As described in subsection 4.1.1, an AHU can be shut off during unoccupied hours. Office and educational buildings are not used 24 hours a day and seven days a week; an AHU is not always operational. In simulations, office building ventilation works from 06:00 to 18:00 and in educational buildings, from 07:00 to 16:00 (Table 4.5). This operation schedule is defined by an occupancy schedule where one-hour ventilation is used before the building is occupied. The AHU is off on weekends when the building is not used. An AHU in dwellings is constantly operational since dwellings can always be occupied.

Table 4.5. Operation schedule of the air handling unit during workdays.

Start time	End time	Office	Apartment	Dwelling
00:00	06:00	0	1	1
06:00	07:00	1	1	1
07:00	16:00	1	1	1
16:00	18:00	1	1	1
18:00	00:00	0	1	1

4.2.4 Description of simulation scenarios

Simulation scenarios are created to validate the methods of the developed ventilation system flexibility management. The object 1 model can have two use cases: office or apartment (Table 4.6). There may be no sensors in the room, only one to measure CO_2 concentration, or all three relevant IAQ parameters (CO_2 concentration, temperature, and relative humidity) may be monitored. The different sensor configurations are used to compare open-loop estimations with those based on measurements. The ventilation system airflow rate is always constant when turned on. Object 2 has one use case and will be used as a dwelling. The ventilation system can have two operation types: CAV or VAV. CO_2 concentration-based proportional control is applied for the VAV type system. Also, different feedback configurations are used where there can be one IAQ sensor in the return air duct and three IAQ sensors in every room. Under three IAQ sensors, three different IAQ parameters are measured: CO_2 concentration, temperature, and relative humidity.

Simulations are conducted on one-year data. Activations are generated according to 2022 mFRR service activation and balancing electricity price data. The simulation is run twice. The first iteration generates the baseline, and the second iteration generates data to validate the accuracy and performance of the developed flexibility management method. A ventilation system operates at its minimum or maximum rate during regulation, depending on the regulation direction.

Table 4.6. Scenarios for ventilation system flexible control.

Scenario no	Object 1		Object 2	
	Room type	IAQ sensors in the room	System type	Sensors' location
1	Office	None	CAV	IAQ sensors in the return air
2	Office	CO_2 sensor	CAV	IAQ sensors in every room
3	Office	All three	VAV	IAQ sensors in the return air
4	Apartment	None	VAV	IAQ sensors in every room
5	Apartment	CO_2 sensor		
6	Apartment	All three		

4.3 Analysis of simulation results

Two different objects are considered, and six scenarios for simulation are implemented. Simulation results show the accuracy of each method, described through the root mean square error (RMSE) and mean absolute percentage error (MAPE).

4.3.1 Object 1: Small room in a building

A ventilation system operates during occupied hours in offices, enabling down-regulations when needed. However, the number of down-regulations activated with sensor feedback is relatively low, with only four during a year-long simulation period (Table 4.7). The open-loop approach expects higher than reality CO_2 concentration; therefore, there are fewer up-regulations and more down-regulations than in scenarios with sensor feedback. Only using CO_2 concentration sensors in estimations will result in around 35% of cases where the temperature limit will be exceeded. Measuring all three IAQ parameters is the best approach where the temperature limit was reached in 4% of cases. However, it caused a reduction in the number of total up-regulations due to temperature boundaries. In around 34% of cases, three IAQ parameter limit conditions were reached during a maximum hour-long regulation.

Table 4.7. Simulation parameters for office.

Parameter	No sensors	CO_2 sensor	All three sensors
Total number of up-regulations	297	301	152
Total number of down-regulation	106	4	4
Number of up-regulations where CO_2 concentration limit was reached	47	90	46
Number of up-regulations where temperature limit was reached	104	105	6
Number of up-regulations where relative humidity limit was reached	0	0	0
Number of up-regulations where at least one of three IAQ parameter limits was reached	132	150	51

A typical ventilation system operates throughout the day in apartment buildings, providing no down-regulations. It enables using an apartment ventilation system at least twice more for up-regulations than for offices (Table 4.8). The open-loop approach again expects higher than reality CO_2 concentration; therefore, there are fewer up-regulations compared to scenarios with CO_2 sensor feedback. Only using CO_2 concentration sensors in estimations will result in around 33% of cases where the temperature limit will be exceeded. Measuring all three IAQ parameters is the best approach, where the temperature limit was reached in around 14% of cases. However, it caused a reduction in the number of total up-regulations due to temperature limits. The relative humidity did not influence the regulations for either the office or the apartment. In around 20% of cases, three IAQ parameter limit conditions were reached during a maximum hour-long regulation.

Table 4.8. Simulation parameters for an apartment.

Parameter	**No sensors**	**CO_2 sensor**	**All three sensors**
Total number of up-regulations	628	635	503
Total number of down-regulation	0	0	0
Number of up-regulations where CO_2 concentration limit was reached	38	40	31
Number of up-regulations where temperature limit was reached	211	208	71
Number of up-regulations where relative humidity limit was reached	0	0	0
Number of up-regulations where at least one of three IAQ parameter limits was reached	235	238	101

4.3.1.1 Power consumption forecast

Power consumption is forecasted using the ARMA(0, 5) model for the office and the ARMA(0, 4) model for the apartment. ARMA model terms are calculated by using the AIC method. The forecast horizon is selected to be 24 hours. Previous week's measurement data forecast the next day's power consumption. Power consumption measurements and the forecast are divided into 5-minute timeslots to have a fast response between ventilation system startups and shutdowns, where the same slot data of the previous week is used to forecast power consumption in the following 24 hours. The 24th-hour forecast with the highest uncertainty is compared with the measured data to calculate the accuracy of the forecast model. One year RMSE is around 0.35 W for the office and 0.17 W for the apartment. The mean absolute percentage error (MAPE) is about 1.2% for the office and approximately 0.6% for the apartment. Figure 4.16 is an example of measured and forecasted power consumption during the first week of November 2022, where regulations can also be seen. There are noticeable differences in the number of regulations in each room type, where the apartment provides more flexibility than the office.

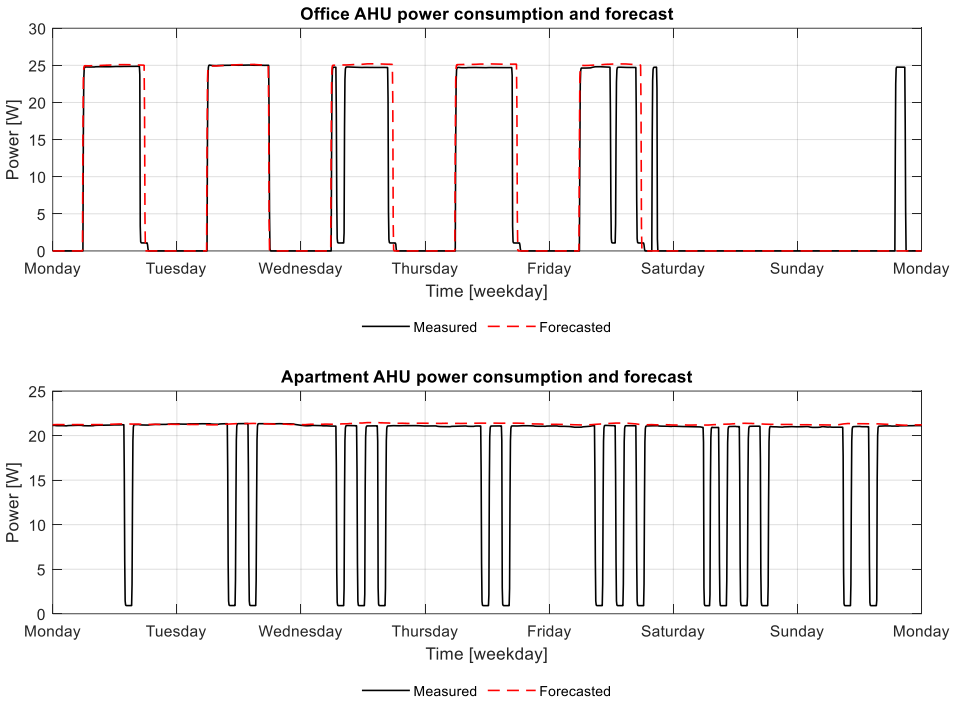

Figure 4.7. Power consumption of office and apartment AHU with regulations.

4.3.1.2 FVR duration estimation

Simulation results show that the temperature has the highest impact on the flexibility for object 1, a small room in a building. It can be seen in Figure 4.8, where an example of one-week FVR duration estimations is shown for the first week of November. The system FVR duration is dictated by CO_2 concentration and temperature. The parameter with short FVR dictates the whole system duration. FVR duration estimations are done for both room types. In the office, the FVR duration is longer during outside working hours since no occupants are in the room. In the apartment, this effect is less noticeable. These results show that depending on the system configuration and if a ventilation system is used to cool a space, the temperature can be more important than CO_2 concentration to estimate ventilation system flexibility. The FVR duration estimations are limited to 60 min as it is the most prolonged delivery period for simulation.

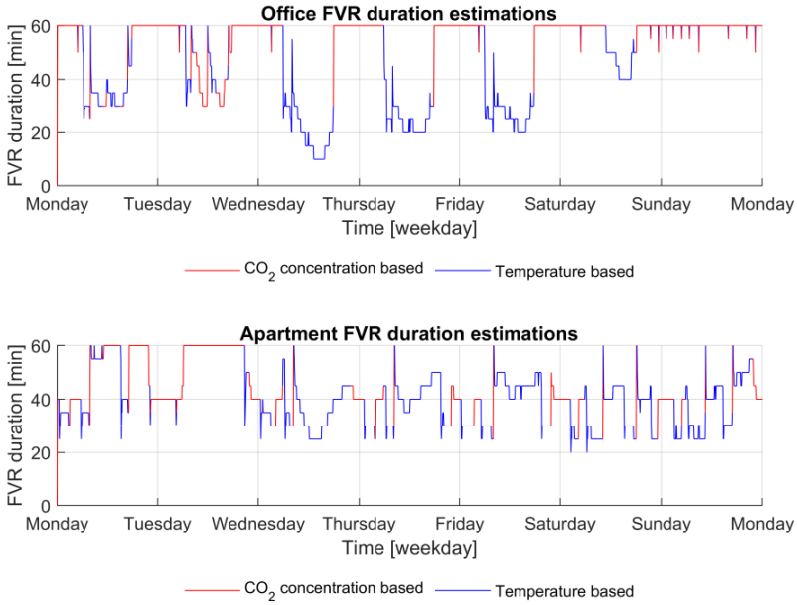

Figure 4.8. FVR duration estimations for office and apartment ventilation systems.

FVR duration estimation residuals for the open-loop approach with no sensors are biased (Figure 4.9) since estimated durations are shorter than the ventilation system can provide. The drawback of this approach is that the actual indoor environment conditions are not known, and it can estimate higher CO_2 concentration levels than in reality. CO_2 concentration based FVR duration estimation residuals are on the positive side for both room types, which is the consequence of using the FVR duration adjustment method. The adjustment method will shorten the estimations based on the consecutive time steps, giving more conservative results. It is good from the occupants' standpoint as an IAQ parameter limit is less likely to be exceeded during a regulation. The temperature has some restrictive effect when all three IAQ sensors are used, which has a negligible effect on CO_2 concentration-based FVR duration estimations. Temperature-based FVR duration estimation residuals are positive, meaning that the temperature boundary is less likely to be exceeded during regulations by implementing the developed method.

The highest inaccuracy in FVR duration estimations was observed with the open-loop approach, where no IAQ sensors are used (Table 4.9). CO_2 concentration-based FVR duration estimations are more accurate for the office than the apartment, which is the effect of the consecutive regulations and different room usage. It can be expected that in actual application, the methods can have even better performance since changes in the IAQ can be included in the estimations. Temperature-based FVR duration estimations show lower accuracy than CO_2 concentration-based estimations since temperature is highly dependent on outdoor conditions. However, the method gives more conservative estimations to avoid exceeding temperature limits during regulations. IAQ parameter limit exceeded for negligible cases when the reserve was activated. It means that during these cases, the FVR duration was estimated to be longer than the ventilation system could provide, causing the IAQ parameter limit to be exceeded during activation. In the office, the CO_2 concentration limit was exceeded for more cases than for the apartment, which is caused by the effect where the reserves were mainly activated during working hours when the office had high occupancy.

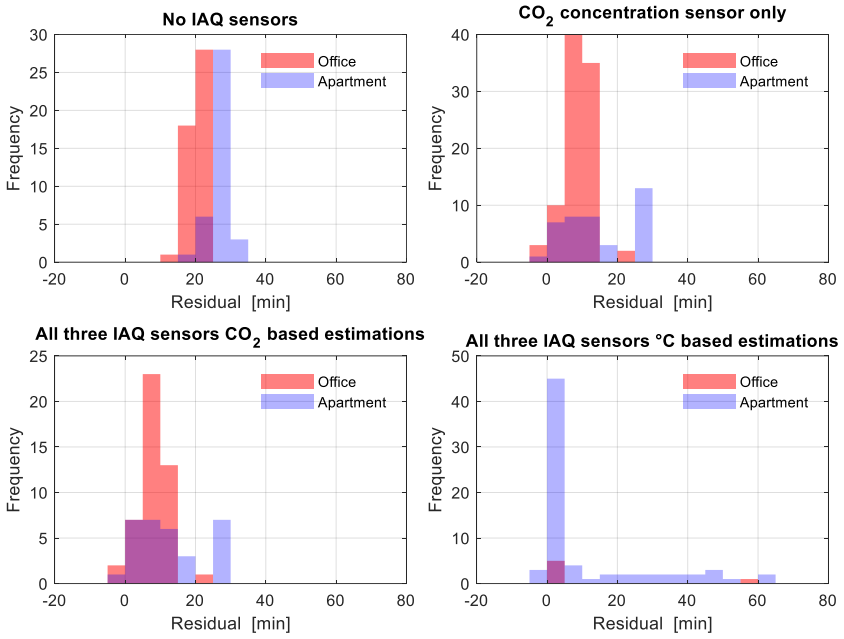

Figure 4.9. Residuals of the FVR duration estimations for object 1.

Table 4.9. Performance of FVR duration estimation methods with object 1.

IAQ sensors in the room		None	CO_2 sensor	All three	
Parameter		CO_2 concentration	CO_2 concentration	CO_2 concentration	Temperature
Office	**RMSE**	18.1 min	7.7 min	7.1 min	22.4 min
	MAPE	38.2%	11.1%	10%	14.1%
	IAQ limit exceeded	0%	1.2%	1.4%	0%
Apartment	**RMSE**	24.5 min	15.7 min	13.7 min	19.1 min
	MAPE	35.8%	15.9%	13.7%	27.1%
	IAQ limit exceeded	0%	0.2%	0.2%	0.6%

4.3.1.3 The ventilation system as a virtual energy storage

Methods to consider a ventilation system as a virtual energy storage (VES) are discussed in section 3.5. These methods were applied to object 1 to analyze the performance of the method and compare to the approach which considers the ventilation system as a typical load that operates at minimum or maximum power consumption level during activation. Unlike conventional energy storage systems, the VES can have SoC higher than 1 (Figure 4.10). It is caused by volatile building usage, where the CO_2 concentration can be at the ambient level during unoccupied hours, causing the SoC to be higher than 1. The SoC for the VES can also be lower than 0, which can occur when the CO_2 concentration boundary is exceeded. SoC below 0 is not the recommended state, but compared to conventional battery energy storage, it does not damage the system. The SoC of the VES is heavily dependent on room usage and fluctuates accordingly. During the weekend, the office is unoccupied, causing the SoC to stabilize around 1 since there is some air

exchange even when the ventilation system is shut down. The selected system is CAV type, where the ventilation rate is at the maximum level. Therefore, SoC is permanently stabilizing around 1.

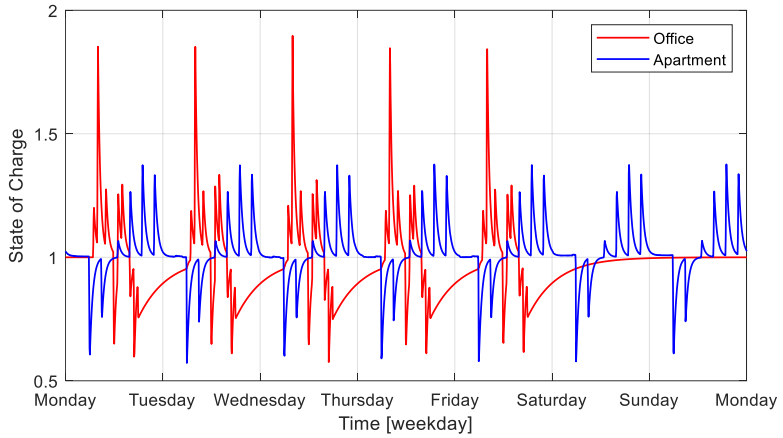

Figure 4.10. Example of a VES state of charge during a week [Paper II].

ARMA(0, 5) model was used to forecast ventilation system power consumption for the office, and ARMA(0, 4) model was used for forecasting in the apartment. The forecasting MAPE is around 1.2% for the office and about 0.6% for the apartment. The forecasting RMSE is approximately 0.4 W for the office and around 0.2 W for the apartment. Down-regulations are only possible for the office (Figure 4.11), where the ventilation system is scheduled to shut down during unoccupied hours. During maximum occupancy hours, there is a slight decrease in the available discharge power caused by the method to provide a higher than minimum ventilation rate to support a 60-minute regulation duration. The apartment can only provide discharge power since the ventilation system is designed to work at its maximum level throughout the day (Figure 4.12). For the apartment, the reduction in available discharge power occurs during night hours when the room usage is the highest.

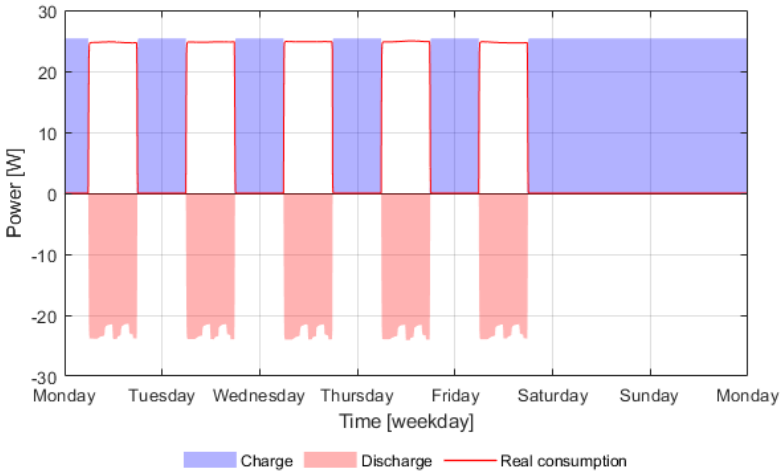

Figure 4.11. Example of VES power consumption, charge, and discharge power of the office during a week [Paper II].

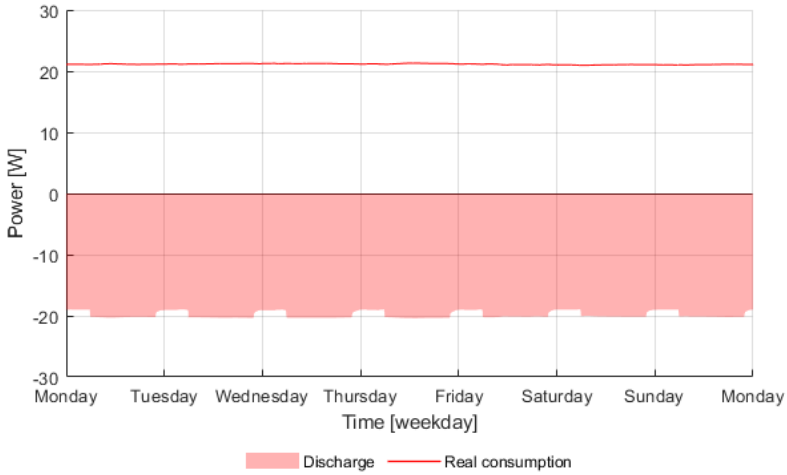

Figure 4.12. Example of VES power consumption and discharge power of the apartment during a week [Paper II].

Residuals of energy capacity estimations are only calculated for regulations where the CO_2 concentration reached its limit, which is less than the total number of regulations conducted during the simulation. Only residuals for up-regulation could be calculated (Figure 4.13) since the minimum CO_2 concentration was not achieved during down-regulations. The energy capacity estimation MAPE is around 15.7% for the office and about 8.3% for the apartment. The energy capacity RMSE is approximately 4.6 Wh for the office and 2.2 Wh for the apartment. For the office, more over-optimistic estimations can be caused by consecutive regulations where the CO_2 concentration cannot recover. There is a problem with thet kind of simulation where estimations cannot be adjusted when the subsequent regulation is activated. Therefore, it can be expected that the accuracy of the VES energy capacity estimation method can be improved with real applications.

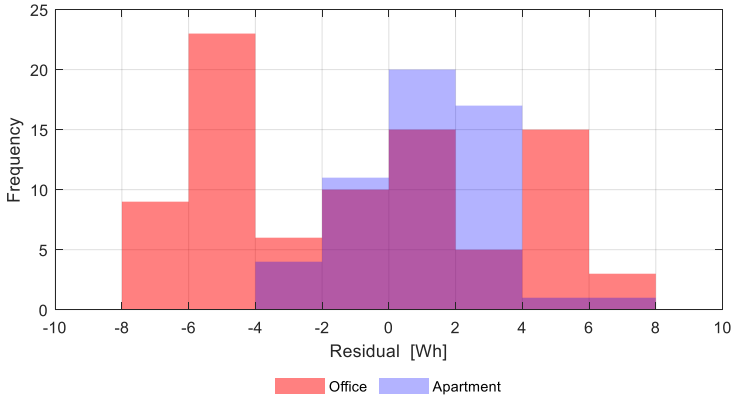

Figure 4.13. Residuals of VES energy capacity estimations for up-regulations [Paper II].

4.3.1.4 Flexibility service activations and pricing

Each hour's price for the flexibility service is calculated based on the CO_2 concentration measurements and costs. For example, upward regulations for the first week of November 2022 are shown in Figure 4.14. The tendered price was calculated using equation (3.24), where comfort cost was derived from the last two weeks' maximum balancing energy price. The reserve was only activated if the tendered price was lower than the balance energy market price. There was mFRR activation and the available capacity for the regulation was more than 10 W. More activations occurred for the apartment than for the office because an apartment ventilation system is running throughout a day. In the office, the ventilation system is shut down during weekend and night hours, which restricts availability for up-regulations, and the tendered price for up-regulations will also drop to 0. A separate figure for down-regulations is not shown since these were rare for the selected object.

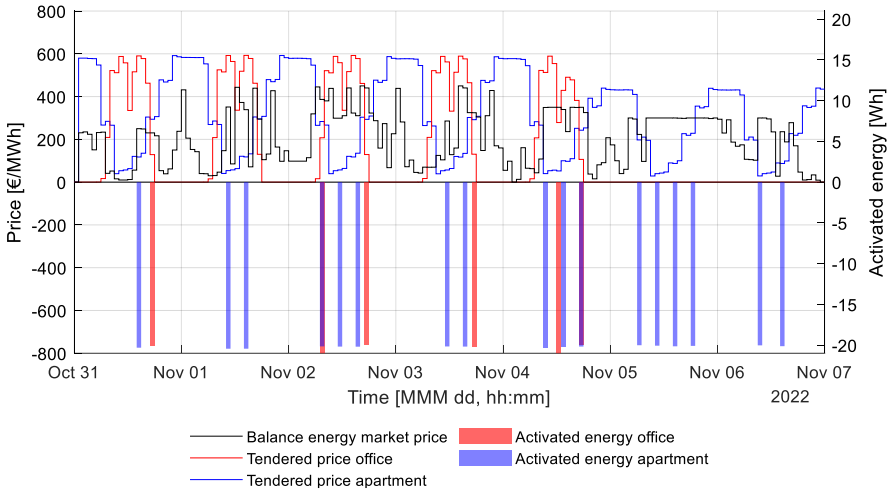

Figure 4.14. Example of flexibility service prices and activation during a week for up-regulations.

Before the financial impact of the regulations can be analyzed, the baseline must be found. It is achieved by measuring ventilation system energy consumption throughout the year without regulations for each room type. In the apartment, the ventilation system's total energy consumption and cost for consumed energy are over two times higher than for the office (Table 4.10).

Table 4.10. Baseline values of energy consumption and cost of energy.

Parameter	Office	Apartment
Energy consumption without regulations	77.8 kWh	186.5 kWh
The total cost of energy without regulations	29.82 €	62.16 €

With the open-loop approach, the energy consumption for the office does not have a significant difference from the baseline (Table 4.11). The reason is a high number of down-regulations as compared to the sensor-based approach. Nevertheless, with the open-loop approach, the total energy cost for a year was reduced by 9.7% for the office and 14.6% for the apartment. With sensors, the total energy consumption was decreased even more since more potential of the ventilation system could be exploited for the

flexibility service. In the office, adding sensors reduced the total energy cost by 1.1% from the baseline. The total energy cost in the apartment was increased by 1% by adding all three IAQ sensors. It is caused by the reduction in the total number of up-regulations due to temperature restrictions. The ventilation system as a VES approach showed the best results in the energy consumption and cost savings' viewpoint. Total energy consumption was reduced by 9.4% for the office and 8.9% for the apartment compared to the baseline. Total energy cost was reduced by 27.3% for the office and 28.9% for the apartment compared to the baseline. The VES approach gave better results since the energy capacity of the ventilation system for regulation is maximized.

Table 4.11. Regulation effect on the energy consumption and cost of energy.

Room type	Scenario	Energy consumption	The total cost of energy
Office	No sensors	77.2 kWh	26.92 €
	CO_2 sensor	74.8 kWh	26.64 €
	All three sensors	74.8 kWh	26.64 €
	As a VES	70.5 kWh	21.67 €
Apartment	No sensors	174.2 kWh	53.06 €
	CO_2 sensor	173.7 kWh	53.04 €
	All three sensors	173.7 kWh	53.69 €
	As a VES	169.9 kWh	44.17 €

4.3.2 Object 2: Single-family house

In the single-family house, the ventilation system runs continuously under normal conditions. It creates the possibility of exploiting the system more for up-regulations than for down-regulations. In total, 374 up-regulations for the CAV type system were conducted; the same value for the VAV type was 257 (Table 4.12). There were zero down-regulations since the capacity for this was insufficient, and the price for regulation was not suitable. The most restrictive IAQ parameter was CO_2 concentration, whose boundary condition reached 82% of cases for the CAV type system and 83% for the VAV type system. In comparison, the temperature limit reached 38% and 31% of cases for the CAV and VAV type system, respectively. Relative humidity had no restrictive effect on regulations with the applied simulation setup.

The same ventilation system is used for CAV and VAV systems with the same maximum and minimum power consumption. It also applies to the ventilation rate. The only difference is in the way the ventilation rate is controlled. The ventilation rate under normal conditions is close to the maximum for the CAV type system. However, for the VAV type system, the ventilation rate depends on the CO_2 concentration in the return air. CO_2 concentration causes a proportional increase in the ventilation rate.

With a maximum of one-hour regulation length, the limit for at least one IAQ parameter was reached for around 78% of cases for the CAV type system and 79% for the VAV. The majority of FVR durations were within 10 minutes. At least 30 minutes of maximum power reduction during up-regulation was provided for 35% of cases for the CAV type system and 37% for the VAV type system. The FVR duration is heavily dependent on the system configuration and building usage. Rooms with higher usage dictate an overall flexibility, and it is reasonable to provide more fresh air to these rooms to increase the FVR duration for the whole system. In dwellings, critical rooms are bedrooms and living rooms.

Table 4.12. Simulation parameters and counts.

Parameter	System type	
	CAV	VAV
Total number of up-regulations	374	257
Total number of down-regulation	0	0
Number of up-regulations where CO_2 concentration limit was reached	280	195
Number of up-regulations where temperature limit was reached	70	45
Number of up-regulations where relative humidity limit was reached	0	0
Number of up-regulations where at least one of three IAQ parameter limits was reached	293	204
AHU maximum power consumption	134 W	134 W
AHU minimum power consumption	6 W	6 W
Maximum ventilation rate	89.9 l/s	89.9 l/s
Minimum ventilation rate	14.4 l/s	14.4 l/s

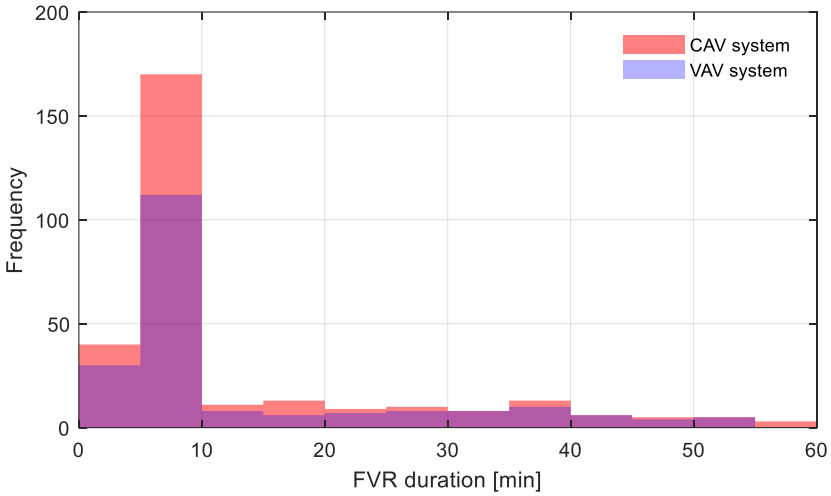

Figure 4.15. Distribution of FVR durations where an IAQ parameter limit was reached.

4.3.2.1 Power consumption forecast

The ARMA(0, 5) model was used to forecast power consumption for both system types. The AIC approach was used to calculate the terms of the ARMA model. 24 hours were chosen as the forecast horizon. The power consumption for the following day was forecasted using measurement data from previous days. For the quick reaction between the ventilation system starting and shutdown, one day was divided into 5-minute timeslots. The forecasts were done for each timeslot separately. The accuracy of the method was determined through the 24th-hour forecast with the most significant uncertainty compared with the observed data. For the CAV and VAV, the RMSE of the annual power consumption forecasts was roughly 1.3 W and 10 W, respectively. For the CAV and VAV, respectively, the MAPE was roughly 0.8% and 6.5%. The inclusion of

stochastic occupancy data hampered the accuracy of the VAV system power consumption forecasts. An illustration of measured and forecasted power consumption for the first week of November is shown in Figure 4.16.

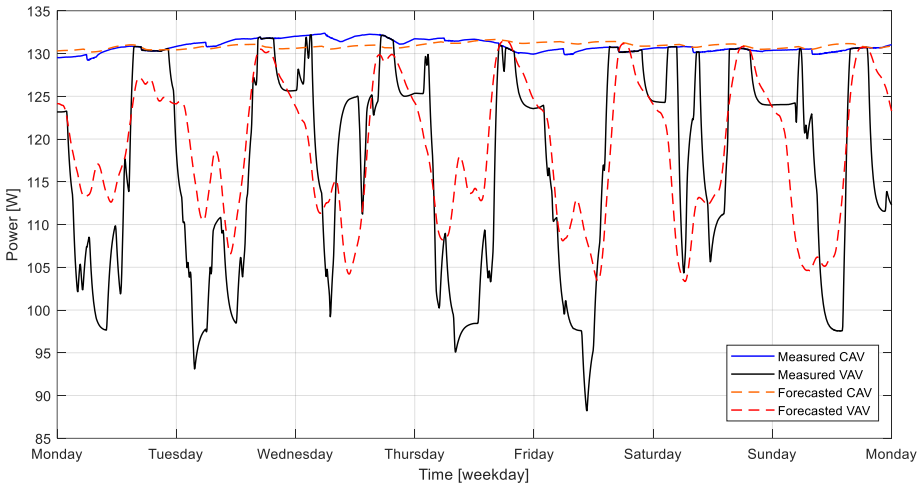

Figure 4.16. Measured and forecasted power consumption of the ventilation system [Paper I].

4.3.2.2 Estimation of FVR duration

Boundary conditions and pollutant generation are both essential for determining the FVR duration. It is necessary to make corrections in boundary conditions in advance if all IAQ sensors are installed in the AHU. The corrections based on data gathered during the second week of January are shown in Figure 4.17. Based on the data from one week, where the 5-minute average is calculated for each timestep within a day, the boundary conditions are adjusted. The occupancy of a room and how uniformly the pollutant concentration is distributed among the rooms are critical factors in the corrections of boundary conditions. The boundary conditions of the two ventilation system types differ slightly.

The simulation results showed that CO_2 concentrations had the most significant impact on flexibility. The first week of November is depicted in Figure 4.18 as an example of a one-week CAV type of ventilation system with estimated FVR durations, where the FVR duration was mainly determined by CO_2 concentration. On the other hand, FVR duration is less affected by temperature. The duration of the entire system is determined by the parameter with the shortest FVR. Since the occupancy profile is the same for both CAV and VAV types of ventilation systems, the FVR durations (Figures 4.18 and 4.19) are comparable. The availability of flexibility is reduced by demand-controlled ventilation, though, as FVR durations are marginally lower. For each system type, two methods – room-based estimations and AHU-based estimations – were used. Room-based estimations used the room with the shortest FVR duration and considered the IAQ sensors in each room. Sensors placed only in the AHU were considered in AHU-based calculations, which also used corrected boundary conditions. The FVR duration profile produced by AHU-based estimations is comparable to that of room-based estimations. However, notable variances can be brought out at stochastic occupancy and created boundary conditions.

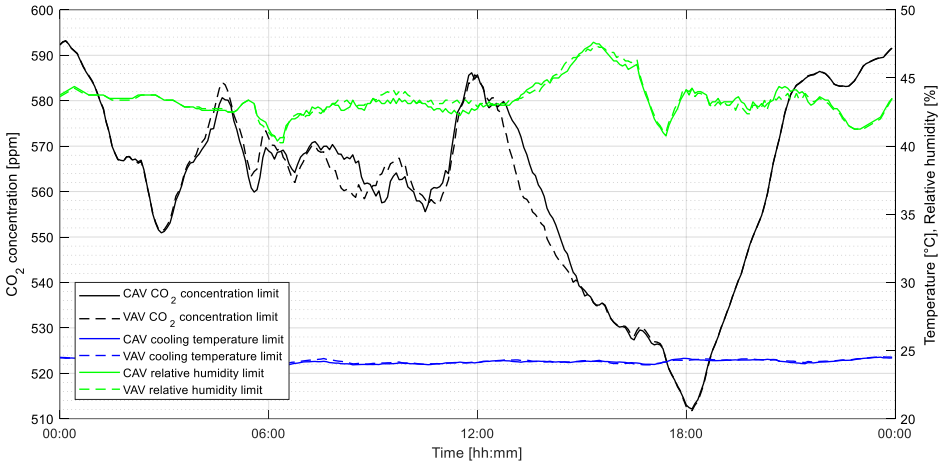

Figure 4.17. Daily IAQ parameter limits after the correction of the boundary condition [Paper I].

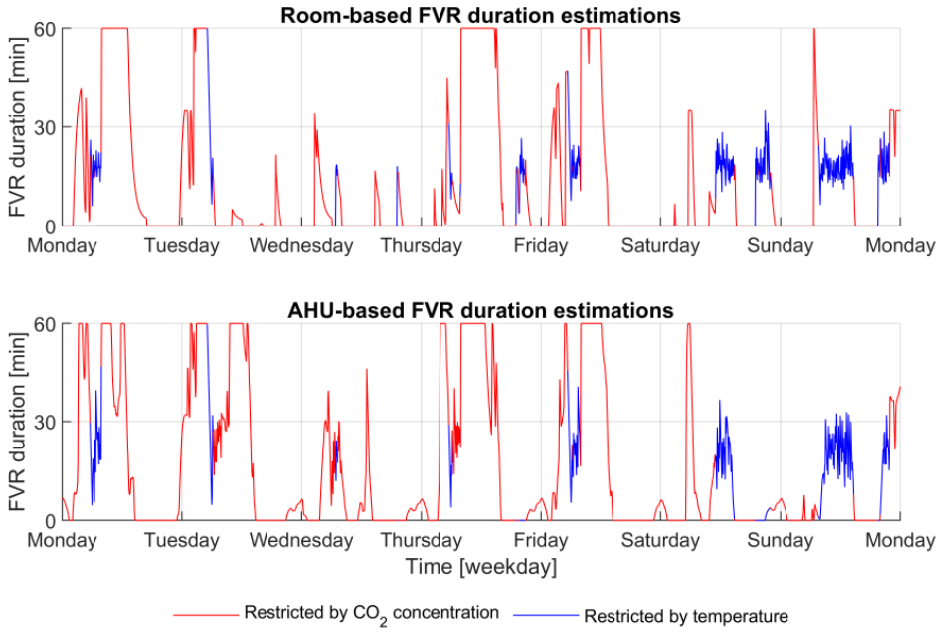

Figure 4.18. Example of one-week FVR duration estimations for a CAV type ventilation system.

The room-based technique was the most accurate way to estimate FVR duration according to residual analysis (Figure 4.20). Room-based approach residuals had a positive bias and provided more conservative FVR durations. It was the reason for applying the FVR duration adjustment method, which reduced the specified timestep estimation according to the following time-step forecasts.

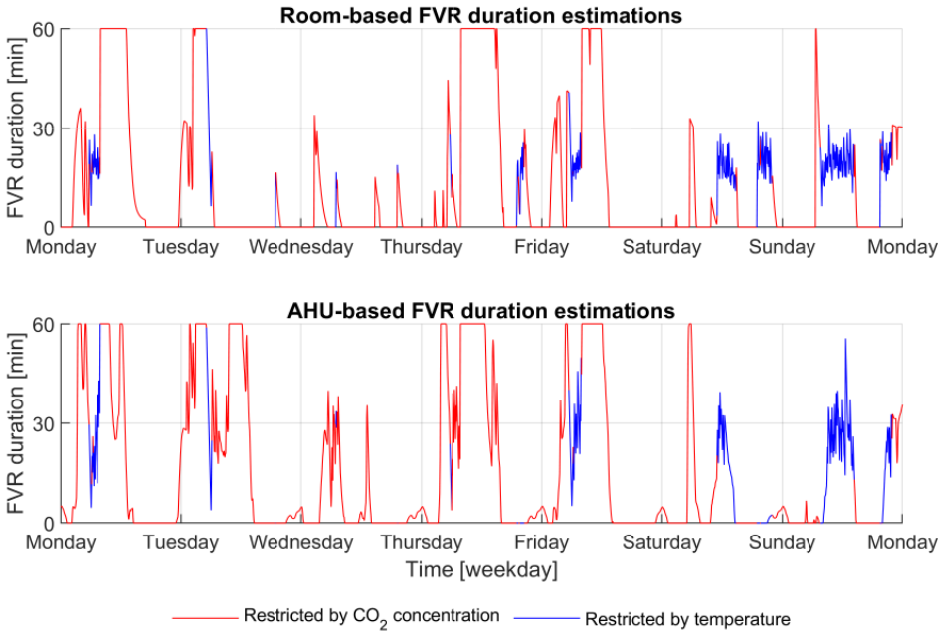

Figure 4.19. Example of one-week FVR duration estimations for a VAV type ventilation system.

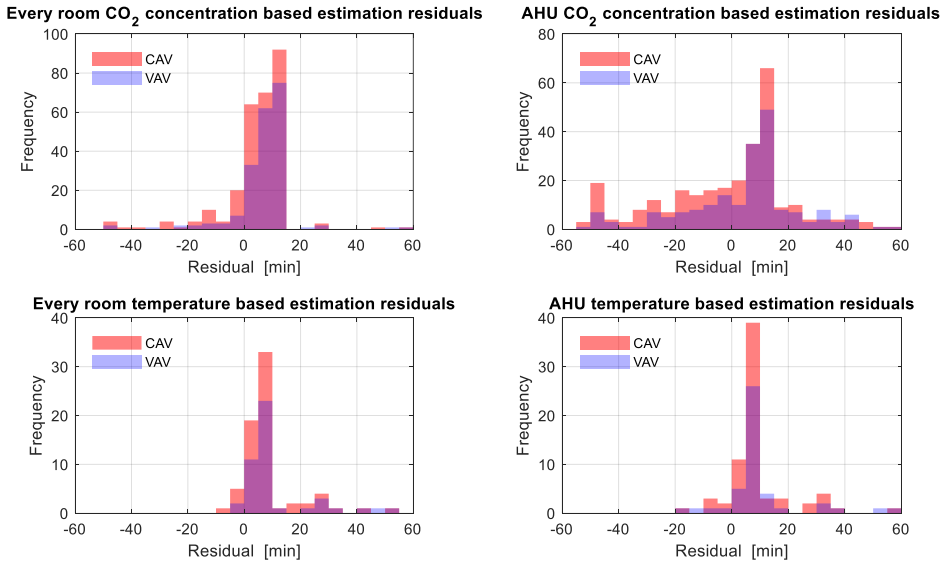

Figure 4.20. Residuals of the FVR duration forecasting.

The highest inaccuracy in FVR duration estimations was observed with the approach where the IAQ sensors were located in the AHU (Table 4.9). CO_2 concentration-based FVR duration estimations are more accurate for the VAV than for the CAV, resulting from fluctuating CO_2 concentration. It can be expected that in actual application, the methods can have even better performance since changes in the IAQ can be included in the estimations. Temperature-based FVR duration estimations showed higher MAPE error

than CO_2 concentration-based estimations since the temperature is highly dependent on outdoor conditions. However, the method gives more conservative estimations to avoid exceeding temperature limits during regulations.

Table 4.13. Performance of FVR duration estimation methods with object 2.

IAQ sensors location		In every room		In the AHU	
Parameter		CO_2 concentration	Temperature	CO_2 concentration	Temperature
Constant Air Volume	**RMSE**	12 min	11 min	23 min	14 min
	MAPE	69%	71%	149%	97%
	IAQ limit exceeded	13.1%	1.6%	31.8%	1.6%
Variable Air Volume	**RMSE**	11 min	14 min	21 min	16 min
	MAPE	67%	74%	122%	89%
	IAQ limit exceeded	7.8%	0.8%	24.9%	1.6%

4.3.2.3 Flexibility service activations and pricing

The cost of operating the ventilation system and the CO_2 concentration measurements were used to determine the cost of providing flexibility. For instance, upward regulations are depicted in Figure 4.21, where the tendered price was computed using equation (3.24), and comfort cost was obtained from the maximum balanced energy price for the previous two weeks. Calculations also considered the highest rate of CO_2 generated during the last two weeks. The reserve was only activated when the tendered price was less than the balance energy market price, the mFRR was activated, and there was more than 10 W of available flexible power for the regulation. The VAV type system was demand-controlled, which resulted in less power that can be used for up-regulations.

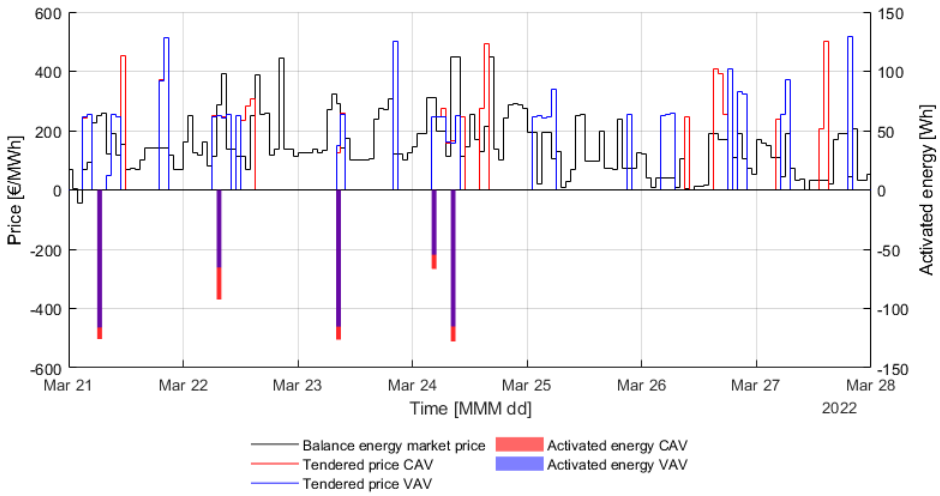

Figure 4.21. Flexibility service prices and activations.

Regulations have little impact on overall energy use in residential buildings because the ventilation system runs continuously (Table 4.14). The total energy used by fans was decreased throughout the simulation period by 1.2% for the CAV system but only by 0.8% for the VAV system. The cost of energy was lowered by 4% for the CAV type system, and for the VAV type system, a decrease of about 2.2% was reached. These percentages can be raised when the profit margins are adjusted for a good balance between system availability to provide service and exploitation, where the ventilation system is used more extensively for flexibility service.

Table 4.14. Regulation effect on energy consumption and cost of energy.

Parameter	**System type**	
	CAV	**VAV**
Energy consumption without regulations	1.152 MWh	1.034 MWh
Energy consumption with regulations	1.138 MWh	1.026 MWh
Total cost of energy without regulations	384.11 €	344.82 €
Total cost of energy with regulations	368.78 €	337.23 €

4.4 Conclusions

This chapter described the validation process of the ventilation system flexibility management methods developed in Chapter 3, based on the state-of-art analysis discussed in Chapter 2. The validation process started with constructing object models: a small room in a building and a single-family house. A year-long simulation was conducted on these objects where the first iteration was done to acquire a baseline, and the second iteration was for testing the performance of the methods. The results addressed power consumption, FVR duration, and economic parameters, where the main observations were:

- ARMA(p, q) model is sufficient to forecast the power consumption of the ventilation system. The forecast MAPE was around 1% for the CAV type systems, and for the VAV type system with a stochastic occupancy profile, the MAPE was 6.5%. According to the Estonian TSO Elering AS [144] up to ± 10% steady-state error is allowed for the mFRR capacity or 0.1 MW, whichever is larger.
- The open-loop approach to estimate FVR duration is used when no IAQ sensors are available, and the goal is to minimize initial investment costs. However, this will result in higher inaccuracies in estimations. From the results of the small room, the variance of residuals is low, but there is a bias that can be removed if parameters are adjusted to actual conditions.
- Placing sensors only in the AHU approach is used when the aim is to lower the initial investment costs while having minimum sensor data. The residual analysis showed higher variability and lower accuracy than placing sensors in each room. Portable sensors are recommended to improve the performance of this approach to tune the corrected boundaries.
- FVR duration estimations based on CO_2 concentration showed an RMSE of 7 min up to 16 min when the fixed occupancy profile was selected and about 12 min when the stochastic occupancy profile was used. Considering that the delivery period is typically not longer than 30 minutes instead of 1 hour,

which was considered in the simulation, it can be assumed that this error is even less in the actual application.

- FVR duration estimations based on temperature showed a RMSE of around 20 min for most scenarios. Therefore, temperature-based FVR duration is more difficult to estimate accurately, but it can be expected that the estimations will also become more accurate with shorter delivery periods.
- The results showed that cost savings are achievable when a ventilation system is integrated into the flexibility service. In the apartment, up to 10% of cost savings were achieved; in the office, up to 15%, and in the single-family house, up to 4%. The cost savings heavily depend on how much the flexibility service exploits the ventilation system. In the single-family house, the CO_2 concentration was already close to the limit, seen from the share of regulations where the CO_2 concentration limit was reached.
- A ventilation system as virtual energy storage is an approach to maximize the energy capacity used for flexibility service. Based on the results, the VES approach increases the total cost savings by twofold compared to operating a ventilation system at a minimum ventilation rate during the activation of the reserve.

The results acquired in this chapter make it possible to implement the developed flexibility management methods on real systems. The experiments conducted in the case studies will be discussed in Chapter 5. In this chapter, two hypotheses were tested. For most cases, the FVR duration is estimated to be shorter than the ventilation system can provide to avoid exceeding limits for IAQ. The second hypothesis is mostly correct since for most cases, the IAQ limits were not exceeded in more than 5% of situations when the reserve was activated. The limit is exceeded more with stochastic occupancy. The third hypothesis is mostly correct since most studied ventilation systems could provide more than half of the cases when the reserve is activated for at least 30 minutes, the maximum amount of power. The exception is the single-family house, where at least 30 minutes of FVR duration was achieved for around 35% of cases. The high pollutant concentration caused this during normal conditions.

5 Case studies with the developed flexibility management methods

In this chapter, developed flexibility methods are experimentally validated on an actual building. First, experimental setups and the experiments are described. Second, the results of the experiments are analyzed, and the performance of the methods is addressed. The aim of the experiments is to discover details that influence the implementation of the developed methods in an actual building that otherwise simulations cannot identify.

Experiments were conducted in the Tallinn University of Technology (TalTech) educational building with a code "SOC" (Figure 4.1), used by the School of Business and Governance. The building is located in Akadeemia tee 3, Tallinn. It is a four-story building with an underground parking area. The total floor area of the building is 10 346 m^2. The installed power of the building is 1.63 MW, and the calculated power consumption is 1.3 MW. The building accommodates lecture rooms, offices, a cafeteria, recreational areas, underground parking, and technical rooms. The SOC building was selected for experiments as it has a wide selection of different ventilation systems and is one of the most modern buildings on the TalTech campus.

Figure 5.1. TalTech SOC educational building.

5.1 Description of the building ventilation systems and experimental setups

Ventilation systems of the TalTech SOC educational building were used to validate the developed flexibility management method. Power consumption of ten ventilation systems was monitored (Table 5.1). The rest of the ventilation systems installed in the building were shut down during the measurement period or had power consumption close to zero. Measurements started on the 16th of June 2021 and ended on the 31st of January 2022. Measurements were taken with a multi-channel energy meter SATEC

BFM136. This energy meter complies with the requirements for accuracy class 0.5S in the standard IEC 62053-21. Most of the systems installed in the SOC building are CAV type, and only two are VAV type. Ventilation systems are also classified as single or multi-zone systems. According to the building design documentation, the total rated power of ventilation systems is 98 kW. The design values differ in actual measurements, and there can be various reasons behind it, such as changes in the equipment, configuration, aging of the system, and leakage through construction.

Table 5.1. Ventilation systems in the TalTech SOC building and the design values.

Code	System type	Multi or single-zone	Fans' rated power, kW	Airflow rate, m^3/s
302SV	CAV	Multi	26.0	6.6
303SV	CAV	Multi	9.5	3.2
304SV	CAV	Multi	16.5	5.7
305SV	VAV	Multi	30.0	8.6
306SV	VAV	Single	9.0	1.8
307S	CAV	Multi	4.0	2.0
307.1V	CAV	Single	1.2	1.3
308V	CAV	Multi	1.2	1.4
309V	CAV	Multi	0.3	0.3
310V	CAV	Single	0.3	0.3

Ventilation systems in the SOC building operate according to a schedule (Figure 5.2). During the daytime, a ventilation system operates at a higher ventilation rate, and during nighttime, a ventilation system operates at a minimum rate or is shut down. The maximum total power consumption of ventilation systems is roughly 35 kW, and the minimum is around 4 kW. Thus, around 31 kW of power can be reduced during the daytime.

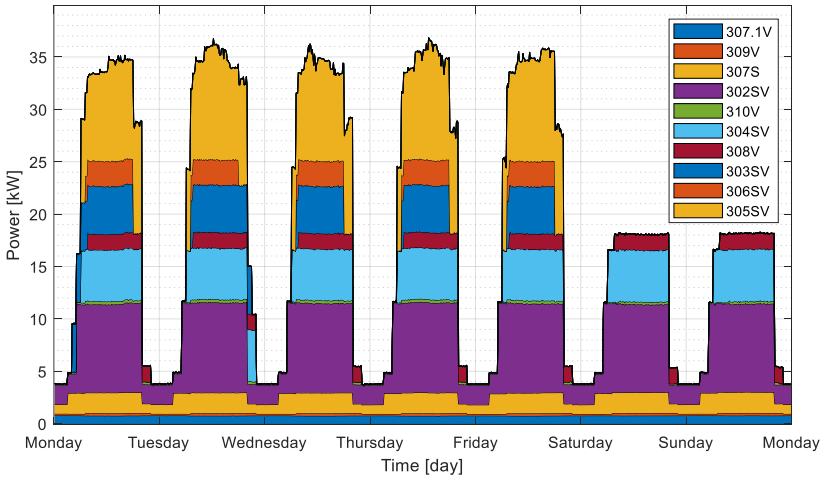

Figure 5.2. Power consumption of SOC building ventilation systems.

5.1.1 Case study 1: Ventilation system 306SV and auditorium room

TalTech auditorium served as the site for the case study. A ventilation system that was mainly servicing one auditorium was used in the study. The chosen auditorium has a floor size of 224.5 m^2, and its estimated indoor air volume is 1122.5 m^3. The auditorium can hold 200 people at a time and has a 1.76 m^3/s designed ventilation rate. The fan rotational frequency of 17 Hz, with around 0.48 m^3/s ventilation rate, was used to determine the lowest permitted airflow rate.

A CO_2 cylinder with attachments to measure and control gas flow was placed in the middle of the auditorium as a source of pollution. The CO_2 cylinder was weighed before and after the experiment to calculate the average CO_2 generation rate. To provide a vertical component to CO_2 pollution and help mix the air, an air mixing fan was positioned close to the CO_2 gas exit nozzle (Figure 5.3). Due to the low temperature of the injected CO_2 gas, which does not mix well with interior air while the air exhaled by people is warmer and has superior mixing capabilities, a mixing fan was necessary. Multiple fresh air inlets bring clean air into the auditorium from below the floor, and one air duct removes polluted air from above, located in Figure 5.3 on the right side of the room.

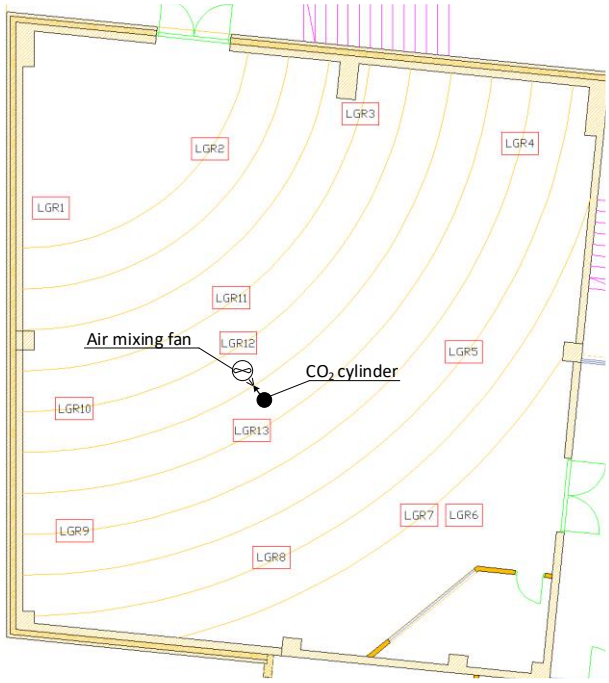

Figure 5.3. The auditorium and measurement equipment layout [Paper III].

IAQ loggers were put in the auditorium, marked LGR1 through LGR13, all of which were placed around 0.8 m, except for LGR6, which was mounted on the extract air orifice at a height of about 3 m. The Evikon E6226 measurement unit (CO_2 level 0 to 10000 ppm) was used to determine the CO_2 concentration. These loggers were placed in the room to provide a clearer picture of the CO_2 distribution inside the auditorium, but their usage to calculate the ventilation system's flexibility was excluded. Only measurements in the extract air duct, suitable for such sensors in most ventilation systems, were used in

flexibility estimations. With little expenditure, the stated flexibility estimation methods can be used for most ventilation systems.

Two fans bring fresh air and remove polluted air from the auditorium as part of a mechanical ventilation system (Figure 5.4). Additionally, the system has an enthalpy heat exchanger configured to run at maximum rotational speed. Air filters, heating, and cooling of the supplied air are additional components of the ventilation system not shown in Figure 5.4.

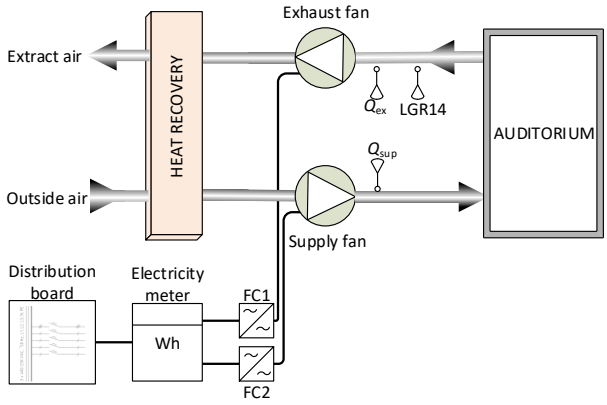

Figure 5.4. Ventilation system 306SV layout and placement of measurement equipment [Paper III].

A timestep of 1 min was used to measure extract and supply airflow rates. A multipurpose indoor air quality meter, Testo 435-4, with a differential pressure range of 0 to 250 Pa and an accuracy of 1 Pa, was used to measure the airflow. A single IAQ logger with a 1-minute timestep was inserted into the extract air duct to measure the CO_2 concentration in the return air. Each fan drive was powered from the HVAC distribution board, and frequency converters FC1 and FC2 were used to control each fan's speed. One electricity meter, model BFM136, was used to measure the individual power consumption of each fan. Measurements logging interval of electricity consumption was 2 min, and average power was saved for each timestep.

5.1.2 Case study 2: Ventilation system 303SV and lecture rooms

Ventilation system 303SV servicing multiple lecture rooms is the point of interest in the second case study. The total floor area connected to the selected ventilation system is 664.1 $m^{2,}$ with a total air volume of around 2324 m^3 (Table 5.2). The ventilation system provides air exchange for the rooms on the second, third, and fourth floors. These rooms are used for lectures, except on the second floor, where there is a recreational area with a floor size of 190.3 m^2. The total airflow rate is 3.36 m^3/s, and the ventilation system power consumption at this rate is approximately 6.2 kW. The minimum rotational frequency of the fan is 15 Hz, with around 1.0 m^3/s ventilation rate and 0.24 kW power consumption. The fan drives have frequency converters that can be operated in the range of 15 to 50 Hz. However, in flexibility estimations, it is considered that the ventilation systems are shut down completely. It is due to complications where the case study used measurements from the lecture rooms, and the ventilation system's operation was not altered since it was not allowed by the system's administrator.

IAQ loggers were installed in each of the 12 lecture rooms connected to the ventilation system. Loggers were placed on the lecturer table with a height of around 0.8 m (Figure 5.5). One of the loggers was placed inside the AHU return air duct to monitor the CO_2 concentration of the extracted air. Lecturers were given pre-filled forms to mark down the number of people inside the lecture room. Since the method calculated the pollutant generation rate, it is possible to derive the number of people from the measurements and compare this data to the written number.

Table 5.2. Rooms connected to ventilation system 303 [145].

Floor	Room number	Floor area, m^2	Room height, m	Airflow rate, m^3/s
II	216	190.3	3.5	0.34
	217	35	3.5	0.21
	218	34.1	3.5	0.26
	219	34.1	3.5	0.24
	220	35	3.5	0.25
	221	35	3.5	0.21
	222	37.2	3.5	0.23
III	315	44	3.5	0.17
	316	44	3.5	0.24
	317	43.7	3.5	0.33
IV	416	44	3.5	0.27
	417	44	3.5	0.34
	418	43.7	3.5	0.27
Total		**664.1**		**3.36**

Figure 5.5. IAQ logger location in a lecture room [145].

IAQ measurements were taken during six weeks, from 7th February 2022 to 17th April 2022. A cap was in between measurements where the loggers were removed from the rooms from 21st March 2022 to 18th April 2022. IAQ was measured with HOBO MX1102A, which measures CO_2 concentration, temperature, and relative humidity (Table 5.3). A timestep of 5 min was used to measure IAQ conditions inside each room, and the AHU return extract air duct. Each fan drive of the ventilation system 303SV was powered from the HVAC distribution board, and frequency converters were used to control each fan's speed. One electricity meter, model BFM136, was used to measure the individual power consumption of each fan. A logging interval of 10 min was selected to measure electricity consumption and average power during each timestep.

Table 5.3. HOBO MX1102A CO_2 logger specification [146].

Parameter	Value
Temperature range	0…50 °C
Temperature measurement accuracy	±0.21 °C
Temperature measurement resolution	0.024 °C at 25 °C
Relative humidity range	1…90%
Relative humidity measurement accuracy	±2% in the range 20…80% ±4.5% in the range 80…90%
Relative humidity measurement resolution	0.01%
CO_2 concentration range	0…5000 ppm
CO_2 concentration measurement accuracy	±(50 ppm + 5% from the reading)
CO_2 concentration measurement resolution	1 ppm

5.2 Analysis of case study results

Two case studies were conducted in the building, and flexibility management methods were tested based on the acquired data. The focus of these studies was on power consumption and FVR duration. The accuracy of each method is described through the root mean square error (RMSE) and mean absolute percentage error (MAPE). Economic aspects are considered for case study 2, where more data was generated for an extended period.

5.2.1 Case study 1: Ventilation system 306SV and auditorium room

On October 9th, 2020, a case study was initiated in the ventilation system servicing an auditorium of an educational building. During the experiment, the regular ventilation rate of the system was changed to minimal (Figure 5.6). The goal was to decrease the system's energy usage and estimate flexibility. The case study was separated into events where something happened or changed during the experiment (Table 5.4). One disturbance was also added where the mixing fan was shortly shut off.

Before being set to the lowest rate, the average power usage of the ventilation system was around 2.43 kW, equivalent to an airflow rate of roughly 1.79 m^3/s. The calculated specific fan power (SFP) was around 1.36 $kW/(m^3/s)$. The system power consumption at the FVR was around 0.17 kW, equivalent to an airflow rate of about 0.48 m^3/s. At the FVR, the calculated SFP was around 0,35 $kW/(m^3/s)$. According to the standard EN 13779, SFP should be less than 2.0 $kW/(m^3/s)$, which the ventilation system complies with. It took around 90 s for the ventilation system to transition from one power level to the next. Therefore, the rate of power change was roughly 25 W/s.

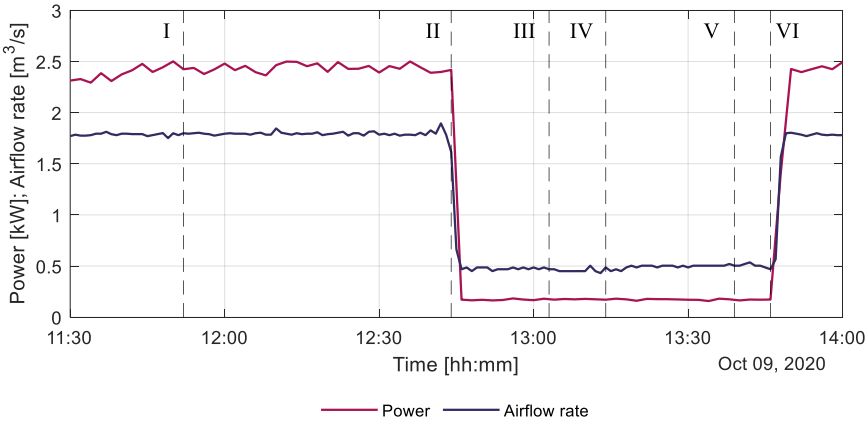

Figure 5.6. The power consumption of the ventilation system and the airflow rate during the experiment [Paper III].

Table 5.4. Events of the case study and schedule [Paper III].

Event	Description	Time
I	Start of the experiment, CO2 gas injection into the auditorium	11:52
II	The ventilation system is switched to the minimum rate	12:44
III	At the start of the disturbance, the CO2 gas mixing fan is switched off	13:03
IV	End of the disturbance, the CO2 gas mixing fan is switched on	13:14
V	The maximum allowable CO2 concentration of 1100 ppm reached	13:39
VI	End of the experiment, the ventilation system returned to regular operation	13:46

5.2.1.1 Power consumption forecast

The ventilation system 306SV was observed for approximately one week, from November 23rd to November 30th, 2020 (Figure 5.7). Results indicate that the ventilation system runs according to schedule, including on weekends. Between 7:00 and 22:00, when the ventilation system is set to operate at the maximum rate, the power consumption can only be reduced during this time window. Between 22:00 and 7:00, the ventilation system is working at its lowest power level, which implies that during that period, the power consumption can only be increased.

The ARMA(0, 2) model was used to forecast power consumption. The AIC approach was used to calculate the terms of the ARMA model. 24 hours were chosen as the forecast horizon. The power consumption for the following day was forecasted using measurement data from previous days. Data for the first two days were used to initialize the forecasting model, and the rest was used to test the model performance. For the quick reaction between the ventilation system starting and shutdown, one day was divided into 2-minute timeslots. The forecasts were done for each timeslot separately. The accuracy of the method was determined through the 24th-hour forecast with the most significant uncertainty compared with the observed data. The RMSE of the power consumption forecasts was roughly 0.04 kW. The MAPE was roughly 2.2%.

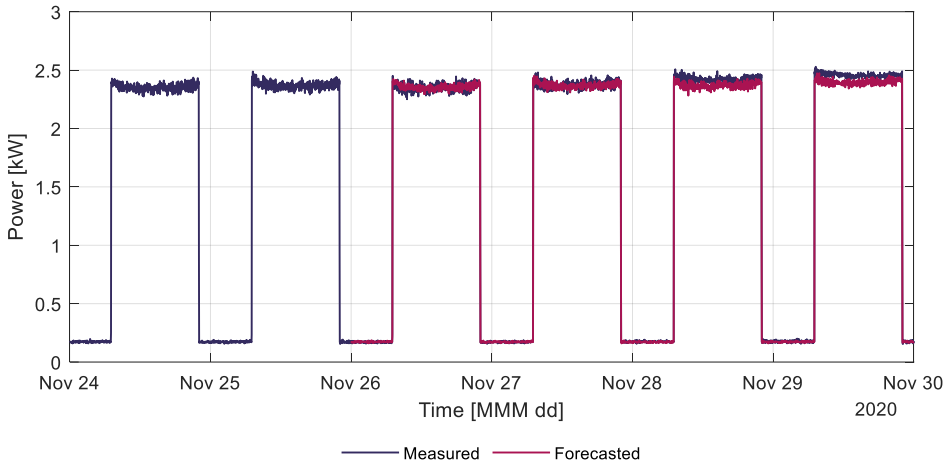

Figure 5.7. Measured and forecasted power consumption of the ventilation system.

5.2.1.2 FVR duration estimation

The valve of the CO_2 cylinder was opened to begin the experiment at 11:52 (Figure 5.8). Throughout the experiment, the CO_2 gas flow rate in the auditorium was maintained at around 22 l/min, equivalent to the CO_2 produced by 66 people, or 33% of the room's occupancy. The ventilation system was forced to operate at the minimum rate from 12:44. The period before this action was utilized to stabilize the CO_2 concentration level in the auditorium and determine how long it could continue operating at its lowest rate. The CO_2 gas mixing fan was turned off at 13:03 and turned back on at 13:14. As a result of inadequate CO_2 gas mixing in the auditorium, this temporarily decreased the concentration of CO_2 in the extract air. The flexibility estimation algorithm recognized this as an unexpectedly low CO_2 generation rate and began calculating the CO_2 concentration in the auditorium using the CO_2 generation data from the preceding five minutes. Only when the ventilation system is forced to work at a rate lower than expected operating conditions to reduce power consumption is this portion of the algorithm active.

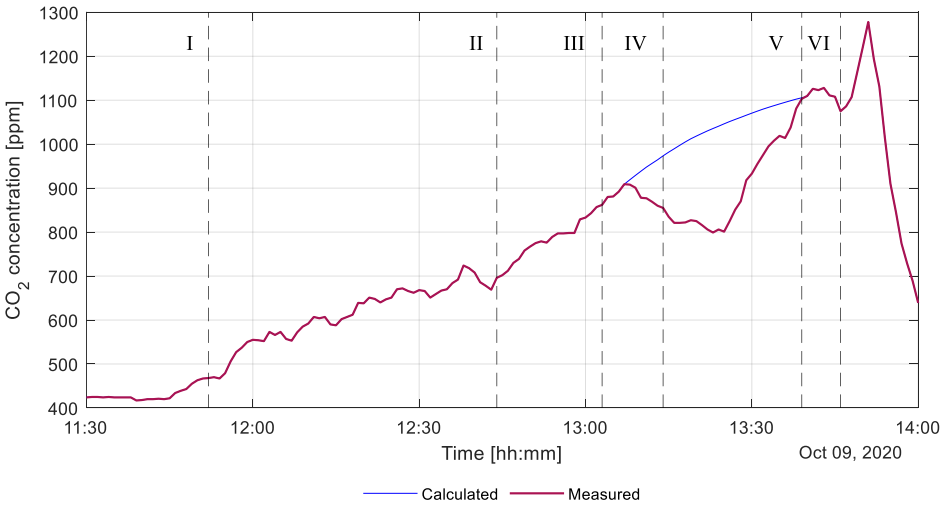

Figure 5.8. CO_2 concentration in extract air during the experiment [Paper III].

It took around 55 minfor the CO_2 concentration to reach and surpass boundary conditions. The estimated FVR duration was 53 min, calculated before the ventilation system was forced to operate at the minimum rate at 12:44. Therefore, the estimation error was 2 min, 4% off from the measured duration. A moving-average filter was used since the initial estimation approach for a shorter operation period generated high fluctuations (Figure 5.9). The filter's window duration was adjusted to 3 min to smooth out more significant oscillations without having too high a lag from the initial estimation. The measured duration indicates the time elapsed after the FVR began until the CO_2 concentration limit was reached. The CO_2 concentration level was estimated from 13:07 as the algorithm detected a negative CO_2 generation rate. The estimated CO_2 concentration reached the boundary of 1100 ppm before it was measured, which is why the estimations are lower than the measured results.

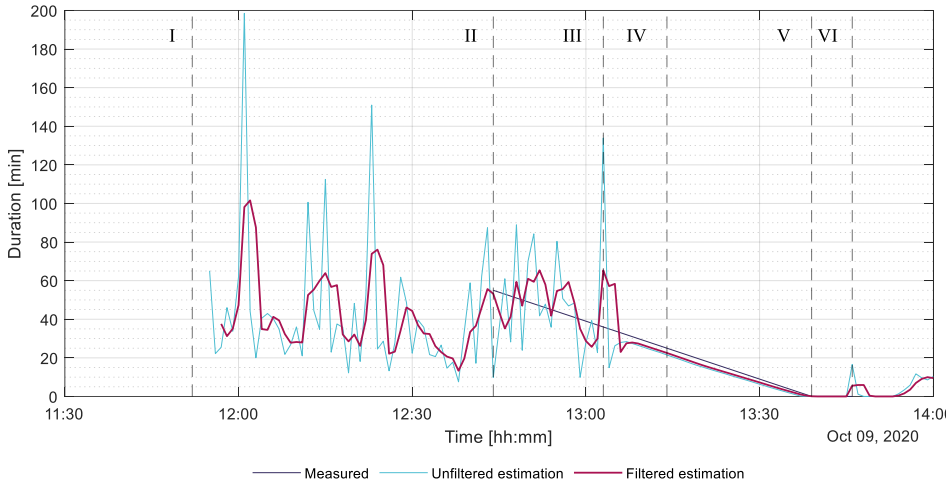

Figure 5.9. Measured and estimated FVR durations [Paper III].

5.2.1.3 IAQ conditions inside the auditorium room

IAQ loggers placed within the lecture room were employed in the case study to get a general outline of the pollutant distribution and overall conditions during the experiment. The average CO_2 concentration inside the auditorium and the CO_2 concentration measured in the extract air duct had a weakly positive correlation during regular operation with a coefficient of about 0.48. Figure 5.10 shows that at normal functioning of the ventilation system, the CO_2 concentration in the extract air was within the range of the CO_2 concentration in the auditorium measured at multiple points. The average CO_2 concentration within the auditorium and CO_2 concentration during the FVR measured inside the extract air duct did not correlate, as shown in Figure 5.10. The reason may be a lack of proper CO_2 gas mixing inside the auditorium or inertia existing between the extracted air and the auditorium's CO_2 concentration change. This experiment should be repeated with persons to understand better the reasons where thorough planning and ethical reasons should be addressed.

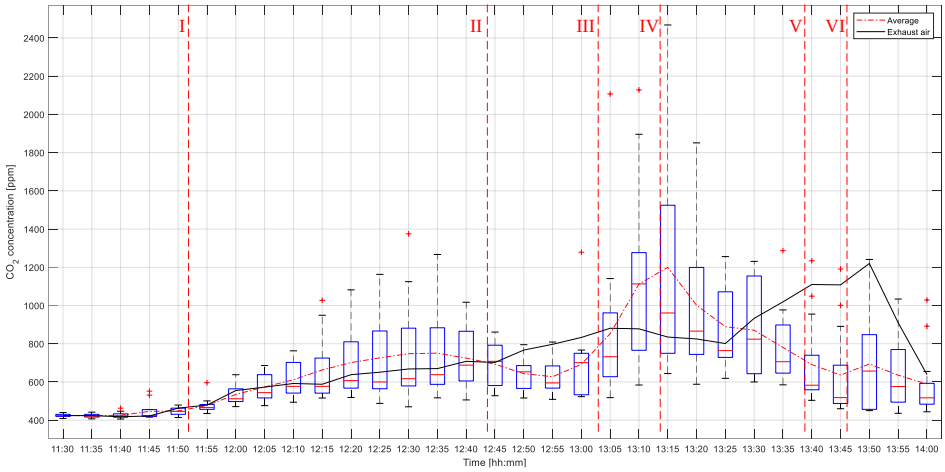

Figure 5.10. Flexibility service prices and activations [Paper III].

5.2.2 Case study 2: Ventilation system 303SV and lecture rooms

In total, 12 lecture rooms are connected to the ventilation system 303SV. The ventilation system runs according to a schedule where it is shut down during unoccupied hours. On Mondays, the ventilation system starts at 4:00 and is shut down at 18:00. On Tuesdays, the ventilation system is started at 7:00 and shut down at 22:00. On all other working days, the ventilation system is started at 7:00 and shut down at 18:00. The ventilation system is shut down during the whole weekend. It allows both up- and down-regulations. However, based on the data acquired during the measurement period, no down-regulations would be conducted on the system. The reason is that the balancing energy price to activate the reserve was unsuitable for the system. There could have been 55 up-regulations during the period starting from 21st March 2022 to 18th April 2022. CO_2 concentration limit would have been reached during 31 regulations or 56% of all the cases. However, in 41 cases, the FVR duration was longer than 30 min, meaning that the ventilation system could support up to 30-minute activations for around 75% of the time.

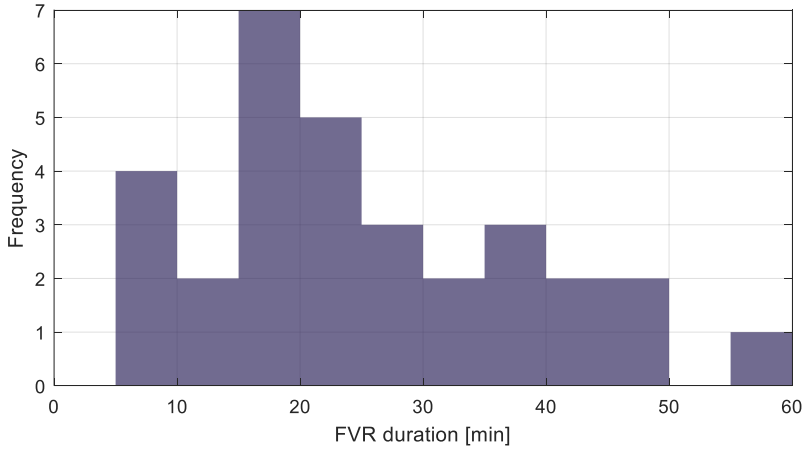

Figure 5.11. Distribution of CO_2 concentration based FVR duration estimates shorter than 60 minutes.

5.2.2.1 Power consumption forecast

The ARMA(0, 2) model was used to forecast the power consumption of the ventilation system 303SV. The AIC approach was used to calculate the terms of the ARMA model. 24 hours were chosen as the forecast horizon. The power consumption for the following day was forecasted using measurement data from previous days. Data from the first two weeks were used to initialize the forecasting model, and the rest was used to test the model's performance. For quick reaction between the ventilation system start and shutdown, one day was divided into 10-minute timeslots. The forecasts were done for each timeslot separately. The accuracy of the method was determined through the 24th-hour forecast, with the most significant uncertainty compared with the observed data. The RMSE of the model during the measurement period was roughly 0.11 kW. The MAPE was roughly 4.3%.

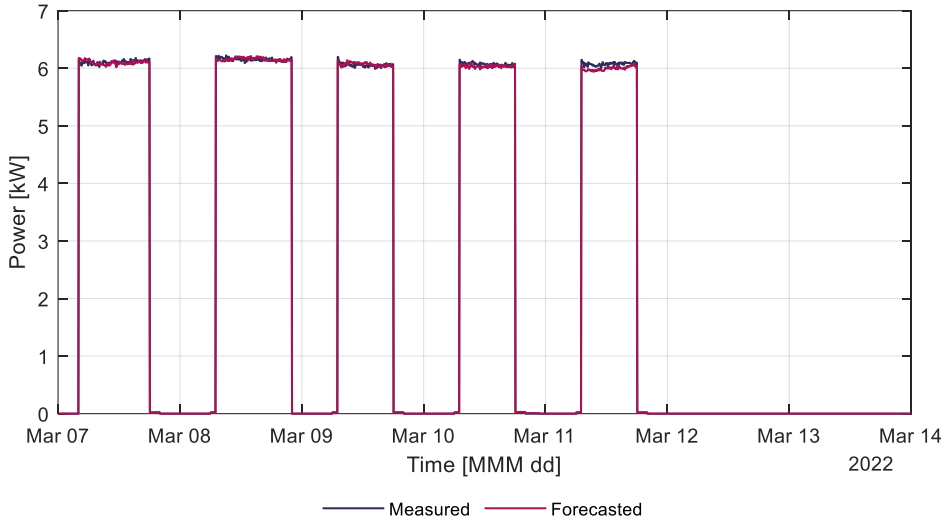

Figure 5.12. Example of measured and forecasted power consumption of the ventilation system.

5.2.2.2 FVR duration estimation

The last week of the monitoring week is depicted in Figure 5.13 as an example of one-week FVR duration estimations. The FVR duration was only determined by the CO_2 concentration. It is due to the reason that inadequate information was acquired on the conditions of the supply air. The temperature and humidity FVR duration method relies on the supply and return air values. Without that, the estimations are inaccurate and cannot be used for flexibility estimations. The the usage profile of the lecture rooms was not the same every week; there were changes in the number of people inside the room, and the time of the lectures changed. However, it can be seen from Figure 5.13 that from Monday to Thursday, rooms were used during working hours, causing a decrease in the FVR duration. There is also a slight decrease on Friday, but it is too small to influence the ventilation system availability for flexibility service significantly.

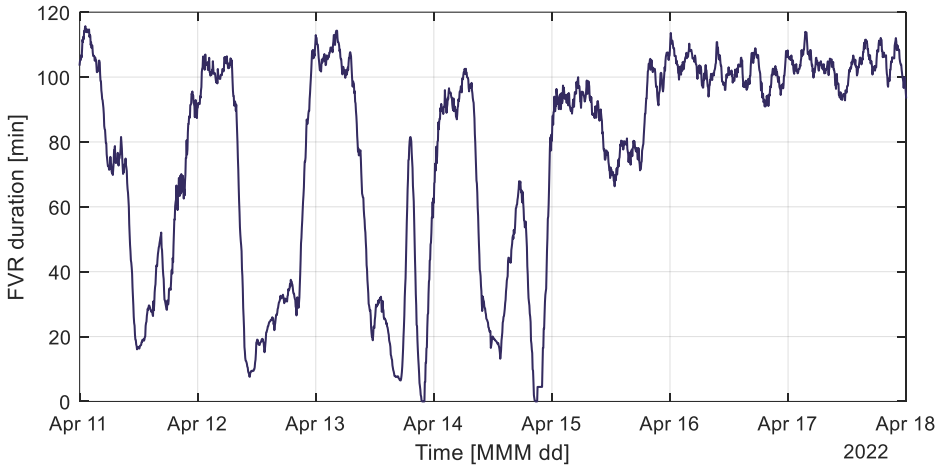

Figure 5.13. Example of one-week FVR duration estimations.

5.2.2.3 Flexibility service activations and pricing

The cost of operating the ventilation system and the CO_2 concentration measurements were used to determine the reduction of cost that it would generate to provide flexibility. For instance, upward regulations are depicted in Figure 5.14, where the tendered price was computed using equation (3.24), and comfort cost was obtained from the maximum balanced energy price for the previous two weeks. Calculations also considered the highest rate of CO_2 generated over the previous two weeks. The reserve was only activated when the tendered price was less than the balance energy market price, the mFRR was activated, and there was more than 100 W of available flexible power for the regulation. It can be seen that during high occupancy hours, the activated energy is lower since the CO_2 concentration will reach its limit faster compared to low occupancy hours, where the ventilation system can be exploited the most. Tendered price also shows the building usage, where the price increases when more people are inside rooms.

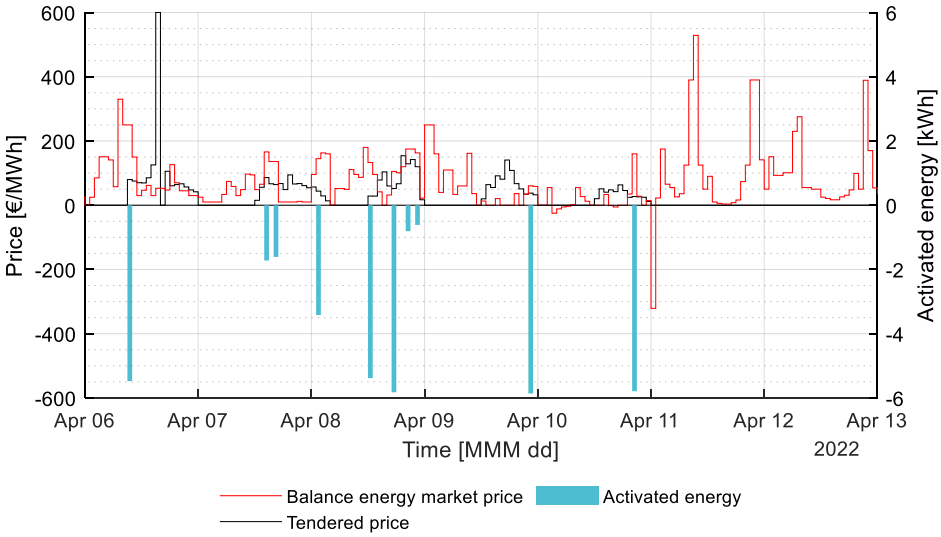

Figure 5.14. Prices and activations of the flexibility service.

With the ventilation system 303SV, no actual regulations were made. The measured power consumption was compared with the calculations done in Matlab. According to the calculations, the total energy of the fans used could decrease throughout the measurement period by 12.5%. The cost of energy could be lowered by 37%. These percentages are prone to changes if the building usage or electricity price changes. During four weeks, the total operation cost of the ventilation system could be reduced by 157 euros, meaning that the annual cost savings could be up to 2000 euros. It is not the only ventilation system in the building, meaning that annual cost savings could be increased even more while providing more flexibility to the grid.

Table 5.5. Regulation effect on energy consumption and cost of energy.

Parameter	**Value**
Energy consumption without regulations	1.68 MWh
Energy consumption with regulations	1.47 MWh
The total cost of energy without regulations	419.48 €
The total cost of energy with regulations	262.85 €

5.3 Conclusions

This chapter described case studies of the flexibility management methods of the developed ventilation system in a building discussed in Chapter 3. The case studies continued the validation process described in Chapter 4, which aimed to test the performance of the management methods in actual usage. Two case studies were performed in one of TalTech educational buildings. The first case study considered a single activation where the room usage was around 1/3. The focus of the second case study was on a multi-zone ventilation system that was monitored for six weeks. The measurement results were used to estimate the flexibility potential of the system. The outcomes addressed power consumption, FVR duration, and economic parameters where the main observations were:

- ARMA(p, q) model is suitable to forecast ventilation system power consumption. The forecast MAPE was around 2.2% for the system in the first case study and 4.3% for the second case study.
- The second case study showed that the ventilation system could provide, in around 75% of cases, the maximum power for up-regulations for at least 30 minutes.
- CO_2 concentration based FVR duration estimation error was 2 min for the first case study at the activation time.
- According to the results acquired from the second case study, it is possible to reduce the total cost of energy by at least 30%.

With the results acquired from this chapter, it is possible to implement the developed flexibility management methods on real systems. Furthermore, the economic findings of this chapter enable the assessment and feasibility studies of integrating ventilation systems in the flexibility service. The fourth hypothesis is correct for most cases where at least 5% of the total cost reduction was noted with the flexibility service. However, in some cases, it can be challenging to achieve. If the system is already operating at the limit, then there are fewer cost savings, but for the case study where the actual ventilation system was monitored, the cost savings could be up to 37%.

6 Conclusions and future work

This doctoral thesis provides novel flexibility management methods for ventilation systems. The developed methods enable the integration of ventilation systems in a flexibility service, thus providing more flexible power to TSOs and other balancing authorities. The findings and results of this thesis are also valuable for building owners who can now reduce energy costs by providing flexibility service with their ventilation systems. In a broader sense, these methods will aid the deployment of renewable energy sources. Besides conventional flexibility sources (e.g., energy storage, power plants), demand-side flexibility where ventilation systems are exploited now has more potential to balance the electric power system.

The developed management methods are created from an aggregator's viewpoint. The flexibility of a ventilation system is described mainly through three parameters: flexible power, FVR duration, and price for the regulation. Flexible power is the amount of power consumption that can be altered. Calculations of the flexible power are based on historical data by implementing the ARMA forecasting model. FVR duration estimations are based on the mass and energy balance analysis. It is achieved by considering the zone size, supply air, return air, and measurement data. The price for the service is calculated for up- and down-regulations separately. During up-regulations, it is crucial to consider buildings with higher usage. The regulation effect is more noticeable, thus causing it to be more expensive. During down-regulations, additional energy consumption is caused by increasing power consumption. It is compensated through a CO_2 concentration level where a higher concentration level provides lower regulation prices.

Flexibility management methods are needed to integrate loads like ventilation systems of different buildings (e.g., residential and commercial) into the flexibility service. However, the available methods described in research papers require further development for implementation in practice. Heating and cooling systems have received much attention from researchers, but the potential of ventilation systems has been left out of focus. Methods described in research papers lack robustness or do not give the building owners or aggregators clear guidelines on implementing these in their systems.

Validation of the developed methods was done with simulations and two case studies. Simulations used data generated with validated building models constructed in IDA ICE. All calculations were done, and the algorithm was written in Matlab. The primary outcomes of the validation process are:

- ARMA(p, q) model is sufficient to forecast ventilation system power consumption. The maximum forecast MAPE of 6.5% was observed with a single-family building with a stochastic occupancy profile. Also, the VAV type system was used for this case, which decreases the accuracy of the forecast.
- The open-loop approach to estimate FVR duration can be a viable option if the occupancy profile does not change over time and the aim is to minimize initial investment costs. From the results of the small room, the variance of residuals is low, but there is a bias that can be removed if parameters are adjusted to actual conditions.
- Placing sensors only in the AHU is also a viable option if the aim is to lower the initial investment costs. The residual analysis showed higher variability and lower accuracy than placing sensors in each room. Portable sensors could be used to improve the performance of this approach to tune the corrected boundaries.

- FVR duration estimations based on CO_2 concentration showed an RMSE of around 8 min when the fixed occupancy profile was selected and around 12 min when the stochastic occupancy profile was used. FVR duration estimations based on temperature showed an RMSE around 20 min for most scenarios. Therefore, temperature-based FVR duration is more difficult to estimate accurately, but it can be expected that the estimations will also become more accurate with shorter delivery periods. Relative humidity had no significant impact on the ventilation system's flexibility.
- The results showed that cost savings are achievable when a ventilation system is integrated into a flexibility service. In the apartment, up to 11% of cost savings were achieved; in the office, up to 15%; in the single-family house, up to 4%; and in the educational building, up to 37%. The cost savings heavily depend on how much the ventilation system can be exploited in the flexibility service. If the IAQ parameters are already near the limit, then there is less possibility to exploit the system in the flexibility service.
- A ventilation system as virtual energy storage is a viable approach to maximize energy capacity and revenue. VES approach can increase the total cost savings twofold compared to operating a ventilation system at a minimum ventilation rate during activation of the reserve.

At the beginning of this research, five main hypotheses were made. Therefore, based on the results discussed in this thesis, the following conclusions and remarks can be made:

1. The development of the ventilation system flexibility management method showed that the hypothesis is correct, as mass and energy balance analysis combined with sensor data enables the estimation of forced ventilation rate duration.
2. For most cases, the IAQ limits were not exceeded in more than 95% of situations when the reserve was activated. High CO_2 concentration in rooms and stochastic occupancy increase the probability that the IAQ limit will be exceeded during a regulation.
3. Most of the studied ventilation systems could provide more than half of the cases when the reserve is activated for at least 30 min, the maximum amount of power. The exception is the single-family house, where at least 30 min of FVR duration was achieved for around 35% of the cases. The high pollutant concentration caused this during normal conditions.
4. ARMA(p, q) models that forecast power consumption 24 h ahead had the MAPE less than 10% for all cases. FVR duration estimation errors of CO_2 concentration were mostly within 10 min, except for a single-family house where the RMSE was 13 minutes. However, temperature-based FVR durations are more challenging to estimate, and the RMSE of 20 min was observed.
5. At least 5% of the total cost reduction is possible with the flexibility service, but in some cases, it can be challenging to achieve. If the system is already operating at the limit, then there are fewer cost savings, but for the case study where the actual ventilation system was monitored, the cost savings could be up to 37%.

6.1 Future work

Future challenges in managing the flexibility of ventilation systems lie in improving and adapting the methods. Due to the complex nature of the problem and the urge to maximize the potential of ventilation systems in the flexibility service, the author has identified the following directions for further research on this topic:

- Identification of the zone volume should be achieved without measuring it separately. In some cases, the actual volume of the zone is difficult to measure due to furniture. Fluctuations in the CO_2 concentration can be used to achieve it.
- Using portable sensors and acquiring environment measurement data from smart devices can be a potential alternative to a dedicated sensor or can be employed to improve the accuracy of the calculations.
- Machine learning approaches can assist and improve the accuracy of the management methods addressed in this thesis. The more data is generated, the more accurate the estimations will be.
- While the methods have been validated in simulations and two case studies, it is crucial to implement this in a real system to further the investigation of the performance of the methods in different conditions.
- The developed pricing model to calculate the price for each activation needs to be further investigated and improved. One improvement is optimizing the profit margins to achieve an optimum between ventilation system exploitation and revenue generation.
- The focus is mainly on industrial and commercial consumers that can provide flexibility. However, methods and products to include households with smaller capacities to the flexibility service are needed.

List of figures

Figure 1.1. Characterization of ventilation systems by system type and control. 15
Figure 1.2. The concept of flexible control of a ventilation system. 16
Figure 1.3. Share of the installed power of the ventilation system for each building type during the last decade. 19
Figure 2.1. Classification of energy flexibility and main sources of flexibility [24]. 20
Figure 2.2. World electricity consumption by sector in 2019 [33]. 21
Figure 2.3. Weighted distribution of electricity consumption in two office buildings [11]. 22
Figure 2.4. Distribution of electricity consumption in Estonian residential buildings [35]. 23
Figure 2.5. Concept of aggregating flexible loads in buildings. 25
Figure 2.6. Example of power spectral density of net demand and allocation of resources to cover the electric system needs [64]. 27
Figure 2.7. Activation process of balancing market reserves [81]. 28
Figure 2.8. Proposed structure of nZEB nanogrid [Paper VI]. 34
Figure 3.1. Flexible power and duration. 36
Figure 3.2. Example of weekly power consumption of a CAV type system. 37
Figure 3.3. Example of weekly power consumption of a single-zone VAV type system. 38
Figure 3.4. Example of weekly power consumption of a multi-zone VAV type system. . 38
Figure 3.5. Occupant schedules for a) educational and b) commercial buildings [127]. 42
Figure 3.6. Occupant schedules for a) office buildings and b) dwellings [127]. 42
Figure 3.7. Dependence of the regulation price on a) CO_2 generation rate for up-regulation and b) CO_2 concentration for down-regulation. 51
Figure 3.8. Rebound effect of a VAV type ventilation system..... 52
Figure 3.9. Algorithm selection procedure for flexibility management. 54
Figure 3.10. Implementation of the flexibility management methods [Paper I]. 55
Figure 3.11. Available flexible power of a ventilation system at time t. 56
Figure 3.12. Energy capacity dependence on CO_2 concentration in a building. 57
Figure 3.13. Energy capacity dependence on the reduction of power consumption. 57
Figure 3.14. CO_2 concentration-based SoC estimation for a ventilation system. 58
Figure 3.15. Dependence of the self-discharge rate on the CO_2 concentration. 59
Figure 4.1. MATLAB and IDA ICE co-simulation process [Paper I]..... 61
Figure 4.2. The room of a building used in simulations [Paper II]..... 66
Figure 4.3. The single-family house used in simulations..... 67
Figure 4.4. Floor plan of the single-family house [Paper I]. 68
Figure 4.5. Room-specific occupancy schedule..... 69
Figure 4.6. System layout of the air handling unit [Paper I]..... 70
Figure 4.7. Power consumption of office and apartment AHU with regulations. 73
Figure 4.8. FVR duration estimations for office and apartment ventilation systems. 74
Figure 4.9. Residuals of the FVR duration estimations for object 1. 75
Figure 4.10. Example of a VES state of charge during a week [Paper II]. 76
Figure 4.11. Example of VES power consumption, charge, and discharge power of the office during a week [Paper II]. 76
Figure 4.12. Example of VES power consumption and discharge power of the apartment during a week [Paper II]. 77
Figure 4.13. Residuals of VES energy capacity estimations for up-regulations [Paper II]. . 77
Figure 4.14. Example of flexibility service prices and activation during a week for up-regulations. 78

Figure 4.15. Distribution of FVR durations where an IAQ parameter limit was reached. . 80
Figure 4.16. Measured and forecasted power consumption of the ventilation system [Paper I]. 81
Figure 4.17. Daily IAQ parameter limits after the correction of the boundary condition [Paper I]. 82
Figure 4.18. Example of one-week FVR duration estimations for a CAV type ventilation system. 82
Figure 4.19. Example of one-week FVR duration estimations for a VAV type ventilation system. 83
Figure 4.20. Residuals of the FVR duration forecasting. 83
Figure 4.21. Flexibility service prices and activations. 84
Figure 5.1. TalTech SOC educational building. 87
Figure 5.2. Power consumption of SOC building ventilation systems. 88
Figure 5.3. The auditorium and measurement equipment layout [Paper III]. 89
Figure 5.4. Ventilation system 306SV layout and placement of measurement equipment [Paper III]. 90
Figure 5.5. IAQ logger location in a lecture room [145]. 91
Figure 5.6. The power consumption of the ventilation system and the airflow rate during the experiment [Paper III]. 93
Figure 5.7. Measured and forecasted power consumption of the ventilation system. .. 94
Figure 5.8. CO_2 concentration in extract air during the experiment [Paper III]. 94
Figure 5.9. Measured and estimated FVR durations [Paper III]. 95
Figure 5.10. Flexibility service prices and activations [Paper III]. 96
Figure 5.11. Distribution of CO_2 concentration based FVR duration estimates shorter than 60 minutes. 96
Figure 5.12. Example of measured and forecasted power consumption of the ventilation system. 97
Figure 5.13. Example of one-week FVR duration estimations. 98
Figure 5.14. Prices and activations of the flexibility service. 98

List of tables

Table 2.1. Baltic mFRR standard product characteristics [85]. 29
Table 2.2. List of algorithms used in energy management systems [103]. 31
Table 2.3. Limit values for energy performance indicator in nZEB. 33
Table 3.1. Building occupancy and ventilation rate ratios to a floor area [127]. 43
Table 3.2. Temperature ranges for normal conditions according to space type and season [127]. 45
Table 3.3. Values for the constants [129]. 46
Table 3.4. Heat generation by human beings in different states of activity [128]. 48
Table 4.1. IAQ categories and values for calculating the ventilation rate [127]. 62
Table 4.2. Building parameters for simulations [127]. 64
Table 4.3. Occupancy schedule according to a room type. 66
Table 4.4. Parameters of the room ventilation system for simulations. 67
Table 4.5. Operation schedule of the air handling unit during workdays. 70
Table 4.6. Scenarios for ventilation system flexible control. 71
Table 4.7. Simulation parameters for office. 71
Table 4.8. Simulation parameters for an apartment. 72
Table 4.9. Performance of FVR duration estimation methods with object 1. 75
Table 4.10. Baseline values of energy consumption and cost of energy. 78
Table 4.11. Regulation effect on the energy consumption and cost of energy. 79
Table 4.12. Simulation parameters and counts. 80
Table 4.13. Performance of FVR duration estimation methods with object 2. 84
Table 4.14. Regulation effect on energy consumption and cost of energy. 85
Table 5.1. Ventilation systems in the TalTech SOC building and the design values. 88
Table 5.2. Rooms connected to ventilation system 303 [145]. 91
Table 5.3. HOBO MX1102A CO_2 logger specification [146]. 92
Table 5.4. Events of the case study and schedule [Paper III]. 93
Table 5.5. Regulation effect on energy consumption and cost of energy. 99

References

[1] European Commission, “Renewable energy directive.” Accessed: May 20, 2021. [Online]. Available: https://ec.europa.eu/energy/topics/renewable-energy/renewable-energy-directive/overview_en

[2] European Commission. Statistical Office of the European Union., “Shedding light on energy in the EU : 2023 interactive publication.,” 2023.

[3] S. Kerscher and P. Arboleya, “The key role of aggregators in the energy transition under the latest European regulatory framework,” *International Journal of Electrical Power and Energy Systems*, vol. 134, no. July 2021, p. 107361, 2022, doi: 10.1016/j.ijepes.2021.107361.

[4] Elering AS, “Sünkroniseerimine Mandri-Euroopaga.” Accessed: May 20, 2021. [Online]. Available: https://elering.ee/sunkroniseerimine

[5] European Commission, “Energy performance of buildings directive.” Accessed: May 20, 2021. [Online]. Available: https://ec.europa.eu/energy/topics/energy-efficiency/energy-efficient-buildings/energy-performance-buildings-directive

[6] Estonian Government, “Minimum requirements for energy performance,” Riigi Teataja. Accessed: May 20, 2021. [Online]. Available: https://www.riigiteataja.ee/en/eli/520102014001

[7] Eurelectric, “Flexibility and aggregation - requirements for their interaction in the market,” 2014.

[8] J. Song, Y. Lee, and E. Hwang, “Time-Frequency Mask Estimation Based on Deep Neural Network for Flexible Load Disaggregation in Buildings,” *IEEE Trans Smart Grid*, vol. 12, no. 4, pp. 3242–3251, Jul. 2021, doi: 10.1109/TSG.2021.3066547.

[9] Z. Li, S. Su, X. Jin, H. Chen, Y. Li, and R. Zhang, “A hierarchical scheduling method of active distribution network considering flexible loads in office buildings,” *International Journal of Electrical Power & Energy Systems*, vol. 131, p. 106768, Oct. 2021, doi: 10.1016/J.IJEPES.2021.106768.

[10] F. Mancini, G. lo Basso, and L. de Santoli, “Energy Use in Residential Buildings: Characterisation for Identifying Flexible Loads by Means of a Questionnaire Survey,” *Energies 2019, Vol. 12, Page 2055*, vol. 12, no. 11, p. 2055, May 2019, doi: 10.3390/EN12112055.

[11] I. Drovtar, J. Niitsoo, A. Rosin, J. Kilter, and I. Palu, “Electricity consumption analysis and power quality monitoring in commercial buildings,” *PQ 2012: 8th International Conference - 2012 Electric Power Quality and Supply Reliability, Conference Proceedings*, pp. 107–112, 2012.

[12] M. Gil-Baez, Á. Barrios-Padura, M. Molina-Huelva, and R. Chacartegui, “Natural ventilation systems in 21st-century for near zero energy school buildings,” *Energy*, vol. 137, pp. 1186–1200, Oct. 2017, doi: 10.1016/J.ENERGY.2017.05.188.

[13] U.S. Department of Energy, “Whole-House Ventilation.” Accessed: Dec. 01, 2021. [Online]. Available: https://www.energy.gov/energysaver/whole-house-ventilation

[14] D. Burmester, R. Rayudu, W. Seah, and D. Akinyele, “A review of nanogrid topologies and technologies,” *Renewable and Sustainable Energy Reviews*, vol. 67, pp. 760–775, Jan. 2017, doi: 10.1016/J.RSER.2016.09.073.

[15] A. Burgio, D. Menniti, N. Sorrentino, A. Pinnarelli, and M. Motta, “A compact nanogrid for home applications with a behaviour-tree-based central controller,” *Appl Energy*, vol. 225, pp. 14–26, Sep. 2018, doi: 10.1016/J.APENERGY.2018.04.082.

[16] Y. Han, X. Xie, H. Deng, and W. Ma, “Central energy management method for photovoltaic DC micro-grid system based on power tracking control,” *IET Renewable Power Generation*, vol. 11, no. 8, pp. 1138–1147, Jun. 2017, doi: 10.1049/IET-RPG.2016.0351.

[17] M. Movahednia, H. Karimi, and S. Jadid, “Optimal hierarchical energy management scheme for networked microgrids considering uncertainties, demand response, and adjustable power,” *IET Generation, Transmission & Distribution*, vol. 14, no. 20, pp. 4352–4362, Oct. 2020, doi: 10.1049/IET-GTD.2020.0287.

[18] Statistics Estonia, “Granted building permits and completed buildings.”

[19] Ettevõtlus- ja infotehnoloogiaminister, “Hoone energiatõhususe miinimumnõuded,” Riigi Teataja. Accessed: Jan. 03, 2022. [Online]. Available: https://www.riigiteataja.ee/akt/113122018014?leiaKehtiv

[20] H. Kuivjõgi, A. Uutar, K. Kuusk, M. Thalfeldt, and J. Kurnitski, “Market based renovation solutions in non-residential buildings – Why commercial buildings are not renovated to NZEB,” *Energy Build*, vol. 248, Oct. 2021, doi: 10.1016/J.ENBUILD.2021.111169.

[21] H. Hao, Y. Lin, A. S. Kowli, P. Barooah, and S. Meyn, “Ancillary Service to the grid through control of fans in commercial Building HVAC systems,” *IEEE Trans Smart Grid*, vol. 5, no. 4, pp. 2066–2074, 2014.

[22] Elering AS, Augstsprieguma tīkls AS, and Litgrid AB, “Baltic Transparency Dashboard.” Accessed: May 22, 2023. [Online]. Available: https://baltic.transparency-dashboard.eu/

[23] Elering AS, “Elering Live.” Accessed: May 22, 2023. [Online]. Available: https://dashboard.elering.ee/en

[24] T. Freire-Barceló, F. Martín-Martínez, and Á. Sánchez-Miralles, “A literature review of Explicit Demand Flexibility providing energy services,” *Electric Power Systems Research*, vol. 209, p. 107953, Aug. 2022, doi: 10.1016/J.EPSR.2022.107953.

[25] I. Mamounakis, D. J. Vergados, P. Makris, E. Varvarigos, and T. Mavridis, “A Virtual MicroGrid platform for the efficient orchestration of multiple energy prosumers,” *ACM International Conference Proceeding Series*, vol. 01-03-October-2015, pp. 191–196, Oct. 2015, doi: 10.1145/2801948.2802012.

[26] A. F. Meyabadi and M. H. Deihimi, “A review of demand-side management: Reconsidering theoretical framework,” *Renewable and Sustainable Energy Reviews*, vol. 80, pp. 367–379, Dec. 2017, doi: 10.1016/J.RSER.2017.05.207.

[27] Pöyry and Imperial College London, “Roadmap for flexibility services to 2030 - A report to the Committee on Climate Change,” 2017.

[28] E. Ercan and E. Kentel, “Optimum daily operation of a wind-hydro hybrid system,” *J Energy Storage*, vol. 50, Jun. 2022, doi: 10.1016/J.EST.2022.104540.

[29] M. M. Bertsiou and E. Baltas, “Management of energy and water resources by minimizing the rejected renewable energy,” *Sustainable Energy Technologies and Assessments*, vol. 52, Aug. 2022, doi: 10.1016/J.SETA.2022.102002.

[30] J. H. Halleraker, M. S. Kenawi, J. H. L’Abée-Lund, T. H. Bakken, and K. Alfredsen, “Assessment of flow ramping in water bodies impacted by hydropower operation in Norway – Is hydropower with environmental restrictions more sustainable?,” *Science of The Total Environment*, vol. 832, p. 154776, Aug. 2022, doi: 10.1016/J.SCITOTENV.2022.154776.

[31] Y. Qiu and F. Jiang, “A review on passive and active strategies of enhancing the safety of lithium-ion batteries,” *Int J Heat Mass Transf*, vol. 184, Mar. 2022, doi: 10.1016/J.IJHEATMASSTRANSFER.2021.122288.

[32] K. W. See *et al.*, “Critical review and functional safety of a battery management system for large-scale lithium-ion battery pack technologies,” *Int J Coal Sci Technol*, vol. 9, no. 1, Dec. 2022, doi: 10.1007/S40789-022-00494-0.

[33] IEA, “World electricity final consumption by sector, 1974-2019, IEA, Paris.” Accessed: Sep. 10, 2021. [Online]. Available: https://www.iea.org/data-and-statistics/charts/world-electricity-final-consumption-by-sector-1974-2019

[34] Global Alliance for Buildings and Construction, “2020 global status report for buildings and construction - towards a zero-emissions, efficient and resilient buildings and construction sector,” 2020. Accessed: Sep. 09, 2022. [Online]. Available: www.globalabc.org.

[35] European Commission, “EU Buildings Factsheets.” Accessed: Sep. 11, 2021. [Online]. Available: https://ec.europa.eu/energy/eu-buildings-factsheets_en

[36] A. R. Coffman, Z. Guo, and P. Barooah, “Characterizing Capacity of Flexible Loads for Providing Grid Support,” *IEEE Transactions on Power Systems*, vol. 36, no. 3, pp. 2428–2437, May 2021, doi: 10.1109/TPWRS.2020.3033380.

[37] H. Tang, S. Wang, and H. Li, “Flexibility categorization, sources, capabilities and technologies for energy-flexible and grid-responsive buildings: State-of-the-art and future perspective,” *Energy*, vol. 219, Mar. 2021, doi: 10.1016/j.energy.2020.119598.

[38] T. Kaschub, P. Jochem, and W. Fichtner, “Solar energy storage in German households: profitability, load changes and flexibility,” *Energy Policy*, vol. 98, pp. 520–532, Nov. 2016, doi: 10.1016/J.ENPOL.2016.09.017.

[39] R. Luthander, J. Widén, D. Nilsson, and J. Palm, “Photovoltaic self-consumption in buildings: A review,” *Appl Energy*, vol. 142, pp. 80–94, Mar. 2015, doi: 10.1016/J.APENERGY.2014.12.028.

[40] R. Kempener, “Clean Energy Solutions Center | Battery Storage for Renewables: Market Status and Technology Outlook,” Abu Dhabi, 2015. Accessed: Aug. 26, 2022. [Online]. Available: https://cleanenergysolutions.org/resources/battery-storage-renewables-market-status-technology-outlook

[41] M. A. López, S. de La Torre, S. Martín, and J. A. Aguado, “Demand-side management in smart grid operation considering electric vehicles load shifting and vehicle-to-grid support,” *International Journal of Electrical Power & Energy Systems*, vol. 64, pp. 689–698, Jan. 2015, doi: 10.1016/J.IJEPES.2014.07.065.

[42] X. Han, T. Ji, Z. Zhao, and H. Zhang, “Economic evaluation of batteries planning in energy storage power stations for load shifting,” *Renew Energy*, vol. 78, pp. 643–647, Jun. 2015, doi: 10.1016/J.RENENE.2015.01.056.

[43] Q. A. Phan, T. Scully, M. Breen, and M. D. Murphy, “Determination of optimal battery utilization to minimize operating costs for a grid-connected building with renewable energy sources,” *Energy Convers Manag*, vol. 174, pp. 157–174, Oct. 2018, doi: 10.1016/J.ENCONMAN.2018.07.081.

[44] G. He, Q. Chen, C. Kang, Q. Xia, and K. Poolla, “Cooperation of Wind Power and Battery Storage to Provide Frequency Regulation in Power Markets,” *IEEE Transactions on Power Systems*, vol. 32, no. 5, pp. 3559–3568, Sep. 2017, doi: 10.1109/TPWRS.2016.2644642.

[45] I. H. Yang and E. J. Nam, “Economic analysis of the daylight-linked lighting control system in office buildings,” *Solar Energy*, vol. 84, no. 8, pp. 1513–1525, Aug. 2010, doi: 10.1016/J.SOLENER.2010.05.014.

[46] F. Rubinstein, L. Xiaolei, and D. S. Watson, “Using Dimmable Lighting for Regulation Capacity and Contingency Reserves in the Ancillary Services Market. A Feasibility Study,” 2010. Accessed: Sep. 01, 2022. [Online]. Available: https://www.osti.gov/servlets/purl/1004218

[47] A. Arteconi *et al.*, “Thermal energy storage coupled with PV panels for demand side management of industrial building cooling loads,” *Appl Energy*, vol. 185, pp. 1984–1993, Jan. 2017, doi: 10.1016/J.APENERGY.2016.01.025.

[48] S. H. Kim, “An evaluation of robust controls for passive building thermal mass and mechanical thermal energy storage under uncertainty,” *Appl Energy*, vol. 111, pp. 602–623, Nov. 2013, doi: 10.1016/J.APENERGY.2013.05.030.

[49] E. Nyholm, S. Puranik, É. Mata, M. Odenberger, and F. Johnsson, “Demand response potential of electrical space heating in Swedish single-family dwellings,” *Build Environ*, vol. 96, pp. 270–282, Feb. 2016, doi: 10.1016/J.BUILDENV.2015.11.019.

[50] B. Kirby, J. Kueck, T. Laughner, and K. Morris, “Spinning Reserve from Hotel Load Response,” *The Electricity Journal*, vol. 21, no. 10, pp. 59–66, Dec. 2008, doi: 10.1016/J.TEJ.2008.11.004.

[51] J. Bode, M. Sullivan, and J. H. Eto, “Measuring Short-term Air Conditioner Demand Reductions for Operations and Settlement | Electricity Markets and Policy Group,” Berkeley, 2012. Accessed: Sep. 02, 2022. [Online]. Available: https://emp.lbl.gov/publications/measuring-short-term-air-conditioner

[52] J. Cai and J. E. Braun, “A regulation capacity reset strategy for HVAC frequency regulation control,” *Energy Build*, vol. 185, pp. 272–286, Feb. 2019, doi: 10.1016/J.ENBUILD.2018.12.018.

[53] H. Hao, Y. Lin, A. S. Kowli, P. Barooah, and S. Meyn, “Ancillary Service to the grid through control of fans in commercial Building HVAC systems,” *IEEE Trans Smart Grid*, vol. 5, no. 4, pp. 2066–2074, 2014, doi: 10.1109/TSG.2014.2322604.

[54] R. D’hulst, W. Labeeuw, B. Beusen, S. Claessens, G. Deconinck, and K. Vanthournout, “Demand response flexibility and flexibility potential of residential smart appliances: Experiences from large pilot test in Belgium,” *Appl Energy*, vol. 155, pp. 79–90, Oct. 2015, doi: 10.1016/J.APENERGY.2015.05.101.

[55] D. Setlhaolo, X. Xia, and J. Zhang, “Optimal scheduling of household appliances for demand response,” *Electric Power Systems Research*, vol. 116, pp. 24–28, Nov. 2014, doi: 10.1016/J.EPSR.2014.04.012.

[56] European Smart Grids Task Force Expert Group 3, “Demand Side Flexibility Perceived barriers and proposed recommendations,” 2019.

[57] R. Kucęba, “Dimensions and Factors that Determine Integration of Small-Scale Sources in the Structures of Virtual Power Plants,” *Production Engineering Archives*, vol. 28, no. 2, pp. 185–192, Jun. 2022, doi: 10.30657/PEA.2022.28.22.

[58] S. Awerbuch and A. Preston, *The Virtual Utility*. Springer US, 1997. doi: 10.1007/978-1-4615-6167-5.

[59] M. Ferrara, A. Violi, P. Beraldi, G. Carrozzino, and T. Ciano, “An integrated decision approach for energy procurement and tariff definition for prosumers aggregations,” *Energy Econ*, vol. 97, p. 105034, May 2021, doi: 10.1016/J.ENECO.2020.105034.

[60] T. Freire-Barceló, F. Martín-Martínez, and Á. Sánchez-Miralles, "A literature review of Explicit Demand Flexibility providing energy services," *Electric Power Systems Research*, vol. 209, Aug. 2022, doi: 10.1016/J.EPSR.2022.107953.

[61] M. Kubli and P. Canzi, "Business strategies for flexibility aggregators to steer clear of being 'too small to bid,'" *Renewable and Sustainable Energy Reviews*, vol. 143, p. 110908, Jun. 2021, doi: 10.1016/J.RSER.2021.110908.

[62] "USEF: WORK STREAM ON AGGREGATOR IMPLEMENTATION MODELS Recommended practices and key considerations for a regulatory framework and market design on explicit Demand Response A solid foundation for smart energy futures".

[63] "Demand Response Activation by Independent Aggregators As Proposed in the Draft Electricity Directive On behalf of EURELECTRIC", Accessed: Sep. 08, 2022. [Online]. Available: www.dnvgl.com

[64] P. Barooah, "Smart Grid Control: Overview and Research Opportunities," J. Stoustrup, A. Annaswamy, A. Chakrabortty, and Z. Qu, Eds., in Power Electronics and Power Systems. Cham: Springer International Publishing, 2019. doi: 10.1007/978-3-319-98310-3.

[65] G. Parkinson, "UBS: closures coal and gas fired power plants in Europe accelerating." Accessed: Sep. 05, 2020. [Online]. Available: https://energypost.eu/ubs-closures-coal-gas-fired-power-plants-europe-accelerating/

[66] T. Kim *et al.*, "An Overview of Cyber-Physical Security of Battery Management Systems and Adoption of Blockchain Technology," *IEEE J Emerg Sel Top Power Electron*, vol. 10, no. 1, pp. 1270–1281, Feb. 2022, doi: 10.1109/JESTPE.2020.2968490.

[67] X. Lai *et al.*, "Critical review of life cycle assessment of lithium-ion batteries for electric vehicles: A lifespan perspective," *eTransportation*, vol. 12, May 2022, doi: 10.1016/J.ETRAN.2022.100169.

[68] T. Raj *et al.*, "Recycling of cathode material from spent lithium-ion batteries: Challenges and future perspectives," *J Hazard Mater*, vol. 429, p. 128312, May 2022, doi: 10.1016/J.JHAZMAT.2022.128312.

[69] L. Meng *et al.*, "Large-Scale Li-Ion Battery Research and Application in Mining Industry," *Energies 2022, Vol. 15, Page 3884*, vol. 15, no. 11, p. 3884, May 2022, doi: 10.3390/EN15113884.

[70] K. W. See *et al.*, "Critical review and functional safety of a battery management system for large-scale lithium-ion battery pack technologies," *Int J Coal Sci Technol*, vol. 9, no. 3, p. 36, 2022, doi: 10.1007/s40789-022-00494-0.

[71] S. Meyn, P. Barooah, A. Bušić, and J. Ehren, "Ancillary service to the grid from deferrable loads: The case for intelligent pool pumps in Florida," *Proceedings of the IEEE Conference on Decision and Control*, pp. 6946–6953, 2013, doi: 10.1109/CDC.2013.6760990.

[72] A. Nayyar, M. Negrete-Pincetic, K. Poolla, and P. Varaiya, "Duration-Differentiated Energy Services with a Continuum of Loads," *IEEE Trans Control Netw Syst*, vol. 3, no. 2, pp. 182–191, Jun. 2016, doi: 10.1109/TCNS.2015.2428491.

[73] A. R. Coffman, Z. Guo, and P. Barooah, "Capacity of flexible loads for grid support: Statistical characterization for long term planning," *Proceedings of the American Control Conference*, vol. 2020-July, pp. 533–538, Jul. 2020, doi: 10.23919/ACC45564.2020.9147252.

[74] H. Hao, B. M. Sanandaji, K. Poolla, and T. L. Vincent, “Aggregate flexibility of thermostatically controlled loads,” *IEEE Transactions on Power Systems*, vol. 30, no. 1, pp. 189–198, Jan. 2015, doi: 10.1109/TPWRS.2014.2328865.

[75] A. R. Coffman, A. Busic, and P. Barooah, “Aggregate capacity for TCLs providing virtual energy storage with cycling constraints,” *Proceedings of the IEEE Conference on Decision and Control*, vol. 2019-December, pp. 4208–4215, Dec. 2019, doi: 10.1109/CDC40024.2019.9028939.

[76] S. Kundu, K. Kalsi, and S. Backhaus, “Approximating flexibility in distributed energy resources: A geometric approach,” *20th Power Systems Computation Conference, PSCC 2018*, Aug. 2018, doi: 10.23919/PSCC.2018.8442600.

[77] F. Lin and V. Adetola, “Flexibility characterization of multi-zone buildings via distributed optimization,” *Proceedings of the American Control Conference*, vol. 2018-June, pp. 5412–5417, Aug. 2018, doi: 10.23919/ACC.2018.8431400.

[78] “EUR-Lex - 32017R2195 - EN - EUR-Lex.” Accessed: Sep. 08, 2022. [Online]. Available: https://eur-lex.europa.eu/legal-content/EN/TXT/?uri=CELEX%3A32017R2195

[79] A. Uk, “DEMAND RESPONSE PARTICIPATION IN DIFFERENT MARKETS IN EUROPE CORE View metadata, citation and similar papers at core,” 2019.

[80] “ACER’s Final Assessment of the EU Wholesale Electricity Market Design,” 2022.

[81] AS “Augstsprieguma tīkls,” E. AS, and L. AB, “Baltic Load-Frequency Control block concept document,” p. 69, 2020, [Online]. Available: https://www.ast.lv/sites/default/files/editor/Baltic_Load_Frequency_Control_concept_document.pdf

[82] “PICASSO.” Accessed: Sep. 08, 2022. [Online]. Available: https://www.entsoe.eu/network_codes/eb/picasso/

[83] “Manually Activated Reserves Initiative.” Accessed: Sep. 08, 2022. [Online]. Available: https://www.entsoe.eu/network_codes/eb/mari/

[84] “TERRE.” Accessed: Sep. 08, 2022. [Online]. Available: https://www.entsoe.eu/network_codes/eb/terre/

[85] Elering AS, AS “Augstsprieguma tīkls,” and LITGRID AB, “Baltic balancing market rules,” 2020.

[86] F. Plaum, R. Ahmadiahangar, A. Rosin, and J. Kilter, “Aggregated demand-side energy flexibility: A comprehensive review on characterization, forecasting and market prospects,” *Energy Reports*, vol. 8, pp. 9344–9362, Nov. 2022, doi: 10.1016/J.EGYR.2022.07.038.

[87] F. Amara *et al.*, “Comparison and Simulation of Building Thermal Models for Effective Energy Management,” *Smart Grid and Renewable Energy*, vol. 6, no. 4, pp. 95–112, Apr. 2015, doi: 10.4236/SGRE.2015.64009.

[88] B. Lehmann, D. Gyalistras, M. Gwerder, K. Wirth, and S. Carl, “Intermediate complexity model for Model Predictive Control of Integrated Room Automation,” *Energy Build*, vol. 58, pp. 250–262, Mar. 2013, doi: 10.1016/J.ENBUILD.2012.12.007.

[89] A. Mirakhorli and B. Dong, “Model predictive control for building loads connected with a residential distribution grid,” *Appl Energy*, vol. 230, pp. 627–642, Nov. 2018, doi: 10.1016/J.APENERGY.2018.08.051.

[90] E. Vrettos, F. Oldewurtel, M. Vasirani, and G. Andersson, “Centralized and decentralized balance group optimization in electricity markets with demand response,” *2013 IEEE Grenoble Conference PowerTech, POWERTECH 2013*, 2013, doi: 10.1109/PTC.2013.6652519.

[91] X. Li, J. Wen, and E. W. Bai, “Building energy forecasting using system identification based on system characteristics test,” *2015 Workshop on Modeling and Simulation of Cyber-Physical Energy Systems, MSCPES 2015 - Held as Part of CPS Week, Proceedings*, May 2015, doi: 10.1109/MSCPES.2015.7115401.

[92] X. Li and J. Wen, “Review of building energy modeling for control and operation,” *Renewable and Sustainable Energy Reviews*, vol. 37, pp. 517–537, Sep. 2014, doi: 10.1016/J.RSER.2014.05.056.

[93] A. Kathirgamanathan, M. De Rosa, E. Mangina, and D. P. Finn, “Feature Assessment in Data-driven Models for unlocking Building Energy Flexibility”, doi: 10.26868/25222708.2019.210591.

[94] R. Yin *et al.*, “Quantifying flexibility of commercial and residential loads for demand response using setpoint changes,” *Appl Energy*, vol. 177, pp. 149–164, Sep. 2016, doi: 10.1016/J.APENERGY.2016.05.090.

[95] E. C. Kara, M. D. Tabone, J. S. MacDonald, D. S. Callaway, and S. Kiliccote, “Quantifying flexibility of residential thermostatically controlled loads for demand response: A data-driven approach,” *BuildSys 2014 - Proceedings of the 1st ACM Conference on Embedded Systems for Energy-Efficient Buildings*, pp. 140–147, Nov. 2014, doi: 10.1145/2674061.2674082.

[96] M. Behl, F. Smarra, and R. Mangharam, “DR-Advisor: A data-driven demand response recommender system,” *Appl Energy*, vol. 170, pp. 30–46, May 2016, doi: 10.1016/J.APENERGY.2016.02.090.

[97] D. S. Kapetanakis, O. Neu, and D. P. Finn, “Prediction of Residential Building Demand Response Potential Using Data-Driven Techniques,” *Building Simulation Conference Proceedings*, vol. 15, pp. 1656–1666, 2017, doi: 10.26868/25222708.2017.439.

[98] S. Prívara, Z. Váňa, E. Žáčeková, and J. Cigler, “Building modeling: Selection of the most appropriate model for predictive control,” *Energy Build*, vol. 55, pp. 341–350, Dec. 2012, doi: 10.1016/J.ENBUILD.2012.08.040.

[99] S. Prívara, J. Cigler, Z. Váňa, F. Oldewurtel, C. Sagerschnig, and E. Žáčeková, “Building modeling as a crucial part for building predictive control,” *Energy Build*, vol. 56, pp. 8–22, Jan. 2013, doi: 10.1016/J.ENBUILD.2012.10.024.

[100] P. Bacher and H. Madsen, “Identifying suitable models for the heat dynamics of buildings,” *Energy Build*, vol. 43, no. 7, pp. 1511–1522, Jul. 2011, doi: 10.1016/J.ENBUILD.2011.02.005.

[101] Z. Wang and Y. Chen, “Data-driven modeling of building thermal dynamics: Methodology and state of the art,” *Energy Build*, vol. 203, p. 109405, Nov. 2019, doi: 10.1016/J.ENBUILD.2019.109405.

[102] A. Kathirgamanathan, M. De Rosa, E. Mangina, and D. P. Finn, “Data-driven predictive control for unlocking building energy flexibility: A review,” *Renewable and Sustainable Energy Reviews*, vol. 135, Jan. 2021, doi: 10.1016/J.RSER.2020.110120.

[103] L. H. M. Truong *et al.*, “Accurate prediction of hourly energy consumption in a residential building based on the occupancy rate using machine learning approaches,” *Applied Sciences (Switzerland)*, vol. 11, no. 5, pp. 1–19, Mar. 2021, doi: 10.3390/app11052229.

[104] I. Walker, B. Less, D. Lorenzetti, and M. D. Sohn, “Development of Advanced Smart Ventilation Controls for Residential Applications,” *Energies 2021, Vol. 14, Page 5257*, vol. 14, no. 17, p. 5257, Aug. 2021, doi: 10.3390/EN14175257.

[105] J. Li, J. Wall, and G. Platt, “Indoor air quality control of HVAC system,” *Proceedings of the 2010 International Conference on Modelling, Identification and Control*, pp. 756–761, 2010.

[106] European Standard, “UNE-EN 15251:2008. Indoor environmental input parameters for design and assessment of energy performance of buildings addressing indoor air quality, thermal environment, lighting and acoustics,” *Aenor*, pp. 1–52, 2008, doi: 10.1520/E2019-03R13.Copyright.

[107] V. L. Erickson and A. E. Cerpa, “Occupancy based demand response HVAC control strategy,” *2nd ACM Workshop on Embedded Sensing Systems for Energy-Efficiency in Buildings (BuildSys’10)*, pp. 7–12, 2010, doi: 10.1145/1878431.1878434.

[108] Z. Yang, B. Becerik-Gerber, N. Li, and M. Orosz, “A systematic approach to occupancy modeling in ambient sensor-rich buildings,” *Simulation*, vol. 90, no. 8, pp. 960–977, 2014, doi: 10.1177/0037549713489918.

[109] Z. Shi, X. Li, and S. Hu, “Direct feedback linearization based control of CO2 demand controlled ventilation,” *ICCET 2010 - 2010 International Conference on Computer Engineering and Technology, Proceedings*, vol. 2, pp. 571–574, 2010, doi: 10.1109/ICCET.2010.5485621.

[110] L. Yu, D. Xie, C. Huang, T. Jiang, and Y. Zou, “Energy Optimization of HVAC Systems in Commercial Buildings Considering Indoor Air Quality Management,” *IEEE Trans Smart Grid*, vol. 10, no. 5, pp. 5103–5113, Sep. 2019, doi: 10.1109/TSG.2018.2875727.

[111] C. Luppe and A. Shabani, “Towards reliable intelligent occupancy detection for smart building applications,” *Canadian Conference on Electrical and Computer Engineering*, pp. 0–3, 2017, doi: 10.1109/CCECE.2017.7946831.

[112] Ettevõtlus- ja infotehnoloogiaminister, “Hoone energiatõhususe miinimumnõuded,” Riigi Teataja. Accessed: Aug. 16, 2023. [Online]. Available: https://www.riigiteataja.ee/akt/113122018014

[113] S. Rauf, A. R. Kalair, and N. Khan, “Variable Load Demand Scheme for Hybrid AC/DC Nanogrid,” *International Journal of Photoenergy*, vol. 2020, 2020, doi: 10.1155/2020/3646423.

[114] I. Roasto, T. Jalakas, and A. Rosin, “Bidirectional Operation of the Power Electronic Interface for Nearly-Zero Energy Buildings,” *2018 20th European Conference on Power Electronics and Applications, EPE 2018 ECCE Europe*, p. 2021, 2018.

[115] L. Martirano, E. Habib, A. Giuseppi, and A. di Giorgio, “Nearly zero energy building model predictive control for efficient heating,” *2018 IEEE Industry Applications Society Annual Meeting, IAS 2018*, pp. 6–11, 2018, doi: 10.1109/IAS.2018.8544632.

[116] E. Hamatwi, I. E. Davidson, J. Agee, and G. Venayagamoorthy, “Model of a hybrid distributed generation system for a DC nano-grid,” *Clemson University Power Systems Conference, PSC 2016*, Apr. 2016, doi: 10.1109/PSC.2016.7462851.

[117] S. Teleke, L. Oehlerking, and M. Hong, “Nanogrids with energy storage for future electricity grids,” *Proceedings of the IEEE Power Engineering Society Transmission and Distribution Conference*, p. 2021, 2014, doi: 10.1109/tdc.2014.6863235.

[118] M. Najafzadeh, I. Roasto, and T. Jalakas, “Energy Router Based Energy Management System for Nearly Zero Energy Buildings,” *2019 IEEE 60th Annual International Scientific Conference on Power and Electrical Engineering of Riga Technical University, RTUCON 2019 - Proceedings*, no. October 2014, pp. 5–10, 2019, doi: 10.1109/RTUCON48111.2019.8982366.

[119] I. Roasto, T. Jalakas, and A. Rosin, “Control of bidirectional grid-forming inverter for nearly zero energy buildings,” *2018 IEEE 59th Annual International Scientific Conference on Power and Electrical Engineering of Riga Technical University, RTUCON 2018 - Proceedings*, 2018, doi: 10.1109/RTUCON.2018.8659848.

[120] I. Roasto, O. Husev, M. Najafzadeh, T. Jalakas, and J. Rodriguez, “Voltage Source Operation of the Energy-Router Based on Model Predictive Control,” *Energies 2019, Vol. 12, Page 1892*, vol. 12, no. 10, p. 1892, May 2019, doi: 10.3390/EN12101892.

[121] I. Cvetkovic *et al.*, “A testbed for experimental validation of a low-voltage DC nanogrid for buildings,” *15th International Power Electronics and Motion Control Conference and Exposition, EPE-PEMC 2012 ECCE Europe*, 2012, doi: 10.1109/EPEPEMC.2012.6397514.

[122] I. Roasto, A. Rosin, and T. Jalakas, “Multiport interface converter with an energy storage for nanogrids,” *Proceedings: IECON 2018 - 44th Annual Conference of the IEEE Industrial Electronics Society*, pp. 6088–6093, Dec. 2018, doi: 10.1109/IECON.2018.8591104.

[123] Y. Chen *et al.*, “Quantification of electricity flexibility in demand response: Office building case study,” *Energy*, vol. 188, Dec. 2019, doi: 10.1016/J.ENERGY.2019.116054.

[124] R. v. Klyuev *et al.*, “Methods of Forecasting Electric Energy Consumption: A Literature Review,” *Energies (Basel)*, vol. 15, no. 23, Dec. 2022, doi: 10.3390/EN15238919.

[125] S. Rotger-Griful, R. H. Jacobsen, D. Nguyen, and G. Sørensen, “Demand response potential of ventilation systems in residential buildings,” *Energy Build*, vol. 121, pp. 1–10, 2016.

[126] A. Nielsen, *Practical Time Series Analysis*. O’Reilly Media, Inc., 2019. Accessed: Jan. 23, 2022. [Online]. Available: https://learning.oreilly.com/library/view/practical-time-series/9781492041641/?ar=

[127] Estonian Centre of Standardisation and Accreditation, “EVS-EN 16798-1:2019+NA:2019 Energy performance of buildings - Ventilation for buildings - Part 1: Indoor environmental input parameters for design and assessment of energy performance of buildings addressing indoor air quality, thermal environment, lighting and acoustics - Module M1-6,” 2019.

[128] ASHRAE, *2013 ASHARE Handbook - Fundamentals*. Atlanta, 2013.

[129] Vaisala, “HUMIDITY CONVERSION FORMULAS - Calculation formulas for humidity,” *Humidity Conversion Formulas*, p. 16, 2013, [Online]. Available: https://www.vaisala.com/sites/default/files/documents/Humidity_Conversion_Formulas_B210973EN-F.pdf

[130] A. Tenwolde and C. L. Pilon, “The Effect of Indoor Humidity on Water Vapor Release in Homes,” *30 Years of Research Proceedings Thermal Performance of the Exterior Envelopes of Whole Buildings X*, pp. 1–9, 2007, [Online]. Available: http://originwww.fpl.fs.fed.us/documnts/pdf2007/fpl_2007_tenwolde001.pdf

[131] P. Lutolf, M. Scherer, O. Megel, M. Geidl, and E. Vrettos, “Rebound effects of demand-response management for frequency restoration,” *2018 IEEE International Energy Conference, ENERGYCON 2018*, pp. 1–6, Jun. 2018, doi: 10.1109/ENERGYCON.2018.8398849.

[132] Trane, “CO2-based demand-controlled ventilation with ASHRAE Standard 62.1-2004,” 2005, [Online]. Available: https://www.trane.com/content/dam/Trane/Commercial/global/products-systems/education-training/engineers-newsletters/standards-codes/admapn017en_1005.pdf
[133] J. Kurnitski, A. Saari, T. Kalamees, M. Vuolle, J. Niemelä, and T. Tark, “Cost optimal and nearly zero (nZEB) energy performance calculations for residential buildings with REHVA definition for nZEB national implementation,” *Energy Build*, vol. 43, no. 11, pp. 3279–3288, Nov. 2011, doi: 10.1016/J.ENBUILD.2011.08.033.
[134] “Validation & certifications - Simulation Software | EQUA.” [Online]. Available: https://www.equa.se/en/ida-ice/validation-certifications
[135] “Liginullenergia eluhooned, väikemajad,” Tallinn, 2017.
[136] RAUSI OÜ and HEVAC OÜ, “Liginullenergia eluhooned, väike eramu. Päikese-elektrisüsteem, tugevvool. Variant 2,” 2017. [Online]. Available: https://kredex.ee/sites/default/files/2019-03/PV_ja_tugevvool_variant_2.pdf
[137] Roofit Solar Energy OÜ, “Liginullenergia eluhooned, väike eramu. Päikese-elektrisüsteem, tugevvool. Variant 1,” 2017. [Online]. Available: https://kredex.ee/sites/default/files/2019-03/PV_ja_tugevvool_variant_1.pdf
[138] Hevac OÜ, “Liginullenergia eluhooned, väike eramu. Soojusvarustus, küte ja ventilatsioon,” 2017. [Online]. Available: https://kredex.ee/sites/default/files/2019-03/Kute_ja_ventilatsioon_3.pdf
[139] TTÜ, “Liginullenergia eluhooned, väike eramu. Energiatõhusus,” 2017. [Online]. Available: https://kredex.ee/sites/default/files/2019-03/Energiatohusus_3.pdf
[140] Tibeco Woodhouse OÜ, “Liginullenergia eluhooned, väike eramu. Arhitektuur,” 2017. [Online]. Available: https://kredex.ee/sites/default/files/2019-03/Arhitektuur_3.pdf
[141] Statistics Estonia, “Dwellings and buildings with dwellings,” Estonia counts 2021. [Online]. Available: https://rahvaloendus.ee/en/results/dwellings-and-buildings-dwellings
[142] T. Häring, T. M. Kull, R. Ahmadiahangar, A. Rosin, M. Thalfeldt, and H. Biechl, “Microgrid Oriented modeling of space heating system based on neural networks,” *Journal of Building Engineering*, vol. 43, p. 103150, Nov. 2021, doi: 10.1016/J.JOBE.2021.103150.
[143] S. Wolf, D. Calì, and M. J. Alonso, “ProccS - An occupancy simulation tool for private households,” 2019. Accessed: Feb. 23, 2022. [Online]. Available: https://www.proccs.org/
[144] Elering AS, “The prequalification process and technical requirements of Manual Frequency Restoration Reserves (mFRR) Service,” 2022. [Online]. Available: https://elering.ee/sites/default/files/2022-07/mFRR%20service_prequalification%20process%20and%20technical%20requirements_20220722.pdf
[145] T. Heinsoo, “Indoor air quality assessment in rooms serviced by a constant air flow ventilation systems,” 2022. Accessed: Aug. 15, 2023. [Online]. Available: https://digikogu.taltech.ee/et/item/d68408fa-c822-4dbb-a22d-18394a4993ed
[146] Onset Computer Corporation, “HOBO MX CO2 Logger (MX1102A) Manual,” 2019. Accessed: Aug. 15, 2023. [Online]. Available: www.onsetcomp.com

Acknowledgements

Primarily, I would like to thank my family for their support and encouragement in my decision to study at Tallinn University of Technology and pursue a doctoral degree. Thank you all my loved family in Võrumaa and friends who have joined and traveled with me on this journey. I thank my parents, Ove and Vaike, who raised me and funded my education. I thank the rest of my family and friends for their support and presence.

I want to thank my supervisors for their counseling and support. I especially want to thank my principal supervisor, Professor Argo Rosin, for guiding and mentoring me. Thank you for seeing the potential in me and showing me the way. Special thanks to my co-supervisor, Senior Researcher Tarmo Korõtko, who assisted me and led me along the way to the details. Many thanks to my co-supervisor from the first years of my Ph.D., Senior Lecturer Indrek Roasto, for mentoring me on academic writing.

I want to thank my colleagues from Tallinn University of Technology for fruitful discussions and meaningful conversations.

This research work has been supported by the European Regional Development Fund (project "Doctoral School of Energy and Geotechnology III"), Estonian Archimedes Foundation (program "Dora Pluss), Estonian Research Council grants (PUT1680 and PSG739), Estonian Centre of Excellence in Zero Energy and Resource Efficient Smart Buildings and Districts ZEBE (grant 2014-2020.4.01.15-0016), European Commission through the H2020 project Finest Twins (grant No. 856602), Estonian Ministry of Education and Research and European Regional Fund (grant 2014-2020.4.01.20-0289). This doctoral thesis was supported by the project "Increasing the knowledge intensity of Ida-Viru entrepreneurship" co-funded by the European Union (2021-2027.6.01.23-0034).

Abstract
Research and development of explicit demand flexibility management methods for ventilation systems

Increasing use of volatile renewable energy sources poses challenges in balancing supply and demand. Therefore, demand-side flexibility is increasingly important for system operators and balancing authorities. Explicit flexibility management methods are needed to integrate loads like ventilation systems of different buildings (e.g., residential and commercial) into the flexibility service. However, the available methods described in research papers require further development for their implementation in practice. Heating and cooling systems have received much attention from researchers, but the potential of ventilation systems has been left out of focus. Therefore, this thesis provides a complete set of novel flexibility management methods for ventilation systems created from an aggregator's viewpoint.

Firstly, the definitions of flexibility and problems to measure it were addressed. It was found that flexible power (how much power consumption can be altered), forced ventilation rate (FVR) duration (how long this forced state can be held), and price for the activation are the main parameters for quantification. Mathematic principles were explained for each parameter, and instructions on implementing these were given.

Secondly, the proposed methods were validated on a building model constructed and simulated in IDA ICE. The data processing and flexibility management methods were applied in MATLAB. It was found that FVR duration estimations based on CO_2 concentration have a mean error of 8 to 12 min. FVR duration estimations based on temperature showed a mean error of around 20 min for most scenarios. The results showed that cost savings are achievable when a ventilation system is integrated into a flexibility service. For example, in the apartment, up to 11% of cost savings were achieved; in the office, up to 15%; and in the single-family house, up to 4%. The cost savings heavily depend on how much the ventilation system can be exploited in the flexibility service.

Finally, the developed methods were tested on a real ventilation system. Two case studies were conducted. It was found that there can be problems in implementing these methods, but all difficulties arising during the validation process were addressed and solved.

In conclusion, the goals set were achieved. From the results obtained from simulations and case studies, the developed management methods are applicable for ventilation system flexibility management. By considering potential cost savings, this topic should raise the attention of building owners and aggregators. Implementing the developed methods was aided with guidelines for system integrators on selecting appropriate methods and where to find the needed data.

Lühikokkuvõte
Ventilatsioonisüsteemidele otsese energiapaindlikkuse juhtimismeetodite uurimine ja arendamine

Suurenev muutlike taastuvenergiaallikate kasutuselevõtt tekitab väljakutseid tootmise ja tarbimise tasakaalustamisel. Seetõttu on koormuse energiapaindlikkusel süsteemi operaatorite ja bilansihaldurite jaoks üha suurem tähtsus. Otsese energiapaindlikkuse juhtimismeetoid on vajalikud integreerimaks koormusi paindlikkusteenusesse nagu erinevate hoonete (näiteks elamute ja äriruumide) ventilatsioonisüsteemid. Siiski nõuavad teaduspublikatsioonides kirjeldatud meetodid praktikas rakendamiseks täiendavat arendamist. Küll on teadlased pööranud palju tähelepanu kütte- ja jahutussüsteemidele, kuid ventilatsioonisüsteemide potentsiaal on jäänud tähelepanuta. Seetõttu pakub see doktoritöö välja uudse paindlikkuse juhtimismeetodite komplekti ventilatsioonisüsteemide jaoks, mis on välja töötatud agregaatori vaatepunktist.

Esmalt käsitleti paindlikkuse mõistet ja selle mõõtmisega seotud probleeme. Teadustööde ülevaatest selgus, et olulised paindlikkuse mõõtmiseks vajalikud parameetrid on paindlik võimsus (kui palju energiatarbimist saab muuta), sunnitud ventileerimise hulga (FVR) kestus (kui kaua seda sunnitud olekut saab hoida) ja teenuse aktiveerimise hind. Iga parameetri jaoks on lahti selgitatud matemaatilised põhimõtted ning lisatud juhised, kuidas neid rakendada.

Teiseks valideeriti väljatöötatud meetodid hoone mudelil, mis oli loodud ja simuleeritud programmis IDA ICE. Andmete töötlemist ja paindlikkuse juhtimise meetodeid rakendati MATLAB-is. Selgus, et FVR kestuse hinnangud, mis põhinesid CO_2 kontsentratsioonil, olid keskmise veaga 8 kuni 12 minutit. FVR kestuse hinnangud, mis põhinesid temperatuuril, olid enamuse stsenaariumide puhul keskmise veaga umbes 20 minutit. Saadud tulemused näitasid, et ventilatsioonisüsteemi integreerimisel paindlikkusteenusesse on võimalik saavutada kulude kokkuhoid. Näiteks korteris saavutati kuni 11% kulude kokkuhoidu, kontoris kuni 15% ja ühepereelamus kuni 4%. Kulude kokkuhoid sõltub suuresti sellest, kui palju ventilatsioonisüsteemi paindlikkusteenuses saab ära kasutada.

Lõpuks testiti väljaarendatud meetodeid reaalsel ventilatsioonisüsteemil. Selleks viidi läbi kaks juhtumiuuringut. Valideerimisprotsessi käigus tuvastati reaalsetel süsteemidel probleemid, millele leiti lahendused.

Kokkuvõtteks võib väita, et seatud eesmärgid on täidetud. Simulatsioonide ja juhtumiuuringutest saadud tulemuste põhjal on võimalik öelda, et välja töötatud juhtimismeetodid on ventilatsioonisüsteemidel rakendatavad. Arvestades potentsiaalset kulude kokkuhoidu, peaks antud teema äratama tähelepanu hoonete omanikes ja agregaatorites. Väljatöötatud meetodite rakendamise toetamiseks on doktritöös välja toodud juhised süsteemi integraatoritele sobivate meetodite valikuks ja vajalike andmete hankimiseks.

Appendix

Publication I

Maask, V., Rosin, A., Korõtko, T., Thalfeldt, M., Syri, S., Ahmadiahangar, R. (2023), "Aggregation ready flexibility management methods for mechanical ventilation systems in buildings," Energy and Buildings, vol. 296, Oct. 2023 doi: https://doi.org/10.1016/j.enbuild.2023.113369.

Energy & Buildings 296 (2023) 113369

Contents lists available at ScienceDirect

Energy & Buildings

journal homepage: www.elsevier.com/locate/enb

Aggregation ready flexibility management methods for mechanical ventilation systems in buildings

Vahur Maask [a,b,*], Argo Rosin [a,b], Tarmo Korõtko [a,b], Martin Thalfeldt [a,c], Sanna Syri [a,d], Roya Ahmadiahangar [a,b]

[a] Smart City Center of Excellence (Finest Twins), Estonia
[b] Department of Electrical Power Engineering and Mechatronics, Tallinn University of Technology, Estonia
[c] Department of Civil Engineering and Architecture, Tallinn University of Technology, Estonia
[d] Department of Mechanical Engineering, Aalto University, Finland

ARTICLE INFO

Keywords:
Explicit demand flexibility
Mechanical ventilation systems
Buildings
Flexibility management
Forecasting

ABSTRACT

Increasing use of volatile renewable energy sources causes challenges in balancing supply and demand. Therefore, demand-side flexibility has rising importance for system operators and balancing authorities. Flexibility management methods are needed to integrate loads like ventilation systems of different buildings (e.g., residential and commercial) into flexibility service. However, the available methods described in research papers require further development for implementation in practice. Heating and cooling systems have received much attention from researchers, but the potential of ventilation systems has been left out of focus. Therefore, this paper provides a complete set of novel flexibility management methods for ventilation systems created from an aggregator's viewpoint. The flexibility is quantified through capacity (e.i. the amount of power consumption that can be altered), forced ventilation rate duration, and the tendered price for the service. The proposed methods were tested on a building model constructed and simulated in IDA ICE. The data processing and flexibility management methods were applied in MATLAB. Two types of ventilation systems with different sensor configurations were considered: constant and variable air volume. Forced ventilation rate duration is calculated using energy and mass balance analysis where the root means squared error was 10 to 33 min, depending on the system type, measured parameter, and sensor location. The flexibility service pricing model was tested on the 2022 years' manual frequency restoration reserve (mFRR) activation and balance energy market data.

1. Introduction

Increasing environmental awareness and climate change have pushed the European Union (EU) towards climate neutrality. Renewable Energy Directive [1] will force member states to fulfill at least 32% of overall energy needs with renewable energy by 2030. The long-term strategy is stated by European Green Deal [2], which aims to become the first climate-neutral continent by 2050. According to the Eurostat [3], the share of renewable energy consumption in gross final energy consumption during ten year period from 2010 to 2020 has increased from 14.4% to 22.1% in the EU, while in Estonia, renewable energy share during the same period has increased from 24.6% to 30.2%. This share is increased by dedicated power plants and households with small-scale photovoltaic energy production or wind turbines, as considered in [4]. Increasing the share of distributed volatile renewable energy generation makes maintaining the equilibrium between supply and demand increasingly challenging. This raises the importance of demand response and energy flexibility managed by aggregators, as described in [5]. Electric power system flexibility is the ability to continuously balance the grid by maintaining electricity supply and demand on an equal level [6] while simultaneously providing acceptable service quality to connected loads [7]. Flexibility in an electric system can be characterized through multiple features related to how the flexibility is provided or properties that can be used to quantify the flexibility, as discussed in [8]. Authors of the review [9] differentiated demand-side flexibility into two: implicit and explicit demand flexibility. The implicit demand flexibility takes advantage of indirect or price-based demand response, where consumers change their electricity consumption according to the energy price at a given time. For example, methods described in [10,11] use implicit demand flexibility to achieve cost savings on energy

* Corresponding author at: Department of Electrical Power Engineering and Mechatronics, Tallinn University of Technology, Estonia.
E-mail address: vahur.maask@taltech.ee (V. Maask).

https://doi.org/10.1016/j.enbuild.2023.113369
Received 23 February 2023; Received in revised form 25 May 2023; Accepted 12 July 2023
Available online 16 July 2023
0378-7788/© 2023 Elsevier B.V. All rights reserved.

purchases. Under explicit demand flexibility, the committed flexibility providers adjust their energy generation or consumption according to the electric system's needs, as described in [12]. Individual participation can be considered in explicit demand flexibility services for large prosumers. In all other cases, aggregation is needed to concentrate multiple prosumers' ability to change their consumption or generation to fulfill all the requirements stated by the market operator [13,9]. Therefore, flexibility management, including algorithms and appropriate equipment, is essential for the current and future energy system [14–16].

It has been suggested in the vision of Smart Grids to harness the positive effects of aggregated residential load flexibility in electricity markets [17,18]. Demand flexibility is not only considered for residential buildings but also includes commercial or industrial sectors, where one approach is discussed in the study [19]. In buildings, mechanical ventilation systems are a possible source of flexibility which according to the European Commission [20], consume more than 2% of the energy produced in the European Union. After heating, cooling, and lighting, they are currently the fourth biggest electricity consumer in buildings. The share of ventilation in the energy balance of buildings is expected to increase as the Energy Performance of Buildings Directive (EPBD) [21] proposal of March 14, 2023, sets requirements for the implementation of adequate indoor environmental quality standards in buildings in order to maintain a healthy indoor climate, which most likely increases the total capacity of mechanical ventilation. The proposal also states that various indoor environment parameters shall be continuously measured and used for control in buildings, including CO_2, temperature, and relative humidity. The indoor sources of particulate matter or volatile organic compounds (VOC) are either reported based on the available data at the product level or directly measured where available. The requirements of the EPBD proposal include zero emission, new and existing buildings undergoing a major renovation, and the majority of existing non-residential and public buildings. Therefore, the readiness to utilize building service systems in the coming decades should increase remarkably. The study [22] found that ventilation alone can form up to 12% of the overall energy consumption in office buildings. Heating, cooling, and lighting system energy consumption depends on ambient conditions, as shown in [23], while a ventilation system's power consumption is related to building usage. Therefore, ventilation systems experience fewer seasonal effects on energy flexibility and can be included in the flexibility service throughout the year.

In Estonia, according to the 2022 year manual frequency restoration reserve (mFRR) activations, the average energy used during up-regulation was around 8.7 MWh [24]. The maximum energy used in regulations during the same period was 98.9 MWh. According to the Estonian transmission system operator (TSO) Elering AS [25], the average hourly energy consumption during 2022 was 934 MWh. It is known that ventilation systems consume at least 2% of the total energy produced in the EU, meaning that the maximum potential of ventilation systems is to provide around 19 MWh of energy for flexibility service. It is more than the average energy used during a regulation. Therefore, ventilation systems can have a relatively high potential to provide flexibility.

Research interest has grown in recent years in the field of energy flexibility and harvesting it from heating, ventilation, and air conditioning (HVAC) systems. However, as shown in research papers [26–32], the main focus is on the heating and cooling system considering temperature as the primary indoor environment quality parameter. Much research is done to reduce energy consumption and costs by implementing optimization methods (e.g., mixed integer linear programming) [33–36] or addressing demand response by taking advantage of time-of-use tariffs or real-time electricity price [37–39]. Authors of the research [39] reported that electricity consumption could be decreased by 9% and the electricity purchase costs by 2% by implementing demand response and using a real-time price signal on an educational office building's ventilation system. Another ventilation system's demand response approach is considered in [40], where a study was made for a commercial building to minimize the energy and thermal discomfort costs related to occupants. The HVAC system used for frequency service is studied in [41]. It found that up to 15% of the rated fan power can be implemented in frequency regulation without substantially affecting the building's indoor temperature. Temperature is an essential indoor air quality parameter, but from an energy flexibility standpoint, CO_2 concentration is the primary parameter to measure the ventilation system's flexibility [42].

Residential buildings can have an important role in providing demand-side flexibility. For example, O. W. Olawale, B. Gilbert, and J. Reyna [43] assessed the residential participants' behavior in demand flexibility programs and estimated that residential participants could provide up to 10 GW for flexibility service in the United States. In addition, the authors of the review [44] found that the most popular resources for flexibility services in the residential sector are thermal energy storage and electric appliances. They reported in the review that the energy cost is reduced by 1% to 48% with flexible operations. The study [45] found that flexibility potential in new residential districts is around 290 W per household with an uncertainty of $\pm$ 90 W and around 1290 W per old building. Coordination and negotiation techniques to manage demand-side flexibility are discussed in the study [46], where game theory was the most widely used technique in residential districts. Authors of the research [47] proposed a space heating coordination strategy to provide flexibility service and reported a 13.96% reduction in operation costs.

Characterization and quantification of flexibility are needed to aggregate flexible loads in the scope of explicit demand flexibility. In addition, an important role is played by forecasts and system control. Therefore, flexible load management can be divided into the following parts:

- **Quantification** is needed to measure the flexibility and provide metrics for the aggregator. However, flexibility cannot be quantified through a single metric, so multiple properties, such as capacity, delay, and duration, are considered [8]. Y. Chen et al. [48] have discussed some of the equations to quantify flexibility, but these mainly apply to heating and cooling systems. After all, the composition of the properties is dictated by the aggregator and selected aggregation method.
- **Forecasting** is an essential part of flexibility service to schedule flexible loads and ensure regulation readiness. Short-term forecasts (e.i., from hours to one day or a week) are used to submit tenders to the market operator [49].
- **The interface** is a composition of methods, rules, and hardware to communicate with an aggregator and control flexible loads. This can also include building-level aggregation, where tenders from the whole building's flexible loads are combined and submitted. If an aggregator sends an activation signal, the interface must deliver the required capacity within time constraints.

The studied literature does not give a complete package of methods to manage ventilation system energy flexibility. Furthermore, the available methods are too complicated to implement or lack a guideline for the building owners or aggregators to implement these on their systems. The available research focuses mainly on heating and cooling, while ventilation systems are left out of scope. This paper addresses these problems and proposes methods to manage ventilation system flexibility, which enables the use of ventilation systems in flexibility service. In addition, this paper bridges the gap in research by providing methods and approaches to measure duration and cope with different sensor configurations for ventilation systems. Also, the step-by-step process for co-simulation between two simulation platforms is given. The paper is organized as follows: in section 2, flexibility management methods are described; section 3 gives an overview of the building model and dataset which was used for the validation of the methods; section 4 shows the results of the validation, and in section 5 acquired

results are discussed.

2. Developed flexibility management methods

The properties of electrical flexibility must be understood before management methods can be applied. Electrical flexibility can be expressed through three attributes: direction, availability, and electrical composition [8,50,51]. Each property has a specific role in flexibility service:

- The **direction** can have two states: up or down. The direction of regulation is specified from the grid's perspective. If the power consumption is decreased, then up-regulation is initiated, and vice versa.
- The **availability** can be defined by the starting time and duration, as shown in Fig. 1. The starting time will mark the moment when the regulation is initiated. The duration defines the time window required for regulation and within the power consumption level that can be sustained without exceeding set boundaries.
- The **electrical composition** can be described through power or capacity, which defines how much power can be used for flexibility service. The total energy used for flexibility service can be calculated by combining duration with power. Ventilation systems that use variable frequency drives have ramps in the power consumption, which can be seen as falling and rising proportions in Fig. 1. This can be named a rate of change and must be considered when a selected system is included in the flexibility service.

2.1. Capacity forecasting

The capacity for each timestep can be calculated based on the system's maximum and minimum power consumption, which can be acquired experimentally or by consulting the documentation. For example, the available power for down-regulation and up-regulation can be calculated from the maximum and minimum possible power consumption, as shown in (1). The sign (+ or -) in front of the value dictates the direction of the regulation. To achieve this, power consumption must be forecasted for each timestep.

$$\Delta P_t = \begin{cases} P_{max} - P_t, & \text{down regulation} \\ P_{min} - P_t, & \text{up regulation} \end{cases}, \tag{1}$$

where ΔP_t – available capacity for up or down regulations at timestep t (kW),

P_t– forecasted power consumption for timestep t (kW),

P_{max}– maximum measured or given by documentation power consumption (kW),

P_{min}– minimum measured or given by documentation power consumption (kW).

A ventilation system usually operates according to a schedule that is adjusted based on the building's usage. During unoccupied hours the ventilation system is switched off or operating at a minimum airflow rate. There can be minor fluctuations in power consumption which increase the uncertainty of the forecast. For forecasting, the autoregressive moving average (ARMA) model is used. ARMA model terms p and q will be selected using the Akaike information criterion (AIC) method. The power consumption forecast is based on previously measured power consumption data and not on a ventilation system type or configuration. ARMA model for forecasting the power consumption of a ventilation system can be described as follows:

$$P_t = \alpha + \sum_{i=1}^{p} \beta_i P_{t-i} + \varepsilon_t + \sum_{i=1}^{q} \phi_i \varepsilon_{t-i}, \tag{2}$$

where α – ARMA model constant,

β_i– AR coefficient for the lag i,

P_{t-i}– AR model power consumption lag,

p– the order for the AR model,

ε_t– error terms,

ϕ_i– MA coefficient for the lag i,

ε_{t-i}– MA model error lag,

q– the order for the MA model.

2.2. Duration forecasting

During regulations, a ventilation system is forced to operate below or above its regular rate, allowing it to decrease or increase its power consumption. This paper defines this state as forced ventilation rate (FVR). However, this state cannot be sustained indefinitely because it affects the building's indoor air quality (IAQ). This subsection discusses a method to estimate and forecast the FVR duration. The same approach is also addressed in the study [52], where experimentation was conducted on one ventilation system of an educational building. The proposed method assumes a mixing type of ventilation system. A forecast is based on three main IAQ parameters: CO_2 concentration, temperature, and humidity. Each parameter has its limit condition and nuances in the duration calculation.

The indoor climate of a building is mainly dictated by three indoor

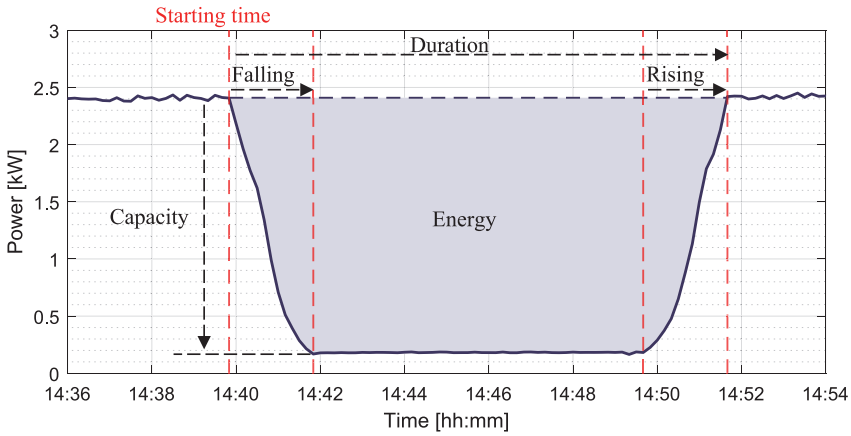

Fig. 1. Example of a ventilation system with variable frequency drive electrical flexibility properties.

air quality (IAQ) parameters: CO_2 concentration, temperature, and humidity. To provide occupants with a healthy and comfortable environment, these three parameters must be between limits given in the standard EN 16798:2019 [53]. Authors of the study [54] suggest placing sensors in both the supply and return air ducts actively monitor contamination or temperature difference. The drawback of this setup is that during the ventilation shutdown, the state of IAQ is unknown, and contamination or temperature can exceed the limits. In addition, placing sensors in each room or space of the building requires higher investment costs and a complex sensor network.

2.2.1. CO_2 concentration

Due to metabolism, persons produce carbon dioxide, which causes the CO_2 concentration in a zone to rise and is correlated with other bioeffluents. Based on the standard EN 12831–1, a zone is a group of rooms with direct or indirect air connection. Without sufficient ventilation, the CO_2 concentration can rise above the allowable limit. However, since this will not happen instantly, the ventilation system can operate at the minimum level for some time. CO_2 concentration-based flexibility duration estimation uses mass balance analysis to calculate the CO_2 generation rate in a building which can be used for duration calculation. Mass balance can be expressed as follows:

$$V\frac{dC}{dt} = G + QC_{amb} - QC, \tag{3}$$

where V – air volume in a zone (m^3),
C– CO_2 concentration in a zone (ppm),
G– CO_2 generation rate (m^3/s),
Q– airflow rate for the zone (m^3/s),
C_{amb}– ambient CO_2 concentration (ppm).

The CO_2 generation rate during the timestep t can be calculated as shown in (4). This equation is derived from the previously mentioned mass balance and is put into a discrete form more suitable for a control system. FVR duration calculation and forecasting are discussed under 2.2.4. The same methods can be used for other pollutants, such as particulate matter and VOCs, since they are also measured in relative values (e.i., the concentration of particles) and subject to mass balance.

$$G_t^{co2} = \frac{V\cdot(C_t - C_{t-1})}{\Delta t} + Q_t\cdot(C_t - C_{amb}), \tag{4}$$

where Δt – timestep length (s).

2.2.2. Temperature

Building ventilation systems can provide thermal comfort to occupants or hold set temperatures for other purposes, which means that when the ventilation system is used for flexibility service, the temperature effect should be included in estimations. In addition, the standard EN 16798-1:2019 specifies temperature ranges according to building type, which can be used in the estimations.

The first law of thermodynamics can be used to estimate energy flows into or out of a zone, as expressed in (5). The difference between the initial and final states of the zone can be expressed through multiple mass flows with uniform properties [55], also adding the heat q generation by people, appliances, and room heating. Mechanical work w can be excluded from the equation because the zone is not doing any mechanical work, and all the energy used by appliances is converted into heat.

$$\sum m_{in}\left(u + pV + \frac{v^2}{2} + gz\right)_{in} - \sum m_{out}\left(u + pV + \frac{v^2}{2} + gz\right)_{out} + q - w = \left[m_{final}\left(u + \frac{v^2}{2} + gz\right)_{final} - m_{initial}\left(u + \frac{v^2}{2} + gz\right)_{initial}\right]_{zone}, \tag{5}$$

where m_{in} – the mass of the entering medium (kg),
m_{out}– the mass of leaving medium (kg),
m_{final}– the final mass of a zone (kg),
$m_{initial}$– the initial mass of a zone (kg),
u– internal energy per unit mass (J/kg),
p – pressure (Pa),
V– specific volume (m^3),
v– velocity of molecules (m/s),
g– local acceleration of gravity (m/s^2),
z– elevation above the horizontal reference plane (m),
q– heat generated inside a zone (J),
w– energy converted into work (J).

A ventilation system can be considered the only way entering and leaving airflow streams can move. All the other mass flows through openings, and walls can be considered in one variable: heat. From (5), only mass internal energy u is needed to estimate the heat generation in a zone, while pressure, volume, velocity, and potential energy have no significant difference. A heat generation rate must be calculated to estimate ventilation system flexibility based on temperature, as shown in (6). FVR duration calculation and forecasting are discussed under 2.2.4.

$$G_t^{heat} = \frac{V\cdot(T_t - T_{t-1})}{\Delta t} + Q_t\cdot(T_t - T_{supply}), \tag{6}$$

where T_t – temperature in a zone at timestep t (K),
T_{t-1}– the temperature at the previous timestep $t-1$ (K),
T_{supply}– supply air temperature (K),
Q_t– ventilation rate at timestep t (m^3/s),
Δt– timestep length (s),
V– zone volume (m^3).

2.2.3. Humidity

The humidity is affected by persons inside the building where moisture is added to inhaled air during exhaling. Also, washing and drying release additional moisture into the inside air. Typically ventilation system is responsible for extracting excess moisture from the building. This means that the humidity effect should be included in estimations when the ventilation system is used for flexibility service.

Commercially available humidity sensors typically measure relative humidity, thus outputting a value that is a percentage of the measured absolute humidity against maximum absolute humidity at a given temperature. However, relative humidity depends on air temperature, which means that relative humidities for entering and leaving air are not comparable due to temperature differences. This issue is resolved by converting the relative humidity level into absolute (g/m^3), which can be calculated as follows:

$$W = \frac{B\cdot C\cdot RH\cdot 10^{\left(\frac{m\cdot T}{T+T_n}\right)}}{100\cdot T}, \tag{7}$$

where T - the temperature of the air (K),
RH - the relative humidity,
B, C, m, T_n– constants which are given in Table 1 [56].

Like the CO_2 concentration estimation, the humidity level inside the building can be estimated by mass balance analysis, as shown in (3). In addition, the humidity generation rate can be calculated, as shown in (8). FVR duration calculation and forecasting are discussed under 2.2.4.

$$G_t^{w} = \frac{V\cdot(W_t - W_{t-1})}{\Delta t} + Q_t\cdot(W_t - W_{supply}), \tag{8}$$

Table 1
Constants for humidity conversion [56].

Constant	Value
B	6.116441
C	2.16679 gK/J
m	7.591386
Tn	240.7263

where W_t – humidity concentration in a zone at timestep t (g/m^3),

W_{supply}– supply air humidity concentration (g/m^3).

2.2.4. Forced ventilation rate duration calculation

Knowing an IAQ parameter X generation rate at a given timestep t, estimation for ventilation system FVR duration can be made as shown in (9). The main restriction for the FVR duration when the ventilation system is operating at lowered power consumption is the boundary condition for the IAQ parameter. There is no lower limit for CO_2 concentration excess above outdoor concentration. This means there is no limitation from the CO_2 concentration perspective to increasing ventilation system power consumption. Although, it must be considered that if, at design conditions, the fan speed is not at the maximum frequency control setpoint, increasing the fan speed above the design value may cause problems with noise or draught. This does not apply to the temperature and humidity range the parameter must be within. Therefore, it must be known what purpose the ventilation system has in addition to air exchange. For example, if the ventilation system is responsible for building heating or indoor air humidification, this must be considered in the duration calculation. This is done by calculating multiple FVR durations for the same parameter and selecting the shortest.

$$\tau_t^X = \frac{V \cdot (X_{limit} - X_t)}{G_t^X - Q_{fvr} \cdot \frac{X_t + X_{limit} - 2 \cdot X_{supply}}{2}}, \tag{9}$$

where X_t – IAQ parameter value in a zone at timestep t (ppm, °C or g/m^3),

X_{limit}– IAQ parameter limit (ppm, °C or g/m^3),

Q_{fvr}– forced ventilation rate (m^3/s).

The FVR duration calculated in (9) is an instantaneous value considering conditions measured during the timestep t. It is not helpful when the forecast for future FVR durations is needed. Therefore, ARMA (p, q) model can be used to calculate future values based on historical data. The ARMA(p, q) model is described in (2), where the power consumption must be replaced with the FVR duration.

The FVR duration forecast must be adjusted according to IAQ parameter generation rate fluctuations. If the subsequent timestep room usage increases, the FVR duration must be shortened as described by (10). This will eliminate overoptimistic estimations where in an actual situation, the FVR can be sustained for a shorter time, or the IAQ parameters will exceed their limits. Each of these adjustments is repeated, and after each iteration, the sum of all FVR duration estimations is calculated and compared with the previous iteration sum, as shown in (11). If they are equal, then the adjustment is completed.

$$\tau_{t,i}^{FVR} = \begin{cases} \tau_{t+1,i-1}^{FVR} + \Delta t, \tau_{t+1,i-1}^{FVR} < \tau_{t,i-1}^{FVR} - \Delta t \\ \tau_{t,i-1}^{FVR}, \quad \tau_{t+1,i-1}^{FVR} \geqslant \tau_{t,i-1}^{FVR} - \Delta t \end{cases} \tag{10}$$

$$\sum_{t=1}^{n} \tau_{t,i}^{FVR} = \sum_{t=1}^{n} \tau_{t,i-1}^{FVR} \tag{11}$$

where $\tau_{t,i}^{fvr}$ – an estimate of FVR duration at time t during correction iteration i,

$\tau_{t,i-1}^{fvr}$– an estimate of FVR duration at time t during correction iteration $i-1$,

Δt– timestep length (s).

2.2.5. Boundary condition correction

One building can consist of multiple zones, each with multiple rooms. To estimate FVR duration, building usage and conditions inside must be known. In many cases, this is causing the need to install additional IAQ sensors in the building. One way to reduce the initial investment costs is to install IAQ sensors in the air handling unit (AHU). However, measurements in the AHU do not represent the actual situation in each room. The pollutant concentration in the AHU for mixing type of ventilation system is the average value for all the zones, as shown in (12). If there are zones with uneven usage, then it can cause a situation where boundary conditions will be exceeded. It is especially troublesome if the ventilation system is forced to operate at its minimum rate. To lessen the flexibility service effect on IAQ and make FVR less noticeable, the solution is restricting ventilation system exploitation and correcting the boundary condition. It is done by narrowing the range where the IAQ parameter can be.

$$X_{return} = \frac{\sum_{i=1}^{n} X_i Q_i}{Q_{return}}, \tag{12}$$

where X_{return} – IAQ parameter value in return air (ppm, °C or g/m^3),

X_i– IAQ parameter value in room i (ppm, °C or g/m^3),

Q_i– airflow rate from the room i (m^3/s),

Q_{return}– airflow rate in the return air duct (m^3/s),

n– total number of rooms.

Occupancy in each room must be measured or estimated to consider uneven occupancy in flexibility calculation. It can be achieved by installing temporary IAQ sensors in rooms of interest and taking measurements for at least one week during normal building usage (i.e., avoid holidays). It is recommended to take repeated measurements at least once a year or after the change in buildings' room usage (i.e., change of tenant).

After the measurements are taken, it is possible to estimate pollutant generation or heat generation according to the floor area of selected rooms, known as specific pollutant generation (SPG). Therefore, the SPG for CO_2 is defined as (m^3/s)/m^2, SPG for temperature is defined as W/m^2, and SPG for humidity is defined as (g/s)/m^2. All the SPGs are calculated according to the CO_2 generation formula as shown in (4), heat generation as shown in (6), and humidity generation as shown in (8).

IAQ parameter limit value can be corrected based on acquired SPGs. The room with the highest SPG for the selected IAQ parameter defines the corrected limit value. Also, rooms are not used equally throughout one day, and the room with maximum SPG can change. Therefore, it is reasonable to calculate the corrected limit value for each timestep. First, the corrected limit value is calculated based on the difference between the upper and lower IAQ parameter limit values multiplied by the room airflow rate and SPG for the selected IAQ parameter. Then, the acquired value is divided by the return airflow rate and the zone's average SPG for all of the rooms in this zone and biased by the IAQ parameter lower limit, which can be calculated as follows:

$$X_t^{limit} = X_{low}^{limit} + \frac{\left(X_{high}^{limit} - X_{low}^{limit}\right) \cdot Q_t^{room} \cdot SPG_t^{room}}{Q_t^{return} \cdot SPG_t^{zone}}, \tag{13}$$

where X_t^{limit} – IAQ parameter limit (ppm, °C, or g/m^3),

X_{low}^{limit}– IAQ parameter lower limit value (ppm, °C, or g/m^3),

X_{high}^{limit}– IAQ parameter upper limit value (ppm, °C, or g/m^3),

Q_t^{room}– airflow rate from the room (m^3/s),

SPG_t^{room}– specific pollutant generation for a room [(m^3/s)/m^2, W/m^2 or (g/s)/m^2],

Q_t^{return}– airflow rate in the return air duct (m^3/s),

SPG_t^{zone}– specific pollutant generation for a zone [(m^3/s)/m^2, W/m^2 or (g/s)/m^2].

2.3. Implementation of methods

Flexibility management methods depend on available measurement data and what is needed for aggregation. This section presents the pricing model and describes the implementation of the developed methods.

2.3.1. Pricing model

The last calculation stage is to find out the energy price for regula-

tions. It is the needed input for the aggregator according to which the amount of regulated energy will be compensated to a building owner. A personalized pricing mechanism is used, as shown in (14). The direction of regulation dictates the ingredients of the final regulation price. If up-regulation is activated and the ventilation system power consumption is lowered, it is needed to compensate for lower IAQ in the zone. It can be done by considering variable building usage, described through the CO_2 generation rate. If the building has low usage, then the cost of regulation is lower, and vice versa. Every regulation introduces changes in the ventilation system, which can contribute to amortization and must be compensated (e.g., switching of contactors, movement of valves, etc.). Amortization costs are neglected in the simulation since these are insignificant for the small-scale system. The down-regulation activation causes additional energy consumption, which introduces costs to the system owner. If the ventilation system's return air CO_2 concentration is higher than the minimum possible CO_2 concentration, the goal is to decrease the CO_2 concentration level by purchasing electricity at a lower price. When the CO_2 concentration is low due to the low occupancy, down-regulation can only be provided if additional costs from grid fees, taxes, and amortization are compensated. Also, the profit margin is included in the regulation price that the building owner dictates.

$$price_t = \begin{cases} \dfrac{\frac{G_t^{co2}}{G_{max}^{co2}} \cdot c_{comf} \cdot \tau_t + c_{amort}}{\Delta P_t \cdot \tau_t} + c_{prof}, & \Delta P_t < 0 \\ \dfrac{C_t - C_{t,min}}{C_{limit} - C_{t,min}} \cdot c_{t,el} - c_{t,fees} - \dfrac{c_{amort}}{\Delta P_t \cdot \tau_t} - c_{prof}, & \Delta P_t > 0 \end{cases}, \quad (14)$$

where $price_t$ – the calculated regulation price at time t (€/MWh),

G_t^{co2}– CO_2 generation rate at time t (m^3/s),

G_{max}^{co2}– maximum estimated CO_2 generation rate (m^3/s),

c_{comf}– the regulation cost on comfort (€/h),

τ_t– duration of regulation at time t (h),

c_{amort}– the regulation cost on amortization (€),

c_{prof}– profit margin for regulations (€/MWh),

ΔP_t– available capacity during the timestep t (kW),

C_t– CO_2 concentration in the return air at time t (ppm),

$C_{t,min}$– minimum CO_2 concentration for maximum airflow rate at time t (ppm),

C_{limit}– CO_2 concentration limit value (ppm),

$c_{t,el}$– electricity price including electricity market price and electricity supplier the profit margin at time t (€/MWh),

$c_{t,fees}$– the sum of all the fees, which include transmission costs and taxes added to consumed energy price at time t (€/MWh).

The forced ventilation rate duration estimation dictates the maximum duration for each regulation. The regulation price is calculated for each period separately. Therefore, the duration of each regulation can be derived as follows:

$$\tau_t = \begin{cases} \tau_t^{FVR}, & \tau_t^{FVR} \leqslant \Delta t \\ \Delta t, & \tau_t^{FVR} > \Delta t \end{cases}, \quad (15)$$

where τ_t^{FVR} – forced ventilation rate duration at time t (h),

Δt– duration between two sequent calculation steps (h).

For down-regulations, the minimum possible CO_2 concentration and CO_2 concentration at a specific time must be estimated ahead. These can be derived from mass balance analysis, as shown in (16) and (17). Minimum CO_2 concentration depends on the maximum airflow and CO_2 generation rates at a selected time. The CO_2 generation rate can be forecasted using the calculated CO_2 generation rate shown in (4) with ARMA(p, q) model.

$$C_{t,min} = \begin{cases} \dfrac{G_t^{co2}}{Q_{max}} + C_{amb}, & G_t^{co2} > 0 \\ C_{amb}, & G_t^{co2} \leqslant 0 \end{cases}, \quad (16)$$

where Q_{max} – maximum ventilation rate (m^3/s).

$$C_t = \frac{2 \cdot V \cdot C_{limit} + 2\tau_t^{fvr,co2} \cdot G_t^{co2} - \tau_t^{fvr,co2} \cdot Q_{fvr} \cdot (C_{limit} - 2 \cdot C_{amb})}{2 \cdot V - \tau_t^{fvr,co2} \cdot Q_{fvr}}, \quad (17)$$

where C_{limit} – CO_2 concentration limit value (ppm),

$\tau_t^{fvr,co2}$– CO_2 concentration based forced ventilation rate duration at time t (s),

Q_{fvr}– forced ventilation rate (m^3/s).

2.3.2. Applying flexibility management methods

In the center of the application is the flexibility management system that connects the building with the aggregator. Flexibility management consists of capacity forecasts, FVR duration forecasts, and regulation prices for the next prediction horizon (Fig. 2). All previously discussed methods must be put into use to achieve this. Different sources of data are used for flexibility management. Real-time data will be gathered directly from sensors and a ventilation system interface. Static data will be acquired from the building's design documentation, ventilation system datasheet, and building owner. Information from the energy supplier is only needed when down regulations are allowed.

All the forecasts are sent to the aggregator, who decides when and how much capacity will be activated. Finally, the activation signal is sent to the flexibility management system, which must achieve the requested power consumption change by forcing the ventilation system to operate at a specific rate.

3. Building model and simulation dataset

A building model and development environment are needed to validate the flexibility management methods and acquire the results. The building model is constructed in IDA Indoor Climate and Energy (IDA ICE), a specialized simulation tool to imitate building behavior. IDA ICE has been validated according to EN 15255:2007, EN 15265:2007, EN 13791, and ASHRAE 140-2004. Reports about test results for validation are available on the EQUA Simulation AB website [57]. MATLAB programming and numeric computing platform are used for scripting, data analysis, and applying flexibility management methods. All the results are acquired by combining IDA ICE with MATLAB.

The whole validation process for the developed flexibility management methods can be divided into five stages (Fig. 3):

I. The building model is configured, and the occupancy schedule is generated. PRN files are used to transfer data between IDA ICE and MATLAB.
II. A year-long simulation is conducted in IDA ICE using all the needed input and the building model. All the measured data gathered from each room and AHU is logged into output files.
III. All the IDA ICE output files are imported into MATLAB, and flexibility management methods are applied. It includes the quantification and forecasting of the ventilation system's energy flexibility. Activations are scheduled based on the 2022 Estonian balancing energy price, day-ahead price, and manual frequency restoration reserve (mFRR) activations.
IV. A year-long simulation is repeated with activations.
V. The data is acquired for IDA ICE, and previously calculated flexibility estimations are compared with measured data. Finally, the dataset is analyzed in MATLAB, and the final results are formulated.

3.1. The building model

The building model is based on a small single-family house, a sample

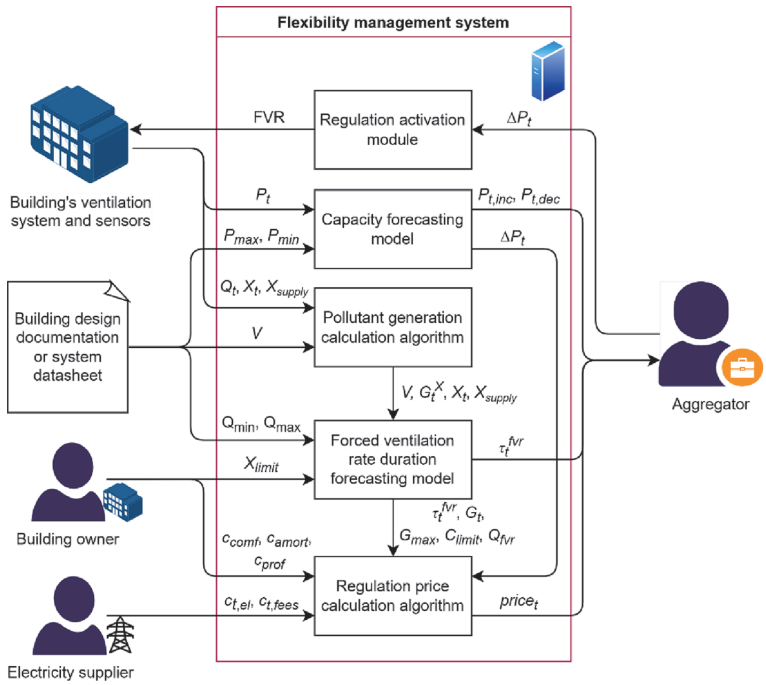

Fig. 2. Implementation of developed methods for ventilation system flexibility management.

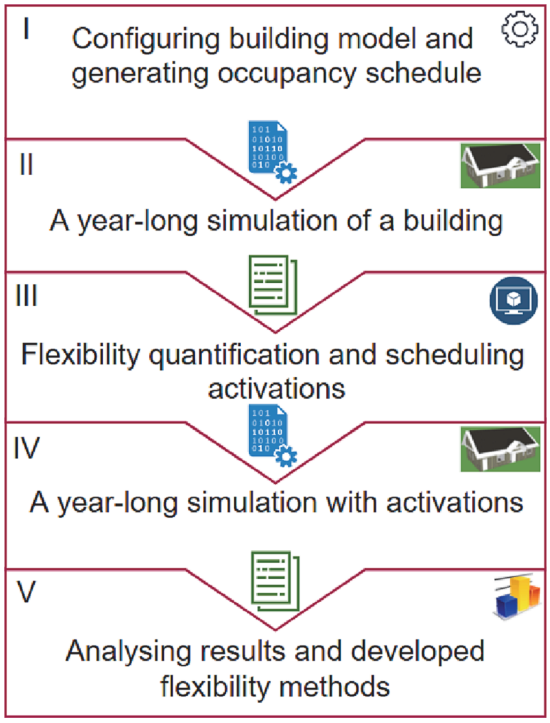

Fig. 3. The validation process of developed flexibility management methods.

building used for redefining the cost-optimality level for new, nearly zero-energy residential buildings in Estonia [58]. The model has been validated previously in a related project, and the relevant documentation is available online [59–63]. The building model represents a single-floor level dwelling with a total floor area of around 100 m^2 and can be considered a typical Estonian single-family house according to the statistics [71].

The building is separated into 11 rooms (Fig. 4) connected to one AHU with heat recovery. The building's occupancy profile is generated for two adults and one child. A simulation model described in the study [64] was used to generate year-long occupancy profiles. The simulation model to generate occupancy profiles was used twice. The first iteration's profiles were applied to the bathroom, bedroom, main bedroom, kitchen, and living room. The second iteration's profiles generated for

Fig. 4. The layout of the building model.

the bathroom and living room were applied to the toilet and office since the model did not support these rooms during the first iteration. This results in the maximum occupancy of the building being five persons, which can be realistic when guests are considered. Occupancy profiles for the utility room, technical room, hall, and vestibule are not generated since it is expected that residents do not stay for long in these rooms. Therefore, the metabolic equivalent of task (MET) of 1.2 is selected for the building model.

The heating of each room is achieved by wall-mounted radiators with a total heating power of 9.65 kW, meaning that the ventilation system is not responsible for providing heat to the rooms. 2 kW air heater is used to warm up the supply air with a heating setpoint of 18 °C if the heat recovery capacity is insufficient. Cooling otherwise is dependent on the ventilation system since the cooling of the rooms is achieved by a cooling heat exchanger installed into the supply air duct. A more comprehensive description of this model is given in the study [65], where a neural network-based building's thermal model was generated.

3.2. Boundary conditions

Boundary conditions are essential parameters that ensure sufficient IAQ in the building and residents' comfort. These conditions must be followed when regulations are conducted. The residents can define boundary conditions or select according to the standard EN 16798–1:2019 indoor climate category II, which states limiting values for IAQ parameters for normal conditions (Table 2). CO_2 concentration, temperature, and relative humidity are selected from the standard as the main IAQ parameters. The standard value for CO_2 concentration for living rooms is 800 ppm, and for bedrooms 550 ppm above ambient concentration. There is no lower limit value for CO_2 concentration, but the concentration cannot be lower than ambient, which in the simulation is assigned to be 400 ppm [66]. Temperature and relative humidity otherwise must be within set limits.

3.3. Simulation dataset

The simulation dataset is generated using a building model constructed in IDA ICE. Each occupied room has an IAQ sensor that measures the room's average CO_2 concentration, temperature, and relative humidity. The AHU sensors are placed in the supply and return air duct (Fig. 5). The supply air temperature, relative humidity, and airflow rate are measured. Since ambient CO_2 concentration in the simulation does not change, measuring it is unnecessary. CO_2 concentration, temperature, and relative humidity are measured in the return air duct. All the measured data is logged into the file imported to MATLAB.

The simulation dataset is divided into two: training and validation. The training data is collected for the first ten weeks starting from the beginning. This data trains forecasting models, performs boundary condition correction, and initializes forecasting models. The validation dataset includes the rest of the 42 weeks. Data from two types of ventilation systems were collected: constant air volume (CAV) and variable air volume (VAV). CAV system operates throughout the day at its nominal level, while the VAV type of system is controlled based on the CO_2 concentration in the return air. In addition, proportional control was applied for the VAV type of system described in the Trane engineers newsletter [67].

Table 2
Boundary conditions for each IAQ parameter.

Parameter	Lower limit	Upper limit
CO_2 concentration in living rooms	400 ppm	1200 ppm
CO_2 concentration in bedrooms	400 ppm	950 ppm
Temperature	23 °C	26 °C
Relative humidity	25%	60%

To generate activations year 2022, balancing energy price and mFRR activations are used. Nord Pool Spot day ahead prices for Estonia, including 20% value-added tax (VAT), were used to calculate electricity prices during normal operating conditions when the ventilation system operated without regulations. To the day-ahead prices, additional fees were added, such as a fixed tariff grid fee of 86.5 €/MWh, renewable energy fee of 13.56 €/MWh, and electricity excise duty of 1.2 €/MWh. During up-regulation, the energy left unconsumed was multiplied by the total electricity price and subtracted from the total cost of consumed energy during the simulation period.

In total, 314 up-regulations for the CAV type of system were conducted; the same value for the VAV type was 230 (Table 3). There were zero down regulations since the capacity for this was insufficient, and the price for regulation was not suitable. The most restricting IAQ parameter was CO_2 concentration, which reached the limit in around 74% of the cases. In comparison, the temperature limit reached 16% to 19% of cases. Relative humidity had no restrictive effect on regulations with the applied simulation setup.

4. Results

The flexibility management methods were applied to the collected dataset. It included training the models and calculating the power consumption and FVR duration forecasts. Forecasted values were compared with measured values to analyze residuals and evaluate the methods' accuracy.

4.1. Power consumption forecast

Power consumption was forecasted using the ARMA(0, 5) model for both system types. ARMA model terms were calculated by using the AIC method. The forecast horizon was selected to be 24 h. Previous days' measurement data was used to forecast the next day's power consumption. One day was divided into 5-minute timeslots where previous days' data forecasted the next 24-hour timeslot value. Dividing data into timeslots allows for quickly respond to ventilation system startups and shutdowns. The 24^{th}-hour forecast with the highest uncertainty was compared with the measured data to calculate the method's accuracy. The year average root means squared error (RMSE) was around 1.3 W for the CAV and 10 W for the VAV. The mean absolute percentage error (MAPE) was around 0.8% for the CAV and around 6.5% for the VAV. Since stochastic occupancy data was used, the VAV system power consumption was more difficult to forecast accurately. Fig. 6 is an example of measured and forecasted power consumption during the first week of November.

4.2. Pollutant generation and FVR duration

Pollutant generation estimation is crucial for FVR duration estimation, and the same is for boundary conditions. If all the IAQ sensors are placed in the AHU, boundary condition correction must be done beforehand. Fig. 7 shows the boundary condition correction based on the data gathered from the second week of January. The boundary conditions were corrected based on one-week data where the 5-minute average was taken for each timestep in a day. Boundary condition correction depended on the room usage and how evenly the pollutant concentration was distributed between rooms. There are minor differences between the boundary conditions of the two ventilation system types.

Simulation results show that CO_2 concentration had the highest impact on flexibility. Fig. 8 shows an example of a one-week CAV type of ventilation system FVR duration estimations for the first week of November, where the FVR duration was dictated mainly by CO_2 concentration. In contrast, the temperature has less impact on FVR duration. The parameter with the shortest FVR duration dictates the whole system duration. VAV type of ventilation system FVR durations (Fig. 9) are

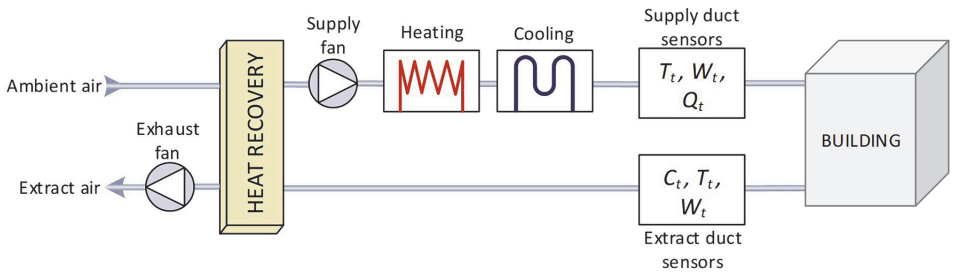

Fig. 5. The layout of the AHU and the location of sensors.

Table 3
Regulations and AHU parameters.

Parameter	System type	
	CAV	VAV
Total number of up-regulations	314	230
Total number of down-regulation	0	0
Number of up-regulations where CO_2 concentration limit was reached	232	172
Number of up-regulations where temperat. limit was reached	52	43
Number of up-regulations where relative humidity limit was reached	0	0
AHU maximum power consumption	134 W	134 W
AHU minimum power consumption	6 W	6 W
Maximum ventilation rate	89.9 l/s	89.9 l/s
Minimum ventilation rate	14.4 l/s	14.4 l/s

similar to CAV since the occupancy profile is the same. However, FVR durations are slightly lower, meaning demand-controlled ventilation lowers the available flexibility. Two approaches were conducted for each system type: room-based and AHU-based estimations. Room-based estimations considered IAQ sensors in each room and used the shortest FVR duration room. AHU-based estimations considered only sensors in one location in the AHU and implemented corrected boundary conditions. AHU-based estimations give a similar FVR duration profile as room-based estimations but have significant deviations that can be caused by stochastic occupancy and the generated boundary conditions.

In residual analysis, regulations were used where CO_2 concentration and temperature limit were reached (Fig. 10). Also, regulations, where the limit was reached within 5 min after the regulation could is conducted were excluded since the simulation timestep is 5 min. The most accurate approach to estimate FVR duration was the room-based approach. Where CO_2 concentration-based estimations RMSE is around 13 min for CAV and 10 min for VAV, temperature-based FVR duration estimation RMSE is around 20 min for the CAV system and around 13 min for VAV. Room-based estimation residuals were biased to the positive side, giving more conservative values. It was the cause of using the FVR duration adjustment algorithm, which decreases given timestep estimation according to the future forecasted values. AHU-based FVR duration estimations were less accurate than the room-based approach. CO_2 concentration-based estimations RMSE was around 33 min for the CAV system and 24 min for VAV. Temperature-based estimation RMSE was around 26 min for the CAV system and 19 min for VAV.

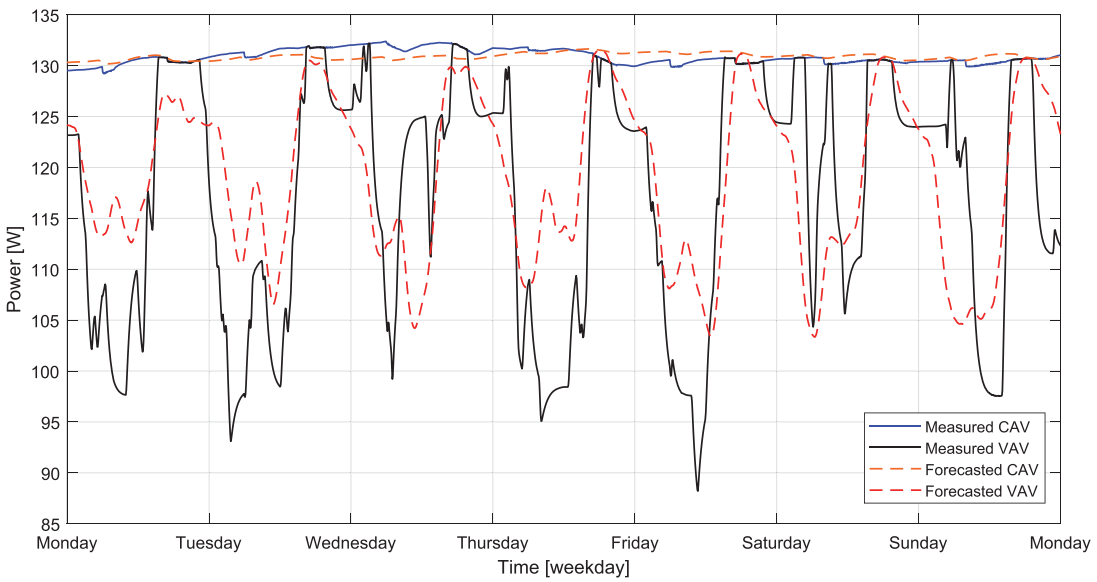

Fig. 6. Measured and forecasted power consumption of the ventilation system.

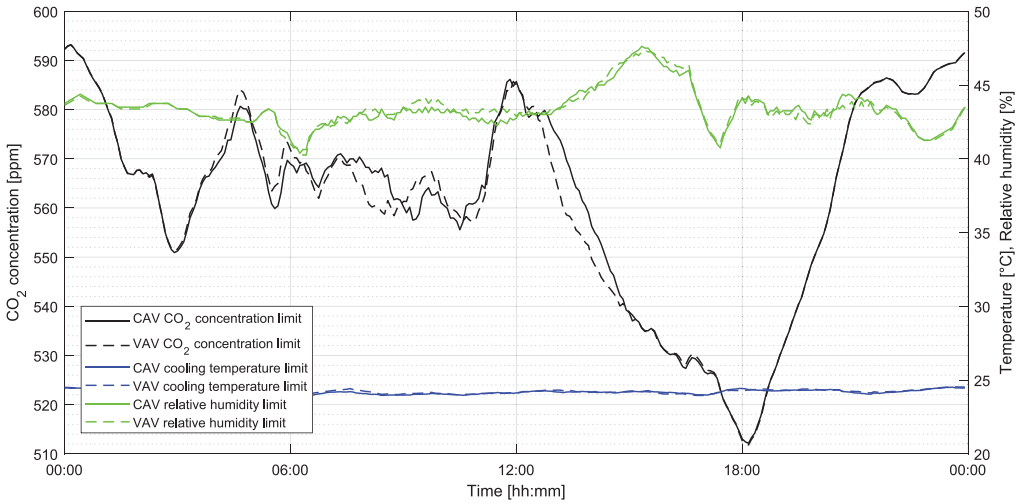

Fig. 7. Daily IAQ parameters' limits after the boundary condition correction.

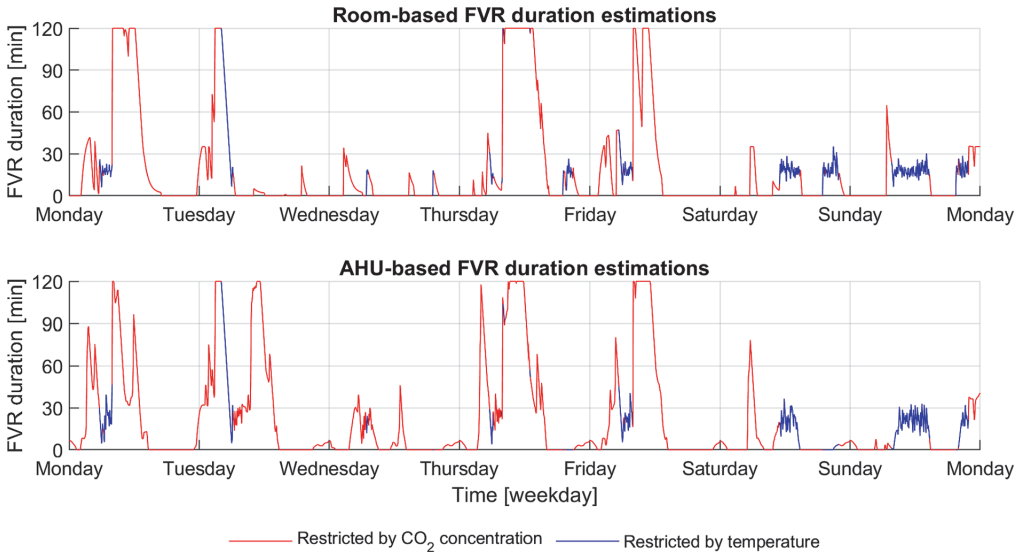

Fig. 8. FVR duration estimations for CAV type of ventilation system.

4.3. Flexibility service activations and pricing

Each hour's price for the flexibility service was calculated based on the CO_2 concentration measurements and costs. For example, upwards regulations are shown in Fig. 11, where the tendered price was calculated using equation (14), where comfort cost was derived from the last two weeks' maximum balancing energy price. The last two weeks' maximum CO_2 generation rate was also used in calculations. Activation of the reserve was only conducted if the tendered price was lower than the balance energy market price, there was mFRR activation, and the available capacity for the regulation was more than 10 W. VAV type of system activated energy was lower than CAV since this system is demand-controlled that causes lower power consumption.

4.4. Discussion

According to the Estonian transmission system operator (TSO), Elering AS [68] up to $\pm$ 10% steady-state error is allowed for the mFRR capacity or 0,1 MW, whichever is larger. Therefore, 0.8% MAPE for the CAV system power and 6.5% MAPE for the VAV power consumption forecasting is sufficient. Furthermore, considering the minimum capacity of 1 MW, this error can be compensated by aggregating multiple ventilation systems where the effect of leveling-off forecasting errors can be achieved [69].

To estimate FVR duration, the room-based approach is the most accurate, where CO_2 concentration-based RMSE for the CAV system is around 13 min and for the VAV type of system around 10 min. Considering the simulation timestep of 5 min, the resolution to calculate

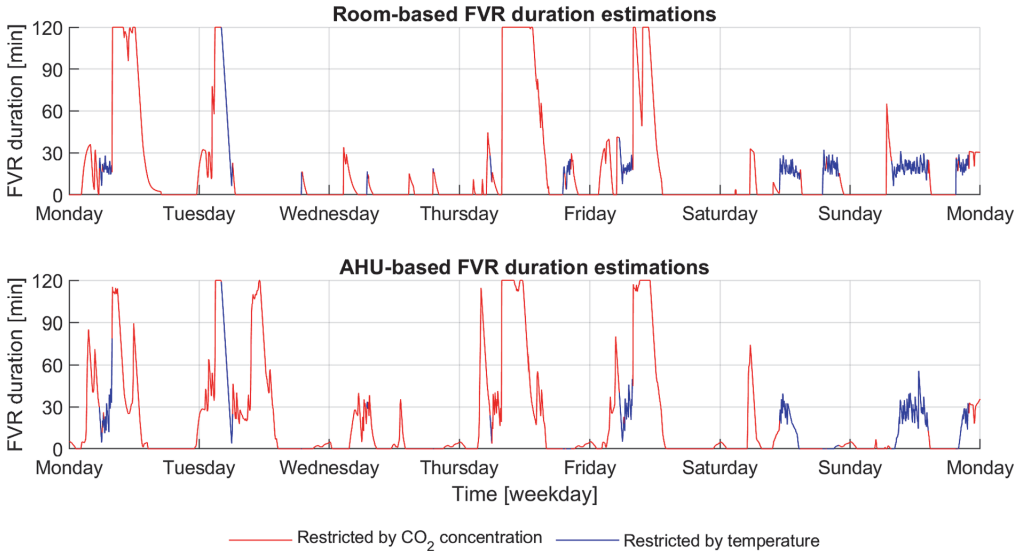

Fig. 9. FVR duration estimations for VAV type of ventilation system.

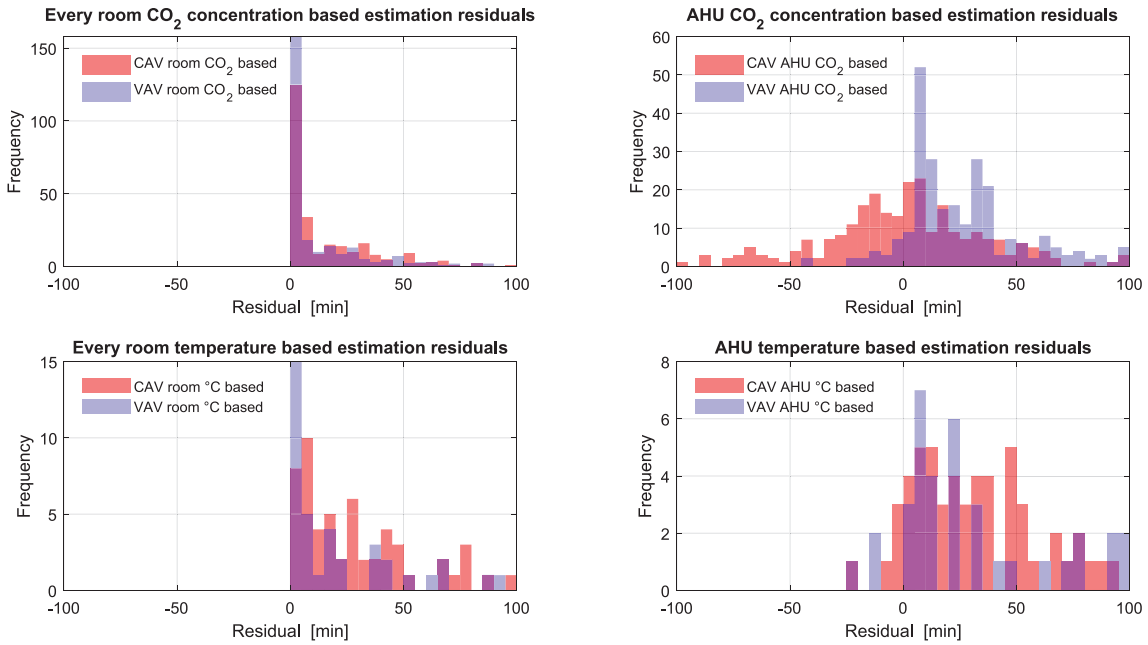

Fig. 10. Residuals of the FVR duration forecasting.

residual can, at maximum, be 5 min. Therefore, mass balance-based FVR estimations are usable in flexibility service. Moreover, residuals of FVR estimations are positive, which means that the IAQ during activations is less likely to be jeopardized. AHU-based estimations are less accurate but can have acceptable performance depending on the building layout and type. It can be backed by the fact that the selected building had stochastic usage, whereas nine-to-five office buildings can have this more consistent throughout a day or week. Also, demand-based ventilation and fewer fluctuations in pollutant concentration can increase the accuracy, as seen from the VAV type of system.

The price to activate the available capacity is the third important parameter tested according to the Estonian balance energy market price and mFRR activations during 2022. The ventilation system operates all day in residential buildings, so regulations have little effect on the total energy consumption. During the simulation period, the total energy consumption of fans was reduced by 1.1% for the CAV system, and VAV

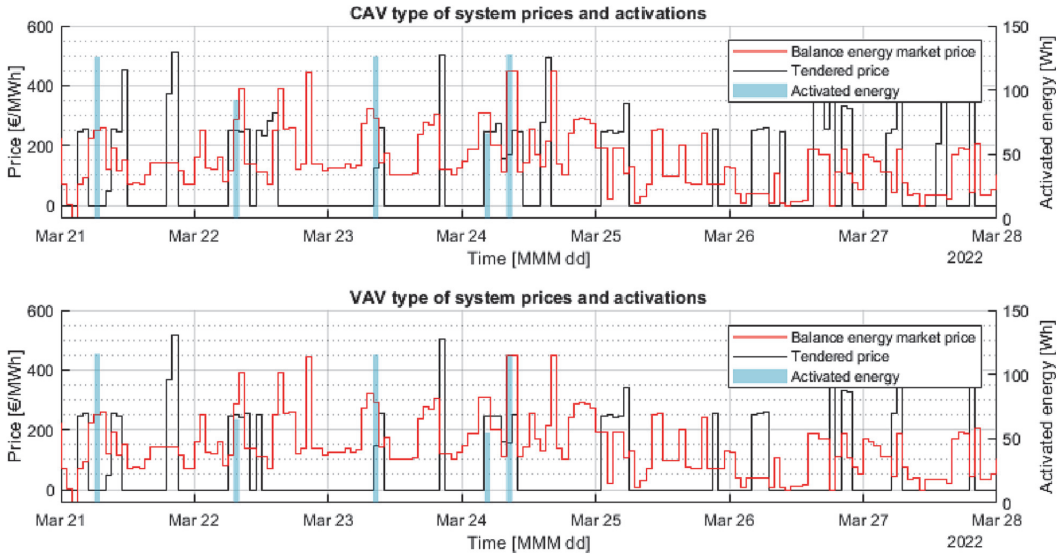

Fig. 11. Flexibility service prices and activations.

type of system, only a 0.7% reduction was noticed (Table 4). The cost of energy was reduced by 4% for the CAV type of system, and around 2.2% reduction was achieved for the VAV type of system. These percentages can be increased when higher profit margins are selected, and the ventilation system is exploited more for the flexibility service. Also, in the energy calculations, air heaters and cooling systems were left out since this paper focuses on fans. It can be expected that with the desynchronization of the Baltic states from the IPS/UPS frequency area [70], the flexibility service will have more use, and there will be more activations.

Table 4
Ventilation system energy consumption and cost of energy during the simulation period.

Parameter	System type	
	CAV	VAV
Energy consumption without regulations	1.152 MWh	1.034 MWh
Energy consumption with regulations	1.139 MWh	1.027 MWh
The total cost of energy without regulations	384.11 €	344.82 €
The total cost of energy with regulations	368.91 €	337.10 €

5. Conclusions

This paper provides a complete set of novel methods to quantify ventilation system energy flexibility developed from an aggregator's viewpoint. Developed methods open the possibility of integrating new and existing buildings with ventilation systems in a flexibility service. In contrast to existing methods and assumptions in the relevant literature, the proposed flexibility management methods employ robust and universal physical rules that are easier for aggregators and building owners to comprehend. Compared to machine learning approaches, the proposed methods require less training, and their performance does not rely on hyperparameters. The methods were tested on the example building model constructed in the IDA ICE simulation platform. A ventilation system's flexibility is quantified through capacity, FVR duration, and the tendered price for the service. ARMA model was used to forecast power consumption for CAV and VAV systems. A forecasting error of 0.8% for the CAV type of system and 6.5% for the VAV type of system was observed.

Two cases to measure IAQ and calculate FVR duration were discussed. In the first case, IAQ is only measured inside AHU, where boundary condition correction was implemented. The second case discussed the possibility of installing sensors in each room which achieved more accurate duration estimations. If exceeding IAQ limits during some regulations is not an issue, installing sensors only in AHU can lower initial investment costs and accelerate the integration process.

The proposed methods were tested, and results were analyzed in multiple stages. First, initial data was generated in IDA ICE which was imported to MATLAB to quantify the flexibility and generated regulation activations by altering the AHU operation schedule. Then, the simulation was rerun in IDA ICE with regulations, and acquired data was used to compare with estimated values. From the financial aspect, the cost of energy consumed was decreased by 4% for the CAV type of system and 1.1% for the VAV type of system. The profitability and optimizing parameters in the price model are subjects for further study.

Declaration of Competing Interest

The authors declare the following financial interests/personal relationships which may be considered as potential competing interests: Argo Rosin reports financial support was provided by European Commission. Tarmo Korõtko reports financial support was provided by Estonian Ministry of Education and Research and European Regional Development Fund. Roya Ahmadiahangar reports financial support was provided by Estonian Research Council.

Data availability

Data will be made available on request.

Acknowledgment

This work has been supported by the European Commission through the H2020 project Finest Twins grant No. 856602; and by the Estonian Ministry of Education and Research and European Regional Fund grant 2014-2020.4.01.20-0289. Additional support was acquired from the Estonian Research Council grant PSG739.

References

[1] European Commission, "Renewable energy directive." https://ec.europa.eu/energy/topics/renewable-energy/renewable-energy-directive/overview_en (accessed May 20, 2021).

[2] European Commission, "A European Green Deal." https://ec.europa.eu/info/strategy/priorities-2019-2024/european-green-deal_en (accessed May 20, 2021).

[3] Eurostat, "Renewable energy statistics," 2022. https://ec.europa.eu/eurostat/statistics-explained/index.php?title=Renewable_energy_statistics#Share_of_renewable_energy_more_than_doubled_between_2004_and_2020 (accessed November 22, 2022).

[4] A. Annuk, W. Yaïci, M. Lehtonen, R. Ilves, T. Kabanen, and P. Miidla, "Simulation of Energy Exchange between Single Prosumer Residential Building and Utility Grid," *Energies 2021, Vol. 14, Page 1553*, vol. 14, no. 6, p. 1553, Mar. 2021, doi: 10.3390/EN14061553.

[5] S. Kerscher, P. Arboleya, The key role of aggregators in the energy transition under the latest European regulatory framework, Int. J. Electr. Power Energy Syst. 134 (2022) 107361.

[6] R. Ahmadiahangar, T. Häring, A. Rosin, T. Korõtko, and J. Martins, "Residential Load Forecasting for Flexibility Prediction Using Machine Learning-Based Regression Model," *Proceedings - 2019 IEEE International Conference on Environment and Electrical Engineering and 2019 IEEE Industrial and Commercial Power Systems Europe, EEEIC/I and CPS Europe 2019*, pp. 2–5, 2019, doi: 10.1109/EEEIC.2019.8783634.

[7] Y. Chen, P. Xu, J. Gu, F. Schmidt, W. Li, Measures to improve energy demand flexibility in buildings for demand response (DR): a review, Energy Build 177 (2018) 125–139, https://doi.org/10.1016/j.enbuild.2018.08.003.

[8] F. Plaum, R. Ahmadiahangar, A. Rosin, J. Kilter, Aggregated demand-side energy flexibility: a comprehensive review on characterization, forecasting and market prospects, Energy Rep. 8 (Nov. 2022) 9344–9362, https://doi.org/10.1016/J.EGYR.2022.07.038.

[9] T. Freire-Barceló, F. Martín-Martínez, Á. Sánchez-Miralles, A literature review of Explicit demand flexibility providing energy services, Electr. Pow. Syst. Res. 209 (2022) 107953.

[10] D. Aussel, L. Brotcorne, S. Lepaul, L. von Niederhäusern, A trilevel model for best response in energy demand-side management, Eur J Oper Res 281 (2) (Mar. 2020) 299–315, https://doi.org/10.1016/J.EJOR.2019.03.005.

[11] T. Kumamoto, H. Aki, M. Ishida, Provision of grid flexibility by distributed energy resources in residential dwellings using time-of-use pricing, Sustain. Energy Grids Networks 23 (Sep. 2020), 100385, https://doi.org/10.1016/J.SEGAN.2020.100385.

[12] A. NOUICER, L. MEEUS, and E. DELARUE, "The economics of explicit demand-side flexibility in distribution grids : the case of mandatory curtailment for a fixed level of compensation," 2020, Accessed: November 24, 2022. [Online]. Available: https://cadmus.eui.eu/handle/1814/67762.

[13] M. Ferrara, A. Violi, P. Beraldi, G. Carrozzino, T. Ciano, An integrated decision approach for energy procurement and tariff definition for prosumers aggregations, Energy Econ 97 (May 2021), 105034, https://doi.org/10.1016/J.ENECO.2020.105034.

[14] P. Arboleya, M.A. Kippke, S. Kerscher, Flexibility management in the low-voltage distribution grid as a tool in the process of decarbonization through electrification, Energy Rep. 8 (Jun. 2022) 248–256, https://doi.org/10.1016/J.EGYR.2022.01.076.

[15] A. Martín-Crespo, S. Saludes-Rodil, and E. Baeyens, "Flexibility management with virtual batteries of thermostatically controlled loads: Real-time control system and potential in spain," *Energies (Basel)*, vol. 14, no. 6, Mar. 2021, doi: 10.3390/EN14061711.

[16] F. Lezama, J. Soares, B. Canizes, Z. Vale, Flexibility management model of home appliances to support DSO requests in smart grids, Sustain Cities Soc 55 (2020) 102048.

[17] R.A. Ahangar, A. Sheykholeslami, Bulk Virtual Power Plant, a Novel Concept for Improving Frequency control and Stability in Presence of Large Scale RES 4 (2014) 1017–1044.

[18] R. AhmadiAhangar, A. Rosin, A.N. Niaki, I. Palu, T. Korõtko, A review on real-time simulation and analysis methods of microgrids, Int. Trans. Electr. Energy Systems 29 (11) (2019) 1–16, https://doi.org/10.1002/2050-7038.12106.

[19] L. Aleixo, A. Rosin, H. Sæle, A. Z. Morch, O. S. Grande, and I. P. Sintef, "Ecogrid EU project - Real time price based load control and economic benefits in a wind production based system," *IET Conference Publications*, vol. 2013, no. 615 CP, pp. 10–13, 2013, doi: 10.1049/cp.2013.1253.

[20] "Ventilation units | European Commission." https://ec.europa.eu/info/energy-climate-change-environment/standards-tools-and-labels/products-labelling-rules-and-requirements/energy-label-and-ecodesign/energy-efficient-products/ventilation-units_en (accessed November 14, 2022).

[21] European Parliament, "Directive of the European Parliament and of the Council on the energy performance of buildings (recast)," 2023. Accessed: May 24, 2023. [Online]. Available: https://www.europarl.europa.eu/doceo/document/A-9-2023-0033_EN.html.

[22] I. Drovtar, J. Niitsoo, A. Rosin, J. Kilter, and I. Palu, "Electricity consumption analysis and power quality monitoring in commercial buildings," *PQ 2012: 8th International Conference - 2012 Electric Power Quality and Supply Reliability, Conference Proceedings*, pp. 107–112, 2012.

[23] A. Franco, L. Miserocchi, and D. Testi, "HVAC energy saving strategies for public buildings based on heat pumps and demand controlled ventilation," *Energies (Basel)*, vol. 14, no. 17, Sep. 2021, doi: 10.3390/EN14175541.

[24] Elering AS, Augstsprieguma tikls AS, and Litgrid AB, "Baltic Transparency Dashboard." https://baltic.transparency-dashboard.eu/ (accessed May 22, 2023).

[25] Elering AS, "Elering Live." https://dashboard.elering.ee/en (accessed May 22, 2023).

[26] Q. Gao, M. Demoulin, H. Wang, S. Riaz, and P. Mancarella, "Flexibility Characterisation from Thermal Inertia of Buildings at City Level: A Bottom-up Approach," *UPEC 2020 - 2020 55th International Universities Power Engineering Conference, Proceedings*, Sep. 2020, doi: 10.1109/UPEC49904.2020.9209795.

[27] Y. Chen, P. Xu, Z. Chen, H. Wang, H. Sha, Y. Ji, Y. Zhang, Q. Dou, S. Wang, Experimental investigation of demand response potential of buildings: combined passive thermal mass and active storage, Appl. Energy 280 (2020) 115956.

[28] M. Tavakkoli, S. Fattaheian-Dehkordi, M. Pourakbari-Kasmaei, M. Liski, M. Lehtonen, Bonus-Based Demand Response Using Stackelberg Game Approach for Residential End-Users Equipped with HVAC System, IEEE Trans Sustain Energy 12 (1) (Jan. 2021) 234–249, https://doi.org/10.1109/TSTE.2020.2989583.

[29] A.C. Duman, H.S. Erden, Ö. Gönül, Ö. Güler, A home energy management system with an integrated smart thermostat for demand response in smart grids, Sustain Cities Soc 65 (2021) 102639.

[30] C. Pathiravasam, G.K. Venayagamoorthy, Distributed demand response management for a virtually connected community with solar power, IEEE Access 10 (2022) 8350–8362, https://doi.org/10.1109/ACCESS.2022.3141772.

[31] M. Gough, S.F. Santos, M. Lotfi, M.S. Javadi, G.J. Osorio, P. Ashraf, R. Castro, J.P. S. Catalao, Operation of a technical virtual power plant considering diverse distributed energy resources, IEEE Trans. Ind. Appl. 58 (2) (2022) 2547–2558.

[32] S. Faddel, Q.Z. Sun, G. Tian, Modeling and coordination of commercial buildings in distribution systems, IEEE Trans. Ind. Appl. 58 (2) (2022) 1654–1663, https://doi.org/10.1109/TIA.2022.3145768.

[33] M. Jelić, M. Batić, and N. Tomašević, "Demand-side flexibility impact on prosumer energy system planning," *Energies (Basel)*, vol. 14, no. 21, Nov. 2021, doi: 10.3390/en14217076.

[34] D. Chao, P. Chakraborty, T. Nishikawa, A.E. Motter, Hierarchical power flow control in smart grids: enhancing rotor angle and frequency stability with demand-side flexibility, IEEE Trans. Control. Netw. Syst. 8 (3) (Sep. 2021) 1046–1058, https://doi.org/10.1109/TCNS.2021.3070665.

[35] C. Utama, S. Troitzsch, J. Thakur, Demand-side flexibility and demand-side bidding for flexible loads in air-conditioned buildings, Appl Energy 285 (2021) 116418.

[36] L. Langer, "An optimal peer-to-peer market considering modulating heat pumps and photovoltaic systems under the German levy regime," *Energies (Basel)*, vol. 13, no. 20, Oct. 2020, doi: 10.3390/en13205348.

[37] S. Xu, L. Yu, X. Lin, J. Dong, and Y. Xue, "Online distributed price-based control of DR resources with competitive guarantees," in *13th ACM International Conference on Future Energy Systems, e-Energy*, Association for Computing Machinery (ACM), Jun. 2022, pp. 17–33. doi: 10.1145/3538637.3538836.

[38] H. Golmohamadi, K.G. Larsen, P.G. Jensen, I.R. Hasrat, Hierarchical flexibility potentials of residential buildings with responsive heat pumps: a case study of Denmark, J. Build. Eng. 41 (2021) 102425.

[39] B. Vand, K. Martin, J. Jokisalo, R. Kosonen, A. Hast, Demand response potential of district heating and ventilation in an educational office building, Sci. Technol. Built. Environ. 26 (3) (Mar. 2020) 304–319, https://doi.org/10.1080/23744731.2019.1693207.

[40] L. Yu, D. Xie, C. Huang, T. Jiang, Y. Zou, Energy optimization of hvac systems in commercial buildings considering indoor air quality management, IEEE Trans. Smart Grid 10 (5) (Sep. 2019) 5103–5113, https://doi.org/10.1109/TSG.2018.2875727.

[41] H. Hao, Y. Lin, A.S. Kowli, P. Barooah, S. Meyn, Ancillary service to the grid through control of fans in commercial Building HVAC systems, IEEE Trans. Smart Grid 5 (4) (2014) 2066–2074.

[42] V. Maask, T. Haring, R. Ahmadiahangar, A. Rosin, and T. Korotko, "Analysis of ventilation load flexibility depending on indoor climate conditions," *Proceedings of the IEEE International Conference on Industrial Technology*, vol. 2020-February, pp. 607–612, Feb. 2020, doi: 10.1109/ICIT45562.2020.9067153.

[43] O. Wonuola Olawale, B. Gilbert, J. Reyna, Aggregate residential demand flexibility behavior: a novel assessment framework, Sustain. Energy Technol. Assess. 56 (2023) 103073.

[44] H. Li, Z. Wang, T. Hong, M.A. Piette, Energy flexibility of residential buildings: a systematic review of characterization and quantification methods and applications, Adv. Appl. Energy 3 (2021) 100054.

[45] S. Martinez, M. Vellei, J. Le Dréau, Demand-side flexibility in a residential district: What are the main sources of uncertainty? Energy Build 255 (2022) 111595.

[46] M. Hu, F.u. Xiao, S. Wang, Neighborhood-level coordination and negotiation techniques for managing demand-side flexibility in residential microgrids, Renew. Sustain. Energy Rev. 135 (2021) 110248.

[47] Z. Dong, X. Zhang, Y. Li, G. Strbac, Values of coordinated residential space heating in demand response provision, Appl. Energy 330 (Jan. 2023), 120353, https://doi.org/10.1016/J.APENERGY.2022.120353.

[48] Y. Chen, Z. Chen, P. Xu, W. Li, H. Sha, Z. Yang, G. Li, C. Hu, Quantification of electricity flexibility in demand response: office building case study, Energy 188 (2019) 116054.

[49] R.V. Klyuev, I.D. Morgoev, A.D. Morgoeva, O.A. Gavrina, N.V. Martyushev, E. A. Efremenkov, Q.i. Mengxu, Methods of forecasting electric energy consumption: a literature review, Energies (Basel) 15 (23) (Dec. 2022) 8919.

[50] C. Eid, P. Codani, Y. Chen, Y. Perez, R. Hakvoort, Aggregation of demand side flexibility in a smart grid: a review for European market design, Int. Conf. European Energy Market, EEM vol. 2015-August (Aug. 2015), https://doi.org/10.1109/EEM.2015.7216712.

[51] X. Jin, Q. Wu, H. Jia, Local flexibility markets: Literature review on concepts, models and clearing methods, Appl. Energy 261 (Mar. 2020), 114387, https://doi.org/10.1016/J.APENERGY.2019.114387.
[52] V. Maask, A. Mikola, T. Korõtko, A. Rosin, M. Thalfeldt, J. Kurnitski, M. Thalfeldt, Contributions to ventilation system demand response: a case study of an educational building, E3S Web of Conferences 246 (2021) 11001.
[53] Estonian Centre of Standardisation and Accreditation, "EVS-EN 16798-1:2019+NA:2019 Energy performance of buildings - Ventilation for buildings - Part 1: Indoor environmental input parameters for design and assessment of energy performance of buildings addressing indoor air quality, thermal environment, lighting and acoustics - Module M1-6," 2019.
[54] F. Shariatzadeh, C.B. Vellaithurai, S.S. Biswas, R. Zamora, A.K. Srivastava, Real-time implementation of intelligent reconfiguration algorithm for Microgrid, IEEE Trans Sustain Energy 5 (2) (Apr. 2014) 598–607, https://doi.org/10.1109/TSTE.2013.2289864.
[55] ASHRAE, *2013 ASHARE Handbook - Fundamentals*. Atlanta, 2013.
[56] Vaisala, "HUMIDITY CONVERSION FORMULAS - Calculation formulas for humidity," *Humidity Conversion Formulas*, p. 16, 2013, [Online]. Available: https://www.vaisala.com/sites/default/files/documents/Humidity_Conversion_Formulas_B210973EN-F.pdf.
[57] "Validation & certifications - Simulation Software | EQUA." https://www.equa.se/en/ida-ice/validation-certifications.
[58] "Liginullenergia eluhooned, väikemajad," Tallinn, 2017.
[59] RAUSI OÜ and HEVAC OÜ, "Liginullenergia eluhooned, väike eramu. Päikese-elektrisüsteem, tugevvool. Variant 2," 2017. [Online]. Available: https://kredex.ee/sites/default/files/2019-03/PV_ja_tugevvool_variant_2.pdf.
[60] Roofit Solar Energy OÜ, "Liginullenergia eluhooned, väike eramu. Päikese-elektrisüsteem, tugevvool [Online]. Available: Variant 1," (2017) https://kredex.ee/sites/default/files/2019-03/PV_ja_tugevvool_variant_1.pdf.
[61] Hevac OÜ, "Liginullenergia eluhooned, väike eramu. Soojusvarustus, küte ja ventilatsioon," 2017. [Online]. Available: https://kredex.ee/sites/default/files/2019-03/Kute_ja_ventilatsioon_3.pdf.
[62] Ttü, "Liginullenergia eluhooned, väike eramu [Online]. Available: Energiatõhusus" (2017) https://kredex.ee/sites/default/files/2019-03/Energiatohusus_3.pdf.
[63] O.Ü. Tibeco Woodhouse, "Liginullenergia eluhooned, väike eramu [Online]. Available: Arhitektuur," (2017) https://kredex.ee/sites/default/files/2019-03/Arhitektuur_3.pdf.
[64] S. Wolf, D. Calì, M.J. Alonso, R. Li, R.K. Andersen, J. Krogstie, H. Madsen, Room-level occupancy simulation model for private households, J Phys Conf Ser 1343 (1) (2019) 012126.
[65] T. Häring, T.M. Kull, R. Ahmadiahangar, A. Rosin, M. Thalfeldt, H. Biechl, Microgrid oriented modeling of space heating system based on neural networks, J. Build. Eng. 43 (Nov. 2021), 103150, https://doi.org/10.1016/J.JOBE.2021.103150.
[66] Á. Muelas, P. Remacha, A. Pina, E. Tizné, S. El-Kadmiri, A. Ruiz, D. Aranda, J. Ballester, Analysis of different ventilation strategies and CO2 distribution in a naturally ventilated classroom, Atmos. Environ. 283 (2022) 119176.
[67] Trane, "CO2-based demand-controlled ventilation with ASHRAE Standard 62.1-2004," 2005, [Online]. Available: https://www.trane.com/content/dam/Trane/Commercial/global/products-systems/education-training/engineers-newsletters/standards-codes/admapn017en_1005.pdf.
[68] Elering AS, "The prequalification process and technical requirements of Manual Frequency Restoration Reserves (mFRR) Service," 2022. [Online]. Available: https://elering.ee/sites/default/files/2022-07/mFRR%20service_prequalification%20process%20and%20technical%20requirements_20220722.pdf.
[69] Elering AS, AS "Augstsprieguma tikls," and LITGRID AB, "Baltic balancing market rules," 2020.
[70] "Synchronisation with continental Europe | Elering." https://elering.ee/en/synchronization-continental-europe (accessed February 13, 2023).
[71] Statistics Estonia, Dwellings and buildings with dwellings, Estonia counts (2021). https://rahvaloendus.ee/en/results/dwellings-and-buildings-dwellings.

Publication II

Maask, V., Rosin, A., Korõtko, T. (2023), “Virtual Energy Storage Model of Ventilation System for Flexibility Service,” 17th IEEE International Conference on Compatibility, Power Electronics and Power Engineering, CPE-POWERENG 2023 (1–6). IEEE.

Virtual Energy Storage Model of Ventilation System for Flexibility Service

Vahur Maask
Department of Electrical Power Engineering and Mechatronics
Tallinn University of Technology
Smart City Center of Excellence (Finest Twins)
Tallinn, Estonia
vahur.maask@taltech.ee

Argo Rosin
Smart City Center of Excellence (Finest Twins)
Department of Electrical Power Engineering and Mechatronics
Tallinn University of Technology
Tallinn, Estonia
ORCID 0000-0002-6485-1037

Tarmo Korõtko
Smart City Center of Excellence (Finest Twins)
Department of Electrical Power Engineering and Mechatronics
Tallinn University of Technology
Tallinn, Estonia
ORCID 0000-0002-7368-1797

***Abstract*—Virtual Energy Storage is a concept where flexible loads are used as conventional battery energy storage. This is a useful approach to provide flexibility service and avoid large expenses on energy storage equipment. This paper proposes novel methods to describe a ventilation system as a Virtual Energy Storage. These methods enable the possibility to use ventilation systems in flexibility service while requiring less data and parametrization than currently available methods. The mass balance analysis is used to derive robust methods to calculate power capacity, energy capacity, State of Charge, etc. Methods are tested with a simulation on an object which is constructed in IDA ICE. In the simulation two use cases are considered: office and apartment. Based on the year 2022 price data and reserve activations the total costs of energy could be decreased by up to 35% if the system is used in flexibility service.**

Keywords—demand-side flexibility, ventilation systems, virtual energy storage, manual frequency restoration reserve

I. Introduction

The European Union (EU) is moving toward climate neutrality as a result of rising environmental consciousness and climatic changes. According to Eurostat [1], during the ten years from 2010 to 2020, the share of renewable energy consumption in gross final energy consumption increased across the EU from 14.4% to 22.1%, while it increased from 24.6% to 30.2% in Estonia. Distributed volatile renewable energy generation has made it more challenging to maintain the balance between supply and demand in the electric power system. This emphasizes the significance of demand-side flexibility [2] and demand response managed by aggregators as outlined in [3].

A Virtual Energy Storage (VES) is a concept where controllable components of the electric power system are used similarly to the conventional energy storage system to provide grid services. These components can be small-capacity conventional energy storage, flexible loads, distributed generators, etc. [4]. The main aim of a VES is to store surplus energy or release it when needed similar to charging or discharging a battery energy storage system (BESS). Using buildings' flexible loads in a VES has several benefits compared to a conventional energy storage system [5], [6] which are lower initial investment costs, soft boundaries (e.g. minimum and maximum indoor temperature), necessity (e.i. most of the buildings need systems to ensure indoor climate and comfort), etc. [4], [7].

Models and methods to describe a VES have been of interest to many researchers. Studies [8]–[10] have focused on air conditioning systems and provided models to calculate power capacity, energy capacity, duration of a charging cycle, and duration of a discharging cycle. K. Vijayalakshmi, K. Vijayakumar, and K. Nandhakumar [8] have reported that 92% accuracy can be achieved by using artificial neural networks to forecast energy capacity. Modeling thermostatically controlled loads as a VES, with the primary emphasis on building heating systems, is another popular topic. Researchers of the study [11] have proposed a temperature-based method to calculate the state of charge of thermostatically controlled loads. It is found by the authors of the research article [12] that with the use of the heating system as a VES the power consumption can be reduced by 20% with a 2 °C adjustable setpoint.

Exploiting mechanical ventilation systems in flexibility service has been an elevated interest in the research. Temperature-based ventilation management is taken into account to provide grid services in studies [13], [14]. J. Wang, S. Huang, D. Wu, and N. Lu [15] proposed physics-based thermal models coupled with machine-learning algorithms to attain the needed power level where a ventilation system is viewed as a VES. It was discovered in [15] that 15% of the rated fan power can be employed to offer grid services without endangering occupants' thermal comfort. S. Rotger-Griful, R. H. Jacobsen, D. Nguyen, and G. Sørensen [17] discussed the potential application of a ventilation system in demand response. They claim that a single 13 kW ventilation system in a 12-story apartment building can achieve a 4.5 kW of power increase and 1.0 kW of power reduction without jeopardizing indoor air quality (IAQ). In the study [16] it was experimentally found that at 33% room usage the selected ventilation system can operate for up to 55 minutes at a minimum ventilation rate.

A few studies consider ventilation systems as VES and the main focus is on heating and cooling systems. Studies that discuss ventilation systems as flexible loads are concentrated on thermal constraints, but according to the study [17] the most restricting parameter is CO_2 concentration. In the studied literature machine learning techniques were widely used, but these methods need a vast amount of data and training to achieve sufficient performance. This can be a problem in a real application. Therefore, this paper proposes a novel and robust mass balance analysis based approach to describe a ventilation system as a VES. The paper is organized as follows: in section 2, methods are described to calculate important metrics for a VES, in section 3 object model and simulation process is explained, and section 4 discusses the results of the conducted analysis.

II. Methods to Quantify Virtual Energy Storage

Charateristizing a VES is essential for quantification. This paper is focused on the following characteristics, which allow quantifying a VES similar to a conventional energy storage system:

- State of Charge (SoC),
- Power capacity,
- Energy capacity,
- Self-discharge rate.

A. State of Charge

A ventilation system based VES SoC can be described through CO_2 concentration in a building because this parameter is directly connected to building usage and is affected by occupants. Depending on the system type and building usage the SoC of the VES can be fluctuating throughout the day. CO_2 concentration in a building can be derived through the use of a mass balance analysis equation as follows:

$$V\frac{dC}{dt} = G + QC_{amb} - QC, \tag{1}$$

where V – air volume in a building (m^3),
C – CO_2 concentration in a building (ppm),
G – CO_2 generation rate (m^3/s),
Q – airflow rate for the building (m^3/s),
C_{amb} – ambient CO_2 concentration (ppm) [18].

The CO_2 generation rate during the timestep t can be calculated as shown in (2). This equation is derived from the previously mentioned mass balance and is put into a discrete form which is more suitable for a control system. The CO_2 generation rate is needed to calculate the SoC for timestep t and estimate the energy capacity.

$$G_t = \frac{V \cdot (C_t - C_{t-1})}{\Delta t} + Q_t \cdot (C_t - C_{amb}), \tag{2}$$

where C_{t-1} – CO_2 concentration during previous timestep $t-1$ (ppm),
Δt – timestep length (s).

When SoC is at 1 then the CO_2 concentration is at a minimum level which can be calculated through maximum ventilation rate Q_{max} and the CO_2 generation at the selected timestep as shown in (3). In a normal situation, the CO_2 concentration cannot be lower than the ambient. Since the building usage changes throughout the day then the minimum CO_2 concentration also changes accordingly. When SoC is at 0 then the CO_2 concentration has reached its limit C_{limit}. The maximum CO_2 concentration limit is a fixed parameter and therefore does not change. The actual SoC is the relative CO_2 concentration in a building at each timestep as shown in (4).

$$C_{t,min} = \begin{cases} \frac{G_t}{Q_{max}} + C_{amb}, & G_t > 0 \\ C_{amb}, & G_t \le 0 \end{cases} \tag{3}$$

$$SoC_t = \frac{C_t - C_{limit}}{C_{t,min} - C_{limit}} \tag{4}$$

B. Power capacity

The available power capacity at a specific timestep can be calculated from the system's maximum and minimum power consumption. These values can be taken from the documentation of the system or can be measured on-site. The VES charging power $P_{t,ch}$ for timestep t can be calculated through the forecasted power consumption P_t for this timestep considering the maximum power consumption P_{max} as shown in (5). The VES discharging power $P_{t,ch}$ can be calculated the same way but considering the minimum power consumption P_{min} as shown in (6).

$$P_{t,ch} = P_{max} - P_t \tag{5}$$

$$P_{t,disch} = P_t - P_{min} \tag{6}$$

Affinity laws, also known as fan laws can be used to describe the relationship between power consumption and the airflow rate [18]. Where fan rotational speed N can also be used instead of airflow rate. These relations are depicted in (7) and are defined through two operational points. Usually measured, predicted, or nominal values are used to derive one value from others.

$$\frac{P_1}{P_2} = \left(\frac{N_1}{N_2}\right)^3 = \left(\frac{Q_1}{Q_2}\right)^3 \tag{7}$$

The real ventilation system does not follow affinity laws exactly and typically there is higher power consumption at the minimum ventilation rate Q_{min} which can be caused by losses and self-consumption of the fan drive. Therefore, power consumption bias P_{bias} is calculated through maximum and minimum ventilation power consumption and airflow rate as shown in (8). The power consumption for the timestep t is calculated using affinity law which states the dependence between airflow rates and power consumption as shown in (9).

$$P_{bias} = \frac{P_{min} - P_{max}\left(\frac{Q_{min}}{Q_{max}}\right)^3}{1 - \left(\frac{Q_{min}}{Q_{max}}\right)^3} \tag{8}$$

$$P_t = (P_{max} - P_{bias}) \cdot \left(\frac{Q_t}{Q_{max}}\right)^3 + P_{bias} \tag{9}$$

Based on the affinity laws ventilation system's power consumption has a non-linear dependence on the airflow rate. Meaning that decreasing the airflow rate by twofold will decrease the power consumption by 8 times. This creates the possibility to decrease airflow rate less than required and lower the influence on IAQ. If the length of regulation duration τ_t is known or is forecasted then the VES charging power can be calculated as shown in (10). This is achieved by calculating the airflow rate based on the demand and replacing Q_t in (9). Before the discharge power can be calculated CO_2 generation rate must be known which can be done by using (2). Power consumption at a specific time is also an important parameter that can be forecasted by using the appropriate method. In this paper, the autoregressive moving average (ARMA) model is used for forecasting which is tuned by implementing the Akaike information criterion (AIC) method. It must be checked that discharging power does not exceed the calculated value shown in (6).

$$P_{t,disch} = \left[\frac{\tau_t \cdot G_t - V \cdot (C_{limit} - C_t)}{\tau_t \cdot Q_{max} \cdot \frac{C_t + C_{limit} - 2C_{amb}}{2}}\right]^3 \cdot (P_{bias} - P_{max}) + P_t - P_{bias} \tag{10}$$

C. Energy capacity

A VES differs from a BESS by the way the energy capacity can be estimated. A ventilation system can exceed its boundary conditions without causing irreversible damage to the system. During charging the ventilation system consumes more energy to lower the CO_2 concentration. From the CO_2 concentration viewpoint, the ventilation system can consume an infinite amount of energy during the charging cycle. CO_2 concentration cannot go below the minimum level and the duration when the CO_2 concentration reaches the minimum level can be calculated as shown in (11). Otherwise, the duration of the forced ventilation rate must be considered in energy calculations which can be depicted as shown in (12). During discharging the ventilation system consumes less energy and the air exchange rate is lowered which causes CO_2 concentration to rise. During discharging cycle ventilation system can operate at a lower power consumption level for a limited time which is dictated by the CO_2 concentration limit. This method to calculate the duration was tested in the case study [16] where one ventilation system in an educational building was used.

$$\tau_{t,ch} = \frac{V \cdot (C_{t,min} - C_t)}{G_t \cdot Q_{max} \cdot \sqrt[3]{\frac{P_t + P_{t,ch} - P_{bias}}{P_{max} - P_{bias}} \cdot \frac{C_t + C_{t,min} - 2C_{amb}}{2}}} \tag{11}$$

$$\tau_{t,disch} = \frac{V \cdot (C_{limit} - C_t)}{G_t \cdot Q_{max} \cdot \sqrt[3]{\frac{P_t - P_{t,disch} - P_{bias}}{P_{max} - P_{bias}} \cdot \frac{C_t + C_{limit} - 2C_{amb}}{2}}} \tag{12}$$

Calculated durations can be used to estimate energy capacity. Before energy capacity can be calculated an adjustment in discharging duration estimations must be conducted. This means that if the next timestep duration estimation is shorter which can be caused by an increase in building usage then the estimated discharging duration must be shortened as shown in (13). This process is repeated and after each iteration, the sum of all duration estimations is calculated and compared with the previous iteration as shown in (14). If they are equal then the adjustment is completed. There is no need to adjust the charging durations since charging has a positive effect on IAQ.

$$\tau_{t,i} = \begin{cases} \tau_{t+1,i-1} + \Delta t, & \tau_{t+1,i-1} < \tau_{t,i-1} - \Delta t \\ \tau_{t,i-1}, & \tau_{t+1,i-1} \geq \tau_{t,i-1} - \Delta t \end{cases}, \tag{13}$$

where $\tau_{t,i}$ – an estimate of duration at timestep t during correction iteration i,
$\tau_{t,i-1}$ – an estimate of duration at timestep t during previous correction iteration $i - 1$.

$$\sum_{t=1}^{n} \tau_{t,i} = \sum_{t=1}^{n} \tau_{t,i-1} \tag{14}$$

Finally, the energy capacity can be calculated, but since the duration is calculated in seconds then it must be converted into hours as follows:

$$E_t = P_t \cdot \tau_t / 3600 \tag{15}$$

D. Self-discharge rate

CO_2 concentration has always some stable level which is dependent on the CO_2 generation rate and the ventilation rate. This stable level causes the effect of self-discharge or self-charge of the VES. Self-discharge takes place when the CO_2 concentration level is lower than the stable level and self-charge happens when the CO_2 concentration level is higher than the stable level. The self-discharge or self-charge rate can be calculated as follows:

$$k_t = \frac{P_t - P_{min}}{\Delta t} \cdot \frac{V \cdot (C_{limit} - C_t) \cdot 3600}{G_t \cdot Q_{min} \cdot \frac{C_t + C_{limit} - 2C_{amb}}{2}} - \frac{P_{t-1} - P_{min}}{\Delta t} \cdot \frac{V \cdot (C_{limit} - C_{t-1}) \cdot 3600}{G_{t-1} \cdot Q_{min} \cdot \frac{C_{t-1} + C_{limit} - 2C_{amb}}{2}}, \tag{16}$$

where k_t – self-discharge or self-charge rate at time t (Wh/s),
P_{t-1} – ventilation system power consumption at time $t - 1$ (W),
C_{t-1} – CO_2 concentration at time $t - 1$ (ppm),
Δt – duration between two sequent timesteps (s).

E. Pricing model

The VES pricing model is needed to provide flexibility to the grid and grant financial incentives for the VES owner. Activations for up or down regulations are conducted in the simulation based on the pricing model. A personalized pricing mechanism is used to achieve this as shown in (17). The direction of regulation dictates the ingredients of the final regulation price. If up-regulation is activated and the ventilation system power consumption is lowered then it is needed to compensate for lower IAQ in the building. This can be done by considering variable building usage which can be described through the CO_2 generation rate. If the building has low usage then the cost of regulation is lower and vice versa. If down-regulation is activated and the ventilation system's power consumption is increased then this causes additional energy consumption which must be compensated. If the ventilation system return air CO_2 concentration is higher than the minimum possible CO_2 concentration then the goal is to decrease the CO_2 concentration level by purchasing electricity at a lower price. When the CO_2 concentration is low due to the low or non-existent occupancy then down-regulation is provided if the additional costs are compensated. Also, the profit margin is included in the regulation price which is dictated by the building owner.

In the simulation, the year 2022 balancing energy price, Nord-Pool day-ahead, and manual frequency restoration reserve (mFRR) activations in Estonia are used to calculate the regulation price and determine the need to activate the VES reserve. Maximum CO_2 generation is the maximum value of the previous two weeks. The previous two weeks' maximum balancing energy price is used for the regulation cost on comfort. The profit will be split between the VES owner and the aggregator and therefore the fixed profit margin is 0.

$$price_t = \begin{cases} \frac{G_t}{G_{max}} \cdot c_{comf} + c_{prof}, & \Delta P < 0 \\ \frac{C_t - C_{t,min}}{C_{limit} - C_{t,min}} \cdot c_{t,el} - c_{t,fees} - c_{prof}, & \Delta P > 0 \end{cases} \tag{17}$$

where $price_t$ – the calculated regulation price at timestep t (€/kWh),
G_{max} – maximum CO_2 generation rate (m^3/s),
c_{comf} – the regulation cost on comfort (€/MWh),
c_{prof} – profit margin for regulations (€/MWh),
ΔP – change of power consumption during regulation (kW),
$C_{t,el}$ – electricity price including electricity market price and electricity supplier margin at timestep t (€/kWh),
$C_{t,fees}$ – the sum of all the fees which include transmission costs and taxes added to consumed energy price at timestep t (€/MWh).

III. Object Model and Simulation Process

The VES methods are applied to the object model which is constructed in IDA Indoor Climate and Energy (IDA ICE). IDA ICE is a specialized simulation tool to imitate building behavior and it has been validated according to the standards EN 15255:2007, EN 15265:2007, EN 13791, and ASHRAE 140-2004. VES quantification methods are applied and analysis is conducted in Matlab.

A. Object model

The object is a room that is a part of a single-story building (Fig. 1). Air exchange is provided by an independent ventilation system that is used in simulations. The ventilation system is configured to operate at a constant air volume (CAV). The room floor area is 13.84 m^2 and the height is 2.7 m. For comparison purposes, this object is configured for two use cases: office and apartment.

The room type is changed through changes in occupancy, ventilation system operation schedule, and ventilation rate (Table I). The occupancy schedule depends on the weekday and time. Hourly occupancy schedule is acquired from the standard EN 16798-1:2019 and accordingly, offices are not used during weekends and nighttime which means that building usage at this time equals 0.

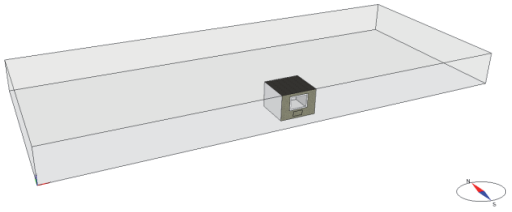

Fig. 1. The room of a building used in simulations

TABLE I. Parameters for Simulation

Parameter	Symbol	Office	Apartment
Air volume in a building, m^3	V	37.4	37.4
Ventilation rate, l/s	Q_t	15.31	13.05
Occupancy, pers/m^2	-	0.0588	0.0353
Minimum ventilation rate, l/s	Q_{min}	1.99	1.95
Maximum ventilation rate, l/s	Q_{max}	15.31	13.05
Minimum AHU power consumption, W	P_{min}	0.87	0.91
Maximum AHU power consumption, W	P_{max}	25.4	21.6
Maximum CO_2 concentration, ppm	C_{limit}	700	700

The standard EN 16798-1:2019 gives guidelines on how to control the ventilation system during unoccupied periods. If the ventilation system is shut off then the minimum amount of air must be delivered to a building before occupation. This minimum amount is 1 volume of the building that must be ventilated within 2 hours. If the ventilation rate is lowered during the unoccupied period then the total airflow for diluting emissions from the building must be at least 0.15 l/(s·m^2) in all rooms. The ventilation rate of around 0.15 l/(s·m^2) is also used during regulations when ventilation system power consumption is lowered. Depending on the selected standard the CO_2 concentration limit can vary [19]. In this paper, the CO_2 concentration limit of 700 ppm is selected which is the lowest limit which is given by the standards. This will ensure more data points where the concentration limit is reached.

B. Simulation process

The developed methods described in the previous section are applied as a co-simulation between IDA ICE and Matlab. The simulation process can be divided into stages (Fig. 2) where each stage can be described as follows:

I The object model is configured in IDA ICE and the occupancy and ventilation system operation schedule is generated.

II One year simulation is conducted and power, airflow, and CO_2 concentration data are acquired with 5-minute resolution.

III The acquired data is processed in Matlab and all the parameters which quantify VES are calculated. Based on the year 2022 balancing energy price, day-ahead price, and mFRR activations ventilation system operation schedule is altered to imitate regulations.

IV One year simulation is repeated in IDA ICE with regulations.

V Data is acquired from IDA ICE and previously calculated VES parameters are compared in the context of energy capacity and cost reduction.

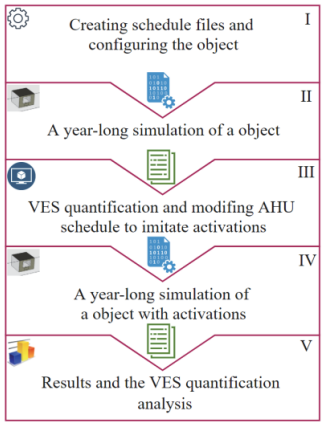

Fig. 2. Stages of the simulation process

IV. Results

Unlike conventional energy storage systems the VES can have SoC higher than 1 (Fig. 3). This is caused by the preventilation effect and volatile building usage where the CO_2 concentration can be lower than the estimated minimum

CO_2 concentration. Since the selected system is CAV type the ventilation rate is at a maximum which means that SoC is stabilizing around 1.

ARMA(0, 4) model is suitable for CAV type of ventilation system power capacity forecasting. The forecasting mean absolute percentage error (MAPE) is around 1.2% for the office and around 0.6% for the apartment. The forecasting root means squared error (RMSE) is around 0.4 W for the office and around 0.2 W for the apartment. Down-regulations are only possible for the office type of room (Fig. 4) where the ventilation system is scheduled to shut down during unoccupied hours. During maximum occupancy hours, the discharge power is decreased to achieve a 60-minute regulation duration which for the apartment is always during night hours (Fig. 5).

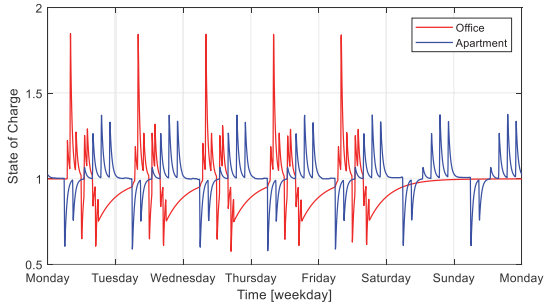

Fig. 3. One week state of charge of a VES

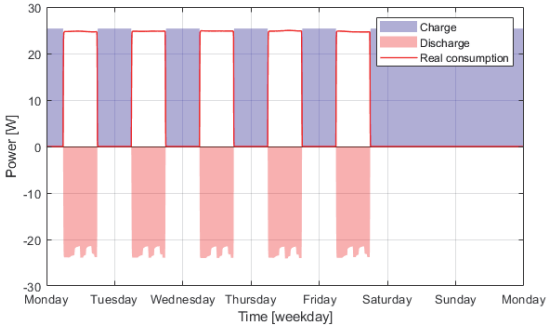

Fig. 4. VES charge and discharge power of the office during a week

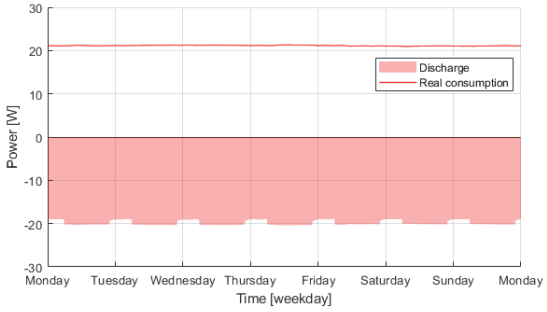

Fig. 5. VES discharge power of the apartment during a week

Residuals of energy capacity estimations are only calculated for regulations where the CO_2 concentration reached its limit which is less than the total number of regulations conducted during the simulation. Only residuals for up-regulation could be calculated (Fig. 6) since during down-regulation the minimum CO_2 concentration was not achieved. The energy capacity estimation MAPE is around 14% for the office and around 9% for the apartment. The energy capacity RMSE is around 4 Wh for the office and 2 Wh for the apartment. For the office, there are more over-optimistic estimations that can be caused by the consecutive regulations where the CO_2 concentration cannot recover. This is a problem with this kind of simulation where estimations cannot be adjusted when the next regulation is activated.

Price and mFRR activation data from the year 2022 are used in simulations. Fig. 7 is an example of regulation prices and activated energy capacity for Friday and Saturday. Since the ventilation system is shut down during the weekend then there are no up-regulations for the office and the tendered price is 0.

The CO_2 concentration limit is reached at around 12% of regulations in the office and around 5% for the apartment (Table II). Since there are mainly up-regulations then the total energy consumption during the year decreased by around 12% for the office and 9% for the apartment. The cost of energy decreased even more since the up-regulations generated positive cash flow and also the amount of energy during the regulation was left unconsumed. The total cost of energy was decreased by around 35% for the office and around 30% for the apartment.

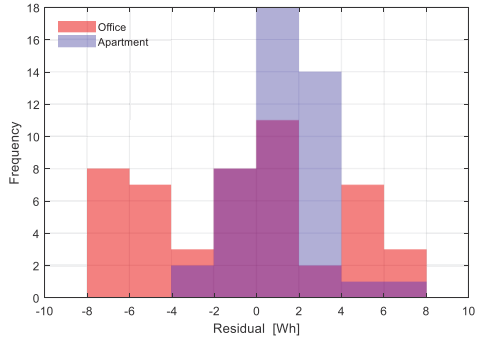

Fig. 6. Residuals of a VES energy capacity forecast for up-regulations

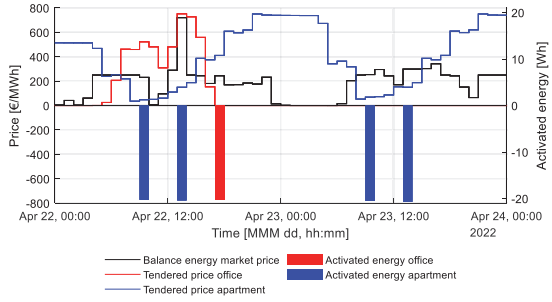

Fig. 7. Prices and energy activations of up-regulation

TABLE II. SIMULATION RESULTS

Parameter	Office	Apartment
Total number of up-regulations	412	856
Total number of down-regulations	3	0
Number of up-regulations where CO_2 concentration limit was reached	49	44
Number of down-regulations where CO_2 concentration minimum value was reached	0	0
Energy consumption without regulations	78 kWh	186 kWh
Energy consumption with regulations	69 kWh	169 kWh
The total cost of energy without regulations	29.80 €	62.16 €
The total cost of energy with regulations	19.31 €	43.63 €

V. CONCLUSIONS

This paper proposes methods to describe ventilation systems as VES. These methods are used to model ventilation system flexibility to provide services to the electric system. These methods are tested on the object model constructed in IDA ICE. The object model is roughly a 14 m^2 room that has two use cases: office and apartment. The year 2022 electricity price and mFRR service activation data are used to analyze the performance of methods. The energy capacity estimation method has a MAPE of 14% for the office and 9% for the apartment.

A year-long simulation showed that by using a ventilation system as a VES and providing flexibility service the system operation costs can be reduced. The cost of consumed energy is decreased by around 35% for the office and by around 30% for the apartment. This creates a good incentive for building owners to allow the aggregator to use their system for the flexibility service. Compared to existing methods described in research papers the developed methods described in this paper are more complete where each VES parameter can be calculated. The methods are based on physical principles which are easier to follow and implement in the real system compared to gray or black box models.

In future work, the VES quantification methods are applied to real buildings, and the aggregation of multiple buildings with different ventilation systems is employed. This will generate more data to conduct a comprehensive analysis of the methods' performance.

ACKNOWLEDGMENT

This study was financed by the Doctoral School of Energy and Geotechnology - III, supported by the European Union, European Regional Development Fund (Tallinn University of Technology's ASTRA "TTÜ arenguprogramm aastateks 2016-2022"). Additional support was received from the European Commission through the H2020 project Finest Twins grant No. 856602; and the Estonian Ministry of Education and Research and European Regional Fund grant 2014-2020.4.01.20-0289.

REFERENCES

[1] Eurostat, "Renewable energy statistics," 2022. https://ec.europa.eu/eurostat/statistics-explained/index.php?title=Renewable_energy_statistics#Share_of_renewable_energy_more_than_doubled_between_2004_and_2020 (accessed Nov. 22, 2022).

[2] S. Mishra, H. Koduvere, I. Palu, R. Kuhi-Thalfeldt, and A. Rosin, "Assessing demand side flexibility with renewable energy resources," *EEEIC 2016 - International Conference on Environment and Electrical Engineering*, Aug. 2016, doi: 10.1109/EEEIC.2016.7555546.

[3] S. Kerscher and P. Arboleya, "The key role of aggregators in the energy transition under the latest European regulatory framework," *International Journal of Electrical Power and Energy Systems*, vol. 134, no. July 2021, p. 107361, 2022, doi: 10.1016/j.ijepes.2021.107361.

[4] M. Cheng, S. S. Sami, and J. Wu, "Benefits of using virtual energy storage system for power system frequency response," *Appl Energy*, vol. 194, pp. 376–385, May 2017, doi: 10.1016/J.APENERGY.2016.06.113.

[5] A. Rahmoun, A. Armstorfer, J. Helguero, H. Biechl, and A. Rosin, "Mathematical modeling and dynamic behavior of a Lithium-Ion battery system for microgrid application," *2016 IEEE International Energy Conference, ENERGYCON 2016*, Jul. 2016, doi: 10.1109/ENERGYCON.2016.7513977.

[6] R. Ahmadiahangar *et al.*, "Energy Storage Expansion Planning in Microgrid," *Proceedings - 2020 IEEE 14th International Conference on Compatibility, Power Electronics and Power Engineering, CPE-POWERENG 2020*, pp. 433–437, Jul. 2020, doi: 10.1109/CPE-POWERENG48600.2020.9161502.

[7] A. Rosin, S. Link, M. Lehtla, J. Martins, I. Drovtar, and I. Roasto, "Performance and feasibility analysis of electricity price based control models for thermal storages in households," *Sustain Cities Soc*, vol. 32, pp. 366–374, Jul. 2017, doi: 10.1016/J.SCS.2017.04.008.

[8] K. Vijayalakshmi, K. Vijayakumar, and K. Nandhakumar, "Prediction of virtual energy storage capacity of the air-conditioner using a stochastic gradient descent based artificial neural network," *Electric Power Systems Research*, vol. 208, Jul. 2022, doi: 10.1016/J.EPSR.2022.107879.

[9] S. Kumar, V. Krishnasamy, R. Kaur, and N. K. Kandasamy, "Virtual Energy Storage-Based Energy Management Algorithm for Optimally Sized DC Nanogrid," *IEEE Syst J*, vol. 16, no. 1, pp. 231–239, Mar. 2022, doi: 10.1109/JSYST.2021.3050779.

[10] Y. Ji, Q. Xu, K. Luan, and B. Yang, "Virtual energy storage model of air conditioning loads for providing regulation service," *Energy Reports*, vol. 6, pp. 627–632, Feb. 2020, doi: 10.1016/J.EGYR.2019.11.130.

[11] Y. Zhou, Y. Wu, Z. Dong, D. Fan, and S. Zhang, "TCL Aggregators Based on Virtual Battery Model Participate in Energy Transaction," *2021 IEEE IAS Industrial and Commercial Power System Asia, I and CPS Asia 2021*, pp. 633–638, 2021, doi: 10.1109/ICPSASIA52756.2021.9621565.

[12] X. Zhang, W. Gao, Y. Li, Z. Wang, Y. Ushifusa, and Y. Ruan, "Operational performance and load flexibility analysis of japanese zero energy house," *Int J Environ Res Public Health*, vol. 18, no. 13, Jul. 2021, doi: 10.3390/IJERPH18136782.

[13] J. Wang, S. Huang, D. Wu, and N. Lu, "Operating a commercial building HVAC load as a virtual battery through airflow control," *IEEE Trans Sustain Energy*, vol. 12, no. 1, pp. 158–168, 2021.

[14] H. Hao, Y. Lin, A. S. Kowli, P. Barooah, and S. Meyn, "Ancillary Service to the grid through control of fans in commercial Building HVAC systems," *IEEE Trans Smart Grid*, vol. 5, no. 4, pp. 2066–2074, 2014.

[15] J. Wang, S. Huang, D. Wu, and N. Lu, "Operating a commercial building HVAC load as a virtual battery through airflow control," *IEEE Trans Sustain Energy*, vol. 12, no. 1, pp. 158–168, 2021.

[16] V. Maask, A. Mikola, T. Korõtko, A. Rosin, and M. Thalfeldt, "Contributions to ventilation system demand response: A case study of an educational building," *E3S Web of Conferences*, vol. 246, Mar. 2021, doi: 10.1051/E3SCONF/202124611001.

[17] V. Maask, T. Haring, R. Ahmadiahangar, A. Rosin, and T. Korotko, "Analysis of ventilation load flexibility depending on indoor climate conditions," *Proceedings of the IEEE International Conference on Industrial Technology*, pp. 607–612, 2020.

[18] S. Rotger-Griful, R. H. Jacobsen, D. Nguyen, and G. Sørensen, "Demand response potential of ventilation systems in residential buildings," *Energy Build*, vol. 121, pp. 1–10, 2016.

[19] G. Wei *et al.*, "A review and comparison of the indoor air quality requirements in selected building standards and certifications," *Build Environ*, vol. 226, p. 109709, Dec. 2022, doi: 10.1016/J.BUILDENV.2022.109709.

Publication III

Maask, V., Mikola, A., Korõtko, T., Rosin, A., Thalfeldt, M. (2021), “Contributions to ventilation system demand response: a case study of an educational building,” Cold Climate HVAC & Energy 2021 (1–6). E3S Web of Conferences.

Contributions to ventilation system demand response: a case study of an educational building

Vahur Maask[1,2*], *Alo* Mikola[1,3], *Tarmo* Korõtko[1,2], *Argo* Rosin[1,2], and *Martin* Thalfeldt[1,3]

[1]Smart City Center of Excellence, Tallinn University of Technology, 19086 Tallinn, Estonia
[2]Department of Electrical Power Engineering and Mechatronics, Tallinn University of Technology, 19086 Tallinn, Estonia
[3]Department of Civil Engineering and Architecture, Tallinn University of Technology, 19086 Tallinn, Estonia

Abstract. The increasing share of volatile renewable energy in the electricity grid increases the importance of load flexibility and Demand Response for balancing electricity supply with demand. Flexible loads in office buildings (e.g. educational buildings) are heating, ventilation, and air conditioning (HVAC) systems. This paper focuses on ventilation systems as flexible loads for providing ancillary services to the grid. A number of studies consider ventilation system control based only on demand or discuss possibilities of improving system performance. Previous studies provide little or no information about ventilation system flexibility, e.g. amount of power modulation, the rate of change, and the duration of how long the power level can be held. The described information is required by aggregators to provide load aggregation services for transmission system operators (TSO). This paper proposes a robust and model-free approach to estimate ventilation system flexibility according to CO_2 concentration in extracted air. The proposed approach includes power regulation boundaries for the ventilation system and duration estimation when operating at the selected boundary. A case study is conducted on a ventilation system, which services an auditorium of an educational building. The current paper analyzes the proposed robust approach for estimating ventilation system flexibility and compares estimation to measured results.

1 Introduction

By introducing distributed volatile renewable energy generation to the electricity grid the balance between electricity supply and demand is becoming difficult to maintain and predict. This is the reason why Demand Response (DR) as a source for energy flexibility is becoming important to provide ancillary services to the grid to maintain system stability. Flexibility can be characterized by the amount of power modulation, the duration of forced power level, the rate of change, the response time, location, etc. [1].

According to the European Commission buildings consume around 40% of the energy produced in the European Union [2]. In commercial buildings, heating, ventilation, air conditioning, and lighting systems are the biggest energy consumers, where ventilation systems alone account up to 12% of the overall energy consumption [3]. While the usage of heating, cooling, and lighting is dependent on ambient conditions, their utilization in DR programs can be limited. Nonetheless, the thermal capacity of a building and its use to provide flexibility has been studied in [4], [5]. Ventilation systems on the other hand, are well suited to provide ancillary services to the grid. The load flexibility of ventilation systems is dictated by indoor air quality (IAQ) as it must provide the defined minimum requirements for indoor climate at all times. The standard CEN/TR 16798 states minimum requirements for three main IAQ parameters: CO_2 concentration, temperature, and humidity.

The use of ventilation systems for providing load flexibility has been of elevated interest of research. Studies [6], [7] consider temperature based ventilation control to provide grid services. A ventilation system is considered as virtual battery storage in [6] where physics-based thermal models and machine-learning techniques are combined to achieve the required power level. In [7] HVAC system was studied to provide frequency regulation services where it was found that 15% of the rated fan power can be used to provide grid services without jeopardizing occupants' thermal comfort. The potential use of a ventilation system in DR is discussed in [8], where the authors state that a single 13 kW ventilation system in a 12-story apartment building can provide 4.5 kW of power increase and 1.0 kW of power reduction when needed without compromising IAQ. Ventilation system shutdown when needed is discussed in [9] where it is found that CO_2 concentration has the highest impact on ventilation system flexibility and the minimum duration for a residential building with a space volume of 100 m^3 is 5 minutes. Mikola et al. [10], [11] have shown that the CO_2-based tracer gas methods are suitable for the ventilation performance evaluation and they have also confirmed that in many cases the fully mixed ventilation is achieved.

* Corresponding author: vahur.maask@taltech.ee

© The Authors, published by EDP Sciences. This is an open access article distributed under the terms of the Creative Commons Attribution License 4.0 (http://creativecommons.org/licenses/by/4.0/).

The studied literature does not consider all parameters that characterize flexibility and proposed methods for harvesting flexibility are tailored to function in specific systems, which means it is not universally applicable in other types of systems. One mentioned approach was to use machine-learning techniques, but to implement this approach, a vast amount of data is needed. This paper diminishes the lack of research in the given field by proposing a universal, model-free, and robust method to estimate ventilation system flexibility. Mass balance analysis is used to estimate a ventilation system load flexibility based on CO_2 concentration. This approach can be used in parallel with machine-learning methods to immediately include the selected ventilation system into an aggregator's portfolio, which can afterward be taken over by artificial intelligence. The paper is organized as follows: in section 2, the experiment setup for conducting the case study and the method for estimating ventilation system flexibility are given, and section 3 discusses the results of the conducted case study.

2 Method

This paper is based on a case study conducted in an auditorium of an educational building and the ventilation system servicing it. In this chapter, the equipment used to conduct this case study and the methodology to estimate load flexibility for the ventilation system is covered.

2.1 Experiment setup

The case study was carried out in an auditorium of a building at the Tallinn University of Technology. The experiment included a ventilation system that was servicing only the selected auditorium. The floor area of the selected auditorium is 224.5 m^2 and the estimated volume of indoor air is 1122.5 m^3. The maximum occupancy of the auditorium is 200 persons and the designed ventilation rate is 1.76 m^3/s. The minimum allowable ventilation rate was set by the fan drive frequency of 17 Hz which is around 0.48 m^3/s.

A pollution source, a CO_2 cylinder with accessories to measure and regulate gas flow, was placed in the center of the auditorium. The CO_2 cylinder was weighted before and after the experiment to estimate the average CO_2 generation rate during the experiment. An air mixing fan was placed close to the CO_2 gas outlet to introduce a vertical component into CO_2 pollution and to assist in mixing the air (Figure 1). The use of a mixing fan was required due to the low temperature of the injected CO_2 gas that does not mix well with indoor air, while the air exhaled by persons is warmer and has better mixing properties. Fresh air is introduced to the auditorium from beneath the floor with multiple fresh air inlets and polluted air is extracted from above with one air duct which can be located in Figure 1 at the right part of the room plan.

IAQ loggers were placed into the auditorium marked as *LGR1* to *LGR13* that are located at the height of around 0.8 m, except *LGR6* that is installed on the extract air outlet at the height of around 3 m. The level of CO_2 was measured using the Evikon E6226 measurement unit (CO_2 level 0 to 10000 ppm). These loggers are added to have a better overview of CO_2 distribution inside the auditorium, but they are not used to estimate the ventilation system flexibility. Ventilation system flexibility estimations use only a single CO_2 concentration sensor located in the extract air duct, which is the preferred placement for such sensors in most ventilation systems. The described flexibility estimation methodology can be applicable for most ventilation systems with minimal investments.

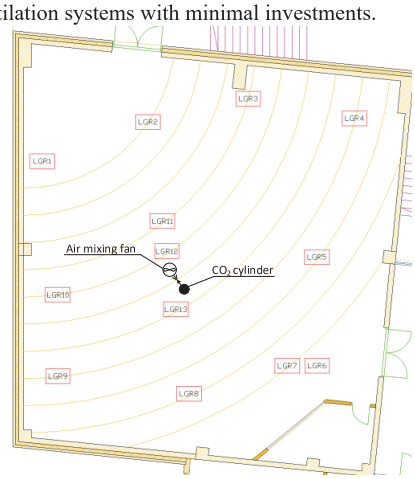

Figure 1. The auditorium and measurement equipment layout.

A mechanical ventilation system is used to change the auditorium air, where two fans are used to supply fresh air and to extract polluted air (Figure 2). The system also includes rotary heat recovery which was set to operate at a maximum rotational speed. The ventilation system also includes air filters, preheating and -cooling of the supply air that are not included in Figure 2.

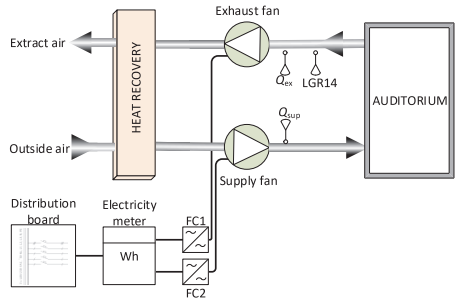

Figure 2. The ventilation system layout with added measurement equipment.

Airflow rates for extract and supply air were measured with a timestep of 1 minute. To measure the airflow, a multifunction indoor air quality meter Testo 435-4 (differential pressure 0 to 250 Pa and accuracy ±1 Pa) was used. One IAQ logger was installed into the extract air duct which measures extract air CO_2 concentration with a timestep of 1 minute. Each fan

speed is regulated with frequency converters *FC1* and *FC2* where each fan drive is powered from the distribution board. Each fan power consumption is measured separately with one electricity meter BFM136. This electricity meter complies with accuracy requirements stated in IEC 62053-22 for class 0.5S. The time interval for power consumption measurements is selected to be 2 min.

2.2 Flexibility prediction

Two main parameters that need to be predicted for flexibility estimation are (a) the amount of power modulation and (b) the duration of how long the power level can be held. The amount of power modulation can be estimated based on historical data where the assumption that each day the ventilation system is operating with the same load pattern is made. The amount of load modulation can be expressed as the available power increase P_{inc} or decrease P_{dec} which can be calculated as follows:

$$P_{inc} = P_{max} - P_i \quad (1)$$

$$P_{dec} = P_i - P_{min} \quad (2)$$

where P_{max} and P_{min} are ventilation unit power consumption at maximum and minimum ventilation rate which in this study are named as forced ventilation rate (FVR). The power consumption of the ventilation system at the time i is expressed as P_i.

The duration for the selected power level is defined by IAQ, where the CO_2 concentration is measured to be used in estimations. The standard CEN/TR 16798-2 states limit conditions for IAQ, where the maximum allowable CO_2 concentration for educational buildings is around 1100 ppm.

A mass balance analysis can be used to estimate CO_2 concentration in a space where the assumption is made that CO_2 concentration can be expressed as a single variable C. The change of CO_2 concentration in a given space is dependent on CO_2 generation (G), ambient CO_2 concentration (C_0), ventilation rate (Q), and the space volume (V). The mass balance equation for mixing ventilation can be expressed as follows [8]:

$$V\frac{dC}{dt} = G + QC_0 - QC \quad (3)$$

CO_2 generation must be known to estimate ventilation system flexibility. Based on measurements CO_2 generation rate can be calculated as shown in (4). This equation is derived from (3) and is put into a discrete form which is more suitable for a control system.

$$G_i = \frac{V \cdot (C_i - C_{i-1})}{\Delta t} + Q_i \cdot (C_i - C_0) \quad (4)$$

Knowing the CO2 generation rate at a given timestep, estimation for ventilation system flexibility according to CO_2 concentration can be made as shown in (5). When the ventilation system is working at the minimum ventilation rate to provide power decrease then CO_2 concentration starts rising until the upper limit is reached. Therefore, (5) can be used to estimate the duration when the CO_2 concentration in a space will reach its boundary. The main restriction for the duration when the ventilation system is operating at lowered power consumption is the upper limit of CO_2 concentration. There is no lower limit for CO_2 concentration, which means that there is no limitation to increase ventilation system power consumption in the CO_2 concentration perspective.

$$\tau_i = \frac{V \cdot (C_{limit} - C_i)}{G_i - Q_{min} \cdot \frac{C_i + C_{limit} - 2C_0}{2}} \quad (5)$$

CO_2 concentration and airflow measurements can have fluctuations that do not correlate due to disturbances or measurement reading lag. This will cause unrealistic flexibility estimations (e.g. estimated duration for FVR is infinitely long). To have a good estimation, these values must be filtered. In this paper, the maximum duration τ_{max} is chosen to be 5 hours, which was selected based on the results of the case study. All estimations that exceed this limit are considered unreasonable and will be replaced by an alternative estimation based on the average CO_2 generation during the last 5 minutes, which can be calculated as follows:

$$\tau_i > \tau_{max} \Longrightarrow G_i = \frac{1}{n}\sum_{k=1}^{n} G_{i-k} \quad (6)$$

The same principle as described previously is used when unexpected negative CO_2 generation is detected at times the ventilation system is forced to operate at a minimum rate. The CO_2 generation data of the previous 5 minutes will be used to calculate the new duration estimation and also the next CO_2 concentration, using (3).

3 Results

In this section, results from the power consumption measurement of the selected ventilation system are discussed to estimate the amount of power modulation available at each hour of the day. A case study is conducted to estimate the duration of how long FVR can be held until the CO_2 concentration reaches its limit. Based on acquired data the proposed method to estimate the ventilation system flexibility can be studied.

3.1 Amount of power modulation

The available amount of power modulation can be estimated statistically based on historical data. In this study, the ventilation system was monitored for one week from 23rd November to 30th November 2020. Results show that the ventilation system is operating

with the same schedule on all days, including weekends (Figure 3). The ventilation system is scheduled to operate at the maximum rate between 7:00 and 22:00 which means that between this time window ventilation system power consumption can only be decreased. The ventilation system is operating at the minimum rate between 22:00 and 7:00 which means that during this time the ventilation system power consumption can only be increased. Transitions from maximum rate to minimum and vice versa conducted at 7:00 and 22:00 do not happen immediately which causes outliers in the data.

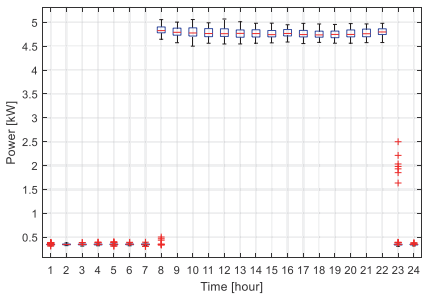

Figure 3. Studied ventilation system power consumption during one day.

During the operation at maximum ventilation rate, the average power consumption of the ventilation system was around 4.77 kW, where the maximum deviation of 0.56 kW was metered between 9:00 and 10:00. During the operation at the minimum ventilation rate, the average power consumption of the ventilation system was around 0.35 kW, where the deviation between the maximum and minimum value was less than 0.1 kW. Based on the measurements carried out, it can be estimated that the amount of power modulation for the selected system is around 4.42 kW.

3.2 Case study

A case study was conducted on the 9th of October, where the ventilation system that services an auditorium of an educational building was switched from normal to minimum operation (Figure 4). The objective was to reduce the power consumption of the system and to estimate the load flexibility. The case study was divided into events where one disturbance caused by the mixing fan was added (Table 1).

The average power consumption of the ventilation system before switching it to the minimum rate was around 4.88 kW which corresponds to the airflow rate of approximately 1.79 m^3/s. Calculated specific fan power (SFP) before the FVR was around 2,73 $kW/(m^3/s)$. During operation at the FVR, the system power consumption was around 0.34 kW, which corresponds to the airflow rate of approximately 0.48 m^3/s. Calculated SFP at the FVR was around 0,71 $kW/(m^3/s)$. According to the standard EN 13779, SFP should be less than 2.0 $kW//(m^3/s)$, which means that the ventilation system has poor efficiency at maximum ventilation rate. The ventilation system took around 90 seconds to reach from one power level to another which means that the rate of power change was approximately 50 W/s.

Table 1. The case study events and schedule.

Event	Description	Time
I	Start of the experiment, CO_2 gas injection into the auditorium	11:52
II	The ventilation system is switched to the minimum rate	12:44
III	Start of the disturbance, the CO_2 gas mixing fan is switched off	13:03
IV	End of the disturbance, the CO_2 gas mixing fan is switched on	13:14
V	The maximum allowable CO_2 concentration of 1100 ppm reached	13:39
VI	End of the experiment, the ventilation system is returned to normal operation	13:46

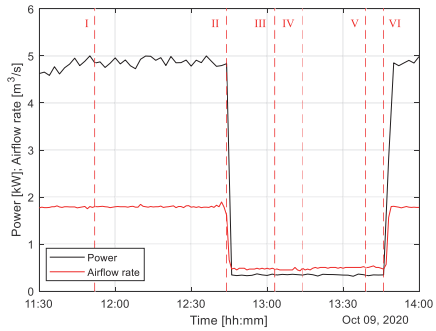

Figure 4. The ventilation system power consumption and airflow rate during the experiment.

The experiment started at 11:52 with the opening the valve for the CO_2 cylinder (Figure 5). During the experiment, the CO_2 gas flow rate into the auditorium was kept around 22 l/min which is roughly equal to the CO_2 generated by 66 persons, which corresponds to 33% of room usage. At 12:44, the ventilation system was switched to operate at the FVR. The time before this action was used to stabilize the CO_2 concentration in the auditorium and to estimate the time duration of how long the ventilation system can be held at the minimum rate. At 13:03 the mixing fan for CO_2 gas was switched off and at 13:14 its operation was restored. This caused a temporary decrease of CO_2 concentration in extract air, which was the result of poor CO_2 gas mixing in the auditorium air. The flexibility estimation algorithm identified this event as an unexpected negative CO_2 generation rate and started to calculate the CO_2 concentration in the auditorium based on the CO_2 generation data of the previous 5 minutes. This part of the algorithm is only activated when the ventilation system is forced to operate at a certain rate that is below normal operating condition to achieve a decreased power consumption.

The boundary for CO2 concentration was reached at 13:39 after which the ventilation system operated for 7 minutes at the lowest rate. At 13:46, the ventilation system was set to operate at the normal rate and the

valve for the CO_2 cylinder was closed, which marked the end of the experiment. Poor mixing of the CO_2 gas with the air inside the auditorium resulted in a high CO_2 concentration. The build-up of the CO_2 concentration is not expected when the CO_2 is generated by people inside the auditorium instead of a gas dispensing system.

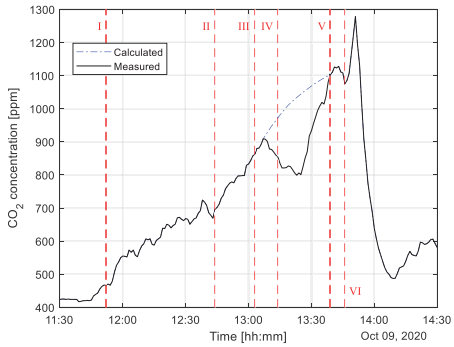

Figure 5. CO_2 concentration in extract air during the experiment.

The amount of power modulation achieved in the experiment in accordance with the analytical estimation shown in Figure 3. The duration of the period where the CO_2 concentration reached or exceeded boundary conditions was around 55 minutes. The estimated duration which was calculated at 12:44 was around 53 minutes, which means that the error of the estimation was 2 minutes or 4%. The initial estimation method for reduced operation duration produced fluctuating results, which is why a moving-average filter was implemented (Figure 6). The window of length of the filter was set to 3 minutes that smoothed larger fluctuations and did not cause significant lag from the initial estimation. The measured duration shows how much time was left until the CO_2 concentration boundary was reached from the start of the FVR. At 13:07, the algorithm detected an unexpected negative CO_2 generation rate, which meant that the CO_2 concentration level was estimated and the measurements did not affect the duration estimation. The estimated CO_2 concentration reached the boundary of 1100 ppm before it was measured which is why the estimations are lower than measured results.

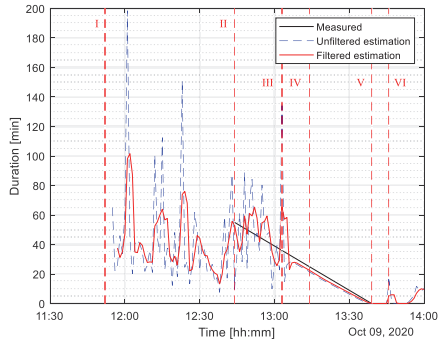

Figure 6. Measured and estimated durations for forced ventilation rate.

In this paper, IAQ loggers located inside the auditorium were used to have an overview of conditions in the auditorium during the experiment. During normal operation, it was found that there is a weak positive correlation with a coefficient of approximately 0.48 between the CO_2 concentration measured inside the extract air duct and the average CO_2 concentration inside the auditorium. It can be seen from Figure 7 that during the ventilation system normal operation the extract air CO_2 concentration was in the range of CO_2 concentration inside the auditorium measured in multiple points. During the period when the ventilation system operated at the FVR CO_2 concentration measured inside the extract air duct and average CO_2 concentration inside the auditorium did not correlate, which can be also seen from Figure 7. This can be caused by poor mixing of CO_2 gas in the auditorium or inertia between the auditorium and the extracted air measurements. To have a better understanding of the reasons this experiment should be repeated with real persons, where thorough planning and ethical reasons should be addressed.

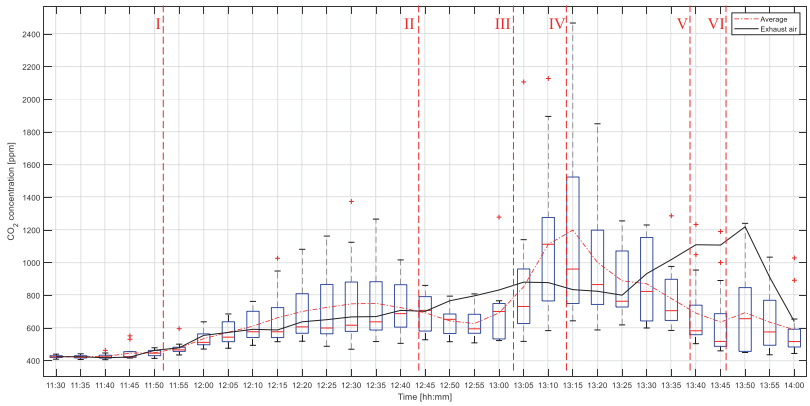

Figure 7. CO_2 concentration in the auditorium and the extract air.

4 Conclusion

In this paper, a method to estimate ventilation system load flexibility was proposed. To test the method, a case study was conducted in one auditorium of an educational building, where air exchange was provided by one ventilation system. The case study included the investigation of ventilation system power consumption, the impact of FVR on the CO_2 concentration, and how it affects flexibility. Three main flexibility parameters were considered: the amount of power modulation, the rate of change, and the duration how of long the minimum power level can be held.

The amount of power change was estimated with statistical analysis and it is found that during measurements ventilation system operated at two scheduled power levels. During daytime or working hours the ventilation system is operating at the maximum ventilation rate which corresponds to approximately 4.77 kW. During night hours the ventilation system operates at the minimum rate and the power consumption is around 0.35 kW. This means that available power modulation is around 4.42 kW, but according to the schedule, the ventilation system power consumption can only be decreased during the daytime. The rate of change was measured during the experiment and it is found to be around 50 W/s for the selected system.

The duration of how long FVR can be held is based on mass balance analysis. Firstly, the CO_2 generation is calculated based on the extract air CO_2 concentration change, airflow rate, and space volume. Secondly, based on the calculated CO_2 generation rate estimation for the duration is made. High fluctuations and unrealistic estimations are filtered out. The experiment showed that with 33% of auditorium usage the ventilation system can operate at the minimum rate for 55 min while the estimated duration was around 53 min. To keep the developed method robust and applicable for different ventilation systems, only one CO_2 sensor in the extract air duct of the ventilation system is used, thus the developed method does not consider non-uniformity in CO_2 concentration. It is the distinct aim of the authors to avoid the limitation of the developed method to only selected ventilation systems, due to alternating locations of the CO_2 sensor. Based on the results, the proposed method can be used to estimate ventilation system flexibility.

Future work considers more ventilation systems and buildings to have a higher amount of available power to regulate. Typically, ventilation systems are configured to operate according to building occupancy, thus to have sufficient load flexibility available, commercial and residential buildings should be combined. In the study pollution source was CO_2 gas which was injected into the auditorium from the gas cylinder, but in further studies, heaters should be added to introduce conditions that are closer to reality. Method to estimate duration will be improved by considering the inertia in CO_2 concentration, adding historical data to the estimation, and including multi-zone ventilation systems, where estimations can be based on the highest CO_2 concentration zone. Also, changing the CO_2 concentration limit according to a space size, air exchange type, and airflow rate should be addressed in further studies.

This work was supported by Estonian Centre of Excellence in Zero Energy and Resource Efficient Smart Buildings and Districts ZEBE, grant 2014-2020.4.01.15-0016 funded by European Regional Development Fund. This work has also been supported by the European Commission through the H2020 project Finest Twins (grant No. 856602).

References

[1] Eurelectric, “Flexibility and aggregation - requirements for their interaction in the market,” 2014. [Online]. Available: http://www.eurelectric.org/media/115877/tf_bal-agr_report_final_je_as-2014-030-0026-01-e.pdf.

[2] European Commission, “Energy performance of buildings directive.” https://ec.europa.eu/energy/topics/energy-efficiency/energy-efficient-buildings/energy-performance-buildings-directive_en (accessed Jan. 15, 2021).

[3] I. Drovtar, J. Niitsoo, A. Rosin, J. Kilter, and I. Palu, “Electricity consumption analysis and power quality monitoring in commercial buildings,” *PQ 2012 8th Int. Conf. - 2012 Electr. Power Qual. Supply Reliab. Conf. Proc.*, pp. 107–112, 2012.

[4] T. Häring and A. Rosin, “Thermal Modelling of a Control Center for Flexibility Analysis in nZEB Nanogrids,” in *2020 IEEE 61th International Scientific Conference on Power and Electrical Engineering of Riga Technical University (RTUCON)*, 2020, pp. 1–6.

[5] M. B. Sanjareh, M. H. Nazari, G. B. Gharehpetian, R. Ahmadiahangar, and A. Rosin, “Optimal scheduling of HVACs in islanded residential microgrids to reduce BESS size considering effect of discharge duration on voltage and capacity of battery cells,” *Sustain. Energy, Grids Networks*, vol. 25, pp. 1–15, 2021.

[6] J. Wang, S. Huang, D. Wu, and N. Lu, “Operating a commercial building HVAC load as a virtual battery through airflow control,” *IEEE Trans. Sustain. Energy*, vol. 12, no. 1, pp. 158–168, 2021.

[7] H. Hao, Y. Lin, A. S. Kowli, P. Barooah, and S. Meyn, “Ancillary Service to the grid through control of fans in commercial Building HVAC systems,” *IEEE Trans. Smart Grid*, vol. 5, no. 4, pp. 2066–2074, 2014.

[8] S. Rotger-Griful, R. H. Jacobsen, D. Nguyen, and G. Sørensen, “Demand response potential of ventilation systems in residential buildings,” *Energy Build.*, vol. 121, pp. 1–10, 2016.

[9] V. Maask, T. Haring, R. Ahmadiahangar, A. Rosin, and T. Korotko, “Analysis of ventilation load flexibility depending on indoor climate conditions,” *Proc. IEEE Int. Conf. Ind. Technol.*, pp. 607–612, 2020.

[10] A. Mikola, J. Rehand, and J. Kurnitski, “Air change efficiency of room ventilation units,” *E3S Web Conf.*, vol. 111, pp. 1–8, 2019.

[11] A. Mikola, T.-A. Kõiv, J. Rehand, and H. Voll, “The Usage of CO2 Tracer Gas Methods for Ventilation Performance Evaluation in Apartment Buildings,” 2017, pp. 27–28.

Publication IV

Ferrantelli, a., Aljas, H. K., Maask, V., Thalfeldt, M. (2021), “Tenant-based measured electricity use in 4 large office buildings in Tallinn, Estonia,” Cold Climate HVAC & Energy 2021 (1–10). E3S Web of Conferences.

Tenant-based measured electricity use in 4 large office buildings in Tallinn, Estonia

Andrea Ferrantelli[1], Hans Kristjan Aljas[1], Vahur Maask[2], Martin Thalfeldt[1,3]*

[1]Department of Civil Engineering and Architecture, Tallinn University of Technology, 19086 Tallinn, Estonia
[2]Department of Electrical Power Engineering and Mechatronics, Tallinn University of Technology, 19086 Tallinn, Estonia
[3]Smart City Center of Excellence, Tallinn University of Technology, Ehitajate tee 5, 19086 Tallinn, Estonia

Abstract. The energy performance assessment of buildings during design is usually based on energy simulations with pre-defined input data from standards and legislations. Typically, the internal gain values and profiles are based on EN 16798-1. However, studies have shown that the real electricity use of plug load and lighting varies more smoothly than in the profiles of EN 16798-1 where zero occupancy outside working hours is assumed. This might result in sub-optimal building solutions due to inadequate building performance simulation input data. The aim of this work is to structure and analyse data from a total of 196 electricity meters in 4 large office buildings in Tallinn, Estonia. Typically, 3 to 8 electricity meters were installed per floor with the consumption coming mainly from plug loads and electric lighting. The data had been gathered between the years 2016-2020 with either 1 or 24 hour time steps, depending on the building and the electricity meter. 3 out of the 4 buildings had an average normalized energy usage slightly below the modelling value calculated according to EN16798-1. Some office spaces stood out with an abnormally high electricity consumption; however, the 24-hour distributions were fairly compact, meaning quite steady consumption patterns. When looking at the dispersion of energy consumption per 24h, averaged over all given offices in a building, no outliers stood out, either. This means that there are not many days when the average consumption and internal heat gains of all offices were simultaneously well below the mean. Additionally, major events like holidays and the COVID19-induced lockdown show up well on the graphs, but also planned changes in occupancy can be seen.

1 Introduction

Office buildings are well known to consume about 40% of the total energy share of the European building sector [1]. As the European Union (EU) has set long-term targets to reduce carbon emissions and energy consumption significantly, improving the energy-efficiency of office buildings is a priority. To this aim, researchers and designers are now focusing on structural improvement as well as on smart technologies, which can align building operation and occupants' needs.

Such alignment is a crucial characteristic of modern approaches: the heating system is now viewed as a means for temperature control rather than just emitting heat to rooms. It has been indeed demonstrated that internal and solar heat gains of intermittently operated buildings such as office buildings (OB) can cover the majority of heat losses [2].

This happens because heat gains from people, equipment and lighting as well as ventilation heat loss have a large impact on heat balance. The fluctuating heat gains and non-demand based ventilation operation make the thermal behaviour dynamic. This is not accounted for in the current design methods, whose conservative and simplistic approach of accounting heat gains results in over-dimensioned and sub-optimally operated systems. On the contrary, the dynamics of heat balance and energy performance of a modern OB require a fairly complex analysis to be performed with advanced computational methods. Building performance simulations (BPS) provide a powerful tool in this sense already at the design stage: for instance, in Estonia it is mandatory to use dynamic (namely, hourly-based) BPS for calculating the Energy Performance Certificate (EPC) of commercial and residential buildings.

Unfortunately, even with simulations there often exists a sizeable difference between calculated and actual energy performance of buildings. Calì et al. [3] demonstrated that the consumed energy can be up to 3 times larger than the calculated estimates; occupants' behaviour was identified as one of the causes of the performance gap in addition to errors in installation and operation of the buildings. Several studies have therefore developed modelling strategies based on the monitored use of OBs, focusing either on occupancy [4], lighting [5] or plug loads/computers [6] measurements. It became immediately clear that the real electricity use of plug load and lighting varies more smoothly than in the profiles of default occupancy schedules building codes and standards, such as the EN 16798-1 [7], where zero occupancy outside working hours is assumed. More

* Corresponding author: andrea.ferrantelli@taltech.ee

© The Authors, published by EDP Sciences. This is an open access article distributed under the terms of the Creative Commons Attribution License 4.0 (http://creativecommons.org/licenses/by/4.0/).

often than not, plug loads and lighting consumption are indeed sizeable also outside occupied hours [8] [9]; significant variances between daily electricity uses of single occupants or office rooms do exist as well. It is thus necessary to track the OB's energy use during the entire 24 hours period, and to study how the measurements correlate with more sophisticated occupancy schedules. This knowledge can then be implemented into accurate BPS for guiding simulation-based design decisions. Reducing the size and cost of heating and cooling systems, simultaneously increasing their efficiency, will then lead towards a new generation of dynamic sizing methods for the heating and cooling of office buildings.

In this paper we lay down such experimental groundwork, which is critical for identifying the typical use of equipment and lighting in office buildings in order to develop methods for e.g. integration into building simulations in order to reduce energy use, improve tenants' comfort, building flexibility etc. The aim of this work is structuring and analysing data from a total of 196 electricity meters in 4 large office buildings in Tallinn, Estonia. Three to eight meters were installed per floor, monitoring plug loads and electric lighting. The data had been gathered between the years 2016-2020, with either 1 or 24 hour time steps depending on building and electricity meter.

Table 1 List of relevant properties for all the buildings.

Properties	A	B	C	D
No. of floors (total)	13	13	8	13
Monitored floors	7	12	8	12
Zones per floor	4	4	6	8
Total area monitored (m²)	4938.3	8508.2	4052.0	13989.6
Customer service nr. of offices %	4 19%	2 11.8%	3 7.5%	5 4.2%
Administrative nr. of offices %	9 42.9%	11 64.7%	33 82.5%	107 89.9%
IT nr. of offices %	8 38.1%	4 23.5%	4 10%	7 5.9%
Total	21	17	40	119
Meas. points (total)	32	48	50	102
Outlier %	5.09	11.91	5.01	9.91
Resolution	0.001	0.001	1	1
Original data unit	kWh/h	kWh/h	kWh	kWh
Start date	2019-01-01	2019-01-01	2017-12-08	2018-01-05
End date	2019-12-31	2019-12-31	2020-03-07	2020-03-07

2 Methods

In this section we describe the datasets acquisition and structure, data preprocessing and methods of statistical analysis.

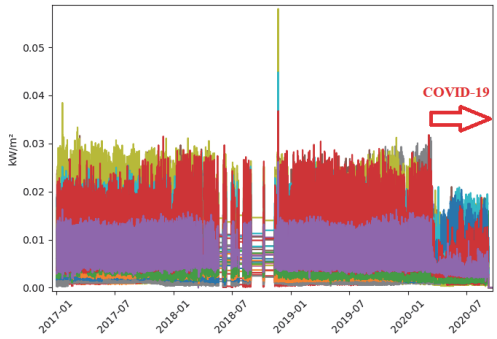

Figure 1 Raw data for Building A.

2.1 Datasets acquisition

This study is based on electricity consumption data acquired from four office buildings located in Tallinn, Estonia (**Table 1**).

Each floor of any building was divided into zones where electricity consumption was metered separately; most of the floors follow a standard layout, only the first and second floor have a larger area.

Each measurement point had three-phase electricity meters that were compatible with a 230/400 VAC voltage system. Measurements were performed with class B meters conforming to EN 50470-3, which had been installed during the construction of the building. The data acquired from the meters was stored in a building management system from which it could be downloaded into a CSV file.

The amount of data from each building ranged from 11 to 27 months. The time resolution of the data was preset by the building management system operator; two buildings displayed hourly data and the other two had daily data (**Table 1**).

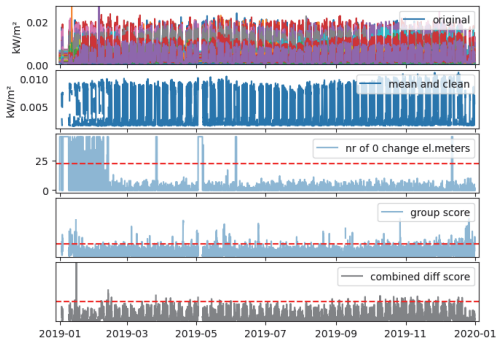

Figure 2 Raw data and outlier predictions for Building B.

2.2 Data preprocessing

2.2.1 Data format

A detailed overview of the building-specific parameters, including floor areas, measurement point counts and time ranges is given in **Table 1**. The original data came in two types of formats. For Buildings A and B, this was a non-cumulative series of hourly kWh consumption readings with 0.001 kWh resolution, for Buildings C and D it was a cumulative series of daily kWh readings with 1 kWh resolution.
The data of Buildings C and D was then converted to a non-cumulative series (kWh/24h) by calculating the differences of two contiguous entries.

In order to give the finalized consumption values in units per square meter, the project documentation of the buildings was used to gain information about the serviced floor areas for each electricity meter. The official areas were given with 0.1m² precision, however, since there were some inconsistencies, we fixed the estimated error at 1m².

2.2.2 Data cleanup

As a first step, some periods of data were left out based on existing knowledge about building occupancy (see **Table 1**). A few electricity meters, which according to the project documentation were labelled as ordinary office meters, were also excluded, since their behaviour and power consumption were significantly different from a typical office meter's pattern, possibly monitoring the consumption of some mechanical equipment.

The COVID-19 impact could also be seen in the graphs as the power usage significantly dropped from March 2020 onwards (**Figure 1**), so the latest cut-off date for all buildings was set to March 7th, 2020.

After visualizing the time-series graphs of used power (kW), numerous other problematic time periods showed up, as in **Figure 1.** These were either affected by stuck readings or by abnormally high peaks. The reasons for such errors could have likely originated from the BMS (Building Management System). One possible explanation for such peaks is the accumulation of used energy while the BMS was shut down since most electricity meters do not log energy consumption with a timestamp. There is also a possibility of external interference in the measurements caused by electromagnetic compatibility issues or poor error mitigation inside the BMS. However, these eventualities have not been verified in the current scenario.

For further analysis of anomalous behaviour and outliers, an algorithm was developed to remove potentially bad data points. Some parameters were adjusted slightly for a couple of buildings for more optimal detection, but the general method is as follows, in the given order:

• If the reading of a single electricity meter at any given time is significantly different from the mean of all meters at that time, exclude the slice. This is necessary to avoid losing outliers after the data has been averaged across a building.

• This step applies only to Buildings A and B (1h timestep). If more than half of the meters show static behaviour, exclude the slice. This is again necessary, since there appeared to be numerous small stops in the readings of individual electricity meters, additionally to the large, synchronized freezes mentioned before.

• Calculate the average consumption across a building at any given time.

• Group the averaged data by weekdays (and hours, if applicable) and exclude points where the value is further than 2 standard deviations of that group's mean.

• Create a combined score of first and second absolute differences of the series, where the second difference has a slightly higher weight. Exclude points where the combined score exceeds a threshold. This helps to remove smaller peaks and abrupt changes.

After visualizing the predictors with this method, some additional time periods stood out with poor behaviour, as can be seen on the left side of **Figure 2**, thus they were left out.

2.2.3 Conversions for distribution analysis (Buildings A and B)

The data for power consumption distribution analysis were given in units kWh/(24h·m²) for compatibility. This has already been achieved with Buildings C and D, but conversion was needed for Buildings A and B.

Since the data had been cleared of outliers, simply summing up the hourly readings of each day could have returned lower than actual results, due to missing values. However, excluding all days that have any missing data would result in a huge loss of data; to reduce the number of lost days, a linear forward interpolation of maximum four hours was thus applied before excluding days with any missing values.

2.2.4 Statistical data analysis

The cleaned-up data were processed with the software R [10] through various packages that allowed exploring distributions as well as performing normality and correlation tests. For Buildings A and B, the 1-hour data were used for daily and weekly analysis, while the monthly assessment used hourly data that were averages of all Mondays, Tuesdays etc. of that month. These correspond to the "average" or "representative" days that are addressed in the next Section.

3 Results

3.1 Boxplots of daily consumption

3.1.1 General

The plots in **Figure 3** to **Figure 6** show distributions of datapoints in kWh/(24h·m²) of each measuring point

in a building. The whiskers of the boxplot are drawn at 5th and 95th percentiles. Green triangles represent arithmetic means and green lines represent medians.

The red, dashed horizontal line represents the reference value used for modelling energy consumption of office buildings, calculated according to EN16798-1 [7]. The value is 0.1089 kWh/(24h·m²), which assumes power consumption of 0.018 kW/m² (0.006 for lights and 0.012 for equipment) at an average usage level of 55%, over an 11h period in a day. The blue horizontal line represents the calculated average consumption of the selected offices in a building.

3.1.2 Analysis

For Buildings B, C and D the average falls only slightly below the reference value, but for Building A the average consumption is significantly higher. It seems that most of the monitored offices in Building A have an average consumption above the reference value, so the high average is not caused by any outstanding offices, rather from a general behaviour of the occupants. **Table 1** displays more administrative than IT offices, however the high consumption should not be related to pc use only. We have no info about employee number either, so no correlations can be generated between user profiles and consumption patterns.

However, the two zones with the highest consumption in Building C are known to be dentist offices. On the far right, a column called "AVG" shows the distribution of average daily consumption values of all the measurement points combined. The variance is quite small, compared to the variance of all other offices in that given building.

This means that there are no large, synchronized swings in the building's total consumption, which can also be seen in **Figure 2** in the graph "mean and clean".

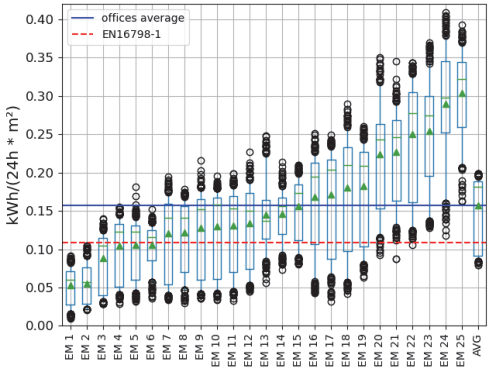

Figure 3 Boxplots for Building A.

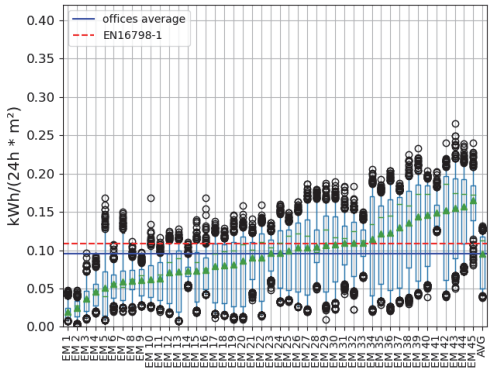

Figure 4 Boxplots for Building B.

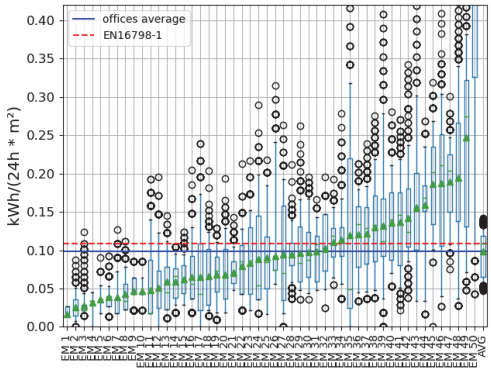

Figure 5 Boxplots for Building C.

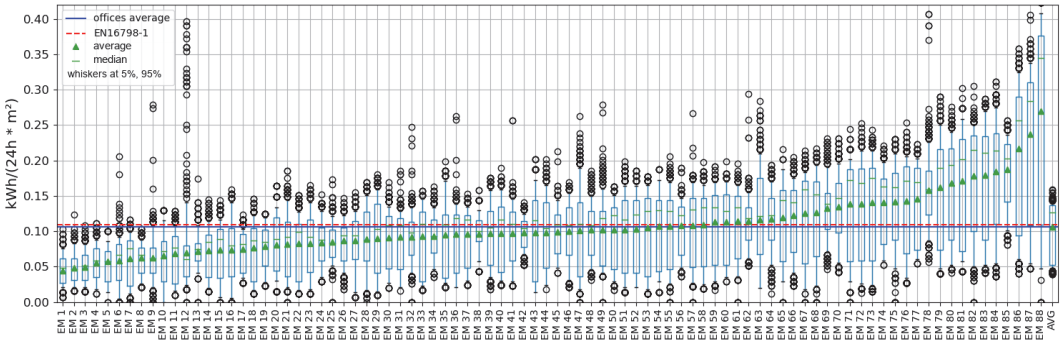

Figure 6 Boxplots for Building D.

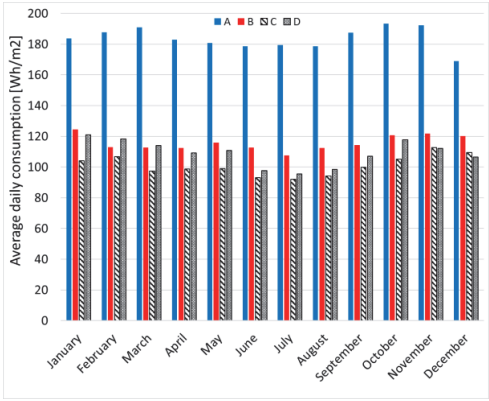

Figure 7 Cumulative daily power consumption, 2019 monthly breakdown for all buildings.

3.2 Monthly analysis and seasonal variations

For each of the four buildings, a monthly breakdown of weekday cumulative consumption [Wh/m2] for the year 2019 was computed. This was obtained, for buildings A and B, by adding all the average hourly values; for buildings C and D cumulative daily values were averaged (24h time step for the data). The result is plotted in **Figure 7** for each building.

Considering the full interval 2016-2020, small differences among the years do exist, whilst the overall pattern does not change qualitatively. Consumption is higher in the Autumn and Spring months, not during the winter as generally expected. For each case, we found very little correlation between climate and tenants consumption: let us remind that only plug load and lighting consumption were monitored, not heating.

Let us consider Building A as an example: a Pearson correlation test returned 0.999 for January versus June, showing a high correlation between winter and summer months. This was confirmed by a Kendall test (more sensitive than the Pearson test) as well.

Furthermore, the same test provided -0.69 and -0.68 for tenants consumption versus, respectively, measured sunshine duration and daily external temperature, which is indicative of a weak correlation. For 2019, the largest consumption was recorded in March, followed by October and November.

It is interesting to investigate the role of sunshine duration more into detail, since our data addressed both equipment plug load and lighting. Since sunshine duration accounts for cloud coverage, differently from daylight hours, it can influence switching lights on and off. A plot of daily average power consumption in function of measured monthly sunshine hours is given in **Figure 8** for Buildings A and B, and in **Figure 9** for C and D. For Building B we used January 2020 data, as the January 2019 data were not sufficient for the statistics. Remarkably, January 2020 was as sunny as March 2019, namely over 3 times sunnier than January 2019. It was also much warmer, with average T=3C versus -3C in 2019. Yet, its average daily consumption was 10% larger than February 2019 (T=1C) and March 2019 (T=2C), confirming the importance of occupancy schedules.

At the building level, **Table 2** features the correlation matrix of 2019 monthly consumption for the four datasets. Building A is fairly uncorrelated from the others, consistently with e.g. **Figure 7**, while B and C seem to be slightly more comparable. Although the fact that A and B have 1hr and C and D have 24hr data hinders any speculation about occupancy patterns, the low overall correlation mirrors the absence of a common climate-induced seasonality in the data.

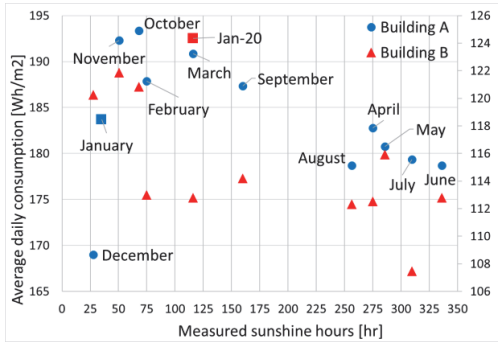

Figure 8 Building A (dots, left axis) and B (triangles, right axis) - Cumulative daily power vs monthly sunshine hours.

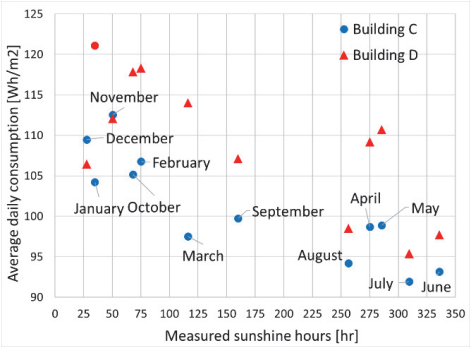

Figure 9 Building C (dots) and D (triangles) - Cumulative daily power consumption versus monthly sunshine hours.

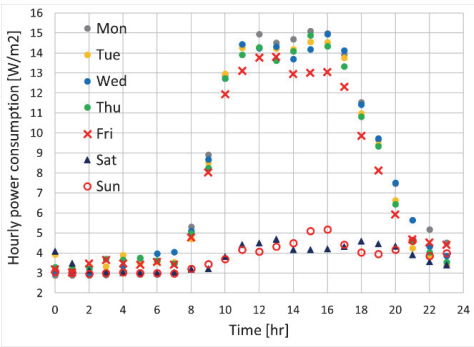

Figure 10 Building A - Tenants' consumption for January 2017, representative week.

Table 2 Correlation matrix for the four datasets, 2019.

	A	B	C	D
A	1.000	0.273	0.333	0.455
B	0.273	1.000	0.636	0.515
C	0.333	0.636	1.000	0.455
D	0.455	0.515	0.455	1.000

3.3 Daily analysis

3.3.1 General considerations

The tenants' electric consumption is illustrated for a representative January 2017 week in **Figure 10**. Notice the sharp decrease at lunch break and the lower consumption for Fridays, as expected.

Qualitatively, the weekday curves do not differ much between winter and summer months, confirming the high correlation already discussed. This agrees with the data distribution, which is sharply bimodal with the two peaks at the histogram extremes for each month.

We recall that Buildings C and D provided only with 24h data, therefore it was not possible to investigate the hourly breakdown as in **Figure 10**. This section will therefore discuss our findings only for A and B.

Considering a specific day with expected full occupancy, we chose a central Wednesday in January 2017. The daily consumption reflects our results for monthly averages: normality is confirmed by QQ (Quantile-Quantile) plots and a Cullen and Frey plot, while histograms show a clear bimodal pattern with modes at the extremes. The statistical parameters of the distribution are an estimated standard deviation (SD) of 4.797, a skewness of 0.288 and a 1.219 kurtosis. The large SD and low kurtosis signify that, despite the substantial data cleanup described in Section 2.2.2, we are still in the presence of outliers, as illustrated in Section 3.1.

3.3.2 Energy consumption prediction formulas for building performance simulations (BPS)

Aiming at using our measurements for implementation into BPS, we generated prediction formulas of energy consumption by adapting to our dataset a bottom-up method that was introduced for domestic hot water data in [11] and then applied to buildings' energy consumption in [12]. The case of [12] addressed a much larger building, with relatively small variances in the hourly consumption profiles for different weeks and months, so it was possible to identify a *unique* representative day whose consumption could be correlated to other days, to cover a full year.

On the other hand, for Building A (and even more for B) too many days had very different profiles, requiring a less simplistic approach. For instance, July 2019 showed the cumulative consumption of the most correlated Monday to be equal to that of the average Monday, while for Tuesdays the difference was remarkable, 5.62%. Preferring an average day to a specific day as representative was therefore more suitable.

Since hour-by-hour prediction in this case is not reliable, we focused on predicting the cumulative energy consumption with the lowest error possible; we also wished to keep smooth interpolation curves to avoid too biased predictions. The procedure followed these steps:

1. The cumulative consumption of *average* days for each month is split into four groups: Mon to Thu (WD), Friday, Saturday and Sunday. The value that is closest to the average is called E_{wd}, E_{Fri}, E_{Sat}, E_{Sun}. For Building B, the corresponding days were February Wednesday, March Friday, June Saturday and September Sunday.

2. Interpolate each of these four reference days and obtain the fit formulas $E_{fit,WD}(t)$ etc. These are our "structural formulas" according to the terminology of [12]. Consumption for a random day can now be predicted by using linear correlations with the formulas

$$E(t) = A * E_{fit,WD}(t) + B, \qquad [W/m2] \quad (1)$$

for weekdays and

$$E_{i,m}(t) = E_{fit,i}(t) * R_{i,m} \qquad [W/m2] \quad (2)$$

for Fridays and the weekend, where i=Fri, Sat, Sun and m=1,...,12. The coefficients A and B are computed by correlating each month with the one corresponding to

the structural formula. For Building B, February holds for weekdays, with coefficients listed in **Table 3**.

Table 3 Monthly correlation formulas for Building B.

Month	A, B (Mon-Thu)	R^2
January	1.0891, 0.0545	0.9739
February	1,0	1
March	0.957, 0.1653	0.9965
April	0.9406, 0.2385	0.991
May	0.9925, 0.1338	0.9963
June	0.945, 0.2415	0.9923
July	0.8788, 0.3439	0.9929
August	0.9478, 0.2147	0.9932
September	0.9785, 0.1522	0.9938
October	1.0452, 0.1172	0.9772
November	1.0753, 0.0216	0.9719
December	1.0374, 0.1425	0.9803

For Friday and the weekend, one should instead use Eq.(2), where

$$R_{i,m} = E_{i,m}/E_{fit,i} \qquad (3)$$

(i=Fri, Sat, Sun) is a non-dimensional coefficient that is computed for each case, given the cumulative energy of the average desired day $E_{i,m}$ (say, for January Friday) and that of the fitted day $E_{fit,i}$. The $R_{i,m}$ coefficients for Building B are listed in **Table 4**.

Table 4 $R_{i,m}$ coefficients for Building B.

Month	Fri	Sat	Sun
1	1.074	1.056	1.079
2	0.973	0.935	0.925
3	1.000	0.984	0.945
4	0.992	0.976	0.947
5	1.019	0.960	1.005
6	0.984	1.000	0.984
7	0.928	0.960	0.959
8	0.974	0.978	0.964
9	0.985	0.978	1.000
10	1.041	1.031	1.021
11	1.044	1.031	1.029
12	1.024	1.042	1.056

Using the above method, we could predict the consumption with small deviations from measurements. The errors ranged from 0.96% to 3% for Mon-Thu, 0.94% to 4.31% for Friday, 0.15% to 3% for weekends.

4 Discussion

During analysis, numerous concerns arose regarding the actual reliability of the data. Inconsistencies in the project documentation, occasionally over-dimensioned electricity meters, numerous logging problems with the BMS and major occupancy changes resulted in a dataset that was far from ideal.

However, it can be shown that computing the error propagation for weighted averages of all electricity meters per unit floor area resulted in negligible final error bounds (0.004 W/m2 on the average). This suggests that installing more meters could produce more accurate data, giving an advantage over measuring everything at the building level only. Additionally, having more meters would allow excluding undesirable zones, which will very likely be present, as well as leaving the ability to distinguish between different types of consumption. It is indeed well known that diverse space-use typologies (distinguished by a combination of tenants' tasks and time-based occupancy) generate a variety of daily consumption profiles, see e.g. [9]; a whole-building zonal analysis would thus allow tailoring the HVAC design to these diverse needs.

One of the data features that could be learned from the box plots comes from the average daily consumption values of all the measurement points combined, which has a small relative variance for that given building. This means indeed that there are no large, synchronized swings in the building's total consumption, which can also be seen in **Figure 2** in the graph "mean and clean".

However, further analysis can be done about the upper, 95th percentile values of individual offices, especially for buildings where hourly data is also available. This could give more information about local peak loads for dimensioning mechanical equipment, as well as finding different correlations.

Our efforts in measuring electricity locally instead of per building showed that it is advisable to invest in measuring electricity locally, rather than being content with measurements at building level, for two reasons. First, the variance induced by diverse types of offices is substantial; this important information disappears if data are aggregated for the whole building. Secondly, our statistical analysis of monthly and daily patterns showed a lower impact of climate and irradiation hours than expected, illustrating the predominant role of occupancy that strongly depends on the specific office typology.

The analysis of monthly consumption brought forward some interesting non-trivial features. First of all, the high correlation between daily profiles during winter and summer months is a signal of a recursive pattern that is not influenced by added sunshine hours.

Figure 8 and **Figure 9** also illustrate that although some correlation with sunshine duration does exist, this is seemingly dominated by the plug load. In **Figure 8**, March dominated over January and February, and April and May over August (Building A). This is common to all the buildings here studied (see also **Table 2**), suggesting a central role of occupancy consistently with [12] and underlining a necessity to address its impact thoroughly.

The daily analysis showed that, although the absence of a standard energy profile was problematic for an hour-by-hour prediction, by focusing instead on the cumulative consumption we managed to establish a procedure that allows implementation into BPS with

good accuracy. The basic idea was that the inconsistencies tend to compensate each other, giving room to some unavoidable tolerance.

5 Conclusions

In this paper we have investigated plug loads and lighting consumption data of four office buildings in Tallinn, Estonia, over a four years period. Data acquisition and preprocessing of some very problematic measurements were discussed into detail, together with a simple, yet effective prediction method for application into BPS towards energy estimates.

Among the other results, we have demonstrated that it is preferable to install more meters rather than measuring everything at the building level, for increased accuracy and for keeping relevant information. Consistently with previous studies, we also found that occupancy patterns are central in determining the electricity consumption.

The definition of a typical office building should therefore be discussed (e.g., IT and administrative work can be quite different in terms of energy use intensity), occupants' density (measured or estimated?), installed plug loads and lighting power etc. These could all provide useful information in order to shift the focus of energy performance research, in order to consider the actual energy use.

We wish to remark that the amount of data analysed is quite remarkable by itself: whilst not providing a fully exhaustive overview of energy consumption in non-residential buildings, it is larger than the average datasets that appear in this type of studies.

Overall, the gathered information has a number of applications on different levels, from tailored predictions aimed at renovations, to refinement of applied predictive modelling strategies, to classification and benchmarking of building energy consumption.

Considering our findings and the above improvements, this study and its developments have the potential to contribute to future calculations of energy performance estimation in office buildings. And even if after COVID-19 we may never go back to the old way of office use, our dataset finds formal application in predictive modelling strategies. It also constitutes a good basis for energy consumption benchmarking, as it provides a baseline upon which future optimisation strategies based on new working styles can be compared.

The authors acknowledge support from the European Regional Development Fund via the Estonian Centre of Excellence in Zero Energy and Resource Efficient Smart Buildings and Districts ZEBE, grant 2014-2020.4.01.15-0016, from the Estonian Research Council through the grant PSG409, from the programme Mobilitas Pluss (Grant No. 2014-2020.4.01.16-0024, MOBTP88) and from the European Commission through the H2020 project FinEst Twins (grant No. 856602). They are also grateful to Andrei Engels for compiling the raw data files.

References

[1] European Commission, "Energy Performance of Buildings," 2020. [Online]. Available: https://ec.europa.eu/energy/topics/energy-efficiency/energy-efficient-buildings/energy-performance-buildings-directive_en. [Accessed 9 December 2020].

[2] M. Thalfeldt, J. Kurnitski and A. Mikola, "Nearly zero energy office building without conventional heating," *Est. J. Eng.,* vol. 19, no. 4, 2013.

[3] D. Calì, T. Osterhage, R. Streblow and D. Müller, "Energy performance gap in refurbished German dwellings: Lesson learned from a field test," *Energy and Buildings,* vol. 127, pp. 1146-1158, 2016.

[4] J. Zhao, B. Lasternas, K. P. Lam, R. Yun and V. Loftness, "Occupant behavior and schedule modeling for building energy simulation through office appliance power consumption data mining," *Energy and Buildings,* vol. 82, pp. 341-355, 2014.

[5] S. Gilani and W. O'Brien, "A preliminary study of occupants' use of manual lighting controls in private offices: A case study," *Energy and Buildings,* vol. 159, pp. 572-586, 2018.

[6] R. M. Tetlow, C. van Dronkelaar, C. P. Beaman, A. A. Elmualim and K. Couling, "Identifying behavioural predictors of small power electricity consumption in office buildings," *Building and Environment,* vol. 92, pp. 75-85, 2015.

[7] E. 16798-1, "Energy performance of buildings - Part 1: Indoor environmental input parameters for design and assessment of energy performance of buildings," CEN, Brussels, Belgium, 2019.

[8] A. C. Menezes, A. Cripps, R. A. Buswell, J. Wright and D. Bouchlaghem, "Estimating the energy consumption and power demand of small power equipment in office buildings," *Energy and Buildings,* vol. 75, pp. 199-209, 2014.

[9] A. Mahdavi, F. Tahmasebi and M. Kayalar, "Prediction of plug loads in office buildings: Simplified and probabilistic methods," *Energy and Buildings,* vol. 129, pp. 322-329, 2016.

[10] R Core Team, "R: A language and environment for statistical computing," R Foundation for Statistical Computing, Vienna, Austria, 2020.

[11] A. Ferrantelli, K. Ahmed, P. Pylsy and J. Kurnitski, "Analytical modelling and prediction formulas for domestic hot water consumption in residential Finnish apartments," *Energy and Buildings,* vol. 143, pp. 53-60, 2017.

[12] A. Ferrantelli, H. Kuivjõgi, J. Kurnitski and M. Thalfeldt, "Office Building Tenants' Electricity Use Model for Building Performance Simulations," *Energies,* vol. 13, p. 5541, 2020.

Publication V

Maask, V., Häring, T., Ahmadiahangar, R., Rosin, A., Korõtko, T. (2020), “Analysis of Ventilation Load Flexibility Depending on Indoor Climate Conditions,” 21st International Conference on Industrial Technology, ICIT2020 (1–6). IEEE.

Analysis of Ventilation Load Flexibility Depending on Indoor Climate Conditions

Vahur Maask, Tobias Häring, Roya Ahmadiahangar, Argo Rosin, Tarmo Korõtko
Department of Electrical Power Engineering and Mechatronics
Tallinn University of Technology
Tallinn, Estonia
Email: vahur.maask@taltech.ee

***Abstract*—Load flexibility and Demand Response are becoming increasingly important to balance the electricity supply and demand. Ventilation systems can be used as flexible loads in an electric power system. A number of studies in the field of load flexibility deal with ventilation system control in reference to measured temperature. However, inadequate attention is paid to the effect of using ventilation shutdown for providing load flexibility to pollutant concentration. This paper presents a ventilation shutdown period estimation according to indoor air quality (IAQ) for different space sizes and numbers of occupants. This study shows how long the ventilation system can be shut down before a pollutant concentration or temperature reaches its boundary considering the average level as an initial condition. Simulations were carried out to demonstrate an application of ventilation system 2-point control and to verify that this will not jeopardize the IAQ for normal conditions.**

Keywords—ventilation, Demand Response, flexibility, indoor climate, number of occupants

I. Introduction

A ventilation system is used to provide fresh air to the building and to extract polluted air. According to the European Commission [1] more than 2% of the energy is consumed by ventilation units in the European Union, which constitutes as the third biggest electricity consumer in a building after heating, cooling and lighting. Furthermore, in office buildings ventilation alone can form up to 12% of the overall energy consumption [2]. The indoor climate of a building is dictated by three indoor air quality (IAQ) parameters: CO_2 concentration, temperature and humidity. To provide a healthy and comfortable environment for occupants, these three parameters must be between limits given in the standard EN 16798.

Electric power system flexibility is the ability to balance the grid continuously by maintaining electricity supply and demand on an equal level [3], while simultaneously providing an acceptable service quality to connected loads [4]. Flexibility is characterized by response time, forced load, delayed load and the amount and duration of aggregated power. The response time characterizes the system inertia to respond to requested changes. Delayed and forced loads are used to decrease peak load and increase valley load. The amount and the duration of aggregated power characterizes both, the demand and supply. Demand-side flexibility can be utilized through Demand Response (DR) programs [5]. It has been suggested in the vision of Smart Grids to harness the positive effects of an aggregated residential load flexibility in electricity markets [6], [7]. In residential buildings, Heating, Ventilation and Air Conditioning (HVAC) systems are a possible source of flexibility. Furthermore, load flexibility is not only considered for residential buildings and can also include commercial or industrial sector where one approach is studied in [8] or a recent trend of electrical vehicles as discussed in [9].

Studies [10], [11] consider temperature based ventilation control while also considering the thermal comfort of occupants. Ventilation DR is considered in [10], where the study was made for a commercial building to minimize the sum of HVAC energy- and thermal discomfort costs related to occupants. In [11] testing was not based on any detailed model but relied on the actual measurement from the experiments performed on site. Both studies did not consider all IAQ parameters and focused merely on temperature. The control of a ventilation system only in reference to measured indoor temperature does not guarantee that other IAQ parameters are within the required limits.

A HVAC system used for providing frequency regulation service is studied in [12]. It is found that up to 15% of the rated fan power can be implemented in the frequency regulation without having a substantial effect on indoor temperature. The DR potential of ventilation systems in residential buildings is discussed in [13], where it is stated that a single 13 kW ventilation system in 12-storey apartment building can provide 4.5 kW of power increase and 1.0 kW of power reduction when needed without compromising IAQ. The outcome of the study was that an automated DR for ventilation systems could be used to provide both, prolonged load sheds and ancillary services, without jeopardizing IAQ. Study [4] shows that buildings can provide a short-term energy flexibility without requiring substantial changes and extra investments in the HVAC system. Mentioned studies do not consider ventilation shutdown as an option to provide load flexibility. Furthermore, existing research mainly focuses on one IAQ parameter while discarding the influence of other parameters on system flexibility.

The authors of [14] monitored indoor air pollutant concentration and climate factors based on the number of occupants and their activities. The measured parameters included particulate matter and the CO_2 concentration. It was found that the pollutant concentration increases along with the increase in the number of occupants and the level of their physical activities. The behavior of occupants was studied in [15], where it was concluded that the CO_2 concentration and the absolute humidity level are in correlation, since during respiration, both the CO_2 and the water vapor are generated. The findings imply that the absolute humidity level can be estimated based on CO2 concentration measurements. In [16], measurements in classrooms were carried out to investigate the dependence of CO2 concentration from ventilation rate and the number of pupils. The study showed that in a poorly ventilated space with the volume of 210 m^3 and an occupancy

978-1-7281-5754-2/20/$31.00 ©2020 IEEE

Authorized licensed use limited to: Tallinn University of Technology. Downloaded on August 17,2023 at 20:51:53 UTC from IEEE Xplore. Restrictions apply.

of 20 persons, the CO_2 concentration rose from 472 ppm to 1732 ppm within 4 hours.

The studied literature does not consider the effect of the number of occupants and the space size on the ventilation flexibility, which is needed for a ventilation system open-loop control methodology. The ventilation system 2-point control and taking advantage of the inertia in pollutant concentration build up is not discussed in present studies. This paper diminishes the lack of research in the given field by estimating a ventilation shutdown period according to the number of occupants and common room sizes. The paper is organized as follows: in section 2 IAQ modeling is given with equations to estimate an allowable ventilation system shutdown time; section 3 gives an overview of the methodology for a flexibility analysis, and section 4 discusses the results.

II. Indoor Air Quality Modeling

The standard EN 16798 states three main parameters and corresponding limits for those parameters to monitor IAQ, which have vital importance in providing a healthy and comfortable environment for occupants. These three parameters are

- CO_2 concentration,
- temperature and
- relative humidity.

IAQ models, which consider the number of occupants and the space size, are needed for simulations to estimate a ventilation shutdown period.

A. CO_2 concentration

To estimate the CO_2 concentration change in a space or building a mass balance analysis is used. It is assumed that the CO_2 concentration of a building or a space can be expressed with a single variable C. The indoor CO_2 concentration depends on the volume of the space (V), the CO_2 generation rate (G), the outdoor CO_2 concentration (C_0), the ventilation rate (Q), and the time (t). The mass balance of the CO_2 concentration can be expressed as follows [13]:

$$V\frac{dC}{dt} = G + QC_0 - QC \tag{1}$$

The CO_2 generated by a person ($Q_{\mathrm{CO_2,gen}}$) during respiration can be estimated as follows [13]:

$$Q_{\mathrm{CO_2,gen}} = \frac{0.00276 \cdot A_D \cdot \mathrm{MET}}{(0.23RQ + 0.77) \cdot 10^3} \tag{2}$$

where A_D is the DuBois surface area, MET is the level of physical activity, and RQ is a respiratory quotient (i.e., the rate of CO_2 produced to oxygen consumed). An average size adult has an A_D of 1.8 m^2 and RQ of 0.83 [13]. The standard EN 16798 states that for residential and office buildings humans are mainly occupied with sedentary activities and therefore the MET value is 1.2.

When the ventilation is shut down, it is assumed that no fresh air is introduced to the building or space (Q = 0). To estimate a ventilation shutdown, period τ (1) can be transformed into a discrete form as presented in (3), where ΔC is the allowable CO_2 concentration change from the initial condition to the limit and K is the number of people in a space or building.

$$\tau = \frac{\Delta C \cdot V}{G} = \frac{\Delta C \cdot V}{K \cdot Q_{\mathrm{CO_2,gen}}} \tag{3}$$

B. Temperature

According to the ASHRAE Handbook – Fundamentals [17], the heat dissipation of a human P_{person} during one hour is 140 W which is considered in the temperature calculations. It is assumed that heat loss through the building envelope is compensated by heat dissipation from appliances and the room heating.

To calculate the coefficient beta with the specific heat capacities (c_p) and densities of wood and air [18]:

$$\beta = \frac{1}{V_{max} \cdot \rho_{air} \cdot c_{p,air} + V_{wood} \cdot \rho_{wood} \cdot c_{p,wood}} \tag{4}$$

using the densities (ρ_x) and c_p values of air and wood.

Considering the number of people (k_i) in a space or building during time step i the temperature change can be calculated as [19]:

$$T_{people} = k_i \cdot P_{person} \cdot \Delta t \cdot \beta \tag{5}$$

The temperature for the next time step:

$$T_{next} = T_i + T_{people} \tag{6}$$

C. Relative humidity

The relative humidity is increased by the human respiration where during exhaling some moisture is added to the inhaled air, which is a function of the room humidity and the temperature as expressed in (7). It is considered that the respiration rate for the average person is 0.12 L/s [20].

$$W_e = 0.202W_i + A + BT_i \tag{7}$$

where W_e is humidity ratio of the expired air, W_i is the humidity ratio of the indoor air, T_i the indoor air temperature, constants A and B have values of 0.0276 and 0.000065, respectively [20].

III. Ventilation System Flexibility Analysis

This paper presents an estimation for a ventilation shutdown period which was conducted on different room sizes and numbers of occupants. According to Statistics Estonia [21], a common two-room apartment is 40 – 49 m^2, a three-room apartment 60 – 79 m^2, and a single family home is at least 100 m^2. An average four-room apartment and an average office in Estonia have space areas of 120 m^2 and 150 m^2, respectively. According to the Estonian Building Code the room height must not be less than 2.5 m, which is considered in space volume calculations. All selected building types and

Authorized licensed use limited to: Tallinn University of Technology. Downloaded on August 17,2023 at 20:51:53 UTC from IEEE Xplore. Restrictions apply.

calculated space volumes proposed in this paper are presented in Table I. In this paper it is estimated that approximately 5% of space is covered by furniture.

TABLE I. SELECTED SPACE TYPES AND VOLUMES.

Space type	Space area, m^2	Space volume, m^3
Two-room apartment	40	100
Three-room apartment	60	150
Four-room apartment	120	300
Single family home	100	250
Office	150	375

According to the study [22] the average CO_2 concentration in a building is 837 ppm, the average temperature 22.6 °C, and the average relative humidity 31%. The standard EN 16798 states limits for a normal IAQ level where the limit for the indoor CO_2 concentration is 1200 ppm. The indoor temperature must be between 20…25 °C for a residential building and between 20…24 °C for an office building during the heating season. The relative humidity must be between 25% - 60% to be considered as a normal condition.

In this paper, three IAQ parameters were selected to simulate the IAQ conditions when the ventilation system is shut down with a different number of people from 1 to 20. In every case, the average level was selected as an initial condition and the time was measured when the IAQ parameter reached its limit. Occupants are the only disturbance source, and other sources (e.g., candles, appliances, pets, etc.) are not considered in this paper.

A single-family house with a space area of 100 m^2 was selected to test proposed method of a ventilation 2-point control according to electricity price. In the simulation the maximum number of people in the building is 5 and the building occupancy throughout the day in hourly resolution (Fig. 1) is based on the methodology for calculating the energy performance of buildings [23]. Simulations were done in MATLAB software.

The ventilation rate was calculated according to the standard EN 16798 which states the following principle:

1) Calculate the total ventilation rate for the residence based on
    a. The floor area – the air change rate for normal conditions is 0.42 L/s per m2;
    b. The number of occupants – the living room and bedroom's outdoor airflow is 7 L/s per person.
2) Select the higher value from the above a) or b) for the total ventilation rate of the residence.

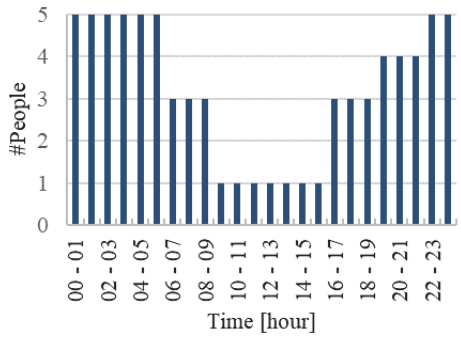

Fig. 1. Residential building hourly occupancy [23].

Considering this principle for a 100 m2 floor area single family home with a maximum occupancy of five people the needed ventilation rate is 42 L/s. A commercially available fan, which is close to the demanded ventilation rate has a 45 W nominal power and a 41 L/s ventilation rate [24]. This fan was selected for simulations and energy cost estimations.

IAQ parameters limit values and a space or building occupancy are the main factors which dictate the ventilation system electric flexibility. Harvesting this flexibility can be achieved through ventilation system 2-point control where ventilation system is shut down during high price period. Motivation to implement 2-point control on ventilation system is to introduce cost savings for end users.

IV. RESULTS

Occupants have the highest influence on the space or building CO_2 concentration level where for a higher number of people the limit is reached in minutes (Fig. 2). While the temperature and the humidity level will take roughly hours and days before reaching the limit (Fig. 3 and 4). Thus, the CO_2 concentration gives the most adequate information about the space ventilation demand and the air quality. For selected two-room apartment, the ventilation cannot be shut down more than two hours for one person and this time is decreased by the increase in the number of people. Five minutes is the minimum ventilation system flexibility considering the most severe case when 20 people occupy the space with a volume of 100 m^3. For larger spaces the shutdown period for the ventilation system can be increased.

If the ventilation system is used for cooling, a differentiation is made between residential and office buildings. In Fig. 3, an office with a space of 375 m3 can be seen as a residential building with a space size close to 250 m3. The shorter period for a ventilation shutdown based on temperature is due to more demanding requirements of office building indoor air temperatures, with the upper limit of 24 °C instead of 25 °C.

Authorized licensed use limited to: Tallinn University of Technology. Downloaded on August 17,2023 at 20:51:53 UTC from IEEE Xplore. Restrictions apply.

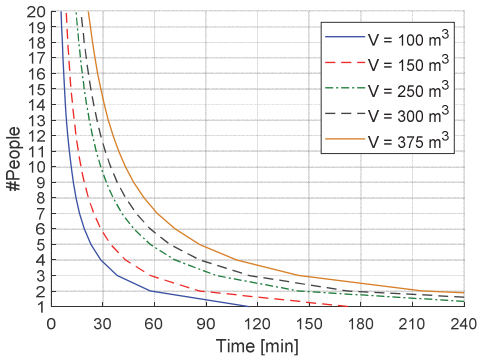

Fig. 2. Ventilation shutdown period dependence on CO_2 concentration.

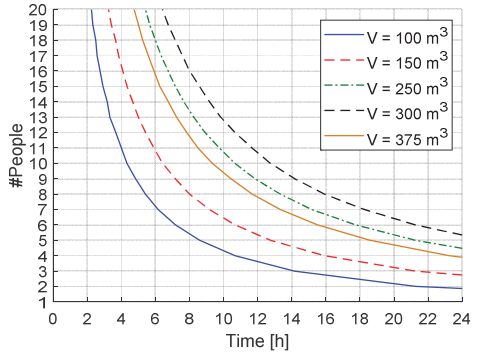

Fig. 3. Ventilation shutdown period dependence on temperature.

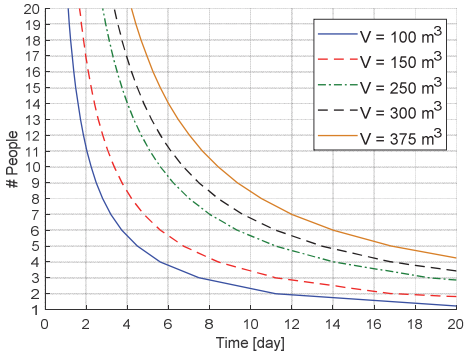

Fig. 4. Ventilation shutdown period dependence on humidity.

Simulations were carried out based on the day-ahead electricity price data from the third to the ninth of December 2018 (Fig. 5) [25]. The depicted energy price is the total price for the end user including all corresponding costs (e.g. price for electricity generation, margins, transmission costs, taxes etc.) that residential consumers pay in Estonia. A two tariff energy metering was considered, where the high tariff period is between 7:00 – 23:00 and the low tariff period is between 23:00 – 7:00 and during weekends [26]. The average CO2 concentration for outdoor air is 400 ppm which is considered in the simulations [1].

Two cases were selected for the simulations:

- Case 1: The ventilation system operates continuously;
- Case 2: The ventilation is shut down for one hour during the maximum price period.

Case 1 is a base condition where no cost savings are present; this is used as a benchmark. Case 2 has no sensor feedback and the space or building IAQ is unknown. The ventilation system shut down duration is selected according to an estimation of a ventilation system shutdown period for a single family home with five occupants, 100 m^2 of space area, and 250 m^3 of space volume.

Each day in the week the ventilation system was shut down for one hour to verify that the ventilation system can be shut down without exceeding the limit for the CO_2 concentration. The CO_2 was selected for the study due to its higher impact on the ventilation shutdown period considered in the previous section. One hour was selected according to the ventilation shutdown period study (Fig. 2). Simulations are based on an open-loop control methodology where the control system has no information about the IAQ. Simulations show the applicability of a ventilation 2-point control and do not consider an optimization of the system. As an example for a dwelling size of 250 m^3 and an occupancy of 5 people the ventilation can be shut down for one hour without exceeding the boundary.

The ventilation shutdown was conducted between 15:00 – 17:00 for most of the days in the week when the electricity price was the highest (Fig. 6). During this timeframe, the building occupancy, according to the methodology described in [23], was 1 to 3 people, which means that ventilation could have been shut down for a longer period. A ventilation system with a nominal power of 45 W the reduced energy consumption for one week is 0.315 kWh, which is approximately 4% of the total energy consumed during continuous operation.

For Case 2, the CO2 concentration boundary of 1200 ppm was not exceeded, and the cost savings on electricity were close to 5% compared to Case 1 (Fig. 7). During the morning high price period which occurred on the second day between 7:00 – 8:00 the CO2 concentration reached close to its boundary. While during the evening high price period the ventilation shut down showed no substantial effect on the CO2 concentration. It can be explained by the occupant behavior that during night hours the residential building has the maximum occupancy which increases the CO2 concentration to its highest level, but during midday the building occupancy is the lowest which decreases the CO2 concentration to its lowest level. This affects the ventilation flexibility in a residential building during the morning and evening high price period where the ventilation can be shut down longer in the evening, because during this time the difference between the CO2 concentration level in a space and its boundary is the largest.

Authorized licensed use limited to: Tallinn University of Technology. Downloaded on August 17,2023 at 20:51:53 UTC from IEEE Xplore. Restrictions apply.

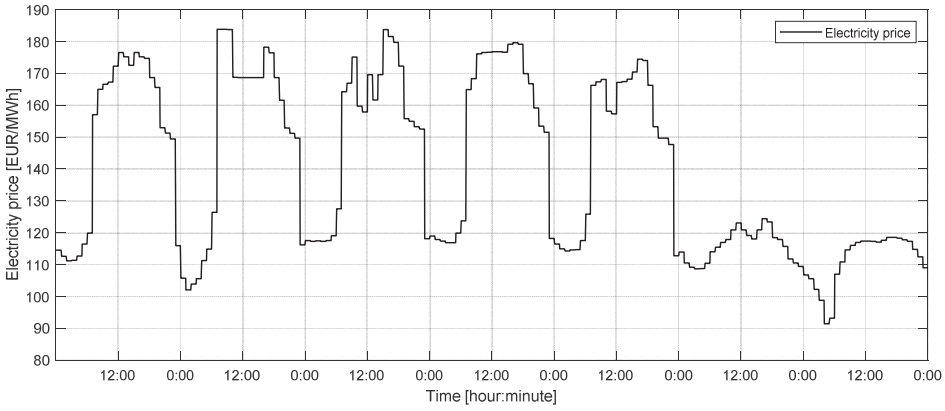

Fig. 5. Electricity price during one week from 3rd to 9th of December 2018 [25].

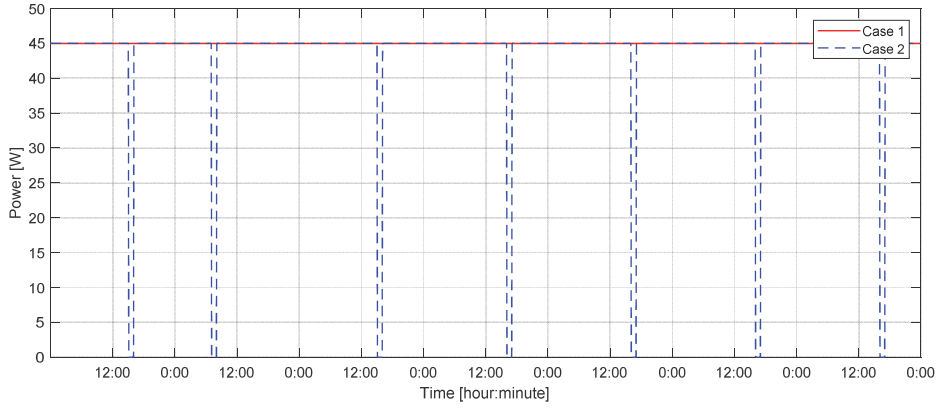

Fig. 6. Ventilation system power consumption during one week without and with ventilation scheduled control.

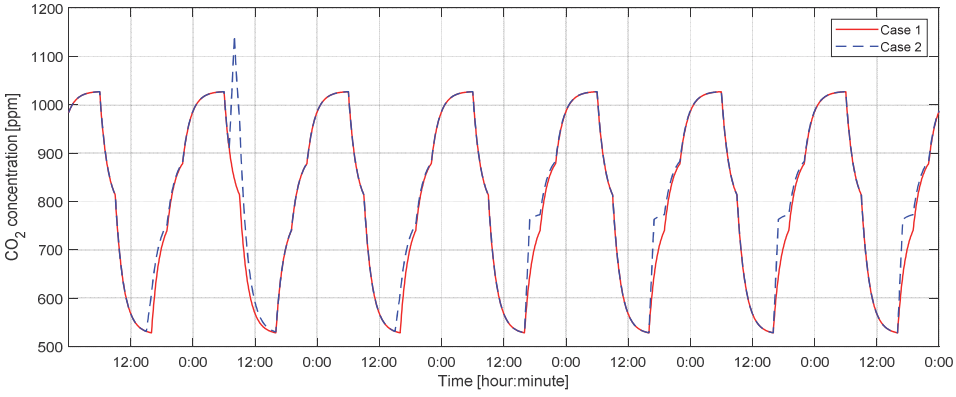

Fig. 7. CO_2 concentration change during one week without and with ventilation scheduled control.

V. Conclusion

The ventilation system can be considered as a flexible load for use in DR programs. A ventilation flexibility by shutdown is possible, where the space size and the number of people dictate the time limit. The minimum time limit for a residential building is 5 minutes considering a space volume of 100 m^3 and an occupancy of 20 people. The CO_2 concentration has the highest impact on the ventilation shutdown period compared to the temperature and the humidity.

It can be concluded from this study that a ventilation system can be shut down for 1 hour when the number of people does not exceed 2, 3, 5, 6, and 7 in a two-room, three-

Authorized licensed use limited to: Tallinn University of Technology. Downloaded on August 17,2023 at 20:51:53 UTC from IEEE Xplore. Restrictions apply.

room, four-room apartment, single-family house and office, respectively. The ventilation shutdown period is approximately 22 times longer for temperature and 270 times longer for relative humidity compared to CO_2 concentration based estimation.

Another contribution of this paper is achieving cost savings by shutting down the ventilation system during a high price period without exceeding the limit parameters for the IAQ. Simulation results showed that up to 5% cost savings could be achieved. This approach is preferable for ventilation systems, which do not have a variable frequency drive and are operating at a fixed ventilation rate.

Future work considers larger commercial buildings (e.g., supermarkets) with powerful ventilation systems. This study considered robust systems without a variable frequency drive and with an open-loop control methodology. The development of a control method and an optimal shut down period for these systems is needed, where the control signal is applied according to the market electricity price or an aggregator demand. Another interesting area for future work may be using the residential building ventilation flexibility in an aggregation level of the power market.

ACKNOWLEDGMENT

This work was supported by the Estonian Research Council grant PUT (PUT1680), and Estonian Centre of Excellence in Zero Energy and Resource Efficient Smart Buildings and Districts ZEBE, grant 2014-2020.4.01.15-0016 funded by European Regional Development Fund. This work has also been supported by the European Commission through the H2020 project Finest Twins (grant No. 856602).

REFERENCES

[1] European Commission, "Ventilation units," [Online]. Available: https://ec.europa.eu/info/energy-climate-change-environment/standards-tools-and-labels/products-labelling-rules-and-requirements/energy-label-and-ecodesign/energy-efficient-products/ventilation-units_en. [Accessed 5 February 2019].

[2] I. Drovtar, J. Niitsoo, A. Rosin, J. Kilter and I. Palu, "Electricity Consumption Analysis and Power Quality Monitoring in Commercial Buildings," *2012 Electric Power Quality and Supply Reliability,* p. 6, 2012.

[3] Roya Ahmadiahangar, Tobias Häring, Argo Rosin, Tarmo Korõtko, João Martins, "Residential Load Forecasting for Flexibility Prediction Using Machine Learning-Based Regression Model," in *IEEE International Conference on Environment and Electrical Engineering and*, Genoa, Italy, 2019.

[4] Y. Chen, P. Xu, J. Gu, F. Schmidt and W. Li, "Measures to improve energy demand flexibility in buildings for demand response (DR): A review," *Energy & Buildings,* vol. 177, pp. 125-139, 2018.

[5] S. Mishra, H. Koduvere, I. Palu, R. Kuhi-Thalfeldt and A. Rosin, "Assessing Demand Side Flexibility with Renewable Energy Resources," in *2016 IEEE 16th International Conference on Environment and Electrical Engineering (EEEIC)*, Florence, 2016.

[6] Roya Ahmadi Ahangar, Abdolreza Sheykholeslami, "Bulk Virtual Power Plant, a Novel Concept for Improving Frequency control and Stability in Presence of Large Scale RES," *International Journal of Mechatronics, Electrical and Computer Technology,* vol. 4, no. 10, pp. 1017-1044, 2014.

[7] Roya AhmadiAhangar, Argo Rosin, Ali Nabavi Niaki, Ivo Palu, Tarmo Korõtko, "A review on real□time simulation and analysis methods of microgrids," *International Transactions on Electrical Energy Systems,* 2019.

[8] L. Aleixo, A. Z. Morch, A. Rosin, O. S. Grande, H. Sæle and I. Palu, "Ecogrid EU project — Real time price based load control and economic benefits in a wind production based system," in *22nd International Conference and Exhibition on Electricity Distribution (CIRED 2013)*, Stockholm, 2013.

[9] Rassõlkin, R. Sell, and M. Leier, "Development Case Study of the First Estonian Self-Driving Car, ISEAUTO," *Electr. Control Commun. Eng,* vol. 14, no. 1, p. 81–88, 2018.

[10] L. Yu, D. Xie, C. Huang, T. Jiang and Y. Zou, "Energy Optimization of HVAC Systems in Commercial Buildings Considering Indoor Air Quality Management," *IEEE Transactions on Smart Grid,* pp. 1-11, 2018.

[11] Q. Hu and F. Li, "Hardware Design of Smart Home Energy Management System With Dynamic Price Response," *IEEE Transactions on Smart Grid,* vol. 4, no. 4, pp. 1878-1887, 2013.

[12] H. Hao, Y. Lin, A. S. Kowli, P. Barooah and S. Meyn, "Ancillary Service to the Grid Through Control of Fans in Commercial Building HVAC Systems," *IEEE Transactions on Smart Grid,* vol. 5, no. 4, pp. 2066-2074, 2014.

[13] S. Rotger-Griful, R. H. Jacobsen, D. Nguyen and G. Sørensen, "Demand response potential of ventilation systems in residential buildings," *Energy and Buildings,* vol. 121, pp. 1-10, 2016.

[14] J. Kim, M. Kong, T. Hong, K. Jeong and M. Lee, "The effects of filters for an intelligent air pollutant control system considering natural ventilation and the occupants," *Science of the Total Environment,* vol. 657, pp. 410-419, 2019.

[15] M.-S. Shin, K.-N. Rhee, E.-T. Lee and G.-J. Jung, "Performance evaluation of CO2-based ventilation control to reduce CO2 concentration and condensation risk in residential buildings," *Building and Environment,* vol. 142, pp. 451-463, 2018.

[16] V. Turanjanin, B. Vučićević, M. Jovanović, N. Mirkov and I. Lazović, "Indoor CO2 measurements in Serbian schools and ventilation rate calculation," *Energy,* vol. 77, pp. 290-296, 2014.

[17] ASHRAE, ASHRAE Handbook - Fundamentals, Atlanta, 2013.

[18] A. Rosin, S. Link, M. Lehtla, J. Martins, I. Drovtar and I. Roasto, "Performance and feasibility analysis of electricity price based control models for thermal storages in households," *Sustainable Cities and Society,* vol. 32, pp. 366-374, 2017.

[19] T. Häring, A. Rosin and H. Biechl, "Using common household thermal storages to support the PV- and battery system in nearly zero energy buildings in off-grid mode," *Sustainable Energy Technologies and Assessments,* vol. 35, pp. 12-24, 2019.

[20] A. TenWolde and C. L. Pilon, "The Effect of Indoor Humidity on Water Vapor Release in Homes," *30 Years of Research Proceedings Thermal Performance of the Exterior Envelopes of Whole Buildings X,* pp. 1-9, 2007.

[21] Statistics Estonia, "REL 2011: Eesti eluruumi keskmine pind ja tubade arv on kasvanud," 19 March 2013. [Online]. Available: https://www.stat.ee/65359?parent_id=32784. [Accessed 15 January 2019].

[22] A. Mikola, A. Hamburg, J. Kurnitski and T. Kalamees, "Rekonstrueeritud korterelamute sisekliima ja energiakasutuse analüüs," Tallinn University of Technology, Tallinn, 2017.

[23] Ministry of Economic Affairs and Communications, "Methodology for calculating the energy performance of buildings," Riigi Teataja, 2013.

[24] FSP, "RS 80 A," Östberg, 2015. [Online]. Available: https://fsp.ostberg.com. [Accessed 20 February 2019].

[25] Nord Pool AS, "Market data," [Online]. Available: https://www.nordpoolgroup.com/. [Accessed 12 December 2018].

[26] A. Rosin, H. Hõimoja, T. Möller and M. Lehtla, "Residential Electricity Consumption and Loads Pattern Analysis," in *Proceedings of the 2010 Electric Power Quality and Supply Reliability Conference*, Kuressaare, 2010.

Authorized licensed use limited to: Tallinn University of Technology. Downloaded on August 17,2023 at 20:51:53 UTC from IEEE Xplore. Restrictions apply.

Publication VI

Maask, V., Rosin, A., Roasto, I. (2018), “Development of Experimental Load Management System for Nearly Zero-Energy Building,” 59th International Scientific Conference on Power and Electrical Engineering of Riga Technical University, RTUCON 2018 (1–5). IEEE.

2018 IEEE 59th International Scientific Conference on Power and Electrical Engineering of Riga Technical University (RTUCON)

Development of Experimental Load Management System for Nearly Zero-Energy Building

Vahur Maask, Argo Rosin, Indrek Roasto
Department of Electrical Power Engineering and Mechatronics
Tallinn University of Technology
Tallinn, Estonia

***Abstract*—Over two third of total electricity produced are consumed by residential and commercial buildings. According to this the nearly zero-energy building (NZEB) with local renewable power sources will play important role to reduce greenhouse gases. Local and intermittent renewable power generation is challenge for power quality and supply reliability of NZEB. It means higher demand for an Energy Management System (EMS) to provide power quality and balance between load and generation. This paper gives a brief overview of EMS for residential buildings. To test an EMS, the behavior of NZEB must be simulated in the laboratory. For this purpose, an experimental system was developed which includes variable load and its control as a part of EMS. Two load simulation methods for load management were studied and experimentally verified.**

Keywords—energy management system; load control; experimental system; nearly zero-energy building

I. INTRODUCTION

Studies have shown that over 60% of total electricity produced in the world is consumed by buildings. This consumption is almost equally divided between residential and commercial buildings [1]. This establishes the direction for energy efficient nearly zero-energy buildings (NZEB). Estonian government has approved a regulation for minimum requirements for energy performance. According to the regulation, buildings erected after 31 December 2018 which belong to the public sector and all other buildings that erected after 31 December 2020 must not exceed the limit values shown in Table I. These values have been established with respect to nearly zero-energy buildings [2].

A nearly zero-energy building is a building that is characterized by sound engineering solutions, built according to the best possible construction practice that employs solutions based on energy efficiency and renewable energy technologies and whose energy performance indicator is greater than 0 kWh/(m2·y) but does not exceed the limit values in Table I. Energy performance indicator is total weighted specific use of delivered energy utilized during standard use of the building, less than the weighted specific use of energy fed into energy networks [2].

NZEB needs an EMS to provide power quality and load balance. The main task is to control local generators, loads and energy storages in such manner that electricity expenses and demand peaks would be kept minimal [3].

TABLE I. LIMIT VALUES FOR ENERGY PERFORMANCE INDICATORS IN NEARLY ZERO-ENERGY BUILDINGS [2]

Building type	kWh/(m2·y)
Small residential buildings	50
Multi-apartment buildings	100
Libraries, office and research buildings	100
Business buildings	130
Public buildings	120
Commerce buildings and terminals	130
Educational buildings	90
Pre-school institutions for children	100
Healthcare buildings	270

The EMS control approaches can be divided in two: fully decentralized and hierarchical control. In fully decentralized approach, the main responsibility is given to controllers of energy generators that must maximize their production to satisfy the demand and probably provide maximum possible export to the grid [3].

In a hierarchical approach, the system is controlled centrally to optimize the general operation. The primary control has the fastest bandwidth compared to other control levels. The main tasks for primary controllers are: voltage and current control of the nanogrid. The secondary control is the EMS that maintains secure and reliable functioning of the nanogrid either in grid-connected or islanded mode. Its control loops operate on slower timescale than a primary controller. The main task for a secondary controller is to provide settings for target real and reactive power. The main objective of the future control systems is to reduce the use of high-speed data connections and the computation of critical tasks [4].

Part of the project of Power Electronics Based Energy Management Systems for Nearly Zero Energy Buildings an experimental system is developed to test EMS and Power Electronic Interface (PEI) behaviour in laboratory conditions. For load simulation an electronic load can be used such as Chroma 63800 or NH Research 4600 Series, both are programmable to simulate linear and non-linear AC loading [5], [6]. In the experimental system covered in this paper real

978-1-5386-6903-7/18/$31.00 ©2018 European Union

Authorized licensed use limited to: Tallinn University of Technology. Downloaded on August 17,2023 at 20:52:31 UTC from IEEE Xplore. Restrictions apply.

loads are needed to simulate multiple appliances and their composition in building's load pattern. Variable AC load is added to the system to provide load simulations in variable power range used in light dimming or electric heater power regulation. To develop appropriate load control method, the variable load is tested, analysed and experimentally verified.

II. Overview of EMS

Search in the database (IEEE Xplore) revealed many articles that address EMS use in nanogrids including renewable energy sources. Different approaches to the EMS have been reported, but some aspects are not covered.

References [7] and [8] include use of on-grid photovoltaic (PV) and battery bank based energy storage (BES) without scheduling time of use of an electric appliance. One approach to manage BES charge and discharge is reported in [7], which considers PV energy production and local energy demand. The main aim is to increase PV energy local consumption by charging BES when PV energy production exceeds local demand. When BES has reached its full charge, the rest of the energy is injected to the grid. BES is only discharged when local demand exceeds PV energy production. BES back-up supply is also under consideration in the outages estimated to last up to 180 minutes. BES price based management is described in [8] where Particle Swarm Optimization is used to optimize multiple variables. In addition to BES management, residents' privacy was also discussed because the central information collecting system was replaced with a local EMS with limited information about demand behavior in residential areas. These two articles neglected the shortening of the investment payback period and did not shift loads in time to maximize the profitability of the system.

Measures for the increase of PV energy local consumption are described in [9] and [10]. Without BES, the EMS is based on controllable loads like a washing machine, a dishwasher, a freezer, an air conditioner, and a water heater. Timestep for demand and local energy production calculations were chosen to be 15 minutes, which is a part of ENTSO-E standard. Studies in [9] and [10] do not analyze the use of electrical energy storage, price based load management and maximization of investment profitability. However, the general aim of EMS is:

- to increase PV energy local consumption as much as possible;
- to maintain a controlled profile according to energy price;
- to minimize PV energy grid injection.

In [11] an interesting concept of energy management is proposed. In that study, demand side management is done by residents. User interface is set up to forecast energy price and PV energy production, so it can notify a user to switch on appliances on more affordable time. Buildings are connected to the grid through a Smart Meter that measures energy consumption in a given time. The article does not address flexible loads that can be controlled centrally and the main focus is on users who must decide by themselves when to turn on electric appliances. In this type of solution, residents comfort and system profitability may be questionable.

On-grid PV with BES and demand side management to maximize PV energy local consumption and to decrease demand peaks are reported in [12] and [13]. Flexible loads were a water heater, a heat pump, a freezer, a washing machine, a dishwasher, and a dryer. BES was only storing PV energy on peak production hours to decrease peak injection to the grid. According to [12], their system was estimated to increase PV energy local consumption by 55% to 65% and decrease peak grid injection by 55%. Electricity price based management and maximization of system profitability were neglected in the above articles.

On-grid PV with BES, demand side and price based management has been addressed in [14], [15] and [16]. Flexible loads were a washing machine, a dryer and a dishwasher. Two price based management systems were considered:

- Time of Use (ToU) offers two or three price levels: "off-peak", "mid-peak" and "peak";
- Real-Time Price (RTP) is based on hourly or half-hour price differences in the energy market.

Two different demand side management methods were considered in [14] and [16]:

- RTPDCPT is a price based management where maximum profit was achieved by charging BES in more affordable night hours;
- CPTBAVP is an average demand based management where energy demand throughout the day is constant, but in this way, at the end of the day, energy in the BES is depleted.

Two PV energy grid injection methods are described in [15]:

- Feed in Tariff where all the PV generated energy is sold to the grid;
- Net Metering where the amount of PV energy, which is not consumed by a building, is injected to the grid.

Two BES management systems were considered:

- PV energy, which is not consumed directly, is stored in BES. This is preferred when the energy price is low;
- Excessive PV energy, which is not consumed directly, is injected to the grid the amount of which does not exceed 0.5 kW and the rest is stored in BES.

References [14] – [16] lack analysis of system profitability and payback period. In these articles, off-grid islanded system operation was not discussed and energy injection back to the grid was kept minimal.

III. Proposed EMS Concept

It is required to do further research in the field of EMS that is suitable for NZEB. Also, smart hardware is needed to maximize system profitability and to ensure residents comfort.

A. Research on EMS

In on-grid operation mode, intelligent price based EMS is needed that would include PV energy production, BES and flexible loads, for example, a water heater, a freezer and room heating. Two approaches can be explored:

978-1-5386-6903-7/18/$31.00 ©2018 European Union

Authorized licensed use limited to: Tallinn University of Technology. Downloaded on August 17,2023 at 20:52:31 UTC from IEEE Xplore. Restrictions apply.

- Maximizing PV energy local consumption to reduce the share of energy taken from the grid;
- Analyzing economic aspects to reduce the payback period and maximizing profitability.

Correlation between these two approaches can be investigated.

In the islanded operation mode, power quality and energy reserve are important. Demand side management and load shifting can improve power quality and reduce the risk of energy reserve depletion. Optimal energy storage reserve for BES must be calculated to provide backup power to the building when grid failure occurs.

B. Description of the experimental system

First goal is to develop an appropriate EMS for NZEB (i.e. nanogrids). Second goal is to test it in real-life situation. To achieve this in the laboratory, a scaled experimental system must be developed. **Error! Reference source not found.** shows the structure of the experimental system for building's energy consumption and EMS behavior simulations.

The experimental system is divided into two main parts: control part as an energy management system and control of PEI and controllable objects as building integrated PV, storage and loads. PEI includes a bidirectional inverter connected to the grid, energy storage and power input of the building. Control of PEI situated on the primary control level is responsible for controlling the bidirectional inverter and the battery DC/DC converter. EMS, which is based on Raspberry Pi, is situated on the secondary control level and is responsible for controlling loads and giving higher level commands to the control system of PEI.

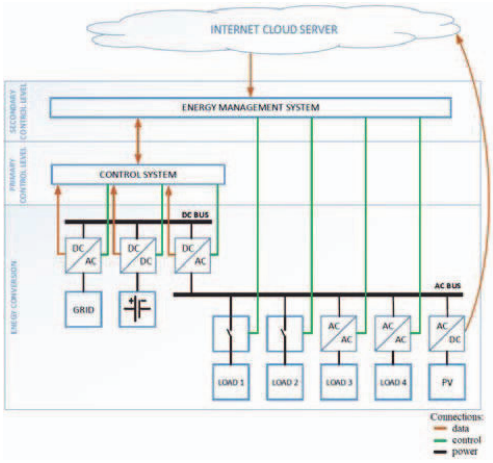

Fig. 1. Structure of the experimental system

For the energy demand simulations of the building in a given timestep, scaled loads "Load 1", "Load 2", "Load 3" and "Load 4" were arranged. Load 1 and load 2 are remotely controlled appliances connected to the grid through smart sockets, which can be wirelessly controlled to simulate load shifting. Load 3 and load 4 are variable loads powered through AC/AC converters controlled by Raspberry Pi. To compare the systems and to find flaws and advantages of each system, two wireless technologies were used: 433 MHz radiofrequency and Wi-Fi. PV with an inverter was added to the system to simulate local power generation. The system is expandable, more devices can be added on the AC or the DC bus.

C. Load control

In the experimental system, AC/AC converters are used to provide a variable load. This variable load can be changed between 0 to 400 W, which is the maximum output power for the dimmer set by manufacturer. From the EMS perspective, this variable load can be seen as dimmable lighting or regulated heater, providing extra control opportunity. Due to the nature of light dimmers, which cut sinus waveform, the output root mean square (RMS) voltage is not linearly dependent on the input 0 to 10 V control voltage. Two different topologies have been considered for use to ensure accurate load control:

- Lookup table;
- Model-based.

The method of lookup table is based on the measurements taken in the range of 0 to 400 W and collected into the table. When a specific load value is required, the program will search an appropriate input control value from that table. Lookup table consist of 32 measured values and linear interpolation is used to obtain the accurate load value.

Model-based method is based on the transfer functions of the dimmer control circuit elements. The light dimmer chosen is controlled by 0 to 10 V analog input voltage. Unfortunately, Raspberry Pi is not supporting analog output, which leads to external digital-analog converter (DAC) use. DAC transfer function is presented in (1), where N is a digital input value for DAC sent from Raspberry Pi, using the I^2C data exchange protocol. DAC maximum output value is 3.3 V, amplified for three times with an operational amplifier.

$$V_{DAC} = \frac{N \cdot 3{,}3 \cdot 3}{4096} \tag{1}$$

Firing angle α of the dimmer is dependent on the DAC output voltage V_{DAC}. Our measurements showed that DAC is not dimming the whole range of sinus waveform and there are upper and lower limitations to be considered in (2).

$$\alpha = -0{,}2629 \cdot V_{DAC} + 2{,}6111 \tag{2}$$

Output RMS voltage is dependent on the supply RMS voltage V_{supply} and firing angle. The transfer function of the dimmer is given in (3) [17].

978-1-5386-6903-7/18/$31.00 ©2018 European Union

Authorized licensed use limited to: Tallinn University of Technology. Downloaded on August 17,2023 at 20:52:31 UTC from IEEE Xplore. Restrictions apply.

$$V_{load} = V_{supply}\sqrt{\frac{1}{\pi}\left(\pi - \alpha + \frac{1}{2}sin\,2\alpha\right)} \quad (3)$$

The final transfer function is the load itself. Power consumed by the load is calculated by (4), which considers RMS voltage on the load and the load resistance R_{load}.

$$P_{load} = \frac{V_{load}^2}{R_{load}} \quad (4)$$

Open-loop control methods have been tested on the experimental system. The load power was increased in 10 W steps from 0 to 400 W (Fig. 2), and measurements were taken with the power analyser. Error means deviation between the reference and the measured power. Our measurements show that the mean error for the model-based method is 1.71% and the mean error for the lookup table is 2.65%. The probability of the error to be in the range of 0 to 4% is 0.93 for the model-based method and for the lookup table it is 0.83 (Fig. 3).

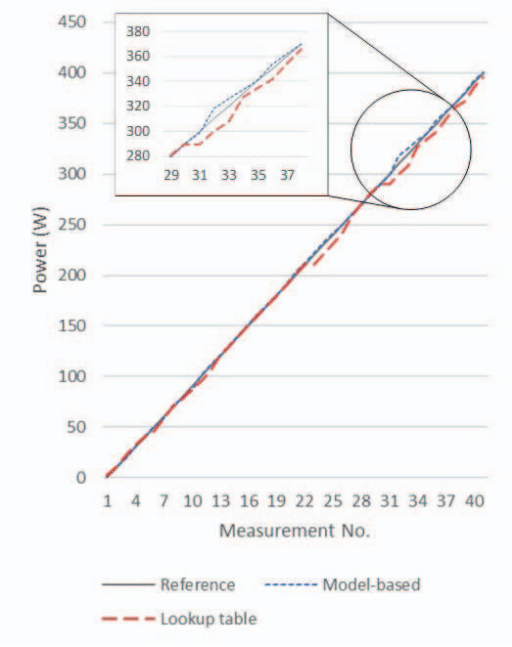

Fig. 2. The behavior of different load control methods

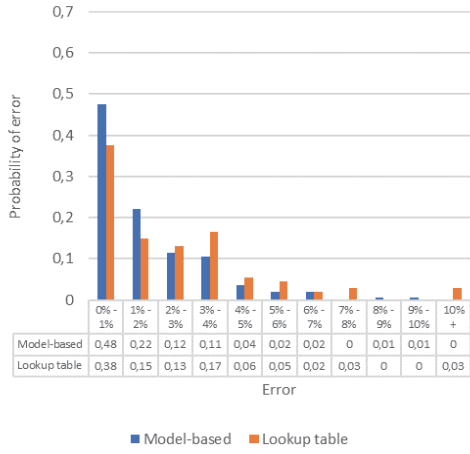

	0% - 1%	1% - 2%	2% - 3%	3% - 4%	4% - 5%	5% - 6%	6% - 7%	7% - 8%	8% - 9%	9% - 10%	10% +
Model-based	0,48	0,22	0,12	0,11	0,04	0,02	0,02	0	0,01	0,01	0
Lookup table	0,38	0,15	0,13	0,17	0,06	0,05	0,02	0,03	0	0	0,03

Fig. 3. Error probability comparison of different methods

IV. Conclusions

Different EMS concepts have been developed but they lack several aspects required for the analysis of EMS. One of the aspects is on-grid and islanded EMS behavior to achieve maximum profitability in normal operation whereas acceptable power quality must be provided during the grid failure.

This paper presents an experimental system for NZEB energy flow simulations. The purpose of the system is to simulate energy consumption of a building and to provide a platform for testing different EMS concepts. The system consists of five parts: bidirectional inverter, BES with DC/DC converter, PV with inverter, EMS based on Raspberry Pi, and different loads that can imitate energy consumption of a building.

Two load simulation methods for load management were studied: lookup table and model-based. Each control method was tested on the experimental system. Results show that mean error for the model-based method is 0,94% smaller than the mean error for the lookup table method. Furthermore, with model-based load control method the error is more probable to occur in the range of 0 to 4% than with the lookup table method. Therefore, the model-based method is more appropriate for use in load control.

Acknowledgment

This work was supported by the Estonian Research Council grant PUT (PUT1680), and Estonian Centre of Excellence in Zero Energy and Resource Efficient Smart Buildings and Districts ZEBE, grant 2014-2020.4.01.15-0016 funded by European Regional Development Fund.

978-1-5386-6903-7/18/$31.00 ©2018 European Union

Authorized licensed use limited to: Tallinn University of Technology. Downloaded on August 17,2023 at 20:52:31 UTC from IEEE Xplore. Restrictions apply.

REFERENCES

[1] A. Rosin, H. Hõimoja, T. Möller, and M. Lehtla, "Residential Electricity Consumption and Loads Pattern Analysis," *Proc. 2010 Electr. Power Qual. Supply Reliab. Conf.*, pp. 111–116, 2010.

[2] Estonian Government, "Minimum requirements for energy performance," *Riigi Teat.*, pp. 1–10, 2014.

[3] N. D. Hatziargyriou, A. Dimeas, A. G. Tsikalakis, J. A. P. Lopes, G. Karniotakis, and J. Oyarzabal, "Management of microgrids in market environment," *2005 Int. Conf. Futur. Power Syst.*, p. 7 pp.-7, 2005.

[4] D. Semënov, G. Mirzaeva, C. D. Townsend, and G. C. Goodwin, "Recent Development in AC Microgrid Control - a Survey," 2017.

[5] Chroma, "Programmable AC Electronic Load – 63800," 2018. [Online]. Available: https://www.chromausa.com/product/programmable-ac-electronic-load-63800/#Overview. [Accessed 2 October 2018].

[6] NH Research, "AC Electronic Load – 4600 Series," 2018. [Online]. Available: https://nhresearch.com/power-electronics-test-systems-and-instruments/ac-dc-electronic-loads/ac-electronic-loads/ac-electronic-load-4600-series/. [Accessed 2 October 2018].

[7] X. Vallvé, A. Graillot, S. Gual, and H. Colin, "Micro storage and demand side management in distributed PV grid-connected installations," *2007 9th Int. Conf. Electr. Power Qual. Util. EPQU*, 2007.

[8] H. Kuo, S. K. Pradhan, C. Wu, P. Cheng, Y. Xie, and L. Fu, "Dynamic Demand - side Management with User' s Privacy Concern in Residential Community," *IEEE Int. Conf. Autom. Sci. Eng.*, pp. 1094–1099, 2016.

[9] A. Baldauf, "A smart home demand-side management system considering solar photovoltaic generation," *5th Int. Youth Conf. Energy*, pp. 1–5, 2015.

[10] L. Martirano *et al.*, "An example of smart building with a km zero energy performance," *IEEE Ind. Appl. Soc. Annu. Meet.*, pp. 1–8, 2017.

[11] J. Kohlmann, M. C. H. Van Der Vossen, J. D. Knigge, C. B. A. Kobus, and J. G. Slootweg, "Integrated Design of a demand-side management system," *2011 2nd IEEE PES Int. Conf. Exhib. Innov. Smart Grid Technol.*, pp. 1–8, 2011.

[12] C. J. C. Williams, J. O. Binder, and T. Kelm, "Demand side management through heat pumps, thermal storage and battery storage to increase local self-consumption and grid compatibility of PV systems," *IEEE PES Innov. Smart Grid Technol. Conf. Eur.*, pp. 1–6, 2012.

[13] S. Janocha, S. Baum, and I. Stadler, "Cost minimization by optimization of electricity generation and demand side management," *2016 Int. Energy Sustain. Conf. IESC 2016*, pp. 1–6, 2016.

[14] S. Pholboon, M. Sumner, and P. Kounnos, "Community power flow control for peak demand reduction and energy cost savings," *2016 IEEE PES Innov. Smart Grid Technol. Conf. Eur.*, pp. 1–5, 2016.

[15] A. N. Ravishankar, S. Ashok, and S. Kumaravel, "Effects of demand side management & storage on renewable energy penetration to the grid," *Proc. 3rd IEEE Int. Conf. Adv. Electr. Electron. Information, Commun. Bio-Informatics, AEEICB 2017*, pp. 329–335, 2017.

[16] S. Pholboon, M. Sumner, and P. Kounnos, "Adaptive Power Flow Control for Reducing Peak Demand and Maximizing Renewable Energy Usage," *5th Int. Electr. Eng. Congr. Pattaya, Thail.*, pp. 8–10, 2017.

[17] N. Mohan, T. M. Undeland, and W. P. Robbins, *Power Electronics: Converters, Applications, and Design*, Third Edit. John Wiley & Sons, 2003.

Vahur Maask received the B.Sc. and M.Sc. degrees in electrical engineering in 2015 and 2017, respectively, from Tallinn University of Technology, Tallinn, Estonia. He is currently working towards the Ph.D. degree and working as early stage researcher at the Tallinn University of Technology in Department of Electrical Power Engineering and Mechatronics. His research interests include modeling and simulation of energy management systems.

978-1-5386-6903-7/18/$31.00 ©2018 European Union

Authorized licensed use limited to: Tallinn University of Technology. Downloaded on August 17,2023 at 20:52:31 UTC from IEEE Xplore. Restrictions apply.

Curriculum vitae

Personal data

Name:	Vahur Maask
Date of birth:	22.09.1993
Place of birth:	Estonia
Citizenship:	Estonian

Contact data

E-mail:	vahur.maask@taltech.ee

Education

2017–2023	Tallinn University of Technology, PhD
2015–2017	Tallinn University of Technology, MSc
2012–2015	Tallinn University of Technology, BSc
2009–2012	Võru Kreutzwaldi Gymnasium, Secondary Education

Language competence

Estonian	Native speaker
English	Fluent
Russian	Basic skills

Professional employment

2018–	Tallinn University of Technology, Junior Researcher
2017–2017	Tallinn University of Technology, Engineer
2015–2015	Ensto Ensek Ltd, development engineer (internship)
2014–2014	Elektrilevi OÜ, protected zone supervision (internship)

Scientific work and Research and Development projects

2021–2023	PSG409, “New generation dynamic sizing methods for heating and cooling systems in intermittently operated buildings”
2021–2022	LEEEE21133, “Providing energy consulting in relation to machine learning models”
2021–2021	LEEAE21059, “Assessment of the reliability of electrical installations with on-site measurements”
2020–2023	EE20107, “Energy flexilibilty service pilot project - Stage 2”
2019–2021	Lep18101, “Proof of concept of an integrated monitoring and diagnostics solution for predictive maintenance of expansion joints”
2017–2021	PUT1680, “Power electronics based energy management systems for net zero energy buildings”
2020–2020	EE20012, “Energy flexilibilty service pilot project - Stage 1”
2018–2018	Lep18038, “Development of a virtual power plant laboratory”
2016–2018	VERT16061, “Strategic Partnership in the field of Mechatronics for innoavative and smart growth of European manufacturing SMEs”
2018–2018	Lep18042, “Composition of a development plan for developing monitoring solutions for compensators in the frame of smart specialisation growth area”
2017–2018	Lep17108, “Preliminary research of the technological solution for monitoring the compensators conditions at site”
2017–2018	Lep17114, “Replacement of electromechanical contactors with semiconductor devices”

Elulookirjeldus

Isikuandmed

Nimi:	Vahur Maask
Sünniaeg:	22.09.1933
Sünnikoht:	Eesti
Kodakondsus:	eestlane

Kontaktandmed

E-post:	vahur.maask@taltech.ee

Hariduskäik

2017–2023	Tallinna Tehnikaülikool, PhD
2015–2017	Tallinna Tehnikaülikool, MSc
2012–2015	Tallinna Tehnikaülikool, BSc
2009–2012	Võru Kreutzwaldi Gümnaasium, reaalsuund

Keelteoskus

Eesti	Emakeel
Inglise	Kõrgtase
Vene	Algtase

Teenistuskäik

2021–2023	PSG409, “Uue generatsiooni dünaamilised meetodid kütte- ja jahutussüsteemide dimensioneerimiseks vahelduva kasutusega hoonetes”
2021–2022	LEEEE21133, “Energeetikaalase konsultatsiooni pakkumine seoses masinõppe mudelitega”
2021–2021	LEEAE21059, “Elektripaigaldise töökindluse hindamine koos kohapealsete mõõdistamistega”
2020–2023	EE20107, “Energiatarbimise juhtimise paindlikkustoote pilootprojekt - 2. etapp”
2019–2021	Lep18101, “Kompensaatorite monitooring kasutuskohas: tehnoloogilise lahenduse kontseptsiooni väljatöötamine”
2017–2021	PUT1680, “Jõuelektroonikal baseeruv energia juhtimissüsteem liginullenergia ehitistele”
2020–2020	EE20012, “Energiatarbimise juhtimise paindlikkustoote pilootprojekt - 1. etapp”
2018–2018	Lep18038, “Virtuaalse elektrijaama arenduslabori väljatöötamine”
2016–2018	VERT16061, “Strateegiline partnerlus mehhatroonika valdkonnas Euroopa väikeste ja keskmise suurusega tootmisettevõtete innovatiivseks ja nutikaks kasvuks (MechMate)”
2018–2018	Lep18042, “Nutika spetsialiseerumise meetme arendusplaani koostamine kompensaatorite monitooringu pilootlahenduste väljatöötamiseks”
2017–2018	Lep17108, “Tehnoloogilise lahenduse eeluuring kompensaatorite monitooringuks kasutuskohas”
2017–2018	Lep17114, “Elektromehhaaniliste kontaktorite asendamine kontaktivabade pooljuhtseadmetega”

ISSN 2585-6901 (PDF)
ISBN 978-9916-80-086-7 (PDF)